IDAHO POWER
An IDACORP Company

Responses to FERC Additional Information Request S-1

Sediment Transport

Final Report
Part 3
Appendices A thru E

Shaun K. Parkinson, P.E.
Engineering Leader

Kelvin Anderson, P.E.
Engineer II

Jeff Conner, P.E.
Engineer II

Hells Canyon Project
FERC No. P-1971-079

February 2005

LIST OF APPENDICES

Appendix A. CH2M Hill reservoir sediment sampling 1
Appendix B. CH2M Hill evaluation of tributary fan volumes 5
Appendix C. CH2M Hill evaluation of sandbar slope stability 9
Appendix D. Explanation of the content on the 5 DVDs included with Hells Canyon AIR S-1..... 13
Appendix E. Tables showing segmentation of unadjusted and flow-adjusted sandbar counts 15

This page left blank intentionally.

Appendix A. CH2M Hill reservoir sediment sampling

This page left blank intentionally.

Sediment Sampling Within Oxbow and Hells Canyon Reservoirs

PREPARED FOR: File

PREPARED BY: Greg Warren

COPIES: Shaun Parkinson / IPC
Kelvin Anderson / IPC
Jeff Conner / IPC
Sherrill Doran / CH2MHILL

DATE: January 6, 2005

Introduction

The purpose of the project was to collect representative samples of sediments from the reservoir bottom and analyze them for particle size distribution and if possible, evaluate the thickness of the sediments that have accumulated on the reservoir bottom.

The study spanned approximately 36 river miles, from just above Hells Canyon Dam at RM 248 to the upper end of Oxbow Reservoir at RM 284. A total of 34 locations were selected for sampling; 13 in Oxbow Reservoir and 21 in Hells Canyon Reservoir. Due to subsurface conditions (i.e. rocky substrate, minimal sediment accumulation), samples were not recovered from all of the proposed locations. Therefore, a total of 6 grab samples were collected from Oxbow Reservoir and 18 were collected from Hells Canyon Reservoir.

The sample locations included areas in the deepest part of the reservoir channel (thalweg), and also along transects perpendicular to the flow direction. The thalweg locations were spaced approximately every 3 miles. The transects consisted of 3 to 5 samples and were typically located below the mouths of selected tributaries.

Attachment A includes maps of Oxbow and Hells Canyon Reservoirs that show the sediment sample locations.

Methods

The proposed sampling locations were located on maps of the reservoirs. The samples were located on the reservoirs using an OMNISTAR Global Positioning System (GPS). The boat used to navigate the reservoirs and collect the samples was a 23-foot Workskiff aluminum V-hull.

At each sample location, the reservoir bottom was sounded to determine the deepest area (thalweg). In areas where fine-grained sediments were suspected, the thickness of the sediments was approximated using a 5- or 10-foot long spud rod (Eakin, 1939). The spud rod is a steel shaft with machined cups at 0.1-foot intervals that is used to determine

sediment thickness and retrieve small samples of the sediments. The spud rod was operated by lowering it over the side of the boat with a rope until it was suspended vertically at least 10 feet above the reservoir bottom. It was then allowed to free-fall through the water into the sediment on the reservoir bottom.

The spud rod was retrieved with the rope and the thickness of the sediment retained on the spud rod was measured and recorded. If no sediment was retained on the initial drop, the spud was deployed again to attempt to retain sediments. A spud rod free of sediment indicated sandy or hard-packed sediment where either the spud could not penetrate, or the sand washed off the spud during retrieval.

The sediment grab samples were collected using a Shipek® sediment sampler manufactured by Wildco. The Shipek collects samples from the upper 0.5 foot of sediment using a spring-loaded, horizontally-rotating bucket that scoops up the sediment. The sampler was lowered to the bottom using a winch mounted to the front of the boat. The sampler was deployed up to three times in order to retrieve samples. If no sediment was recovered after the third attempt, it was noted on a field form along with reasons for lack of recovery. Typically, reasons for lack of sample retrieval included gravelly substrate or very hard-packed sandy material that the sampler bucket could not penetrate.

The sediment samples were transferred from the sampler into stainless steel bowls. The sediment samples were mixed, and representative portions of the sample placed into a clear plastic jar and a plastic baggie. Some of the samples were photographed if notable features were observed. The sample ID, location, date, time, containers, and other notes such as material description and number of sample attempts were recorded on field forms and in a field notebook.

Attachment B includes the sample information including sample location, date and time, water depth, material recovered, laboratory data, and other notes.

Summary of Lab Results

Hells Canyon Reservoir

Hells Canyon thalweg sediments consisted primarily of fine-grained silts, clays, and fine sands between RM 248 and 260. The percent passing #200 sieve (<0.075 mm) for these materials ranged between 48.8 and 93.7 percent. The D_{50} of these finer materials averaged 0.23 mm. Farther up the reservoir above RM 263, sediments consisted primarily of silty sands and gravels with few fine-grained materials. The D_{50} of these coarser materials averaged 4.2 mm, and ranged from 0.13 to 19.0 mm. Along the transects, sediments were more coarse-grained and some represented side-slope deposition.

Oxbow Reservoir

In Oxbow thalweg sediments were typically fine sandy silt between RM 273 and 276. The percent passing #200 sieve (<0.075 mm) for these materials ranged between 38.8 and 67.4 percent. The D_{50} of these finer materials averaged 0.10 mm. (Along the one transect able to be sampled at RM 275.8, sediments were more coarse-grained and some represented side-slope deposition.) Farther up the reservoir above RM 276, sediments consisted primarily of

sands and gravels with few fine-grained materials. The D_{50} of the only sample recovered (RM 279.5) was 0.39 mm.

Complete particle-size distribution curves are included in Attachment C.

References

Eakin, H. M. 1939. In *Sedimentation Engineering*, 1975. American Society of Civil Engineers Manual and Report on Engineering Practice No. 54. New York, NY.

Wildlife Supply Company. 1997-1998 Catalog. 301 Cass Street, Saginaw, MI 48602.

ATTACHMENT A

MAPS OF SAMPLE LOCATIONS

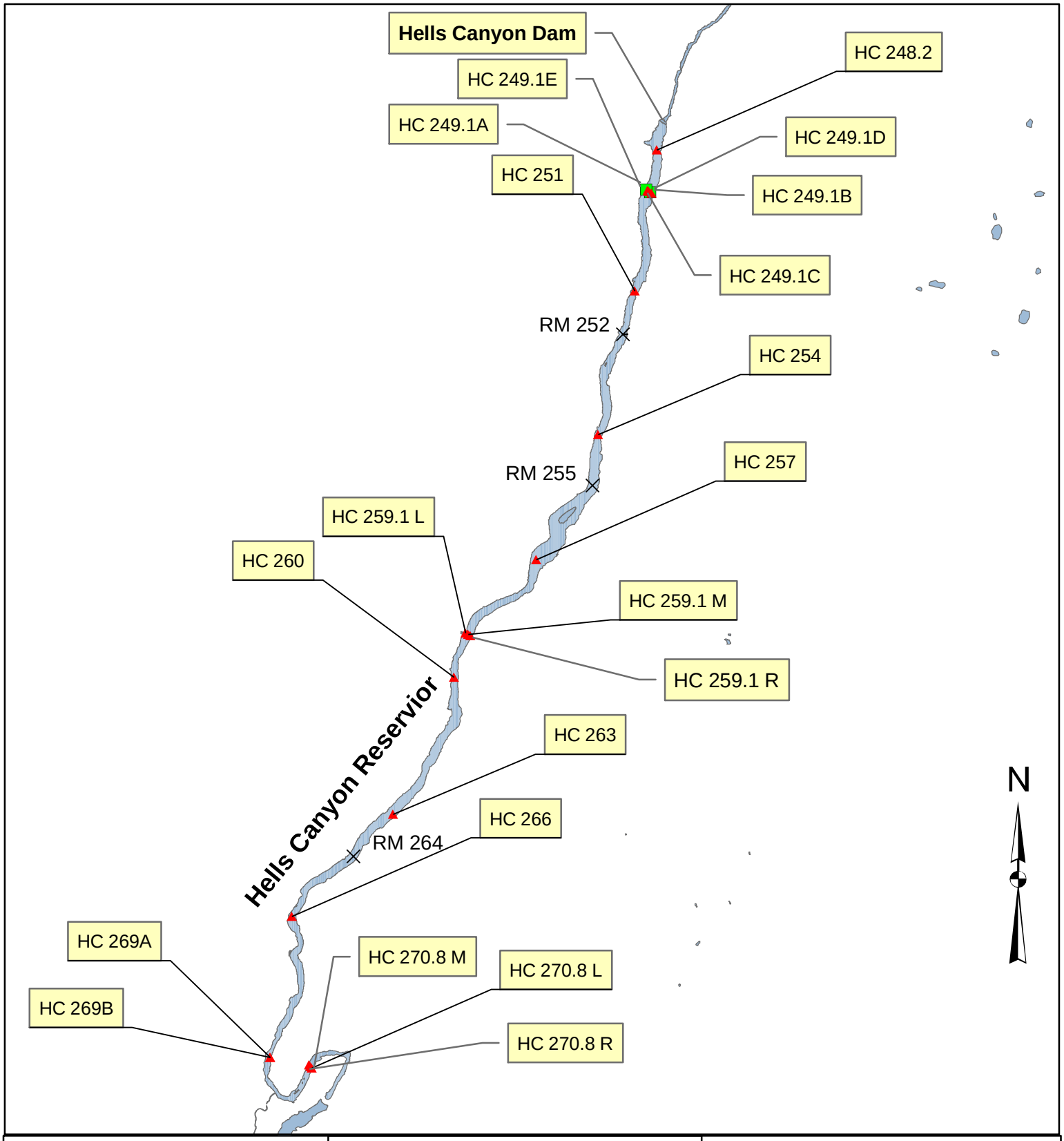

Legend

- No Sample Recovery
- Sampled Location

0 0.5 1 2 3 4 Miles

Area Map

Hells Canyon Reservoir

Sediment Sample Locations

September 2004

CH2MHILL

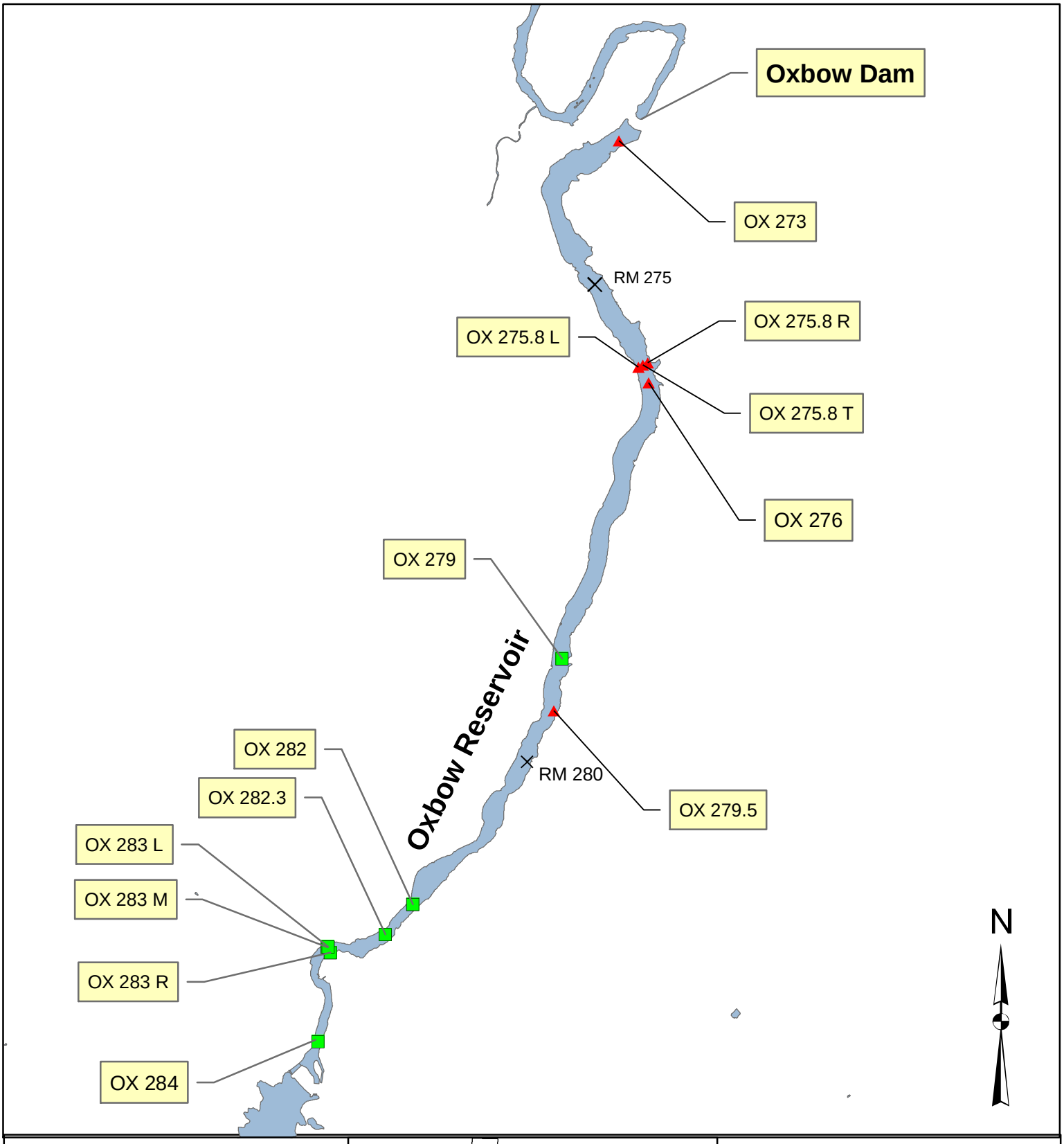

Features Legend

Sampled Locations

No Sample Recovery

1 0.5 0 1 Miles

Area Map

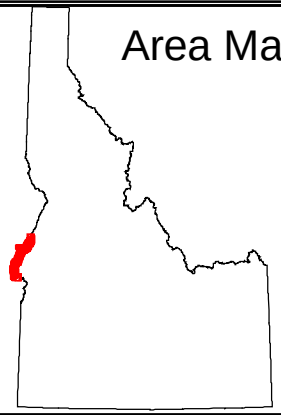

Oxbow Reservoir

Sediment Sample Locations

September 2004

CH2MHILL

ATTACHMENT B

SUMMARY OF SAMPLE INFORMATION

Oxbow - Hells Canyon Reservoir Sediment Sampling

September 27 - 29, 2004

Sample ID (RM[1])	River Mile	Date	Time	Water Depth (ft)	Material[2]	% Passing #200	D_{50} (mm)[3]	Sample Containers	Notes
OX 273	273	9/28/2004	9:12	136	Organic gray to black sandy silt/clay	67.4	n/a	Bag/Jar	Spud = 6.9 ft., Organic reservoir sediment
OX 275.8 T	275.8	9/28/2004	10:09	103	Black to dark gray silty sand	38.8	0.10	Bag/Jar	Spud = 1.1 ft., No odor
OX 275.8 R	275.7	9/28/2004	10:25	64	Silty sand	25.0	0.11	Bag/Jar	No odor
OX 275.8 L	275.9	9/28/2004	10:39	65	Sandy gravel with trace silt	10.6	3.03	Bag/Jar	
OX 276	276	9/28/2004	11:08	112	Organic sandy silt/clay	66.7	n/a	Bag/Jar	
OX 279	279	9/28/2004	11:42	72	Sandy gravel plus bivalve shells	---	---	None	3 attempts, 1st 2 empty
OX 279.5	279.5	9/28/2004	12:26	95	Sand with gravel	2.3	0.39	Bag/Jar	Recovered sample on 2nd attempt
OX 282	282	9/28/2004		62	Gravel/sand	---	---	None	3 attempts, no recovery except scrapings
OX 282.3	282.3	9/28/2004	13:06	25	Rounded gravels and organic debris	---	---	None	3 attempts, poor recovery
OX 283 M	283	9/28/2004	13:23	16	Gravel/sand	---	---	None	3 attempts, no recovery
OX 283 R	282.8	9/28/2004	13:29	6	Gravel/sand	---	---	None	3 attempts, no recovery
OX 283 L	283.2	9/28/2004	13:24	18	Gravel/sand	---	---	None	3 attempts, no recovery
OX 284	284	9/28/2004	13:45	15	Cobbles/gravels substrate	---	---	None	3 attempts, no recovery
HC 248.2	248.2	9/29/2004	8:52	216	Brown to gray to black organic silt/clay with fine sand	87.1	n/a	Bag/Jar	Spud > 5.5 ft., gas bubbles in sample
HC 249.1A	249	9/29/2004	10:07	83	Sandy gravel	6.3	25.0	Bag	Rocky - side slope deposition
HC 249.1B	249.05	9/29/2004	10:18		Fine black silty sand	---	---	None	Poor recovery
HC 249.1C	249.1	9/29/2004	10:33	189	Dark organic silt/clay	93.7	n/a	Bag/Jar	
HC 249.1D	249.15	9/29/2004	10:45	193	Dark organic silt/clay with fine sand	83.8	n/a	Bag/Jar	Spud > 6.75 ft., organic
HC 249.1E	249.2	9/29/2004	11:14		Gravelly	---	---	None	Rocky - side slope deposition, no recovery
HC 251	251	9/29/2004	9:38	183	Organic gray/brown silt/clay	92.2	n/a	Bag/Jar	Spud = 1.1 ft
HC 254	254	9/29/2004	11:35	143	Organic gray/brown silt/clay with trace sand	89.5	n/a	Bag/Jar	Spud = 1.4 ft
HC 257	257	9/29/2004	11:58	104	Dark gray/brown sandy silt	66.5	n/a	Bag/Jar	Spud = 1.4 ft., RM approximate - no gps point
HC 259.1 R	259	9/27/2004	15:42	103	Silt/very fine sand	57.7	n/a	Bag/Jar	
HC 259.1 L	259.1	9/27/2004	15:51	40	Very fine sand with trace silt	7.9	0.20	Bag/Jar	
HC 259.1 M	259.2	9/27/2004	16:03	73	Very fine sand with trace silt	5.5	0.37	Bag/Jar	
HC 260	260	9/27/2004	15:23	105	Very fine sand to silt	48.0	0.08	Bag/Jar	
HC 263	263	9/27/2004	15:02	75	Silty sand	18.8	0.13	Bag/Jar	
HC 266	266	9/27/2004	14:15	48	Sand with trace silt	8.6	0.28	Bag/Jar	
HC 269A	269	9/27/2004	13:32	25	Sandy gravel	0.8	19.0	Bag	
HC 269B	269.1	9/27/2004	13:48	25	Fine sand	2.8	0.62	Bag/Jar	
HC 270.8 L	270.7	9/28/2004	15:00	6	Silty sand	26.9	0.14	Bag/Jar	Very slight odor
HC 270.8 M	270.8	9/28/2004	15:13	8	Gravelly sand with trace silt	7.0	0.74	Bag/Jar	No odor
HC 270.8 R	270.9	9/28/2004	15:28	20	Sandy gravel	4.0	12.77	Bag/Jar	No odor
HC 271.5	271.5	9/28/2004	15:45	5	Boulder/cobble gravels	---	---	None	Could not reach sample location - too shallow

Notes:

1) Sample ID is approximately equal to River Mile location

2) Samples with poor recovery not evaluated for PSD; estimated particle size by recovered materials, bottom characteristics and spud rod probing

3) Samples with >50% passing #200, D_{50} is less than 0.075 mm

OX = Oxbow Reservoir Sample Locations

HC = Hells Canyon Reservoir Sample Locations

R = River right

M, T = Above thalweg

L = River left

A, B, C, D, E = Samples collected along transect perpendicular to flow direction

ATTACHMENT C

PARTICLE SIZE DISTRIBUTION CURVES

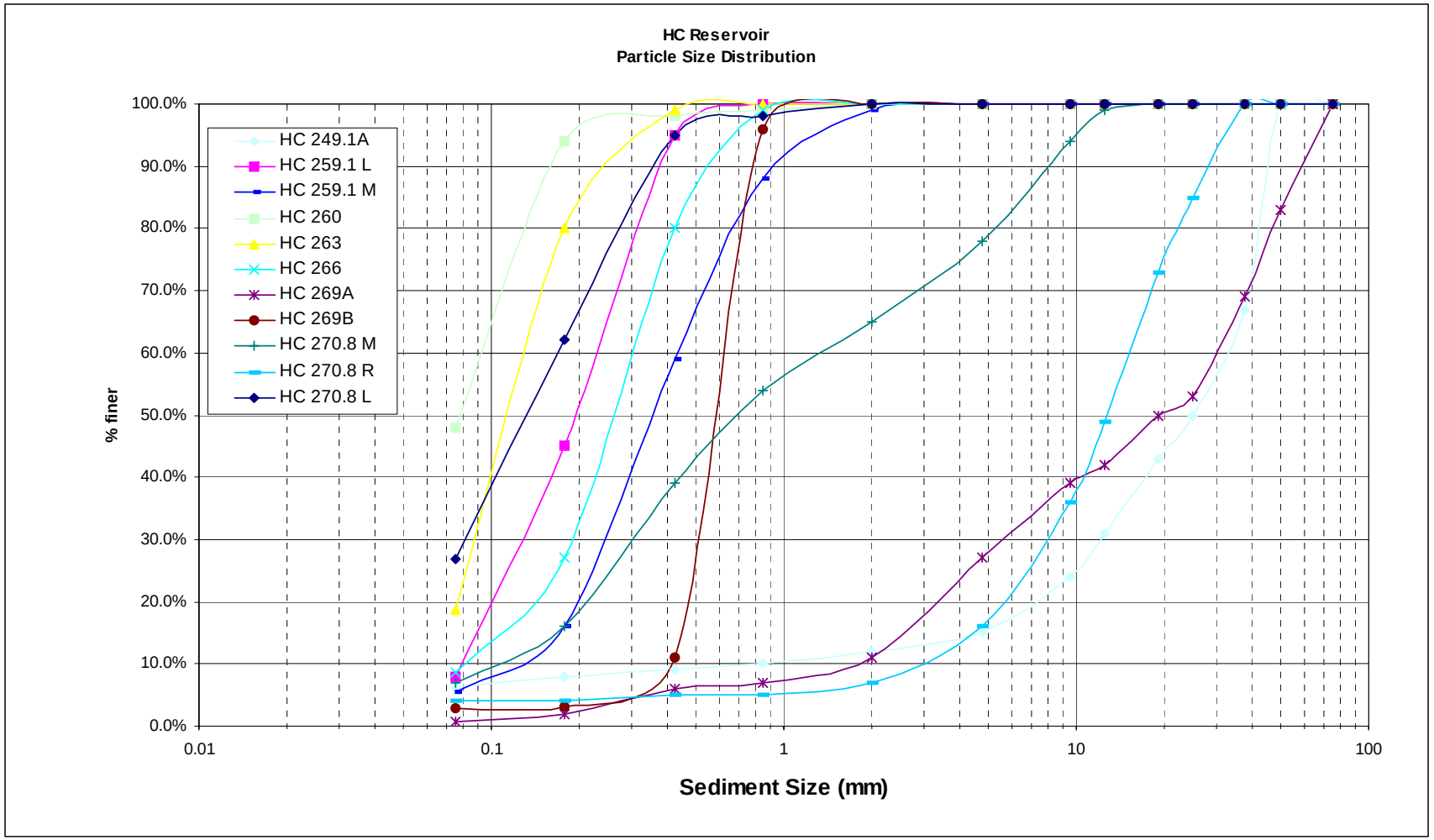
HC Reservoir
Particle Size Distribution
100.0%
90.0%
80.0%
70.0%
60.0%
50.0%
40.0%
30.0%
20.0%
10.0%
0.0%
% finer
0.01
0.1
1
10
100
Sediment Size (mm)
HC 249.1A
HC 259.1 L
HC 259.1 M
HC 260
HC 263
HC 266
HC 269A
HC 269B
HC 270.8 M
HC 270.8 R
HC 270.8 L

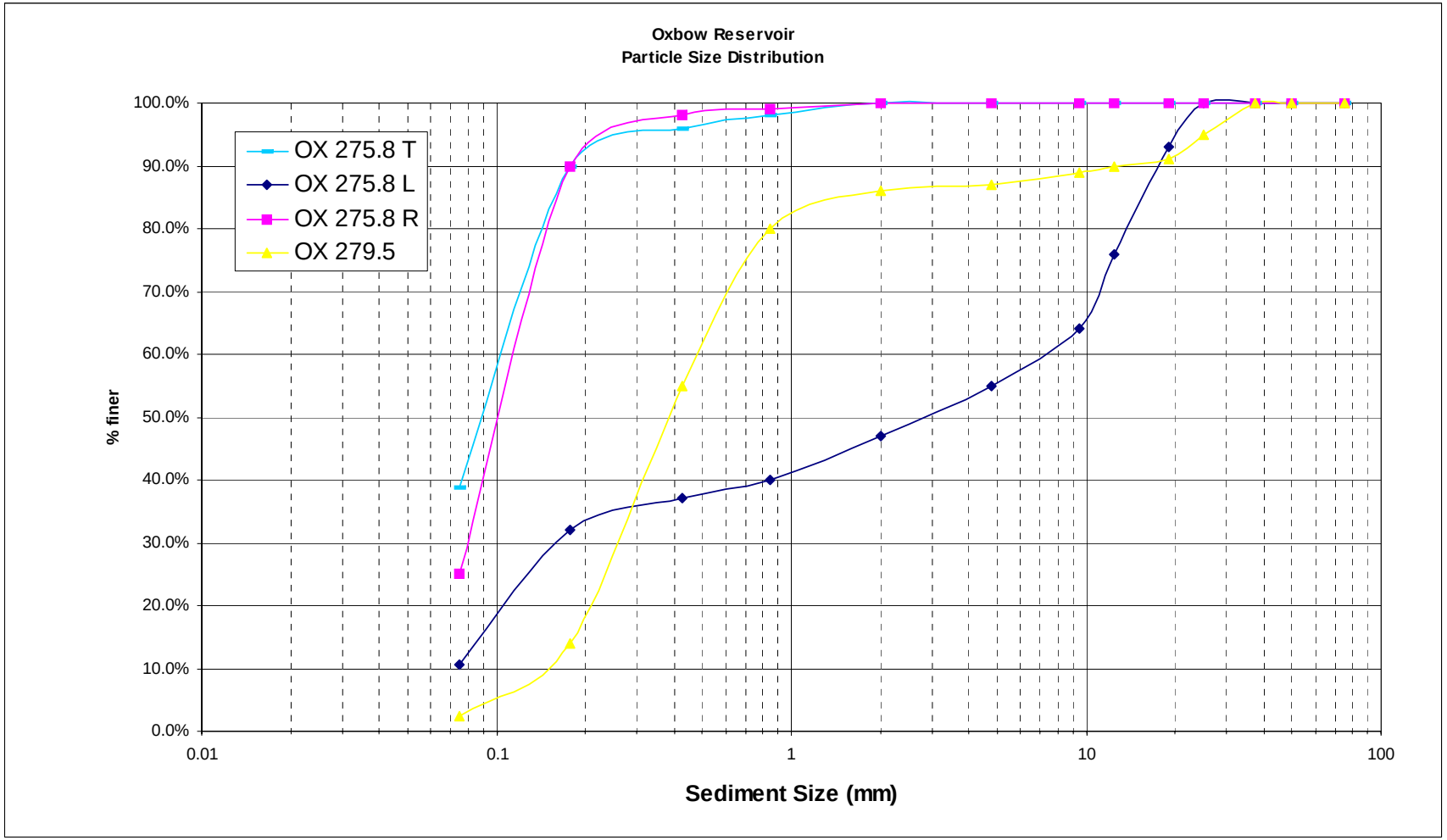
Oxbow Reservoir
Particle Size Distribution
OX 275.8 T
OX 275.8 L
OX 275.8 R
OX 279.5
% finer
100.0%
90.0%
80.0%
70.0%
60.0%
50.0%
40.0%
30.0%
20.0%
10.0%
0.0%
0.01
0.1
1
10
100
Sediment Size (mm)

Appendix B. CH2M Hill evaluation of tributary fan volumes

This page left blank intentionally.

Appendix B PDF goes here

Estimated Sediment Volumes in Selected Tributaries, Brownlee, Oxbow, and Hells Canyon Reservoirs

PREPARED FOR: File

PREPARED BY: Greg Warren/CH2M HILL/BOI

COPIES: Shaun Parkinson/IPC
Jeff Conner/IPC
Kelvin Anderson/IPC
Sherrill Doran/CH2M HILL/BOI

DATE: January 31, 2005

Introduction

Idaho Power Company (IPC) contracted CH2M HILL to estimate post-impoundment sediment deposition volumes in selected tributaries in the Hells Canyon Complex, which includes Brownlee, Oxbow, and Hells Canyon reservoirs. This exercise was conducted during December 2004, in order to address AIRs from FERC as part of the relicensing effort. The purpose of the exercise was to estimate the volume of sediment that has been deposited from selected tributaries into the reservoirs since project completion. The sediment volumes are being estimated in order to obtain a better understanding of the sediment budget for this portion of the Snake River system.

Sediment volumes were estimated for the following tributaries: Brownlee, Dennett, Rock, and Sturgill Creeks in Brownlee Reservoir; Salt Creek in Oxbow Reservoir; and McGraw and Steamboat Creeks in Hells Canyon Reservoir.

Methodology

The following techniques were used to estimate post-impoundment sediment volumes in the tributaries:

- **Geophysics**: Golder and Associates (Golder) collected geophysical data and prepared a report and maps that showed distribution and estimated volumes of sediment deposits that they interpreted to be post-impoundment. Golder's report also describes the geophysical techniques and equipment used.
- **Topographic maps**: Pre-reservoir topographic maps were compared with the bathymetric maps to evaluate the pre-reservoir topography and assess if topographic changes (i.e., depositional events) had occurred since reservoir impoundment. The contours were used to draw longitudinal profiles and cross sections of the drainage topography prior to filling the reservoirs.
- **Bathymetric maps**: Bathymetric maps provided by IPC were used to analyze reservoir bottom topography and identify any deposits that appeared to be post-impoundment,

based primarily on position and geomorphic expression. Sediment deposits, including pre-impoundment alluvial fans, post-impoundment deltaic deposits, debris-flow deposits, and subaqueous slumps were identified on the bathymetric maps. Also, locations of deposits identified by Golder were outlined on these maps for comparison. Profiles and cross-sections of the tributaries were drawn on the bathymetric maps to evaluate slopes, gradients, and estimate the thickness of the sediment deposits. The current reservoir bottom contours were compared with pre-reservoir contours to identify differences that may be the result of post-reservoir deposition.

- **Aerial photographs**: Aerial photographs provided by IPC were used to identify and map sediment deposits and evaluate changes that had occurred since construction of the reservoirs. Post-impoundment color photos and pre-impoundment black-and-white photos were available for comparing existing versus current conditions. These photographs provided visual evidence regarding post-impoundment deposition.

Assumptions

A few general assumptions were applied during the sediment volume calculations. These include:

- Sediment deposition of fine-grained materials such as sand, silt, and clay likely occurs during annual spring runoff, but the largest volumes materials are likely deposited at the tributary mouths as a result of relatively large but infrequent debris-flows. Debris flows are defined in the Dictionary of Geologic Terms as "rapid flowage involving debris (i.e. larger fragments of rocks) of various kinds and conditions". Debris flows are also referred to locally as slides or blow-outs.

- The interval between large depositional events is likely to be longer than time since construction of the HCC. Therefore, estimating the sediment input during a short time interval (especially considering geologic time) may not be representative of the long-term sediment delivery capacity of the tributaries.

- Geomorphic interpretations were used in conjunction with the aerial photographs to determine whether sedimentation occurred during pre- or post-impoundment conditions. A post-impoundment depositional event (i.e., a debris flow) would typically form a deltaic deposit when it enters the slack water. Deltaic deposits are fan-shaped, relatively flat-topped with steeper fronts. However, depending on the energy and velocity of the debris flow, subaqueous fans may form farther out in the reservoirs. Also, in Brownlee reservoir, deltaic deposits have been eroded and re-worked in the tributaries by post-depositional streamflow that occurs while the reservoir is lowered and the deposits are subaerially exposed.

- A rough comparison of drainage basin area vs sediment volume showed little correlation. Therefore it is assumed that existing sediment volumes in each tributary are dependent on numerous factors including infrequent debris flows, localized precipitation events that trigger debris flows, roads and culverts in the drainage basin that may capture sediments, and long-term buildup of sediments in individual tributaries.

- Sediment deposition in Brownlee Reservoir occurs at various levels and locations along the tributary arms, depending on the level of the reservoir at the time of the event. Therefore, in long tributary arms post-impoundment deposits are present over a long distance at a variety of elevations. Post-impoundment deposits in the Brownlee Reservoir tributaries are primarily below full-pool.
- Because of the relatively constant levels of Oxbow and Hells Canyon Reservoirs, post-impoundment sediment deposits are found near the mouth of the tributaries where the debris flows rapidly lose energy as they enter the slack water, and also above full-pool elevations because the reservoir acts as a new "base level" of the tributaries. Some modification of these subaqueous deposits from post-depositional floods and currents may have occurred.
- The sediment volumes estimated represent a "snapshot" in time, based on the available data, and are intended to represent "order-of-magnitude" estimates. At any time in the future, an above-average precipitation year or large thunderstorms could result in large quantities of sediment deposition in a short time, which could substantially alter the volume calculations.

Limitations to Analytical Techniques

- The thickness of the sediment deposits was estimated by using surface contours to estimate the slope angles of tributary side slopes and thus re-create the original valley profiles. Limitations using this technique include error in the contour maps, and interpreting whether the deposits filling the tributaries are pre- or post-impoundment (aerial photographs were used to confirm the age of many of the deposits, but not all). Therefore, if depositional features in the tributaries are interpreted to be post-impoundment whereas they are really be pre-impoundment, the rate and amount of deposition is overestimated.
- The most recent depositional features could be identified on the aerial photographs. However, deposits that preceded the most recent events could not be observed because they are buried by the most recent events. Also, the aerial photographs of Brownlee Reservoir were taken while the reservoir was low and therefore portions of the tributaries that are often inundated were visible. The aerial photographs of Oxbow and Hells Canyon reservoirs were taken during full pool conditions and therefore no subaqueous deposits were visible.
- The contact between pre- and post-impoundment sediments (i.e. the thickness of post-impoundment deposits) could not always be identified using geophysics because of (1) the relatively high density of the deposits, (2) the coarse-grained nature of the sediment deposits resulted in poor reflectors and (3) the lack of density differences between the pre- and post-impoundment deposits was not conducive to geophysical signatures. In other words, if the post-impoundment deposits have similar densities as the pre-impoundment deposits, they cannot be distinguished by geophysical reflection.
- The U. S. Geological Survey topographic maps available are 1:24,000 scale, with 40-foot contours. Therefore the scale and error margin of these maps was sufficiently large to

limit their accuracy when attempting to evaluate relatively small-scale, thin depositional events.

- The sediment volume calculations are intended primarily to be "order-of-magnitude" scale calculations.

Summary and Discussion

The following table shows CH2M HILL's estimated sediment volumes for the seven tributaries, Golder's volume estimates, and discussion of the sediment estimates and interpretation of geomorphic features. Note that Golder's volume estimates were not included in CH2M HILL's estimates.

The post-impoundment sediments interpreted by Golder are typically distinctive lobes of finer-grained sediments interpreted from geophysical data. CH2M HILL's estimates generally cover a larger portion of the tributaries, include coarse-grained materials not able to be identified by the available geophysical techniques, and may also include material deposited above the high-water mark. Therefore, CH2M HILL's volumetric estimates are typically larger than Golder's. Localized, post-impoundment side-hill slumps that resulted from saturation of colluvial materials were not included in the tributary sediment volume estimates.

Maps that outline the interpreted sediment deposits are included as attachments.

Tributary	Estimated Sediment Volume (m^3)	Golder Estimated Sediment Volume (m^3)	Notes and Comments
Steamboat Creek	25,000 (under full pool) 15,000 (above full pool)	10,402	Very irregular topography is evident underwater where this tributary empties into HC reservoir; and includes large rocky knobs, pre-impoundment alluvial fans, and surficial disturbance related to dam construction. CH2M HILL and Golder identified post-impoundment sediment deposits where this tributary meets the reservoir. The post-impoundment aerial photograph showed post-impoundment sediment deposits where the tributary meets the reservoir. The pre-impoundment aerial photographs showed alluvial deposits in the tributary; therefore the sediments interpreted to be post-impoundment may also include pre-impoundment sediments. This site is difficult to interpret because of the excavation, re-grading the area, and other disturbance caused by construction activities.
McGraw Creek	7,500 (under full pool) 100,000 (above full pool)	1,555	The post-impoundment aerial photograph shows large quantities of post-impoundment sediment deposition above the water line. Golder and CH2M HILL both identified subaqueous sediment deposition where the tributary meets the reservoir. The pre-impoundment aerial photographs showed pre-reservoir alluvial fans at the mouth of the tributary, but also showed that there was very little sediment deposition in this tributary prior to reservoir construction. The side slopes of this tributary are steep so the sediments appear to be relatively thick. Golder also identified subaqeous slumps (“slide debris”) on the opposite side of the reservoir.
Salt Creek	4000 (above full pool)	7,413 (includes off-tributary slide debris)	The subsurface morphology at the mouth of the tributary appears to include bedrock outcrops but little or no post-impoundment deposition at the tributary mouth. A relatively small deltaic deposit was identified where the tributary meets the reservoir. Pre-impoundment alluvial fans appear to be present beneath the reservoir surface. Golder identified two subaqueous deposits north and south of the main tributary channel. CH2M HILL interpreted these to be post-impoundment slumps that occurred on steep, saturated slopes away from the tributary and would therefore not be considered part of the sediment budget. Overall, very little subaqueous sediment deposition was identified from this tributary, only the small deltaic deposit where the tributary meets the reservoir.
Brownlee Creek	350,000 (under full pool)	28,885	Post-impoundment aerial photographs showed several post-impoundment deltaic deposits, braided stream channels, and reworked sediments in this long tributary. The pre-impoundment aerial photographs show alluvial deposits in the tributary prior to reservoir construction. However, it is evident on the recent aerial photographs that post-impoundment sediment deposition has occurred. The sediment volume estimate may include pre-impoundment sediments that are part of original Brownlee Creek alluvium. It is estimated that approximately 50 percent of the sediment deposits in the tributary are post-impoundment. The thickness of the post-impoundment sediments that overlie the pre-impoundment alluvium could not be determined. Golder identified two lobes of sediment in this tributary that are interpreted to be post-impoundment.
Dennett Creek	210,000 (under full pool)	46,154	A distinctive deltaic deposit was observed on aerial photographs near the bottom of the tributary, this material is clearly post-impoundment (also identified by Golder as post impoundment). The pre-impoundment aerial photograph showed alluvial deposits in the tributary prior to reservoir construction, therefore the overall sediment volume calculated for this tributary likely includes some pre-impoundment sediments. However, the post-impoundment photos show recent sediment deposits and migration of the creek channel as a result of the sediment deposition.
Sturgill Creek	20,000 (under full pool)	15,440	This is a very narrow, rocky tributary. During the site visit, a well-formed but eroded gravelly deltaic deposit was observed where tributary meets the high-water mark. It appears that overall relatively little post-impoundment deposition has occurred in this tributary, especially considering its drainage basin area. Pre-impoundment stream alluvium was also observed in the tributary on the pre-impoundment aerial photographs.
Rock Creek	250,000 (under full pool)	18,693	This is a long, straight tributary that appears to be filled with primarily post-impoundment sediments based on pre-impoundment topography, current bathymetry, and aerial photographs. Thin alluvial deposits are evident in this tributary on the pre-impoundment aerial photographs whereas the post-impoundment aerial photographs show evidence of recent sediment deposition in the tributary. It is interpreted that approximately 80 percent of the sediment in the tributary is post-impoundment. It appears that remnants of the original channel are evident on the bathymetric maps. Golder identified two lobes of sediments within the tributary that are interpreted to be post-impoundment deposits.

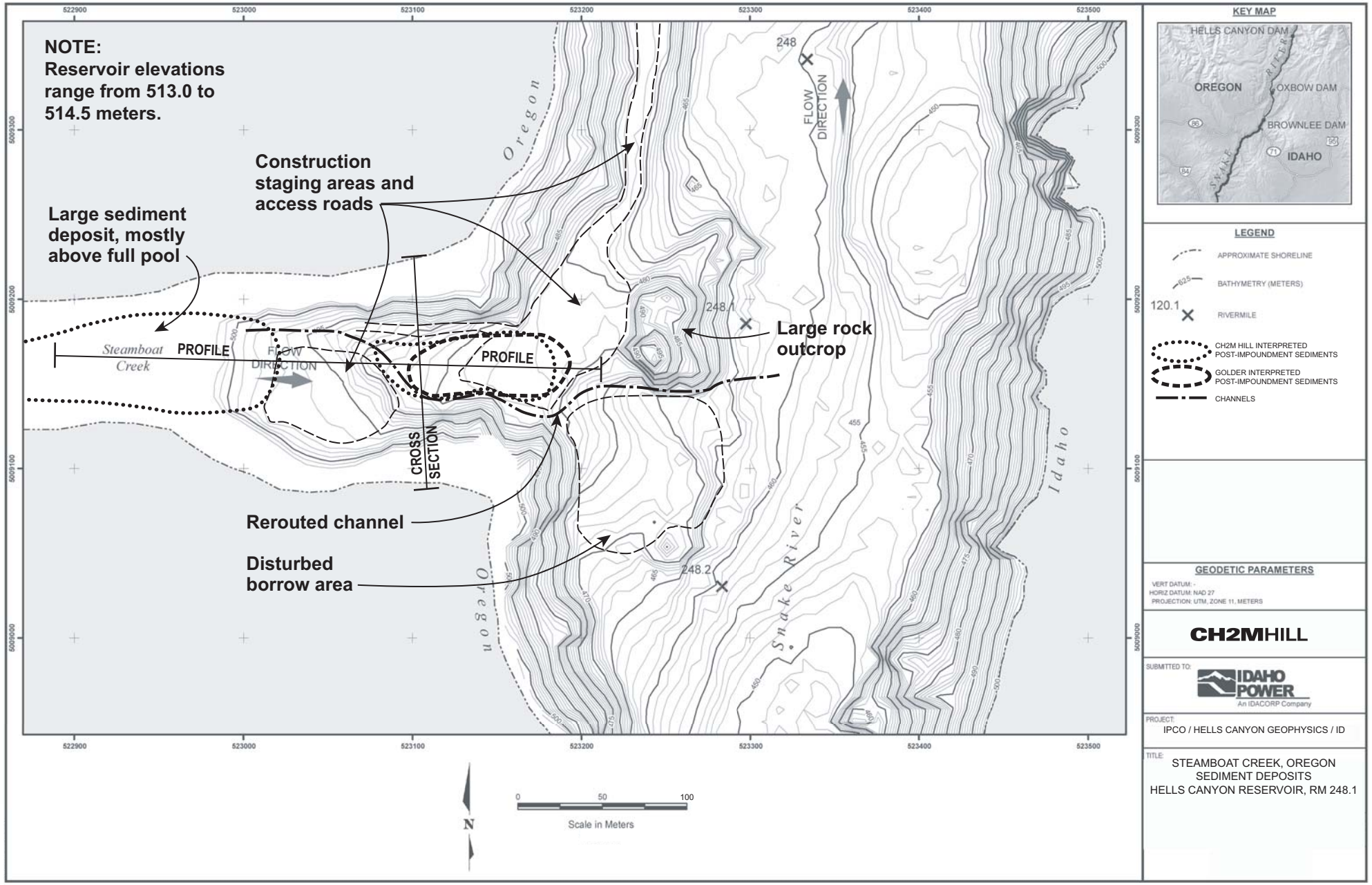

W012005009BOI

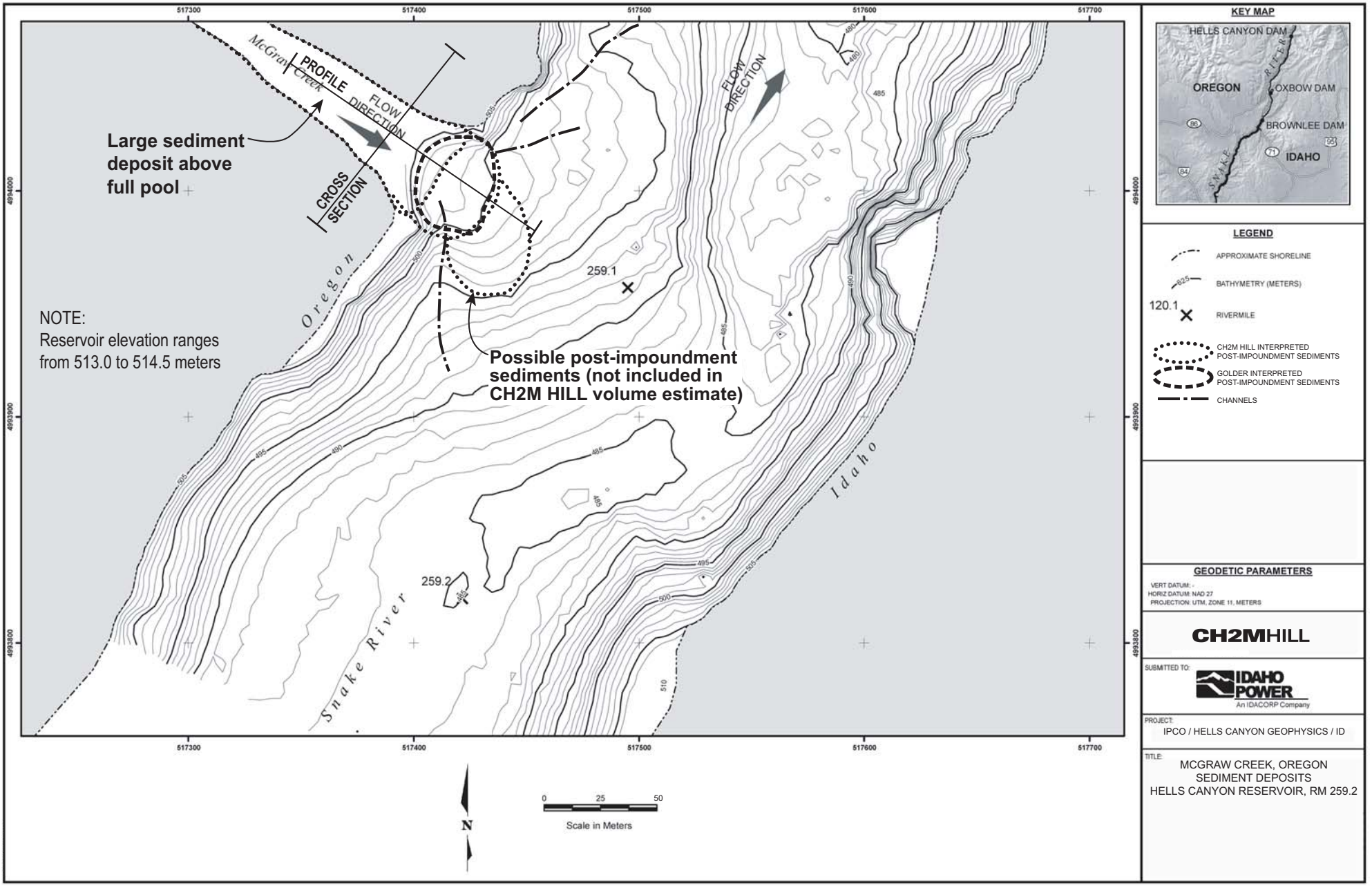

KEY MAP

LEGEND

- APPROXIMATE SHORELINE
- 482.5 BATHYMETRY (METERS)
- 120.1 RIVERMILE
- CH2M HILL INTERPRETED POST-IMPOUNDMENT SEDIMENTS
- GOLDER INTERPRETED POST-IMPOUNDMENT SEDIMENTS
- CHANNELS

GEODETIC PARAMETERS

VERT DATUM: -
HORIZ DATUM: NAD 27
PROJECTION: UTM, ZONE 11, METERS

CH2MHILL

SUBMITTED TO: IDAHO POWER An IDACORP Company

PROJECT: IPCO / HELLS CANYON GEOPHYSICS / ID

TITLE: MCGRAW CREEK, OREGON
SEDIMENT DEPOSITS
HELLS CANYON RESERVOIR, RM 259.2

W012005009BOI

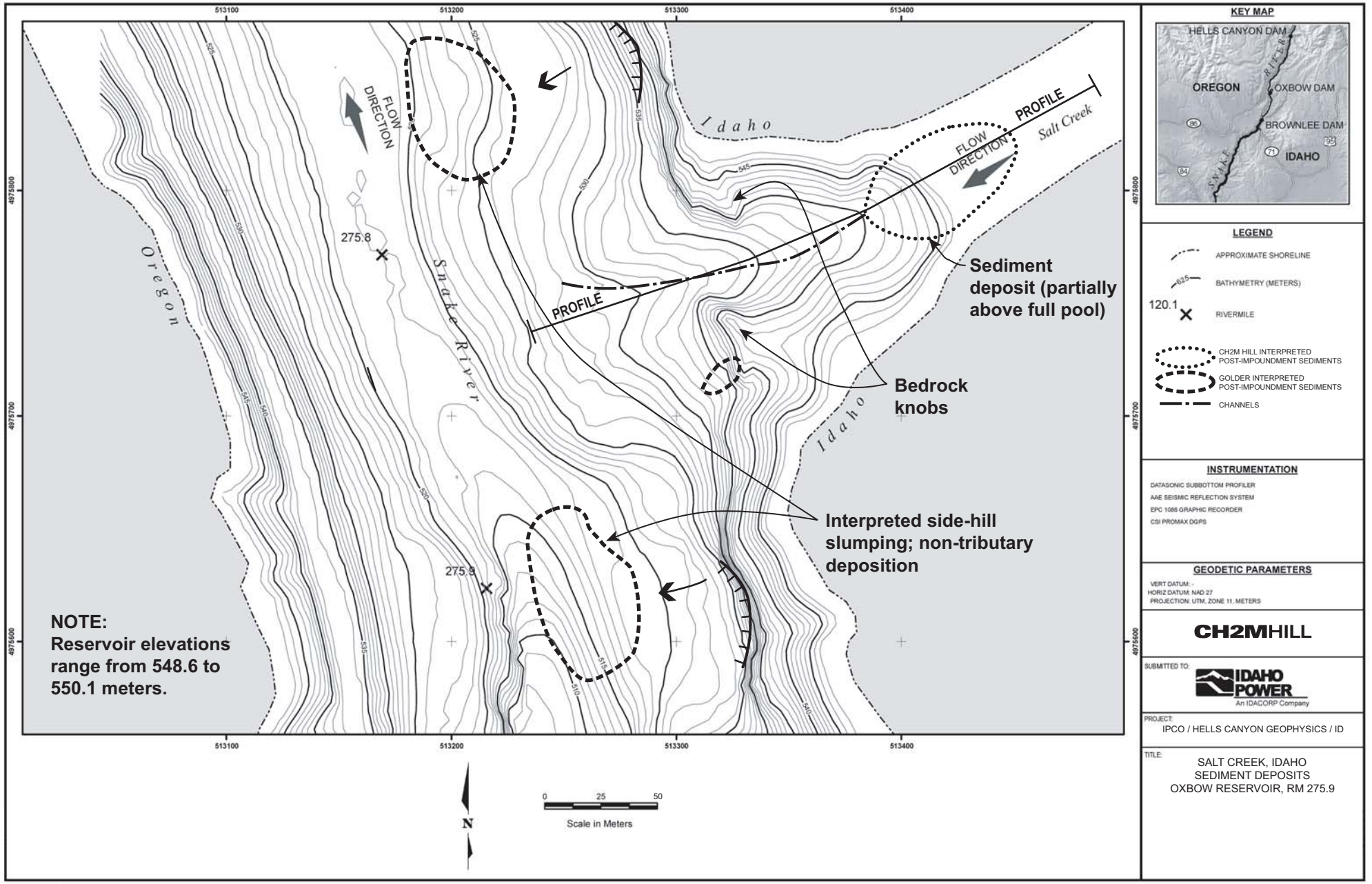

KEY MAP

LEGEND

- APPROXIMATE SHORELINE
- 625 BATHYMETRY (METERS)
- 120.1 RIVERMILE
- CH2M HILL INTERPRETED POST-IMPOUNDMENT SEDIMENTS
- GOLDER INTERPRETED POST-IMPOUNDMENT SEDIMENTS
- CHANNELS

INSTRUMENTATION

DATASONIC SUBBOTTOM PROFILER
AAE SEISMIC REFLECTION SYSTEM
EPC 1086 GRAPHIC RECORDER
CSI PROMAX DGPS

GEODETIC PARAMETERS

VERT DATUM: -
HORIZ DATUM: NAD 27
PROJECTION: UTM, ZONE 11, METERS

CH2MHILL

SUBMITTED TO: IDAHO POWER An IDACORP Company

PROJECT:
IPCO / HELLS CANYON GEOPHYSICS / ID

TITLE:
SALT CREEK, IDAHO
SEDIMENT DEPOSITS
OXBOW RESERVOIR, RM 275.9

W012005009BOI

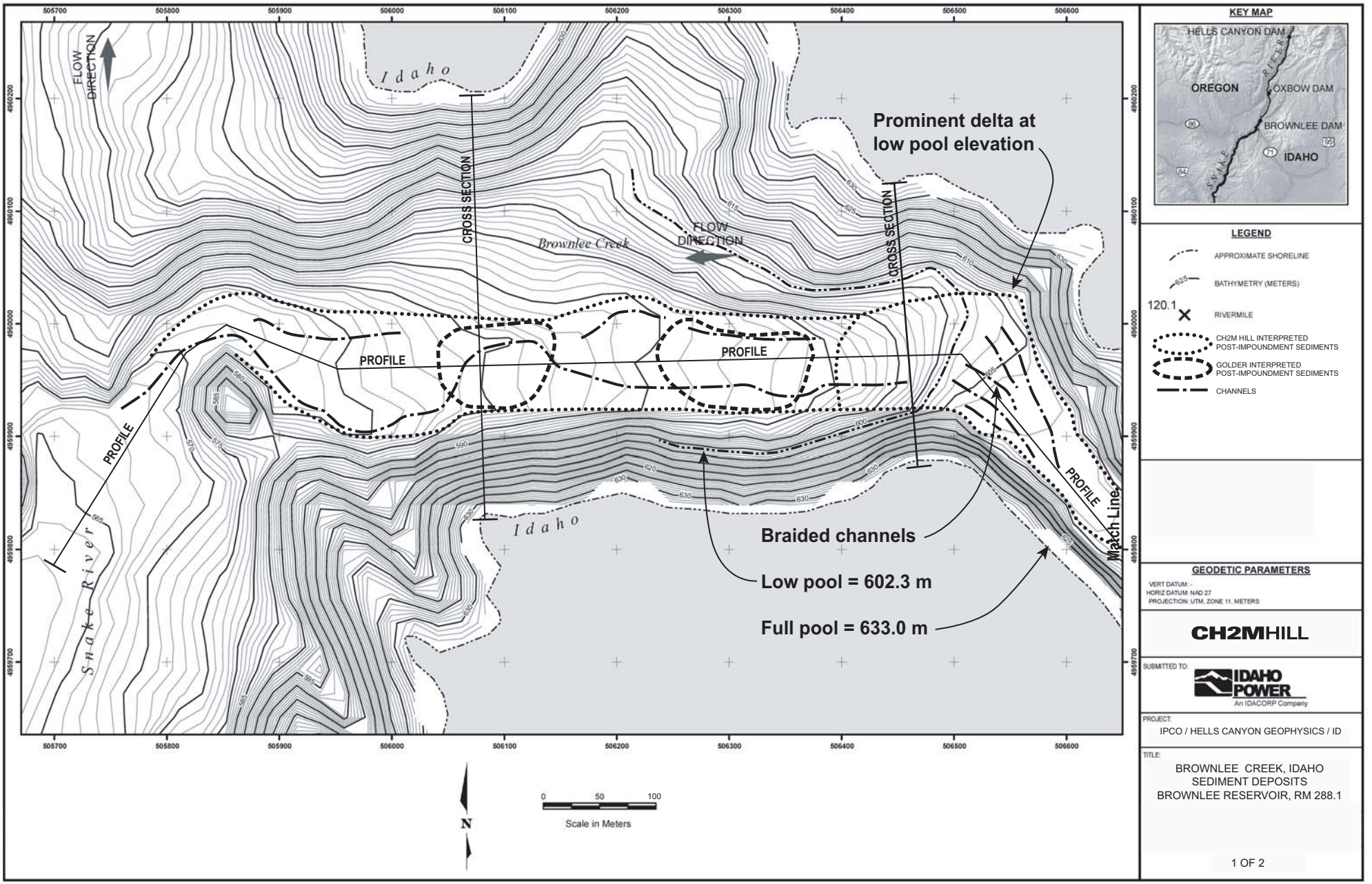

KEY MAP

LEGEND

- APPROXIMATE SHORELINE
- 625 BATHYMETRY (METERS)
- 120.1 RIVERMILE
- CH2M HILL INTERPRETED POST-IMPOUNDMENT SEDIMENTS
- GOLDER INTERPRETED POST-IMPOUNDMENT SEDIMENTS
- CHANNELS

GEODETIC PARAMETERS

VERT DATUM: -
HORIZ DATUM: NAD 27
PROJECTION: UTM, ZONE 11, METERS

CH2MHILL

SUBMITTED TO: IDAHO POWER An IDACORP Company

PROJECT:
IPCO / HELLS CANYON GEOPHYSICS / ID

TITLE:
BROWNLEE CREEK, IDAHO
SEDIMENT DEPOSITS
BROWNLEE RESERVOIR, RM 288.1

W012005009BOI

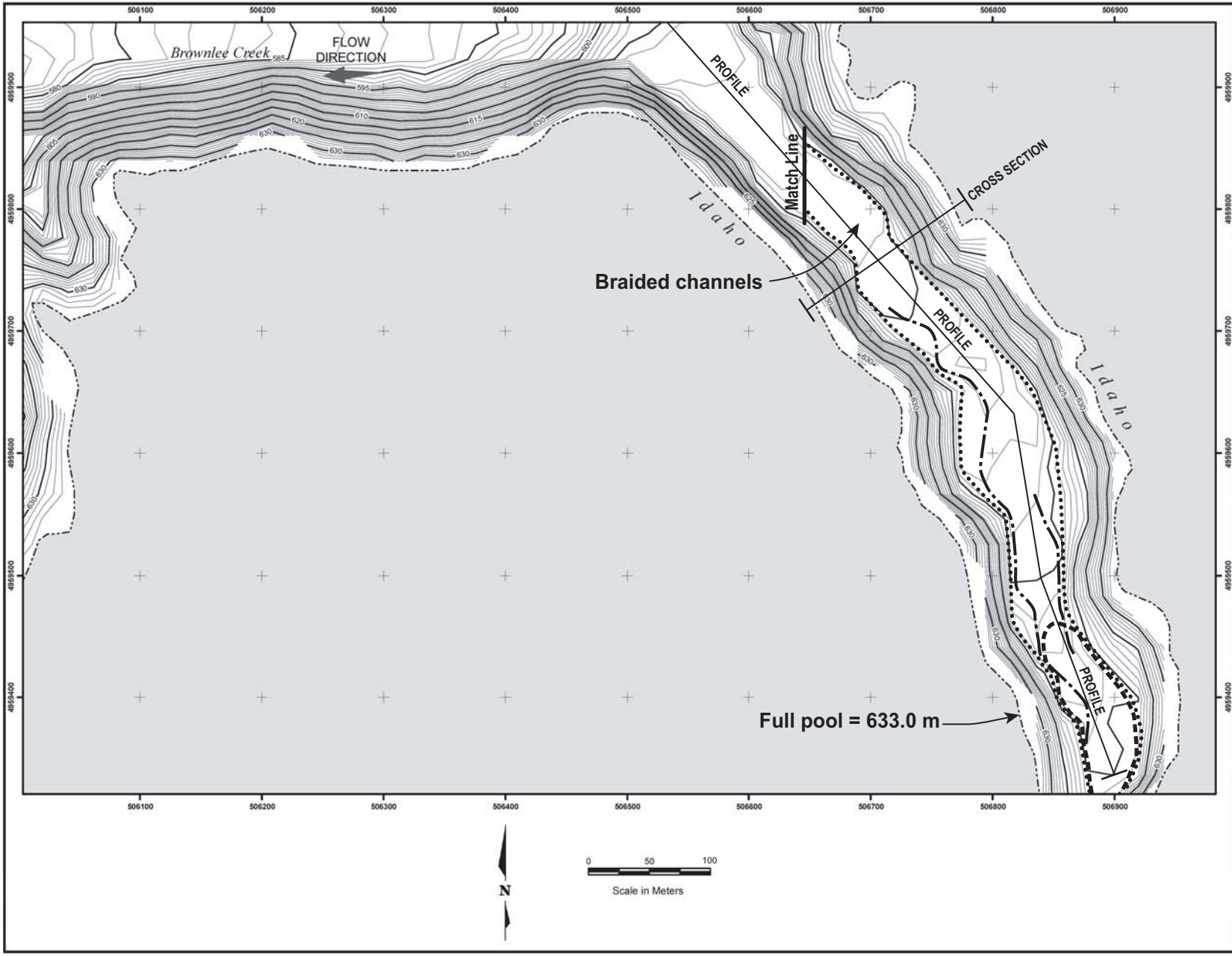

KEY MAP

LEGEND

- APPROXIMATE SHORELINE
- 625 BATHYMETRY (METERS)
- 120.1 RIVERMILE
- CH2M HILL INTERPRETED POST-IMPOUNDMENT SEDIMENTS
- GOLDER INTERPRETED POST-IMPOUNDMENT SEDIMENTS
- CHANNELS

1 OF 2

GEODETIC PARAMETERS

VERT DATUM: -
HORIZ DATUM: NAD 27
PROJECTION: UTM, ZONE 11, METERS

CH2MHILL

SUBMITTED TO: IDAHO POWER An IDACORP Company

PROJECT: IPCO / HELLS CANYON GEOPHYSICS / ID

TITLE:

BROWNLEE CREEK, IDAHO
SEDIMENT DEPOSITS
BROWNLEE RESERVOIR, RM 288.1

2 OF 2

W012005009BOI

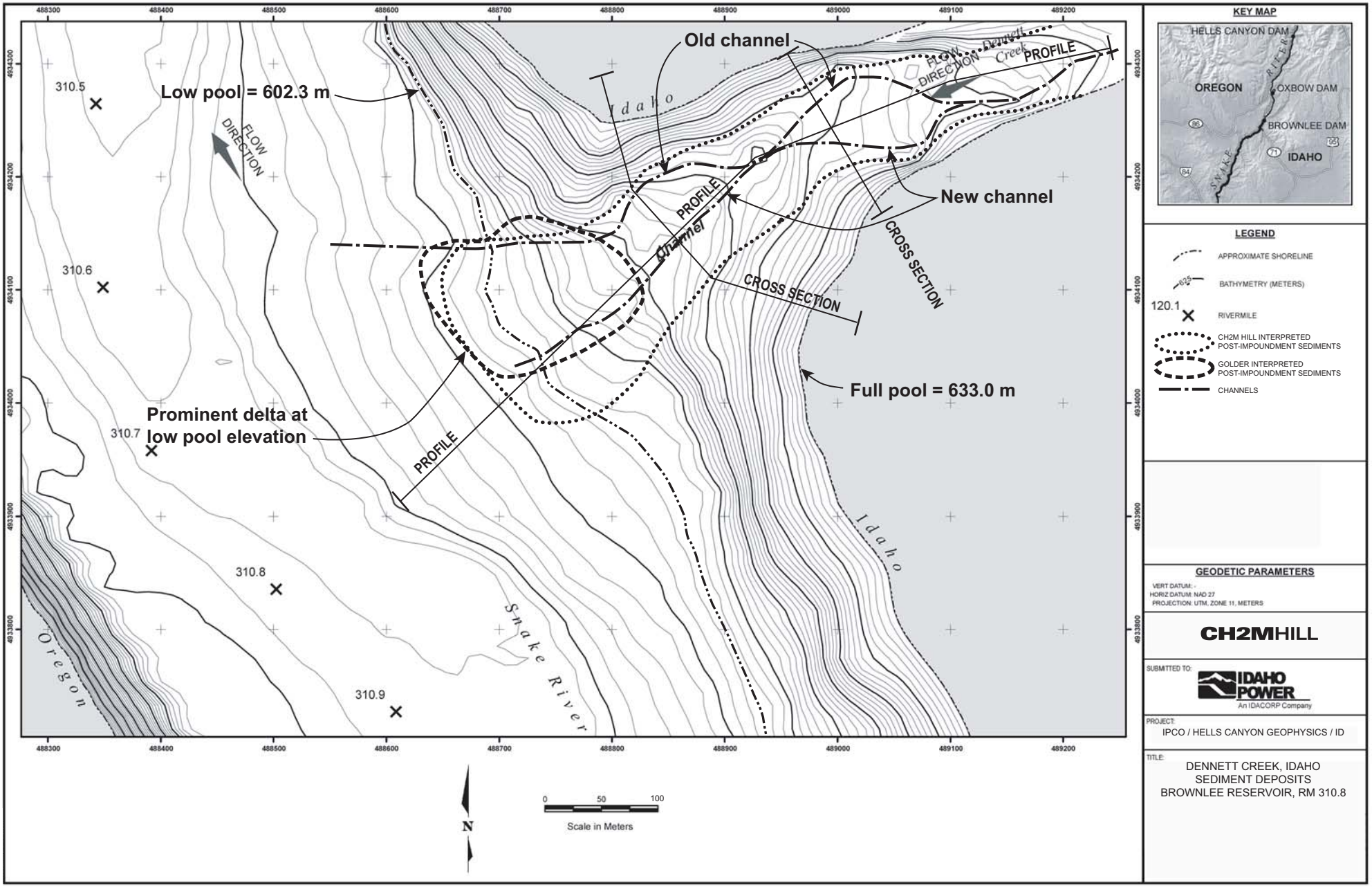

KEY MAP

LEGEND

- APPROXIMATE SHORELINE
- 625 BATHYMETRY (METERS)
- 120.1 RIVERMILE
- CH2M HILL INTERPRETED POST-IMPOUNDMENT SEDIMENTS
- GOLDER INTERPRETED POST-IMPOUNDMENT SEDIMENTS
- CHANNELS

GEODETIC PARAMETERS

VERT DATUM: -
HORIZ DATUM: NAD 27
PROJECTION: UTM, ZONE 11, METERS

CH2MHILL

SUBMITTED TO: IDAHO POWER An IDACORP Company

PROJECT: IPCO / HELLS CANYON GEOPHYSICS / ID

TITLE: DENNETT CREEK, IDAHO
SEDIMENT DEPOSITS
BROWNLEE RESERVOIR, RM 310.8

W012005009BOI

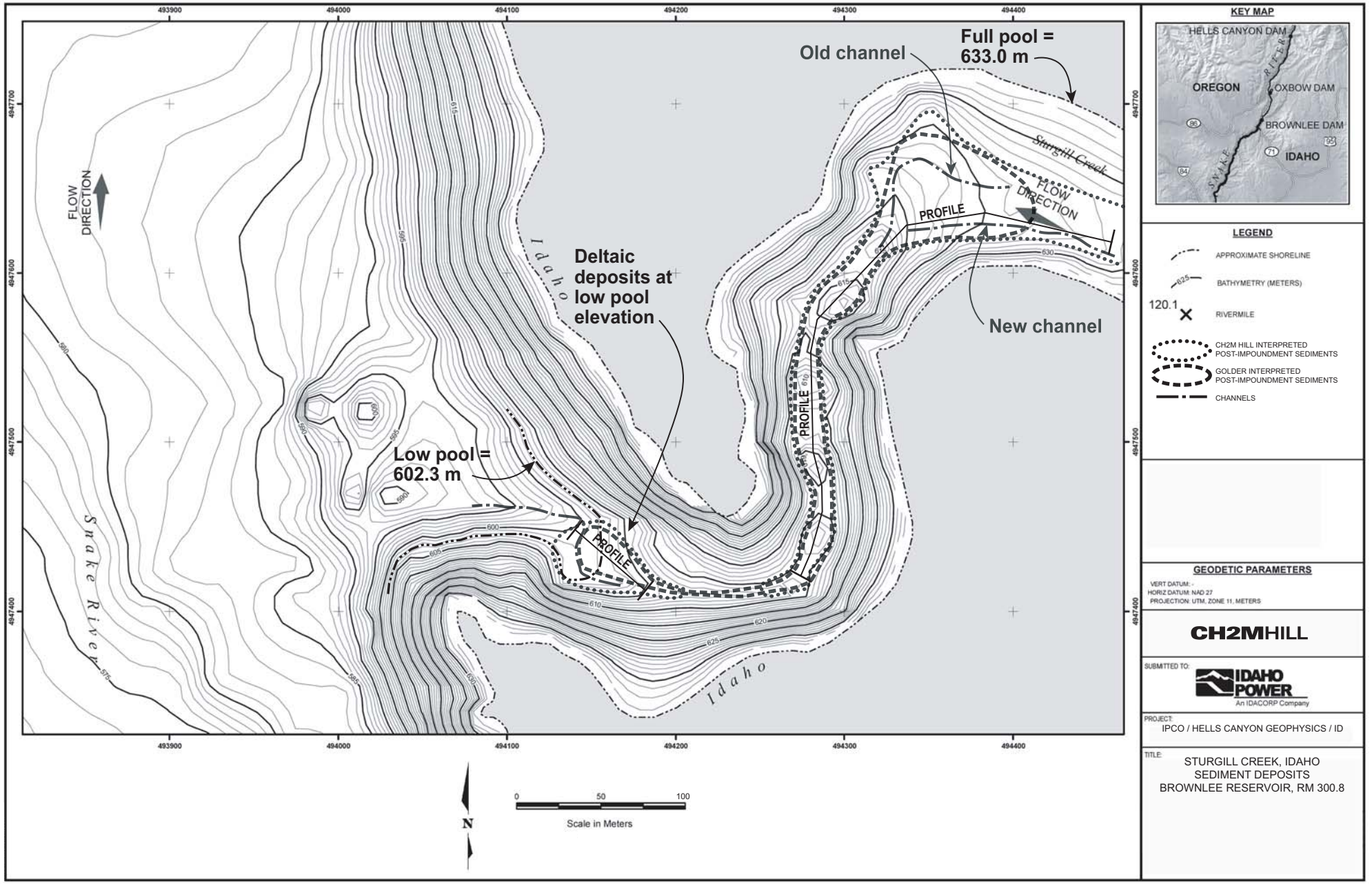

KEY MAP

LEGEND

- APPROXIMATE SHORELINE
- BATHYMETRY (METERS)
- 120.1 RIVERMILE
- CH2M HILL INTERPRETED POST-IMPOUNDMENT SEDIMENTS
- GOLDER INTERPRETED POST-IMPOUNDMENT SEDIMENTS
- CHANNELS

GEODETIC PARAMETERS

VERT DATUM: -
HORIZ DATUM: NAD 27
PROJECTION: UTM, ZONE 11, METERS

CH2MHILL

SUBMITTED TO: IDAHO POWER, An IDACORP Company

PROJECT: IPCO / HELLS CANYON GEOPHYSICS / ID

TITLE: STURGILL CREEK, IDAHO
SEDIMENT DEPOSITS
BROWNLEE RESERVOIR, RM 300.8

W012005009BOI

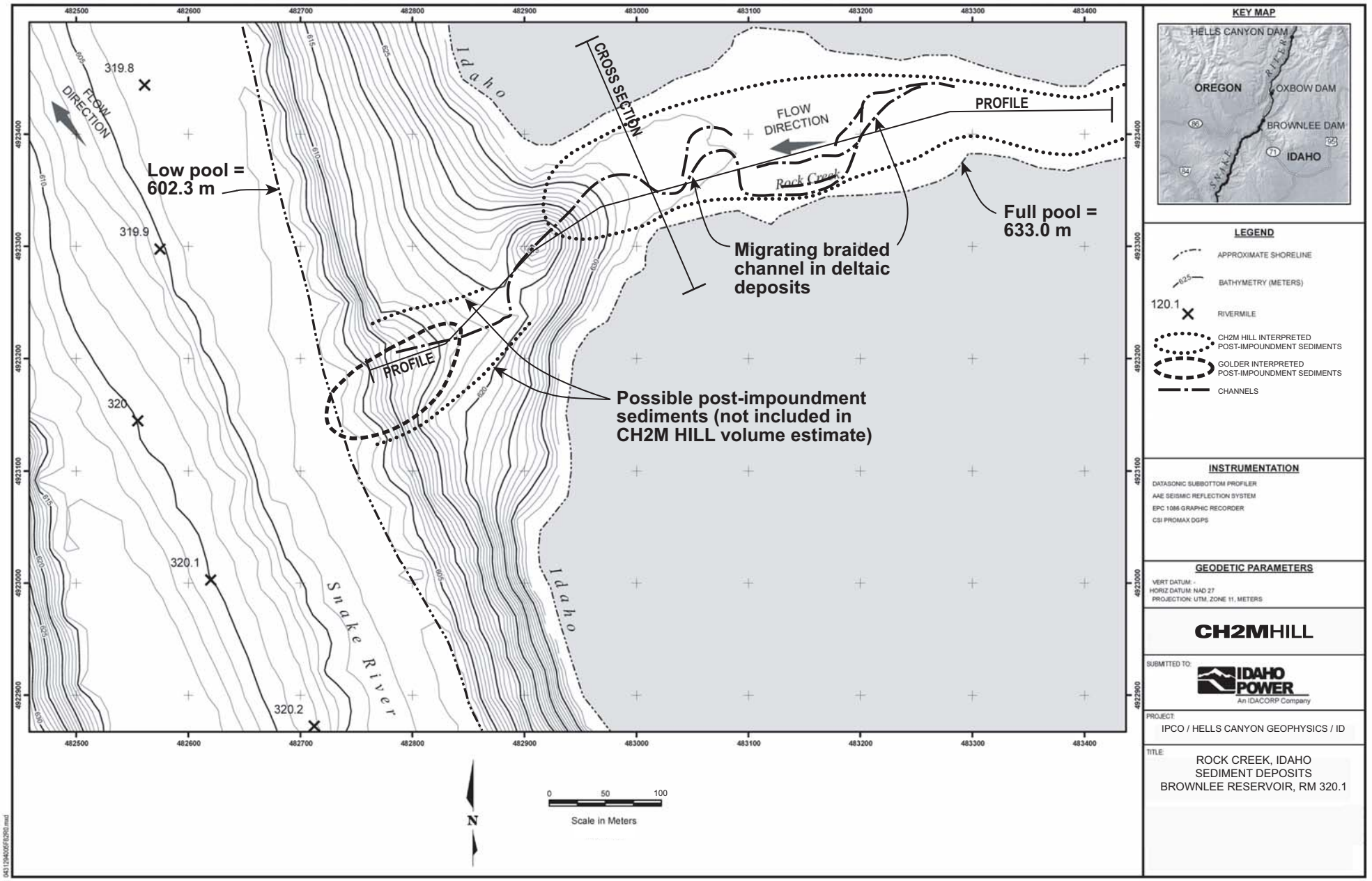

KEY MAP

LEGEND

- APPROXIMATE SHORELINE
- 625 BATHYMETRY (METERS)
- 120.1 RIVERMILE
- CH2M HILL INTERPRETED POST-IMPOUNDMENT SEDIMENTS
- GOLDER INTERPRETED POST-IMPOUNDMENT SEDIMENTS
- CHANNELS

INSTRUMENTATION

DATASONIC SUBBOTTOM PROFILER
AAE SEISMIC REFLECTION SYSTEM
EPC 1086 GRAPHIC RECORDER
CSI PROMAX DGPS

GEODETIC PARAMETERS

VERT DATUM: -
HORIZ DATUM: NAD 27
PROJECTION: UTM, ZONE 11, METERS

CH2MHILL

SUBMITTED TO: IDAHO POWER An IDACORP Company

PROJECT: IPCO / HELLS CANYON GEOPHYSICS / ID

TITLE: ROCK CREEK, IDAHO
SEDIMENT DEPOSITS
BROWNLEE RESERVOIR, RM 320.1

This page left blank intentionally.

Appendix C. CH2M Hill evaluation of sandbar slope stability

This page left blank intentionally.

Hells Canyon—Stability Analysis of Sandbars

PREPARED FOR: Idaho Power Company

PREPARED BY: King Sampaco/SEA
Dean Harris/BOI

COPIES: Steve Miller/BOI
Don Anderson/SEA

DATE: January 24, 2005

1. Introduction

This technical memorandum discusses the results of stability analyses that were conducted for the sandbars in Hells Canyon along the Snake River in Idaho. CH2M HILL was authorized by Idaho Power Company (IPC) to perform geotechnical analysis and evaluation of the stability of the sandbars at three selected sites located downstream of the Hells Canyon Dam, namely: Pine Bar, Fish Trap, and Tin Shed sites.

1.1 Scope

The scope of this stability evaluation was limited to the following tasks:

- Summarizing our understanding of the current state of the practice on stability analysis of sandbar slopes due to rapid drawdown conditions
- Presenting the methodology used to analyze the stability of sandbar slopes in Hells Canyon
- Conducting a series of stability analyses
- Summarizing the results and implications of the stability analyses

The stability analyses were limited to evaluation of stability of sandbar slopes at the three selected locations mentioned above. These analyses were conducted using two loading scenarios for rapid drawdown conditions in the sandbar slopes: (a) load following operation; and (b) flood recession condition. The load following operation scenario represents loading in the slope due to fluctuations in the river water elevation resulting from the operation of the dam. The flood recession scenario represents loading in the slope due to fluctuations in the river water elevation caused by a major flood event in the river.

In both scenarios, slope failure is assumed to be characterized by mass failure or mass wasting at the sandbar areas due to the action of seepage forces in the slope after conditions of rapid drawdown in the river water elevations. Occurrence of slope failures due to rapid drawdown is generally attributed to the development of excess pore water pressures and the removal of the stabilizing external water pressures on the slope. Other processes that could result to erosion of the sandbars such as drag and lift forces from river water that tend to detach and entrain surface particles of the sand, weakening and weathering of the

sandbar particles due to moisture changes, current and wave action, and fluvial transport and erosion of sediments that could lead to scouring at the toe of the slope were not included in these stability evaluations.

1.2 Limitations

This technical memorandum has been prepared for the exclusive use of IPC for specific application to the Hells Canyon Project in accordance with generally accepted geotechnical engineering practice. No other warranty, express or implied, is made.

The analyses, interpretations, and conclusions presented in this technical memorandum were based on subsurface conditions interpreted from the very limited field investigation and laboratory tests conducted for the project and on two loading scenarios of rapid drawdown conditions (that is, load following and flood recession) in the sand bar slopes.

2. Project Description

The study area is the Snake River below the Hells Canyon Complex (HCC). The HCC is composed of Brownlee, Oxbow, and Hells Canyon reservoirs. The reservoirs were primarily constructed for power production, although Brownlee Reservoir has operational requirements related to flood control. Work on the three-dam complex began in 1958 with the construction of Brownlee Dam. Construction of the Oxbow Project occurred in 1961, and Hells Canyon Dam was constructed in 1969. The combined volume of water in the three reservoirs within the HCC is approximately 1.65 million acre-feet. Total usable storage within the three reservoirs is 1,009,478 acre-feet.

The Hells Canyon Project, the third development in the HCC, is also the one farthest downstream on the Snake River. It consists of a concrete gravity dam and integral spillway, intake, and powerhouse at river mile 247.6. Hells Canyon Dam is a 910-foot-long cast-in-place concrete gravity dam with a maximum structural height of 330 feet. The dam impounds a 25-mile reservoir that extends up to the toe of Oxbow Dam. The maximum reservoir depth, from the deepest point in Hells Canyon Reservoir just upstream of the dam to the normal maximum reservoir elevation of 1,688 feet msl (mean sea level), is approximately 240 feet.

3. Mechanics of Sandbar Slope Failures

The mechanics of slope failures in sandbars due to fluctuations in river water elevation are described by Budhu and Gobin (1994) as presented below. This description is based on actual observations of seepage erosion in sandbars located downstream of dams.

> "*When the river rises, water infiltrates into and is stored in the river bank. As the river falls the volume of stored water must drain from the bank. If the rate of fall of the river is greater than the rate at which stored water can exit the bank, then the phreatic surface will be at a higher elevation than the river stage. A seepage face then develops between the river level and the exit point of the bank-stored water. If the seepage velocity of the exiting ground water is sufficiently high, the soil mass can become like viscous fluid and be carried away in suspension by the outflow of water (see Figure 1). The removal of sediments from the sandbars tends to steepen the slopes with concomitant bank or slope failures. Rivulets and gullies (rilling process) are formed below the exit point along the sandbars as the bank-stored water with its sediments rushes downslope toward the river. These rivulets and gullies are*

scoured deeper as the water picks up sediments along its path to the river. Within the river bank deposits and above the exit points, the internal erosion of sediments can form tunnels. The walls of these tunnels eventually collapse as the tunnel becomes deeper and/or adjoining tunnels encroach on one another.

When the river stage is lowered, an elevated pore water pressure distribution remains within the river bank. The residual pore water pressures and removal of stabilizing external water pressure on the face of the bank can lead to slope failures under undrained conditions similar to slope failures in reservoir embankments under rapid drawdown. The mass of material involved in bank slumps under undrained conditions is often very large, in the order of several hundred kilograms. A substantial area of the sandbar can be lost in a few seconds. On occasions, incipient slope failures under undrained conditions may occur during rapid recession of the river stage. That is, the failure plane is initiated but slumping is not discernible. The soil mass is now much weaker than it was prior to the formation of the failure plane. On the next rising river stage, the coupled effect of hydrostatic forces from water that enters the failure plane and tractive scour forces can result in failure of the weakened soil mass, which disintegrates and is taken away by the flow. It is quite easy to confuse this seepage-induced failure to a tractive force-induced failure. The condition that is critical in provoking such failures is a rapid lowering of the river stage caused by a high dam-down-ramping rate, followed by a constant low discharge over a day or more. The latter allows for a prolonged period of seepage out of the sandbar and results in the formation of a more pronounced failure plane."

4. Current Methods on Stability Analysis of Sandbars

Stability of steep river banks has been the subject of considerable study by geotechnical engineers, geomorphologists, and geophysicists. Engineering research has concentrated on development of engineering designs for artificial slopes and embankments, but very little of this work has dealt with very steep slopes, undisturbed soils, complex stratigraphies, and unspecified drainage conditions found in eroding, natural river banks.

4.1 Methods Used in River Mechanics

Stability analyses applicable to very steep (almost vertical) river cliffs associated with eroding, unstable streambanks have been undertaken by researchers in hydraulic engineering and fluvial geomorphology (Osman and Thorne, 1988; Darby and Thorne, 1996). Most of the methods used in river mechanics to analyze the stability of river banks are generally limited to very steep, near-vertical cohesive soil slopes. These available methods are not appropriate for use in generally flat sandbar (non-cohesive) slopes because there is a clear contrast in failure mechanics for these slopes. In non-cohesive bank slopes (such as sandbars), shear strength increases more rapidly with depth than does shear stress, so that critical conditions are more likely to occur at shallow depths. In cohesive bank slopes, shear stress increases more quickly than shear strength with increasing depth so that critical surfaces tend to be located deep within the bank (Terzaghi and Peck, 1967). Noncohesive materials usually fail by dislodgment and avalanching of individual particles or by shear failure along shallow, very slightly curved slip surfaces. Deep-seated failures occur in cohesive materials with a block of disturbed, but more or less intact, bank material sliding into the channel along a curved failure surface.

In 1993, an ASCE Task Committee was established to study the hydraulics, bank mechanics, and modeling of river width adjustment in alluvial channels. Part of the work of this Task Committee was to review the available methods to analyze stream bank stability. Results of this review indicate that, while rapid progress is being made, most existing analyses of bank mechanics are still at the stage of being research tools that are not yet suitable for design applications.

4.2 Modified Infinite Slope Approach

For relatively flat sandbars, Budhu and Gobin (1994) developed a method to determine the limiting slope (subsequently termed the equilibrium seepage slope, ESS) below which slope failures of sandbars due to seepage of bank-stored water would be unlikely. The method is based on the fundamental equation for evaluating the factor of safety (FS) of a saturated, infinite slope with seepage parallel to the face.

The maximum slope of a saturated or dry sandbar without seepage is the angle of internal friction (ϕ) of the sand. Under seepage loading, the FS of a slope is reduced to half of its initial (nonseepage) value. If seepage were to occur to an initially stable saturated or dry infinite slope of homogeneous sand, then the slope angle (α_s) for stability, under seepage parallel to the slope, is reduced from ϕ to:

$$\alpha_s = \tan^{-1} [(\gamma'/\gamma_{sat}) \tan \phi] \quad \ldots\ldots\ldots\ldots (1)$$

in which γ' is the submerged unit weight and γ_{sat} is the saturated unit weight of the sand.

As found in many geotechnical textbooks (e.g., Dunn et al., 1980; Lambe and Whitman, 1969), Equation (1) was derived assuming that the infinite slope was initially inundated with groundwater to the top of the slope, and seepage took place parallel to the slope in a homogeneous sand mass. This assumption is not directly applicable to sandbar deposits because:

- Sandbars are typically aggradated during floods or high river flows (such as during dam discharges) that are of short duration such that the groundwater level in many of the sandbars rarely equilibrates with the high water level; and
- The assumption of seepage parallel to the slope is only reasonable for the lower portion of the seepage face.

Realizing these limitations, Budhu and Gobin (1994) proposed the following graphical approach to establish the ESS, below which slope instability (defined as bank slumps, mass wasting, or slope failures) due to seepage would be "unlikely." The approach is graphically shown in Figure 2 and is explained below:

- The ensuing discharge from the dam will cause water to infiltrate into the sandbar, and at peak discharge the phreatic surface in the sandbar could be represented by the curve ABC. If the peak discharge is held for some period of time, the phreatic surface will move upward, with point A remaining fixed. In such a case, the amount of bank-stored groundwater will increase. In a typical dam operation, the peak discharge is generally held for about 2 to 4 hours.

- For a stable slope under seepage, Equation (1) is approximately valid for the lower portion of the seepage face. Thus, a line of slope α_s drawn from the lowest water elevation after the drawdown intersecting the phreatic surface at B represents the ESS of the lower portion of the active sandbar face (line DB).
- The ESS for the portion of the sandbar above the phreatic surface will be its angle of friction (ϕ) as shown by line BE.
- The slope DBE represents the maximum stable slope of a sandbar under seepage for a cohesionless soil. This surface defines the upper limit for slope stability under seepage and can be further degraded by rilling, tractive scour, wave impacts, and other erosion processes.
- The soil enclosed within DBEHAD constitutes transient sediments that would be in a state of flux. These sediments would accumulate and then disperse in a cyclic pattern following natural environmental conditions (such as floods) and/or operations of the dam.

Field observations suggest that built-up sandbars remain stable during slowly receding floods or high dam discharges but collapse when regular patterns of dam discharges recommence to cause rapid fluctuations. The amount of potentially erodible sediments would increase as the range of fluctuation increases, the minimum stage is lowered, and the period at which peak discharge is held constant increases.

The Budhu-Gobin approach (also referred to in this technical memorandum as the modified infinite slope method) was developed to provide a first approximation to determine the extent of slope instability due to seepage erosion and to aid environmental scientists in determining the range in which biomass would be in a state of flux. The analysis was successfully used to assess the instability of sandbars downstream of Glen Canyon Dam along the Colorado River in Arizona. The validity of the method was supported by ground survey data from the study area. Field instrumentation and monitoring was provided by the United States Geological Survey (USGS).

Since the Budhu-Gobin approach is graphical, the method does not directly provide an estimate of the FS of the slope but instead defines the extent of the slope materials that would be affected (i.e., materials that are in the transient mode) by the fluctuations of the water level. The FS of the slope associated with the ESS established using the Budhu-Gobin approach can be estimated in two ways:

- Given that the procedure is an extended form of the traditional infinite slope analysis method, the FS of the slope could be approximated using the traditional infinite slope equation (see Equation 2 in the later section of this technical memorandum). The estimated FS based on this equation would be conservative in that it assumes that the slope is fully saturated and infinitely long, and thus neglects the other components of the potential failure surface that are above the saturated zone.
- A generalized slope stability computer program could be used to estimate the FS of the potential failure mass for a predetermined failure surface established from the Budhu-Gobin approach. The use of computer programs to analyze stability of slopes is discussed in the following section. This procedure is expected to yield higher and more

realistic estimate of FS but requires considerably more time to perform than using the traditional infinite slope equation.

4.3 Limit Equilibrium Solution

Computer programs are available to analyze the stability of slopes including sandbars. These computer programs typically use a 2-D limit equilibrium method for the general solution of stability problems. Methods of slices or sliding block procedures are employed to calculate the FS against instability of the slope. The program searches for the failure surface having the lowest FS. This is identified by the program as the critical surface, for which a FS is reported. Although the search is automatic, the program can be operated to search for the critical failure surface in different areas of the slope.

The most commonly used computer programs in the geotechnical community include PCSTABL (FHWA, 1987), XSTABL (Sharma, 1992), and UTEXAS (Shinoak Software, 2001). These programs have similar capabilities of performing slope stability computations using various methods of analysis. UTEXAS has the advantage that it can perform more sophisticated two-stage and three-stage stability computations to simulate rapid drawdown loading cases in embankments using the procedures recommended by Duncan et al. (1990). However, UTEXAS requires special strength parameters from triaxial test results. In the absence of triaxial test data, published data in the literature may be used, but these data may not necessarily reflect the real conditions of the soil that comprise the actual slope being analyzed.

Because of their simplicity, it is not uncommon to use PCSTABL or XSTABL to analyze rapid drawdown in embankments although there are doubts as to the accuracy of these programs in rapid drawdown calculations. This is primarily because these programs can only perform single-stage stability computations in which pore pressures and seepage forces may not be properly and accurately represented.

5. General Characteristics of the Sandbars in Hells Canyon

The geotechnical and fluvial characteristics of the sandbars in Hells Canyon were estimated from limited field and laboratory test data. Figures 3 through 5 show the location of the test holes at the three sites. These test holes were advanced using a combination of 2-inch-diameter core and a 3-inch-diameter auger. CH2M HILL conducted the field investigation primarily to obtain information of the mineralogy and grain-size characteristics of the materials from the sandbars.

The maximum depth of the test holes was dictated either by the refusal of the sampler to advance any further or by the caving of the test holes, which typically occurred when groundwater or heaving sand was encountered. Some of the test holes were drilled on the terrace area, specifically for a separate task not related to the stability evaluation of the sandbars. Although not directly related to this study, data from the test holes drilled at the terrace site were used herein to establish an understanding of the variability of subsurface conditions at the project site.

Descriptions of the field investigation for the three sites are summarized below:

- At the Fish Trap site, the field data consisted of four test holes (labeled F1 through F4) advanced to a depth of about 3.0 feet to 5.5 feet to obtain soil samples for field classification and laboratory testing for soil properties. One of the test holes (F2) was cored on the terrace area to a depth of 5.5 feet while the other three were advanced on the sandbar to depths of 3.0 feet to 4.2 feet. Figure 6 shows the visual descriptions of the soil samples recovered from the Fish Trap site.
- At the Pine Bar site, three test holes (P1 through P3) were advanced to a depth of about 3.0 to 8.0 feet. Test hole P1 was cored on the terrace area. Figure 7 shows the visual description of the soil samples recovered from the Pine Bar site.
- At the Tin Shed site, the field data consisted of three test holes (labeled TS1, TS4, and TS5) advanced to a depth of about 1.75 feet to 11.0 feet. TS1 and TS4 were cored on the terrace area while TS5 was advanced on the sandbar. Figure 8 shows the visual descriptions of the soil samples recovered from the Fish Trap site.

Laboratory grain-size tests were conducted on selected samples recovered from the test holes. The grain-size distribution plots for these samples are shown in Figures 9 through 18. These plots can be summarized as follows:

- At the Fish Trap site, the soils at the sandbar area (test holes F1, F3, and F4) were generally poorly graded fine to coarse sand with less than 2% fines (defined as the percent passing the No. 200 sieve). All 10 samples tested were very similar in grain-size distribution. Soils at the terrace area appear to contain more fines, on the order of 1 to 8%. Figures 9 through 12 show the grain-size distribution plots for soils recovered from the Fish Trap site.
- At the Pine Bar site, soils recovered at the bar areas (P2 and P3) were generally poorly graded with less than 1% fines. One of the samples (P3) was very similar in grain-size distribution to bar deposits from the Fish Trap site while the other (P2) was somewhat coarser. Soils at the terrace area appear to be more well-graded and contain more fines, on the order of 2 to 18%. Figures 13 through 15 show the grain-size distribution plots for soils recovered from the Pine Bar site. The terrace deposits at this location are more variable and generally finer in grain-size than for the terrace samples from the Fish Trap site.
- At the Tin Shed site, the soils recovered at TS5 (cored on the sandbar) were poorly graded with less than 2% fines. These materials are different in grain-size characteristics than those determined for the previous sites. As in the other two sites, the soils recovered from the terrace (TS1 and TS4) were more well-graded and contained about 2 to 19% fines. Figures 16 through 18 show the grain-size distribution plots for soils recovered from the Tin Shed site.

Laboratory test data on samples recovered from the test holes appear to indicate that the soils recovered from the terrace contain more fines than those recovered from the sandbars. In general, soils that contain less fines are expected to have higher shear strength than those with more fines.

Laboratory tests were also conducted on the recovered samples from the three sites. These tests consisted of in situ dry unit weights, in situ moisture contents, and direct shear tests. A close examination of the tested samples indicate that there are basically two types of soils that were tested: one is a fine sand with 8% fines and the other is a silty sand/sandy silt with 16 to 57% fines.

The fine sand sample has an in situ dry unit weight of about 92 pcf, moisture content of 17%, and apparent soil cohesion of 90 psf and angle of internal friction of 34 degrees from direct shear tests. The resulting moist unit weight is 107 pcf.

The silty sand samples have an average in situ dry density of 87 pcf, and an average moisture content of about 9%. The range of in situ moist unit weight is 93 pcf to 97 pcf (average of 95 pcf). The angle of internal friction from direct shear tests ranges between 26 and 36 degrees while the apparent soil cohesion ranges between 50 and 130 psf.

6. River Water Level and Discharge Data

As mentioned earlier in this technical memorandum, the stability evaluations for the sandbar slopes were conducted using two loading scenarios: *load following operation* and *flood recession condition*. Streamflow hydrographs showing variations of river surface water elevation and river discharge with time for the three study sites were provided by IPC. For the load following operation scenario, the hydrograph record for 1995 was used as it appears to represent the maximum discharge and drawdown conditions in the river due to the operation of the dam. For the flood recession scenario, the hydrograph record for 1997 appeared to represent the maximum discharge and drawdown conditions in the river due to a flood event.

6.1 Load Following Operation

Figures 19 and 20 show the hydrographs of river water level at the Fish Trap site and discharge data downstream of the dam for the year 1995. The general shape of these hydrographs is very similar to the other two sites except that the water elevations are different as these would vary according to the topographic location of the site. From the information provided by IPC regarding the load following operation of Hells Canyon Dam, it appears that during summer months flow fluctuations downstream of the dam are limited to 10,000 cfs (283 m^3/s). In other times of the year, these fluctuations are typically increased to about 16,000 cfs (453 m^3/s).

A more detailed analysis of the individual hydrographs for each site indicate the following specific characteristics:

- At the Fish Trap site, the river water elevation due to dam operations throughout the year could undergo fluctuations between Elev. 346.5 m and Elev. 348.8 m. The maximum recorded drawdown head occurred sometime in March 6, 1995, when the water level was lowered from Elev. 348.55 m to Elev. 346.93 m, resulting in a maximum drawdown head of 1.6 m (5.3 feet) over a period of about 11 to 12 hours (see Figures 21 and 22).
- At the Pine Bar site, the maximum recorded drawdown head also occurred sometime on March 6, 1995, when the water level was lowered from Elev. 376.85 m to Elev. 375.5 m,

resulting in a maximum drawdown head of 1.32 m (4.3 feet) over a period of about 11 to 12 hours (see Figures 23 and 24).

- At the Tin Shed site, the maximum recorded drawdown head also occurred sometime in March 6, 1995, when the water level was lowered from Elev. 347.0 m to Elev. 345.9 m, resulting in a maximum drawdown head of 1.13 m (3.7 feet) over a period of about 11 to 12 hours (see Figures 25 and 26).

For the three sites, the discharge associated with the above drawdown heads was 26,000 cfs (736 m^3/s) at high water level to 10,000 cfs (283 m^3/s) at low water level.

Other lower load swings were also examined, and these were found to cause fluctuations in river water level between the range of elevations indicated, but at a lesser drawdown head. During summer months, the flow fluctuations in the dam are typically limited to 10,000 cfs (283 m^3/s), but this load swing could occur more frequently than the 16,000 cfs (453 m^3/s) load swing. Analyses of all the three sites for the 10,000 cfs load swing, specifically due to reduction in flow from 20,000 cfs (566 m^3/s) to 10,000 cfs (283 m^3/s) are, thus, included in this technical memorandum. This flow reduction would result to lowering of the water level elevations in the three sites as follows:

- Fish Trap Site: Elev. 348 m to Elev. 346.86 m for a maximum drawdown head of 1.14 m (3.7 feet)
- Pine Bar Site: Elev. 376.39 m to Elev. 375.48 m for a maximum drawdown head of 0.91 m (3.0 feet)
- Tin Shed Site: Elev. 346.57 m to Elev. 345.83 m for a maximum drawdown head of 0.74 m (2.4 feet)

6.2 Flood Recession Condition

Figures 27 and 28 show the water elevation and discharge variations with time for a flood event that occurred in 1997. These hydrograph records indicate that the maximum flood event occurred between December 28, 1996, through January 9, 1997. During this period, the maximum drawdown in the river water elevation at the Fish Trap site occurred between Elev. 353.4 m. and Elev. 349.0 m, indicating a maximum drawdown of 4.4 m (14.0 feet) over a period of about 4.5 days (see Figures 27 and 28). At the Pine Bar site, a maximum drawdown of 3.5 m (11.5 feet) occurred over 4.5 days as a result of recession in the flood water elevation in the river from Elev. 380.7 m to Elev. 377.2 m (Figures 29 and 30). At both sites, the discharge associated with this flood recession was estimated to be about 70,000 cfs over 4.5 days.

The flood recession condition at the Tin Shed site is currently being evaluated in a parallel effort by others and was therefore not included in the scope of work for this task.

7. Methodology

The stability of sandbars at Hells Canyon was evaluated using the modified infinite slope analysis procedure (Budhu and Gobin, 1994) discussed earlier. Selected results of analyses were then verified using the traditional limit equilibrium procedure using the slope stability computer program PCSTABL.

7.1 The Modified Infinite Slope Method

As discussed previously, the modified infinite slope method is basically a graphical procedure that involves estimation of a limiting slope (called the equilibrium seepage slope, ESS) based on shear strength and unit weight of the soil that comprise the slope. Existing slopes steeper than the ESS indicate "likely" failure of the slopes following conditions of rapid drawdown in the river water elevation. Slope failure, in this context, is characterized by mass failure or mass wasting of the slope materials located above the ESS line. According to the modified infinite slope method, the slope materials above the ESS line constitute transient sediments that would accumulate and disperse in a cyclic pattern following conditions of rapid drawdown in the river water elevation due to natural environmental conditions (such as floods) and or operations of the dam.

The modified infinite slope method does not give a quantitative FS but does provide a graphical means of evaluating the limiting slope angle below which failure of sandbar slopes under the drawdown conditions would not be expected to occur. Therefore, the FS was estimated by using the traditional infinite slope equation for saturated slopes. Accordingly, the FS is expressed as:

$$FS = [(\gamma'/\gamma_{sat}) \tan \phi/\tan \beta] \quad \ldots\ldots\ldots\ldots (2)$$

in which β is the slope angle of the existing sandbar slope, ϕ is the angle of internal friction, and γ' and γ_{sat} are as defined in Equation 1.

The infinite slope estimates of FS were performed using a range of values (minimum, maximum, and average) for soil shear strength. The range of values was based on results of very limited laboratory testing conducted on selected samples recovered at the project site. As noted previously, the use of infinite slope equation to determine the FS is conservative.

7.2 Limit Equilibrium Verification

The limit equilibrium solution was conducted on selected slopes to verify the estimated FS from the traditional infinite slope analysis. Limit equilibrium analysis is performed by assuming trial failure surfaces and considering equilibrium of the failure mass based on slope geometry, groundwater conditions, estimated shear strength of the soil, and external loading on the slope. In limit equilibrium analysis, the FS is defined as the factor by which the strength of the soil exceeds the strength needed to maintain stability. Thus, a FS of greater than 1 indicates that the slope is stable.

For this task, the computer program PCSTABL was used to evaluate the FS of selected slopes for comparison with the results of traditional infinite slope analyses. To provide a meaningful comparison of the results, the PCSTABL runs were performed using identical geometry, loading conditions, and soil properties as that of the representative slope analyzed by the traditional infinite slope analysis.

7.3 Stability Evaluation of Hells Canyon Sandbar Slopes

Stability analyses were conducted using slope cross sections or transects generated from surveys of the site. The transects were typically prepared at distance intervals of approximately 45 feet along the length of the sandbar. Figures 31 through 33 show the locations where the transects were cut across each of the sandbar sites.

To minimize the number of cases to be analyzed, the transect slopes generated for each site were examined, and the sites with the most critical slopes were initially selected for analysis. The final choice of the most critical sites was based on a combination of steepness of the existing sandbar slopes and the occurrence of maximum drawdown for the two loading scenarios. The Tin Shed site was excluded in the flood recession scenario for reasons discussed previously.

Based on these criteria, the Fish Trap site was selected for complete analysis using the two loading scenarios while the Pine Bar site was judged to be the more critical for the flood recession scenario. The flood recession analysis conducted for the Fish Trap site was primarily carried out to back up the flood recession analyses for the Pine Bar site. All three sites were analyzed for the 10,000 cfs (283 m^3/s) load swing, which represents the more frequent load following scenario.

In the modified infinite slope analysis, the ESS were first established graphically for all the transects across the three sites. A range of ESS was plotted on these transects in accordance with the range of angles of internal friction and unit weights obtained from the laboratory tests.

PC-STABL was used to estimate the FS of the existing slope generated from Fish Trap transect 9 in order to provide a back-up check of the FS obtained from the traditional infinite slope equation for the load following case. The phreatic surface was specified assuming that drainage would not occur in the sand during the drawdown period. This assumption was made to simulate full saturation of the slope, which is the basic assumption of the traditional infinite slope analyses. This assumption is expected to yield conservative results for entirely homogeneous cohesionless slopes in which some drainage could occur over the drawdown period (that is, approximately 12 hours).

8. Results and Discussion

This section presents and discusses the results of stability analyses of sandbar slopes at the Fish Trap, Pine Bar, and Tin Shed sites.

8.1 Load Following Scenario

This section discusses the results of stability analyses of sandbar slopes for the 16,000 cfs and 10,000 cfs flow fluctuations.

8.1.1 16,000 cfs Flow Fluctuation

Figures 34 through 44 show the slope cross-sections for the 11 transects cut across the Fish Trap site and the water levels before and after drawdown for the 16,000 cfs (453 m^3/s) flow fluctuations in the river. Also shown in these figures are plots of the minimum and maximum ESS, defined by the slope angle α_s. This range in the value of α_s was established using Equation 1 and was found to range between 10 and 14 degrees, depending on the values of unit weight and angle of internal friction of the soil in the slope. The existing slope (β) at this site varies between 5.7 and 13.3 degrees.

For this analysis, the angle of internal friction of the slope was assumed to be 26 degrees, which was the minimum value obtained from the laboratory direct shear tests. This

minimum value was used for conservatism in the analyses and to compensate for uncertainties in soil properties due to the limited amount of data.

As previously discussed, slopes flatter than the ESS are designated as "unlikely" to fail by seepage-induced instability. Slopes steeper than the ESS are designated as "likely" to fail by seepage-induced instability resulting from the specified drawdown in the river water level. Using these criteria, it appears that most of the existing slopes for the Fish Trap site (transects 1 through 9) could be regarded as "unlikely" to fail by instability due to the 16,000 cfs flow fluctuation caused by operation of the Hells Canyon Dam. For the case of transects 10 and 11, where the existing slopes are steeper than the ESS, the potential failure zones (hatched area) are sketched as illustrated in Figures 43 and 44. According to the modified infinite slope method, the slope materials inside the hatched area constitute transient sediments that would accumulate and disperse in a cyclic pattern following conditions of rapid drawdown due to the load following operation in the dam.

The FS of the existing sandbar slopes for the 11 transect sections shown in Figures 34 through 44 were calculated using Equation (2). These calculated FS are summarized in Table 1 and are shown as a range of FS consisting of the minimum, the maximum, and the average. Results of these calculations suggest that, except for the slopes in transects 10 and 11, most of the existing sandbar slopes at the Fish Trap site are "not likely" to fail by the sudden lowering of the river water level as a result of the Hells Canyon Dam operation. The average FS estimated for these slopes range between 1.1 and 1.8 (see Table 1).

PCSTABL was used to analyze Fish Trap transect 9 using the same slope parameters and geometry as those depicted in Figure 42. Both the sliding block and circular failure surfaces were used to develop an understanding for the minimum FS of the submerged slope. Table 2 summarizes the results of the PCSTABL analysis. These results show close agreement between the sliding block and the circular failure modes. The FS estimated for transect 9 ranges between 0.9 and 1.15 (average of 1.0), which closely agrees with the estimates given by Equation 2, as shown in Table 1 (range of 0.9 to 1.2 and average of 1.1). Figures 45 and 46 show typical computer printouts of the PCSTABL analyses for the circular failure modes and for unit weights of 107 pcf and 93 pcf, respectively.

A PCSTABL verification run was also made for transect 10 using the slope geometry shown in Figure 43. As shown in Table 1, the factor of safety of this slope using the traditional infinite slope analysis ranges between 0.8 and 1.0. The modified infinite slope analysis also indicates that the existing slope at this transect exceeds the ESS and that the transient sediments associated with this potential failure surface are as depicted in Figure 43. The results of the PCSTABL analyses for the specified failure surface (hatched zone in Figure 43), however, indicate factor of safety of 1.1 and 1.25 for unit weights of 93 pcf and 107 pcf, respectively. As mentioned in Section 4.1, this higher factor of safety obtained from limit equilibrium analyses using PCSTABL is expected. The discrepancy in the estimated factors of safety further confirms the level of conservatism inherent to both the traditional and modified infinite slope stability methods of analyses.

8.1.2 10,000 cfs Flow Fluctuation

Similar results of analyses using the 10,000 cfs flow fluctuation in river water level are provided in Figures 47 through 79 for all the three sites.

Figures 47 through 57 show the plots of the ESS and water elevations before and after drawdown for the Fish Trap site. The existing slope (β) of the sandbar for this site within the limits of the drawdown elevation varies between 5.7 and 12.7 degrees. Table 3 shows the calculated FS (expressed as minimum, maximum, and average) of the existing sandbar slopes. Except for transects 10 and 11, the calculated average FS appear to vary between 1.0 and 1.8. These results appear to be very similar to that of the 16,000 cfs flow fluctuation.

Similar plots for the Pine Bar site are shown in Figures 58 through 65. The existing slope (β) of the sandbar at this site varies between 5.1 and 14 degrees. Table 4 shows the calculated FS of the existing sandbar slopes for this site. Except at five locations, the calculated average FS varies between 1.0 and 2.0. The five locations where the FSs were calculated to be less than 1.0 are shown in Figure 58 (transect 1), Figure 60 (transect 3), Figure 61 (transect 4), Figure 62 (transect 5), and Figure 63 (transect 6). As shown in these figures, the volume of the sandbar that is considered to be in the transient state is very small due to the smaller magnitude of drawdown (i.e, 3 feet) and the fact that the existing slope within the limits of the drawdown is close to the ESS value. As will be shown in Section 8.2, the flood recession scenario at the Pine Bar site could involve complete overtopping or submergence of the sandbar at this site; in which case the volume of the sandbar material considered to be in the transient state is very large relative to that expected for the 10,000 cfs flow fluctuation.

Figures 66 through 79 show similar plots for the Tin Shed site. The existing slope (β) of the sandbar at this site varies between 2.3 and 9.9 degrees. Table 5 shows the calculated FS of the existing sandbar slopes for this site. Since the existing slope is less than the minimum ESS value of 10 degrees, it is expected that the average FS at this site is at least 1.0 (range of FS is 1.0 to 4.5).

8.1.3 Summary

In summary, the combination of traditional and modified infinite slope analyses indicates that slope failure of the Fish Trap, Pine Bar, and Tin Shed sites due to the load following operation (for both 16,000 cfs and 10,000 cfs flow fluctuations) is not expected. Some portions of the sandbar exceed the slope necessary to maintain stability. However, field observations indicate that the slopes at this portion of the bar may comprise gravel and cobble materials that appear to possess higher strength (particularly due to interlocking) than represented by the shear strength assumed in the analyses (that is, $\phi = 26$ degrees, which is for a loose silty sand).

FS from the traditional infinite slope and limit equilibrium analyses vary depending on whether the minimum, maximum, or average soil properties are used but are typically greater than 1.0 for all transects for even the minimum properties. In design cases where it is necessary to consider potential loss of life or loss of property, a FS of greater than 1.5 is usually required. For a less critical case, a FS of 1.3 would often be acceptable. If the average soil properties determined from laboratory testing are used in conjunction with the fact that the soils comprising the sandbars contain a heterogeneous mix of fine to coarse sand with some interlocking gravel and cobbles, the estimated FS for the majority of the sandbar slopes are expected to be 1.3 or greater.

8.2 Flood Recession Scenario

Infinite slope (modified and traditional) and limit equilibrium analyses of the flood recession case were completed for the Fish Trap and Pine Bar sites. Figures 80 through 87 show the slopes generated from the 7 transects cut across the Pine Bar site. At this site, the existing slopes vary between 11.6 and 24.0 degrees. Also plotted in these figures are the ESS lines representing the equilibrium slopes for the sandbars.

As indicated earlier, the flood recession scenario was analyzed using the hydrograph for the 1997 flood records. In this hydrograph, the maximum drawdown recorded during a flood event was about 11 to 14 feet, occurring over a period of about 4 to 5 days. At the Pine Bar site, this corresponds to lowering the water elevation from Elev. 380.7 m before drawdown to Elev. 377.2 m after drawdown. These water surface elevations primarily result in full submergence of the majority of the sandbars as depicted in Figures 80 through 87. Because of the higher flows associated with the flood event, the fluctuations of the water surface elevation in the river for the flood recession scenario occur on much higher elevations than the load following case.

Tables 6 and 7 show the estimated FS for the flood recession scenario for the Fish Trap and Pine Bar sites, respectively. Results of these analyses indicate that the majority of the slopes are not stable for the flood recession case. The estimated FS are typically less than 1.0. These results suggest that rapid drawdown caused by flood events in the river (that is, flood recession) would have more impact on the sandbar slopes than the load following case arising from fluctuations in the river water elevations due to the dam operation.

9. Summary and Conclusions

Stability analyses were conducted for the sandbars located downstream of the Hells Canyon Dam. The stability analyses were performed using two loading scenarios that define occurrence of rapid drawdown in the sandbar slopes: (a) load following operation, and (b) flood recession condition. In both scenarios, slope failure is assumed to be characterized by mass failure or mass wasting at the sandbar areas due to the action of seepage forces in the slope. The occurrence of slope failure is attributed to the development of excess pore pressures and the removal of the stabilizing external water pressure on the slope.

The stability evaluations were carried out using a combination of three methods, namely: (a) modified infinite slope analysis, (b) traditional infinite slope analysis, and (c) limit equilibrium procedure. The modified infinite slope analysis (Budhu and Gobin, 1994) is a graphical method that is based on the fundamental equation for evaluating the FS of a saturated, infinite slope with seepage parallel to the face. This method was used on this project to determine the extent of slope materials that would be affected by fluctuations of the water level. Traditional infinite slope equation (Equation 2) was used to estimate the FS of the slope analyzed by the modified infinite slope method. On some selected slopes, these FS estimates were verified by limit equilibrium procedure using the computer program PCSTABL.

Results of stability evaluations indicate that failure of sandbar slopes due to load following operation of the dam is not expected. Although some portions of the sandbars have slopes that appear to exceed the slope necessary to maintain stability, field observations of the

materials that comprise the sandbar suggest that the assumptions used in the stability evaluations are very conservative.

Results of analyses for the flood recession scenario indicate that the majority of the sandbar slopes are not stable when subjected to rapid drawdown of water surface elevations in the river during occurrence of major flood events.

Although the flood recession case shows a greater potential to cause instability of the sandbar slopes, it has to be noted that the analysis procedure used to analyze these slopes involves very conservative drainage assumptions (on top of conservative shear strength parameters). That is, the method assumes that very little drainage of the slope will occur during recession of the flood flows. Because the sandbars are composed of sand that are expected to be well draining, this assumption appears to be very conservative. Therefore, it is likely that many of the slopes will be stable during flood recession as long as drawdown occurs slowly enough to allow drainage in the sandbar slopes.

Analysis of the sandbars to make a more precise evaluation of the stability under the two loading scenarios would require adequate survey data to establish the slope geometry and detailed knowledge of the shear strength and permeability characteristics of the slope materials. A considerable effort would be required to collect representative samples in the field and to perform laboratory testing for shear strength and permeability characteristics on these samples. With this information, a more complex and/or sophisticated analyses could be performed. However, there would still be unknown variables that may not be directly quantifiable. These variables include 3-D effects on slope stability due to the limited lateral extent of the sandbars, variations in soil properties, and imperfections in field sampling and laboratory testing among others. Therefore, even though the analysis would be more complex, the accuracy of the results may not necessarily increase substantially.

10. References

ASCE (1988). "*River Width Adjustment. I: Processes and Mechanisms.*" Journal of Hydraulic Engineering, Vol. 124, No. 9, ASCE, pp. 881-902.

Budhu, M and Gobin, R. 1994. "*Instability of Sandbars in Grand Canyon.*" Journal of Hydraulic Engineering, Vol. 120, No. 8, ASCE, pp. 919-933.

Darby, S and Thorne, C. 1996. "*Development and Testing of a River-Bank Stability Analysis.*" Journal of Hydraulic Engineering, Vol. 122, No. 8, ASCE, pp. 443-455.

Duncan, JM, Wright, SG, and Wong, KS. 1990. "*Slope Stability During Rapid Drawdown.*" Proceedings of the H. Bolton Seed Memorial Symposium, Berkeley, CA, May 10-11.

Dunn, I, Anderson, L, and Kiefer, F. 1980. *Fundamentals of Geotechnical Analysis*. John Wiley & Sons, Inc., New York.

FHWA. 1987. *PCSTABL User's Manual*, Federal Highway Administration, Alexandria, Virginia.

Lambe, T and Whitman, R. 1969. *Soil Mechanics*. John Wiley & Sons, New York.

Osman, A and Thorne, C. 1988. "*Riverbank Stability Analysis I: Theory.*" Journal of Hydraulic Engineering, Vol. 114, No. 2, ASCE, pp. 134-150.

Sharma, S. 1992. *XSTABL – An Integrated Slope Stability Analysis Program for Personal Computers, Reference Manual*. Interactive Software Designs, Inc., Moscow, Idaho.

Shinoak Software. 2001. *UTEXAS – A Computer Program for Slope Stability Calculations*, Shinoak Software, Shinoak Drive, Austin, Texas.

Terzaghi, K and Peck, R. 1967. *Soil Mechanics in Engineering Practice*. John Wiley & Sons, New York.

TABLE 1
Estimated Factors of Safety at Fish Trap Site for Load Following Scenario (16,000 cfs Flow Fluctuation)
Infinite Slope Analysis with Seepage Parallel to the Face

Transect Number	Existing Slope Angle, β (degrees)	Factor of Safety, FS		
		Minimum FS (γ_{sat} = 93 pcf)	Maximum FS (γ_{sat} = 107 pcf)	Average FS
1	8.0	1.1	1.5	1.3
2	7.4	1.2	1.6	1.4
3	6.0	1.5	2.0	1.7
4	5.7	1.6	2.1	1.8
5	5.8	1.6	2.0	1.8
6	7.0	1.3	1.7	1.5
7	7.7	1.2	1.5	1.4
8	8.2	1.1	1.4	1.3
9	9.7	0.9	1.2	1.1
10	12.2	0.8	1.0	0.9
11	13.3	0.7	0.9	0.8

Notes:
Based on 1995 hydrograph data. The analysis was conducted for maximum drawdown from Elev. 348.55 m to Elev. 346.93 m due to load following.
Existing slope angles defined by β indicate a break in the slope within the range of drawdown elevations considered in the analyses.
Analysis assumed an angle of internal friction of 26 degrees for the soil within the sandbar.

TABLE 2
Estimated Factors of Safety for Transect 9 at Fish Trap Site Using PCSTABL
Load Following Scenario (16,000 cfs Flow Fluctuation)

Failure Mode	Factor of Safety, FS	
	Minimum FS (γ_{sat} = 93 pcf)	Maximum FS (γ_{sat} = 107 pcf)
Sliding Block	0.9	1.15
Circular Surface	0.9	1.15

TABLE 3
Estimated Factors of Safety at Fish Trap Site for Load Following Scenario (10,000 cfs Flow Fluctuation)
Infinite Slope Analysis with Seepage Parallel to the Face

Transect Number	Existing Slope Angle, β (degrees)	Factor of Safety, FS		
		Minimum FS (γ_{sat} = 93 pcf)	Maximum FS (γ_{sat} = 107 pcf)	Average FS
1	8.3	1.1	1.4	1.3
2	7.4	1.2	1.6	1.4
3	6.3	1.5	1.8	1.7
4	6.0	1.5	1.9	1.7
5	5.7	1.6	2.0	1.8
6	7.1	1.3	1.6	1.5
7	9.7	0.9	1.2	1.1
8	9.1	1.0	1.3	1.1
9	10.0	0.9	1.2	1.0
10	12.7	0.7	0.9	0.8
11	11.9	0.8	1.0	0.9

Notes:
Based on 1995 Hydrograph Records. Used maximum drawdown from Elev. 348.0 m to Elev. 346.86 m in the analyses.
Existing slope angles defined by β indicate a break in the slope within the range of drawdown elevations considered in the analyses.
Angle of internal friction of the soil within the sandbar was assumed to be 26 degrees.

TABLE 4
Estimated Factors of Safety at Pine Bar Site for the Load Following Scenario (10,000 cfs Flow Fluctuation)
Infinite Slope Analysis with Seepage Parallel to the Face

Transect Number	Existing Slope Angle, β (degrees)	Factor of Safety, FS		
		Minimum FS (γ_{sat} = 93 pcf)	Maximum FS (γ_{sat} = 107 pcf)	Average FS
1	10.0	0.9	1.2	1.0
	11.3	0.8	1.0	0.9
2	10.0	0.9	1.2	1.0
3	12.4	0.7	0.9	0.8
	6.8	1.4	1.7	1.5
4	6.3	1.5	1.8	1.7
	14.0	0.6	0.8	0.7
	5.4	1.7	2.2	1.9
5	14.0	0.6	0.8	0.7
	9.9	0.9	1.2	1.0
	5.1	1.8	2.3	2.0
6	8.0	1.1	1.5	1.3
	8.0	1.1	1.5	1.3
	14.0	0.6	0.8	0.7
7	9.4	1.0	1.2	1.1
	8.3	1.1	1.4	1.3
	5.1	1.8	2.3	2.0
	8.8	1.0	1.3	1.2
8	7.4	1.2	1.6	1.4

Notes:
Based on 1995 Hydrograph Records. Used maximum drawdown from Elev. 376.39 m to Elev. 375.48 m in the analysis.
Existing slope angles defined by β indicate a break in the slope within the range of drawdown elevations considered in the analyses.
Angle of internal friction of the soil within the sandbar was assumed to be 26 degrees.

TABLE 5
Estimated Factors of Safety at Tin Shed Site for the Load Following Scenario (10,000 cfs Flow Fluctuation)
Infinite Slope Analysis with Seepage Parallel to the Face

Transect Number	Existing Slope Angle, β (degrees)	Factor of Safety, FS		
		Minimum FS (γ_{sat} = 93 pcf)	Maximum FS (γ_{sat} = 107 pcf)	Average FS
1	3.2	2.9	3.6	3.3
2	2.9	3.2	4.0	3.6
3	2.3	4.0	5.1	4.5
4	8.0	1.1	1.5	1.3
5	4.3	2.1	2.7	2.4
6	9.9	0.9	1.2	1.0
7	6.6	1.4	1.8	1.6
8	4.0	2.3	2.9	2.6
9	3.7	2.5	3.1	2.8
10	5.7	1.6	2.0	1.8
11	6.0	1.5	1.9	1.7
12	3.2	2.9	3.6	3.3
13	9.7	0.9	1.2	1.1
	6.0	1.5	1.9	1.7
14	3.9	2.4	3.0	2.7

Notes:
Based on 1995 Hydrograph Records. Used maximum drawdown from Elev. 346.57 m to Elev. 345.83 m in the analyses.
Existing slope angles defined by β indicate a break in the slope within the range of drawdown elevations considered in the analyses.
Angle of internal friction of the soil within the sandbar was assumed to be 26 degrees.

TABLE 6
Estimated Factors of Safety at Fish Trap Site for Flood Recession Scenario
Infinite Slope Analysis with Seepage Parallel to the Face

Transect Number	Existing Slope Angle, β or β' (degrees)	Factor of Safety, FS		
		Minimum FS (γ_{sat} = 93 pcf)	Maximum FS (γ_{sat} = 107 pcf)	Average FS
1	12.5	0.7	0.9	0.8
	33.4	0.2	0.3	0.3
2	9.5	1.0	1.2	1.1
	21.5	0.4	0.5	0.5
3	10.0	0.9	1.2	1.0
	26.0	0.3	0.4	0.4
4	9.5	1.0	1.2	1.1
	31.6	0.3	0.3	0.3
5	19.1	0.5	0.6	0.5
6	18.7	0.5	0.6	0.5
7	19.7	0.5	0.6	0.5
8	15.1	0.6	0.8	0.7
	32.3	0.3	0.3	0.3
9	6.4	1.4	1.8	1.6
	32.5	0.3	0.3	0.3
10	8.6	1.1	1.3	1.2
	31.3	0.3	0.3	0.3
11	14.6	0.6	0.8	0.7
	38.1	0.2	0.3	0.2

Notes:
Based on 1997 Flood Records. Used maximum drawdown from Elev. 353.4 m to Elev. 349.0 m in the analyses.
Existing slope angles defined by both β and β' indicate a break in the slope within the range of drawdown elevations considered in the analyses.
Angle of internal friction of the soil within the sandbar was assumed to be 26 degrees.

TABLE 7
Estimated Factors of Safety at Pine Bar Site for Flood Recession Scenario
Infinite Slope Analysis with Seepage Parallel to the Face

Transect Number	Existing Slope Angle, β (degrees)	Factor of Safety, FS		
		Minimum FS (γ_{sat} = 93 pcf)	Maximum FS (γ_{sat} = 107 pcf)	Average FS
1	23.2	0.4	0.6	0.5
2	19.9	0.4	0.6	0.5
3	18.8	0.5	0.6	0.5
4	24.0	0.4	0.5	0.4
5	13.5	0.7	0.9	0.8
6	12.2	0.7	0.9	0.8
7	11.9	0.8	1.0	0.9
8	11.6	0.8	1.0	0.9

Notes:
Based on 1997 Flood Records. Used maximum drawdown from Elev. 380.7 m to Elev. 377.2 m in the analysis.
Angle of internal friction of the soil within the sandbar was assumed to be 26 degrees.

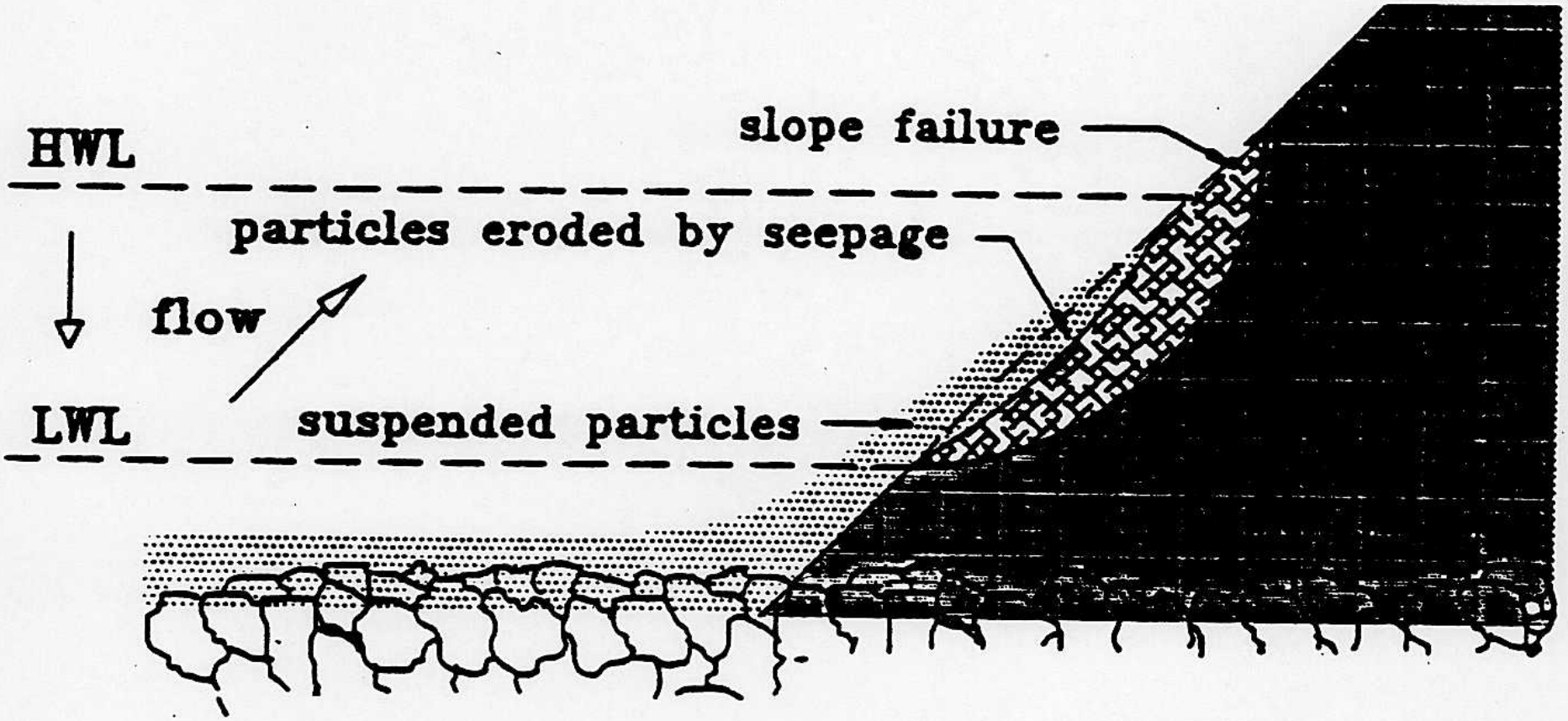

Mechanism of Seepage-Driven Erosion

Figure 1

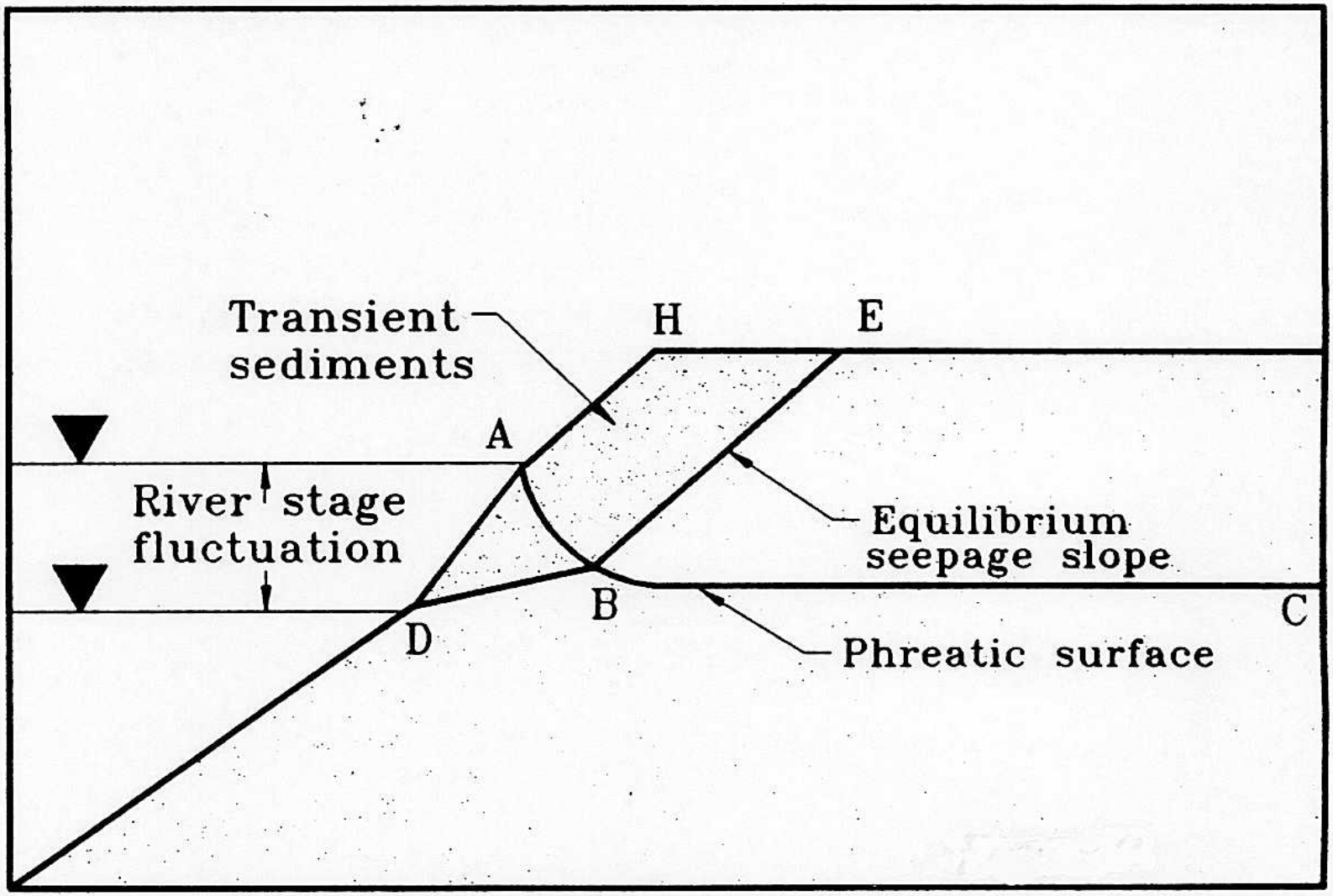
Transient
sediments
H
E
A
River stage
fluctuation
Equilibrium
seepage slope
B
C
D
Phreatic surface

Figure 2

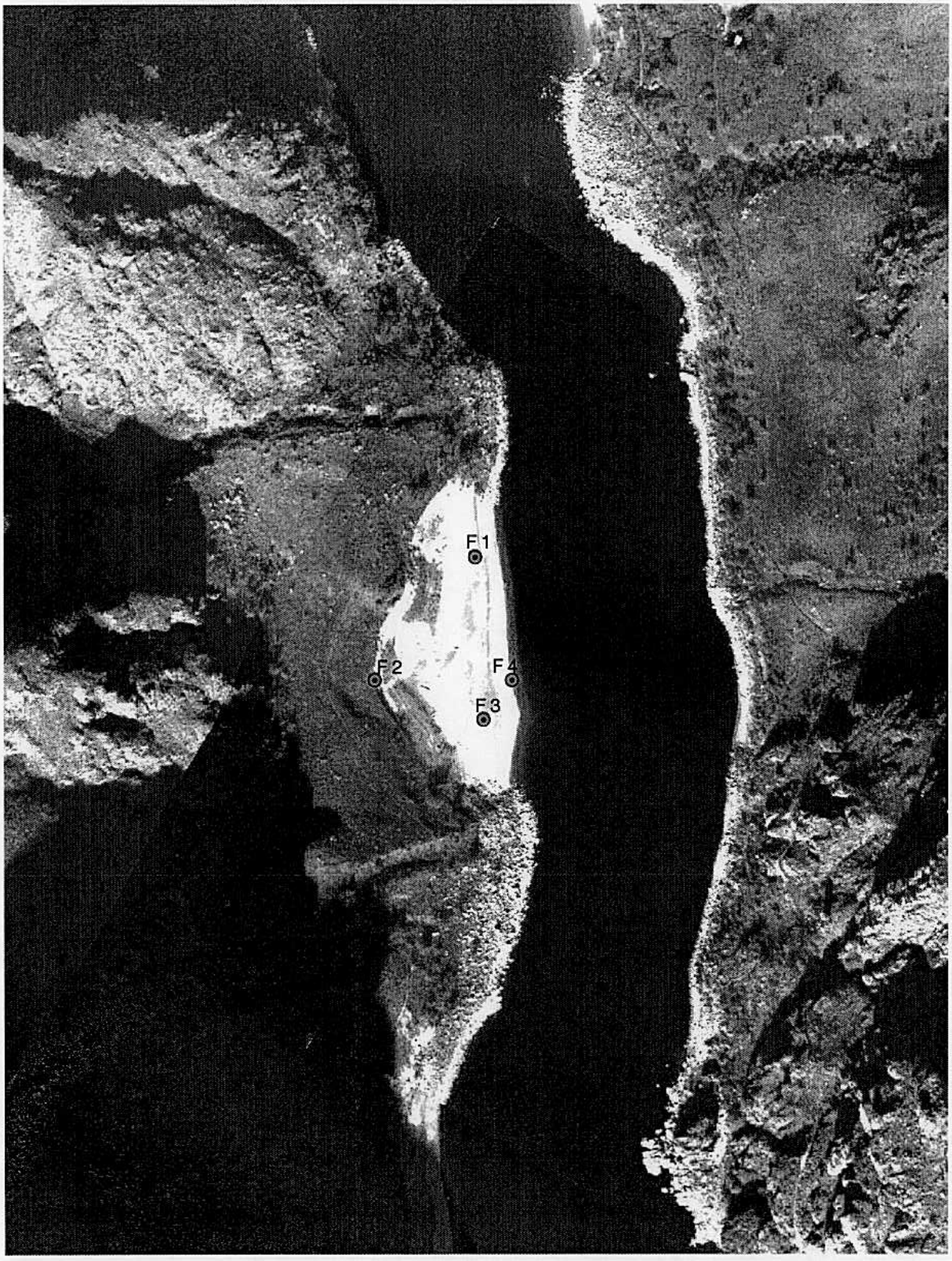

Fish Trap Bar

100 0 100 200 Feet

Figure 3

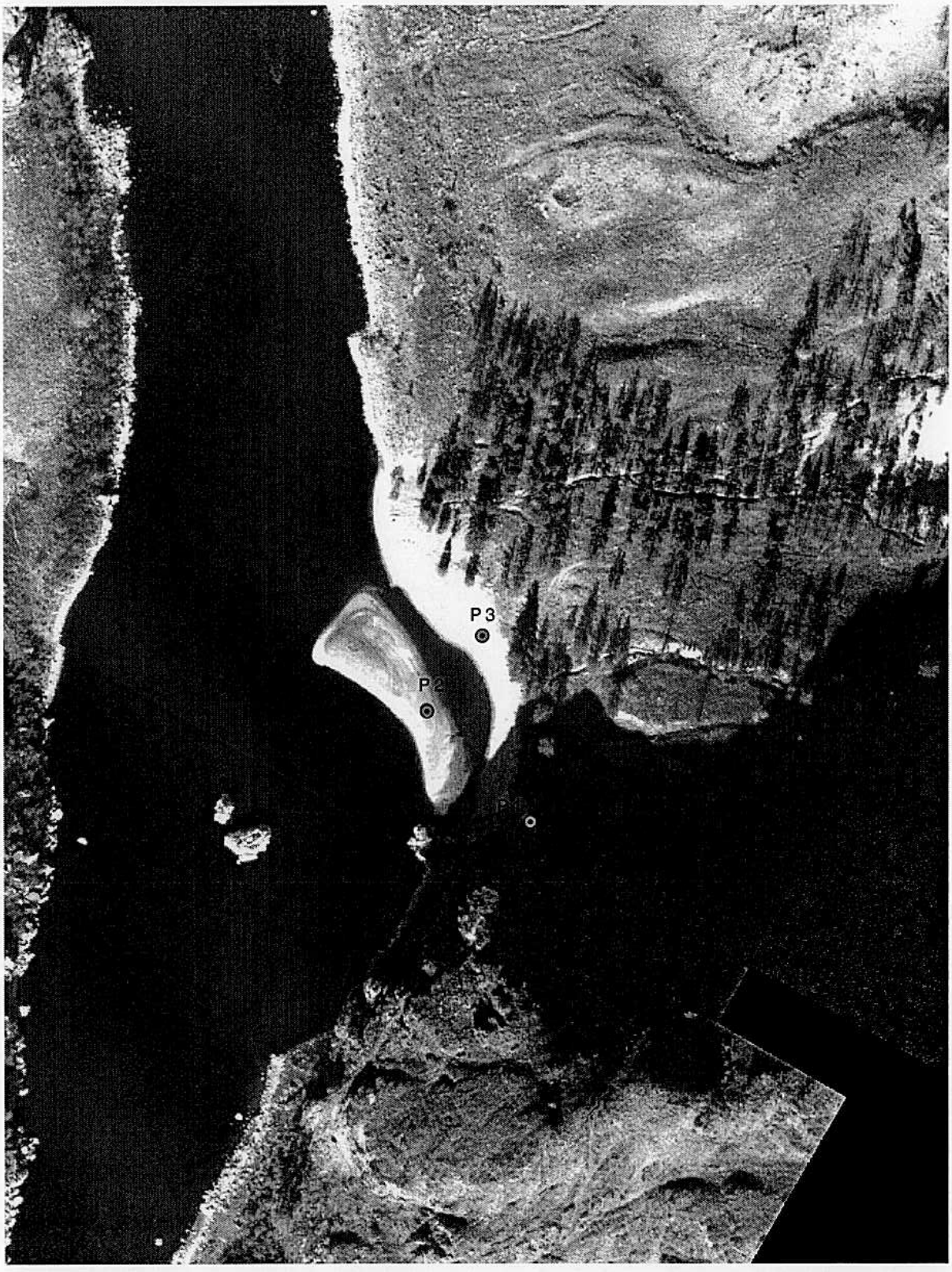

Figure 4

Tin Shed Bar

100 0 100 200 Feet

Figure 5

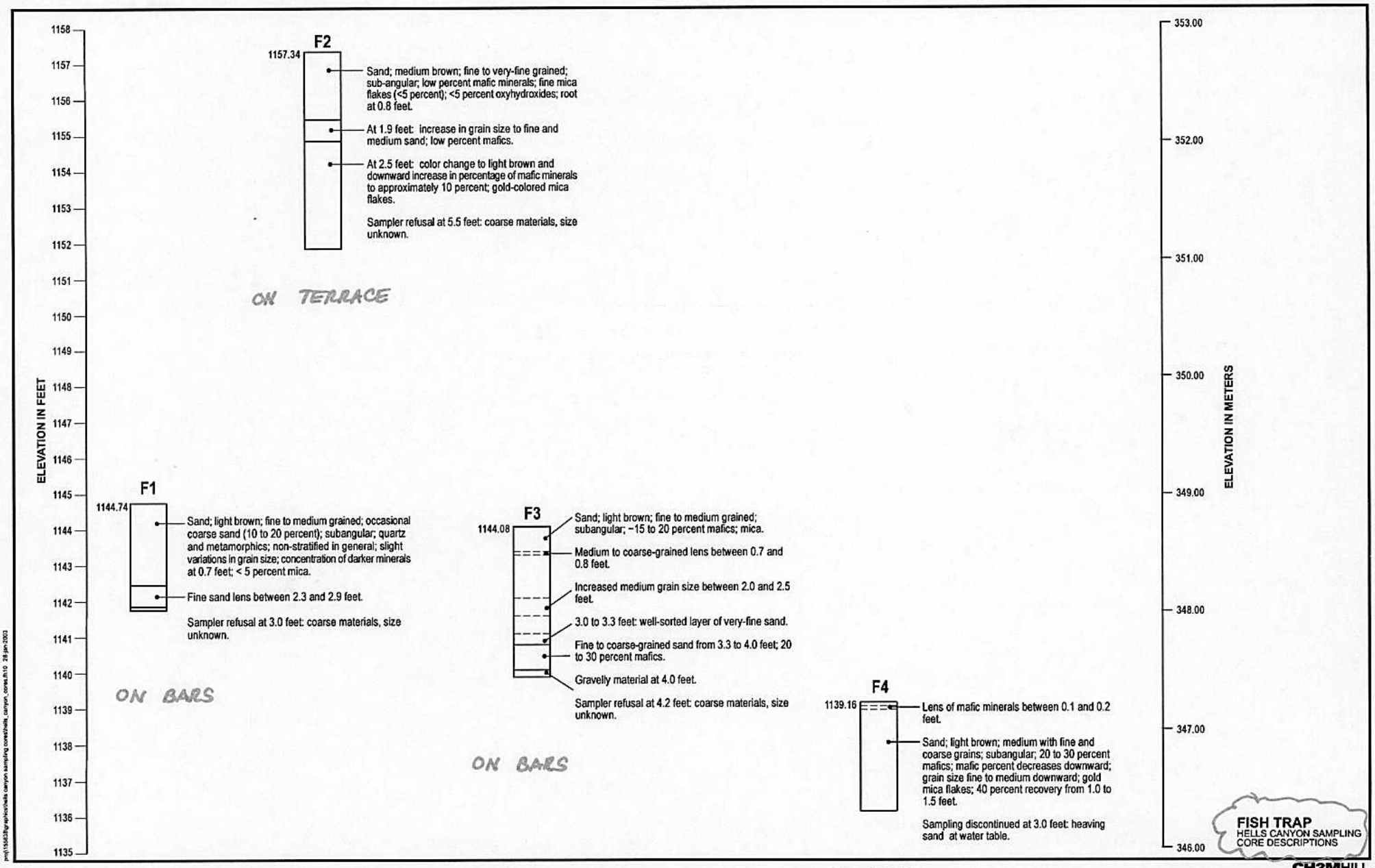
ELEVATION IN FEET
1158
1157
1156
1155
1154
1153
1152
1151
1150
1149
1148
1147
1146
1145
1144
1143
1142
1141
1140
1139
1138
1137
1136
1135
F2
1157.34
Sand; medium brown; fine to very-fine grained; sub-angular; low percent mafic minerals; fine mica flakes (<5 percent); <5 percent oxyhydroxides; root at 0.8 feet.
At 1.9 feet: increase in grain size to fine and medium sand; low percent mafics.
At 2.5 feet: color change to light brown and downward increase in percentage of mafic minerals to approximately 10 percent; gold-colored mica flakes.
Sampler refusal at 5.5 feet: coarse materials, size unknown.
ON TERRACE
F1
1144.74
Sand; light brown; fine to medium grained; occasional coarse sand (10 to 20 percent); subangular; quartz and metamorphics; non-stratified in general; slight variations in grain size; concentration of darker minerals at 0.7 feet; < 5 percent mica.
Fine sand lens between 2.3 and 2.9 feet.
Sampler refusal at 3.0 feet: coarse materials, size unknown.
ON BARS
F3
1144.08
Sand; light brown; fine to medium grained; subangular; ~15 to 20 percent mafics; mica.
Medium to coarse-grained lens between 0.7 and 0.8 feet.
Increased medium grain size between 2.0 and 2.5 feet.
3.0 to 3.3 feet: well-sorted layer of very-fine sand.
Fine to coarse-grained sand from 3.3 to 4.0 feet; 20 to 30 percent mafics.
Gravelly material at 4.0 feet.
Sampler refusal at 4.2 feet: coarse materials, size unknown.
ON BARS
F4
1139.16
Lens of mafic minerals between 0.1 and 0.2 feet.
Sand; light brown; medium with fine and coarse grains; subangular; 20 to 30 percent mafics; mafic percent decreases downward; grain size fine to medium downward; gold mica flakes; 40 percent recovery from 1.0 to 1.5 feet.
Sampling discontinued at 3.0 feet: heaving sand at water table.
ON BARS
353.00
352.00
351.00
350.00
349.00
348.00
347.00
346.00
ELEVATION IN METERS
FISH TRAP
HELLS CANYON SAMPLING
CORE DESCRIPTIONS
CH2MHILL

Figure 6

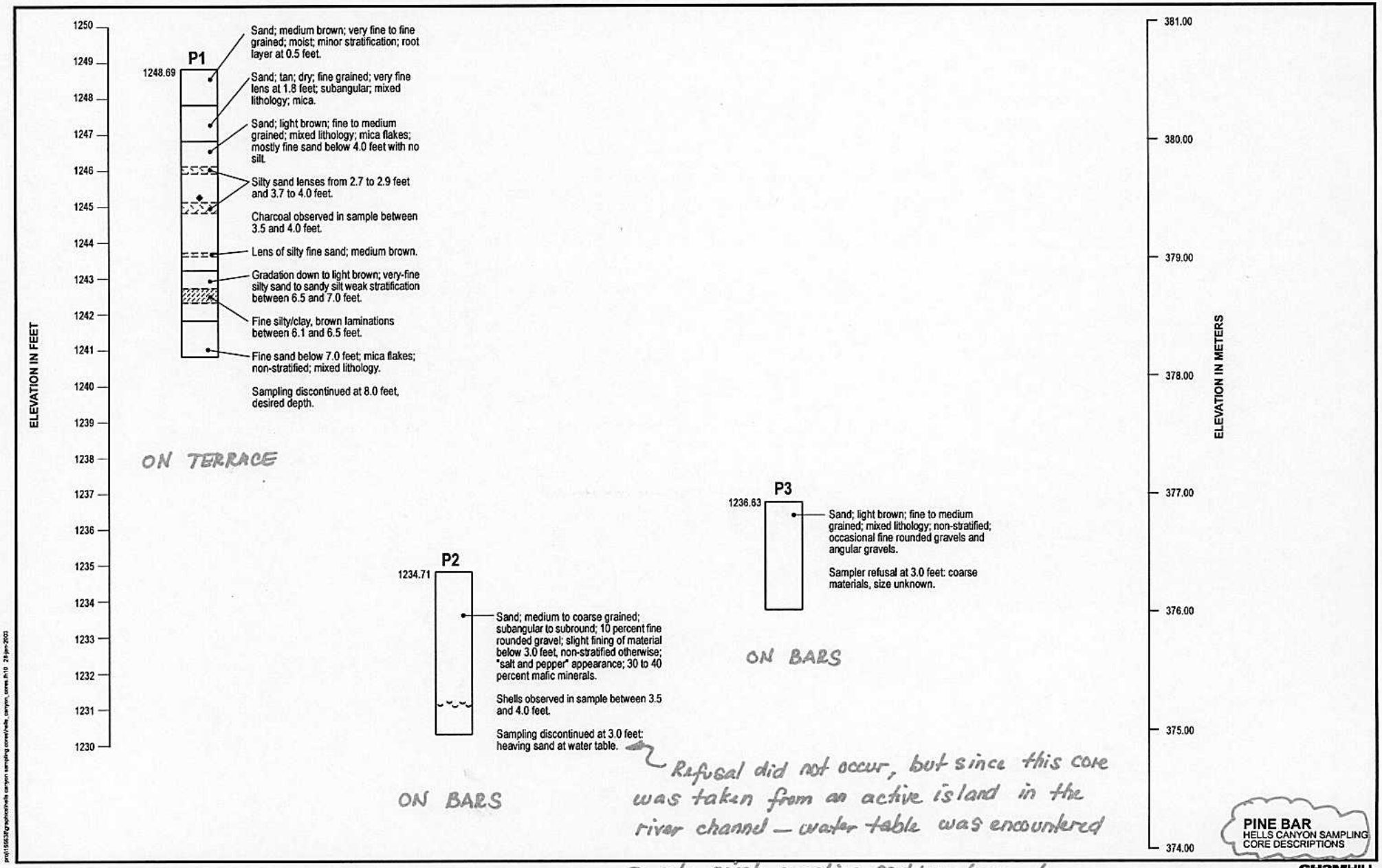
ELEVATION IN FEET
1250
1249
1248
1247
1246
1245
1244
1243
1242
1241
1240
1239
1238
1237
1236
1235
1234
1233
1232
1231
1230
P1
1248.69
Sand; medium brown; very fine to fine grained; moist; minor stratification; root layer at 0.5 feet.
Sand; tan; dry; fine grained; very fine lens at 1.8 feet; subangular; mixed lithology; mica.
Sand; light brown; fine to medium grained; mixed lithology; mica flakes; mostly fine sand below 4.0 feet with no silt.
Silty sand lenses from 2.7 to 2.9 feet and 3.7 to 4.0 feet.
Charcoal observed in sample between 3.5 and 4.0 feet.
Lens of silty fine sand; medium brown.
Gradation down to light brown; very-fine silty sand to sandy silt weak stratification between 6.5 and 7.0 feet.
Fine silty/clay, brown laminations between 6.1 and 6.5 feet.
Fine sand below 7.0 feet; mica flakes; non-stratified; mixed lithology.
Sampling discontinued at 8.0 feet, desired depth.
ON TERRACE
P2
1234.71
Sand; medium to coarse grained; subangular to subround; 10 percent fine rounded gravel; slight fining of material below 3.0 feet, non-stratified otherwise; "salt and pepper" appearance; 30 to 40 percent mafic minerals.
Shells observed in sample between 3.5 and 4.0 feet.
Sampling discontinued at 3.0 feet: heaving sand at water table.
ON BARS
P3
1236.63
Sand; light brown; fine to medium grained; mixed lithology; non-stratified; occasional fine rounded gravels and angular gravels.
Sampler refusal at 3.0 feet: coarse materials, size unknown.
ON BARS
Refusal did not occur, but since this core was taken from an active island in the river channel — water table was encountered @ w/c point sampling could no longer be done due to the sand collapsing.
ELEVATION IN METERS
381.00
380.00
379.00
378.00
377.00
376.00
375.00
374.00
PINE BAR
HELLS CANYON SAMPLING
CORE DESCRIPTIONS
CH2MHILL

Figure 7

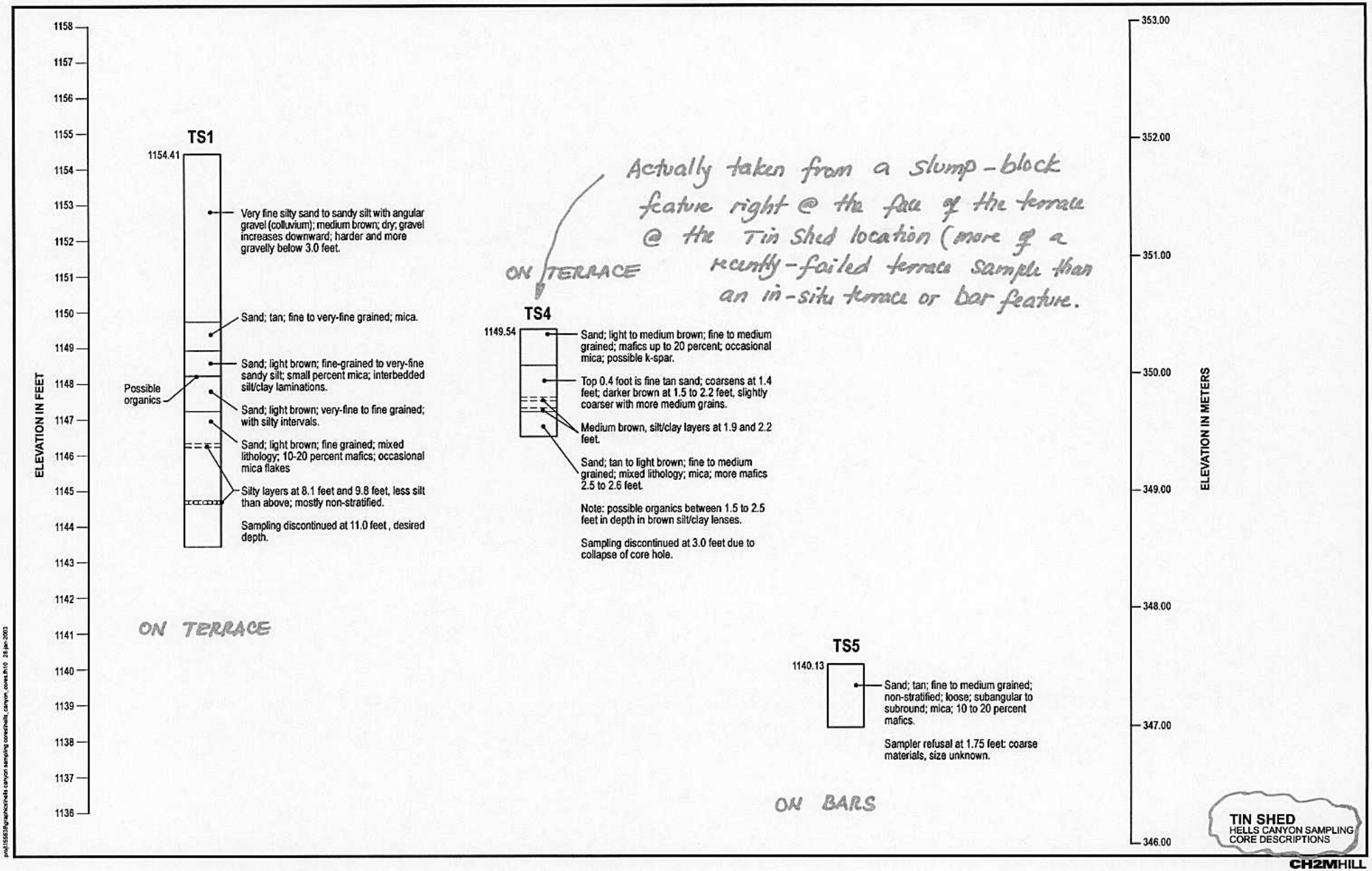
ELEVATION IN FEET
1158
1157
1156
1155
1154
1153
1152
1151
1150
1149
1148
1147
1146
1145
1144
1143
1142
1141
1140
1139
1138
1137
1136
TS1
1154.41
Very fine silty sand to sandy silt with angular gravel (colluvium); medium brown; dry; gravel increases downward; harder and more gravelly below 3.0 feet.
Sand; tan; fine to very-fine grained; mica.
Sand; light brown; fine-grained to very-fine sandy silt; small percent mica; interbedded silt/clay laminations.
Possible organics
Sand; light brown; very-fine to fine grained; with silty intervals.
Sand; light brown; fine grained; mixed lithology; 10-20 percent mafics; occasional mica flakes
Silty layers at 8.1 feet and 9.8 feet, less silt than above; mostly non-stratified.
Sampling discontinued at 11.0 feet , desired depth.
ON TERRACE
Actually taken from a slump-block feature right @ the face of the terrace @ the Tin Shed location (more of a recently-failed terrace sample than an in-situ terrace or bar feature.
ON TERRACE
TS4
1149.54
Sand; light to medium brown; fine to medium grained; mafics up to 20 percent; occasional mica; possible k-spar.
Top 0.4 foot is fine tan sand; coarsens at 1.4 feet; darker brown at 1.5 to 2.2 feet, slightly coarser with more medium grains.
Medium brown, silt/clay layers at 1.9 and 2.2 feet.
Sand; tan to light brown; fine to medium grained; mixed lithology; mica; more mafics 2.5 to 2.6 feet.
Note: possible organics between 1.5 to 2.5 feet in depth in brown silt/clay lenses.
Sampling discontinued at 3.0 feet due to collapse of core hole.
TS5
1140.13
Sand; tan; fine to medium grained; non-stratified; loose; subangular to subround; mica; 10 to 20 percent mafics.
Sampler refusal at 1.75 feet: coarse materials, size unknown.
ON BARS
353.00
352.00
351.00
350.00
349.00
348.00
347.00
346.00
ELEVATION IN METERS
TIN SHED
HELLS CANYON SAMPLING
CORE DESCRIPTIONS
CH2MHILL

Figure 8

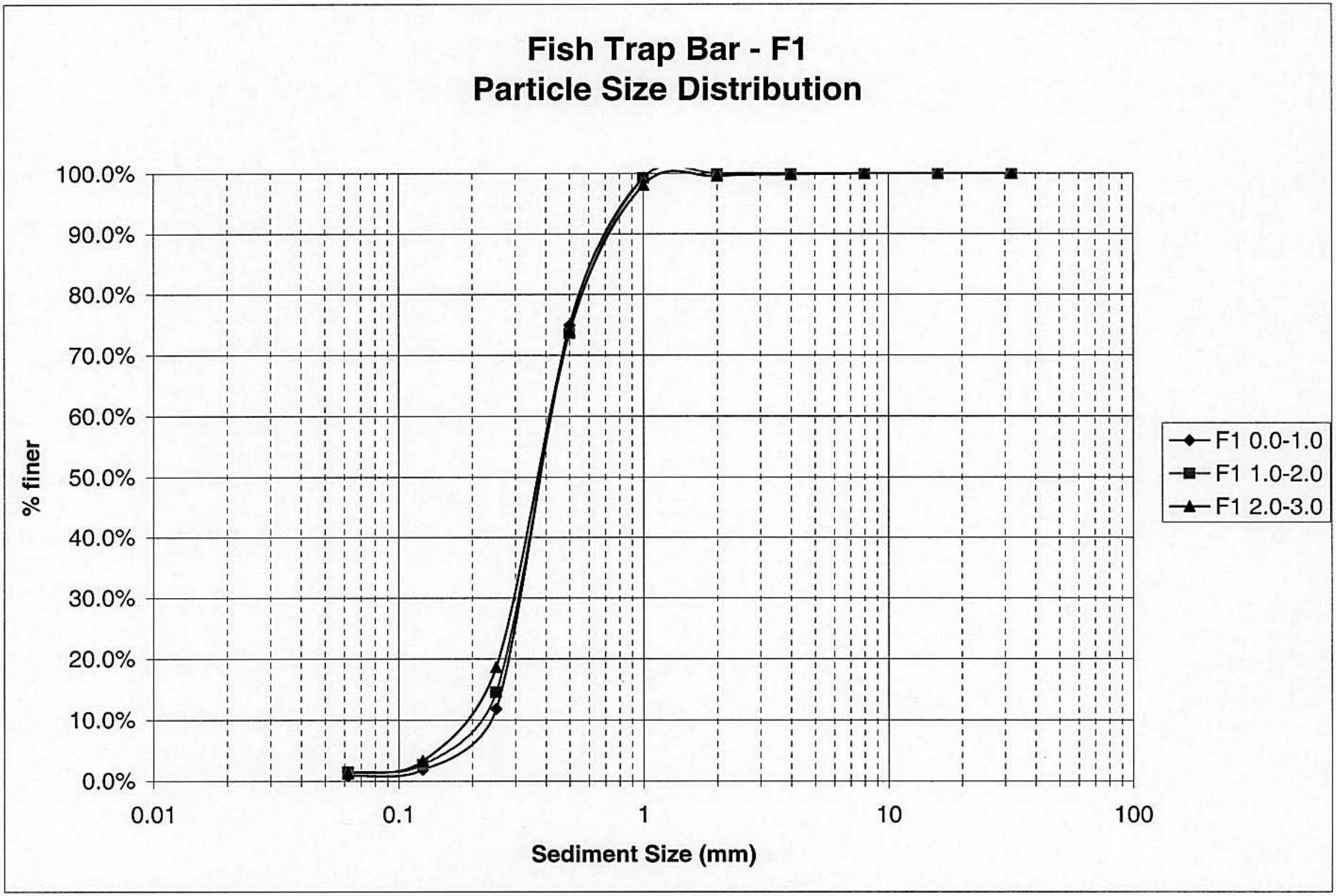
Fish Trap Bar - F1
Particle Size Distribution
100.0%
90.0%
80.0%
70.0%
60.0%
50.0%
40.0%
30.0%
20.0%
10.0%
0.0%
% finer
0.01
0.1
1
10
100
Sediment Size (mm)
F1 0.0-1.0
F1 1.0-2.0
F1 2.0-3.0

Figure 9

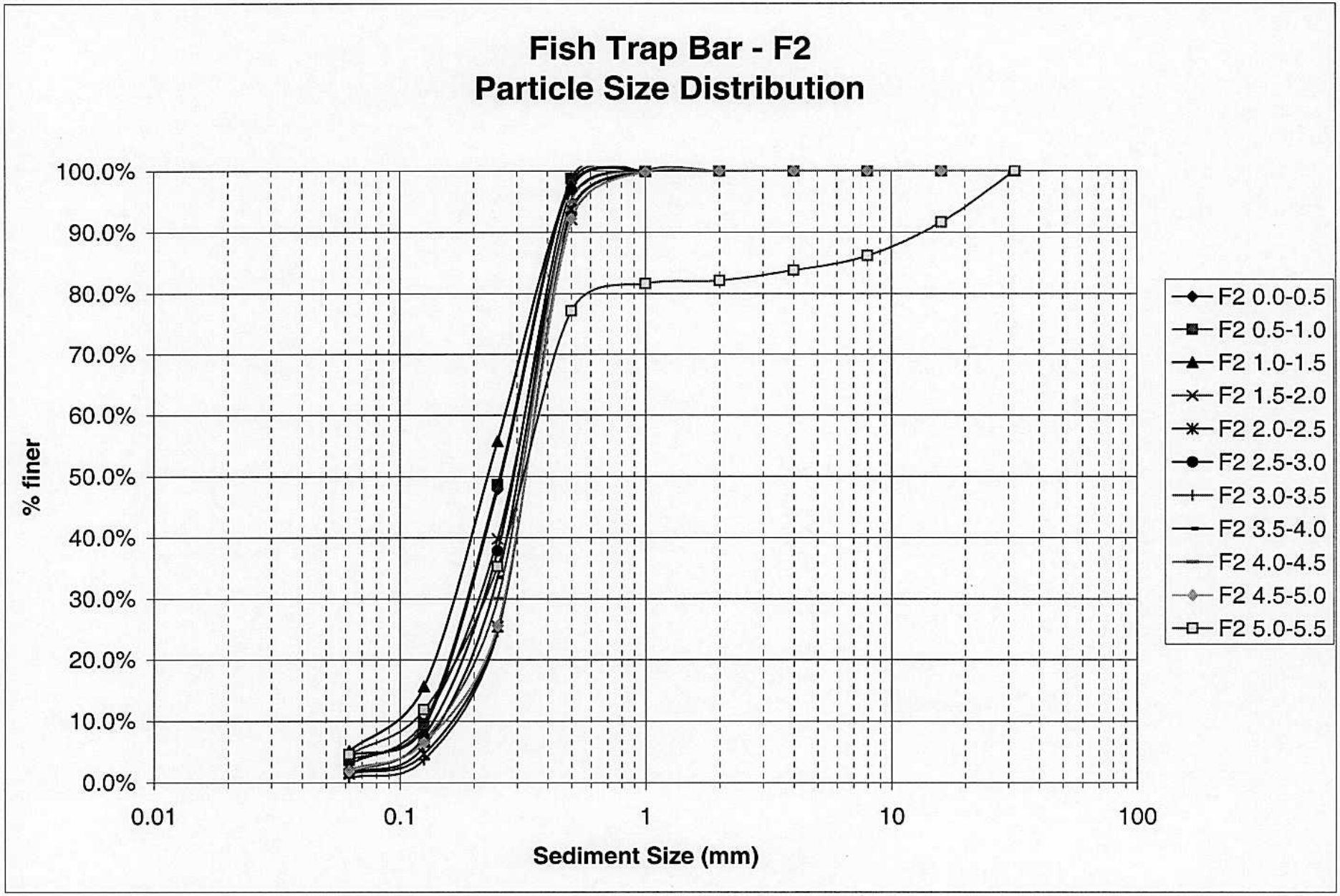
Fish Trap Bar - F2
Particle Size Distribution
100.0%
90.0%
80.0%
70.0%
60.0%
50.0%
40.0%
30.0%
20.0%
10.0%
0.0%
% finer
0.01
0.1
1
10
100
Sediment Size (mm)
F2 0.0-0.5
F2 0.5-1.0
F2 1.0-1.5
F2 1.5-2.0
F2 2.0-2.5
F2 2.5-3.0
F2 3.0-3.5
F2 3.5-4.0
F2 4.0-4.5
F2 4.5-5.0
F2 5.0-5.5

Figure 10

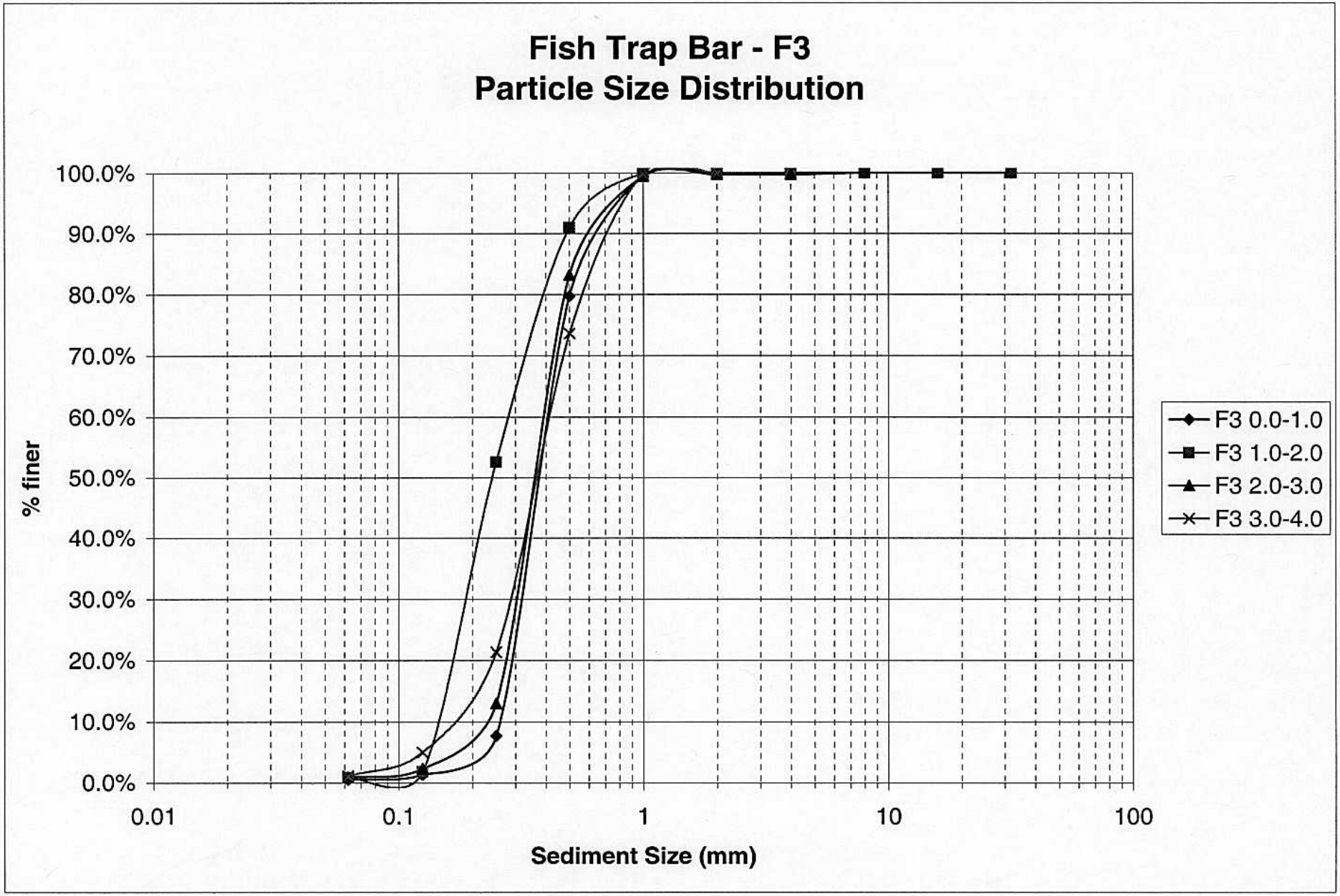
Fish Trap Bar - F3
Particle Size Distribution
100.0%
90.0%
80.0%
70.0%
60.0%
50.0%
40.0%
30.0%
20.0%
10.0%
0.0%
% finer
0.01
0.1
1
10
100
Sediment Size (mm)
F3 0.0-1.0
F3 1.0-2.0
F3 2.0-3.0
F3 3.0-4.0

Figure 11

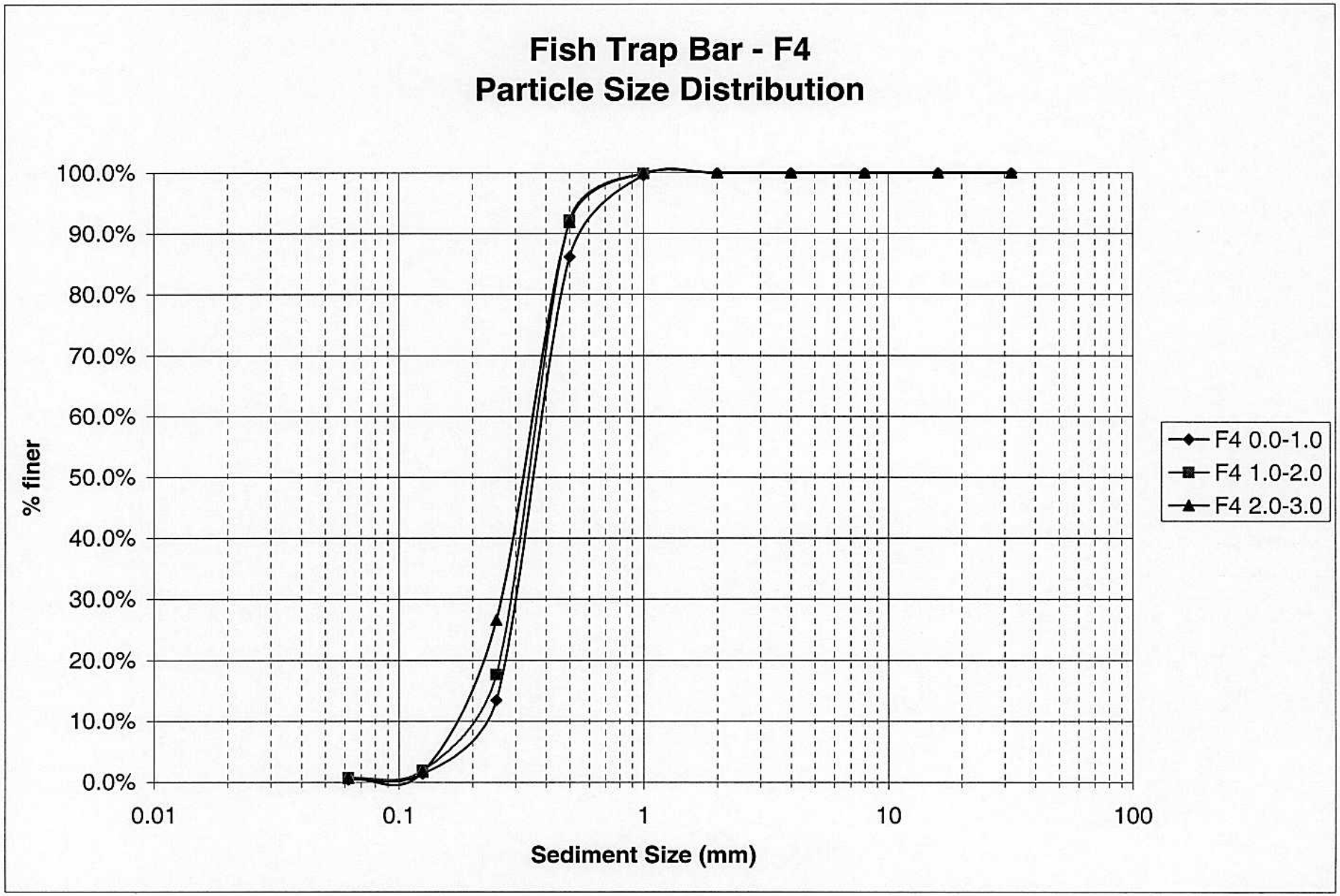
Fish Trap Bar - F4
Particle Size Distribution
100.0%
90.0%
80.0%
70.0%
60.0%
50.0%
40.0%
30.0%
20.0%
10.0%
0.0%
% finer
0.01
0.1
1
10
100
Sediment Size (mm)
F4 0.0-1.0
F4 1.0-2.0
F4 2.0-3.0

Figure 12

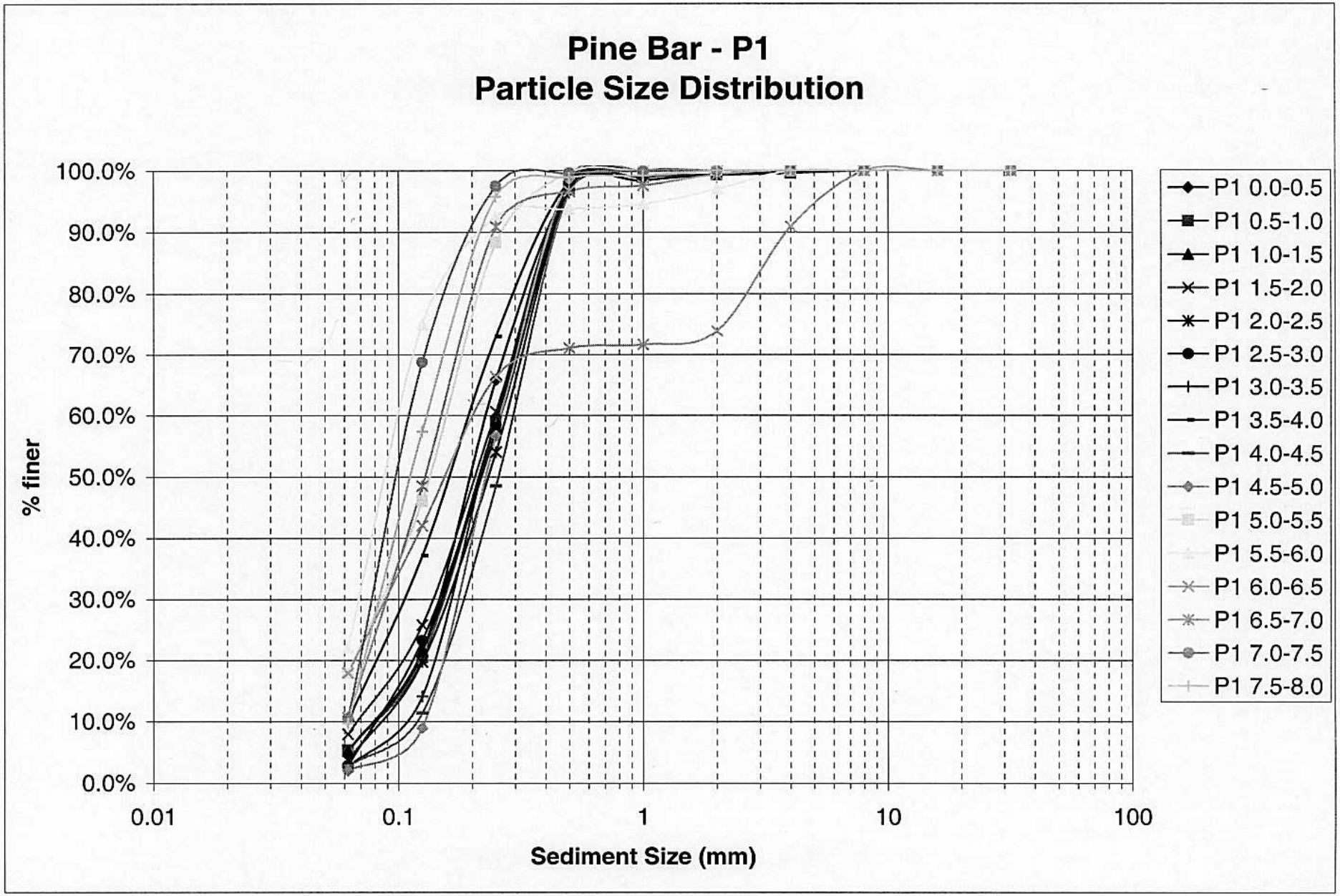
Pine Bar - P1
Particle Size Distribution
100.0%
90.0%
80.0%
70.0%
60.0%
50.0%
40.0%
30.0%
20.0%
10.0%
0.0%
% finer
0.01
0.1
1
10
100
Sediment Size (mm)
P1 0.0-0.5
P1 0.5-1.0
P1 1.0-1.5
P1 1.5-2.0
P1 2.0-2.5
P1 2.5-3.0
P1 3.0-3.5
P1 3.5-4.0
P1 4.0-4.5
P1 4.5-5.0
P1 5.0-5.5
P1 5.5-6.0
P1 6.0-6.5
P1 6.5-7.0
P1 7.0-7.5
P1 7.5-8.0

Figure 13

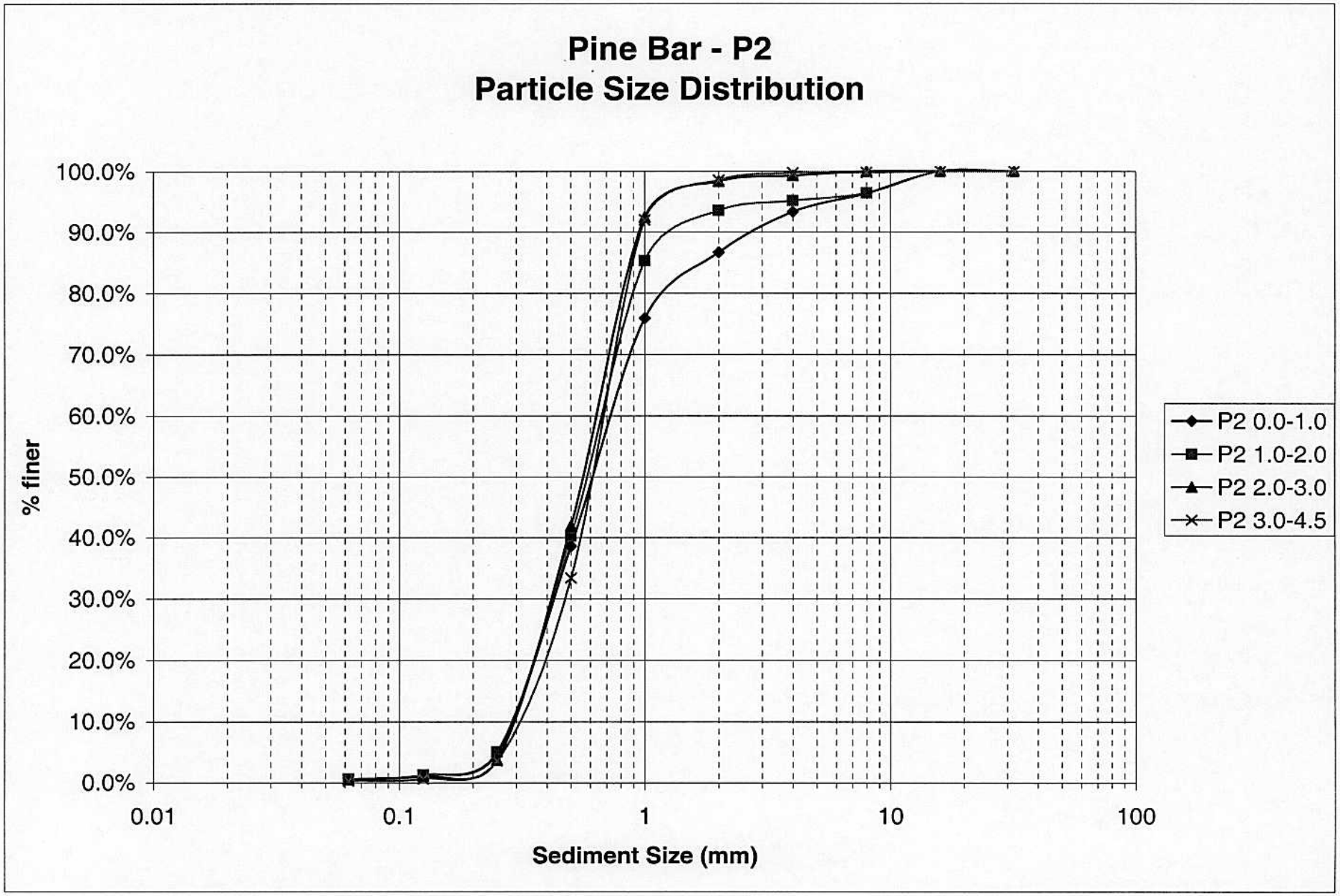
Pine Bar - P2
Particle Size Distribution
100.0%
90.0%
80.0%
70.0%
60.0%
50.0%
40.0%
30.0%
20.0%
10.0%
0.0%
% finer
0.01
0.1
1
10
100
Sediment Size (mm)
P2 0.0-1.0
P2 1.0-2.0
P2 2.0-3.0
P2 3.0-4.5

Figure 14

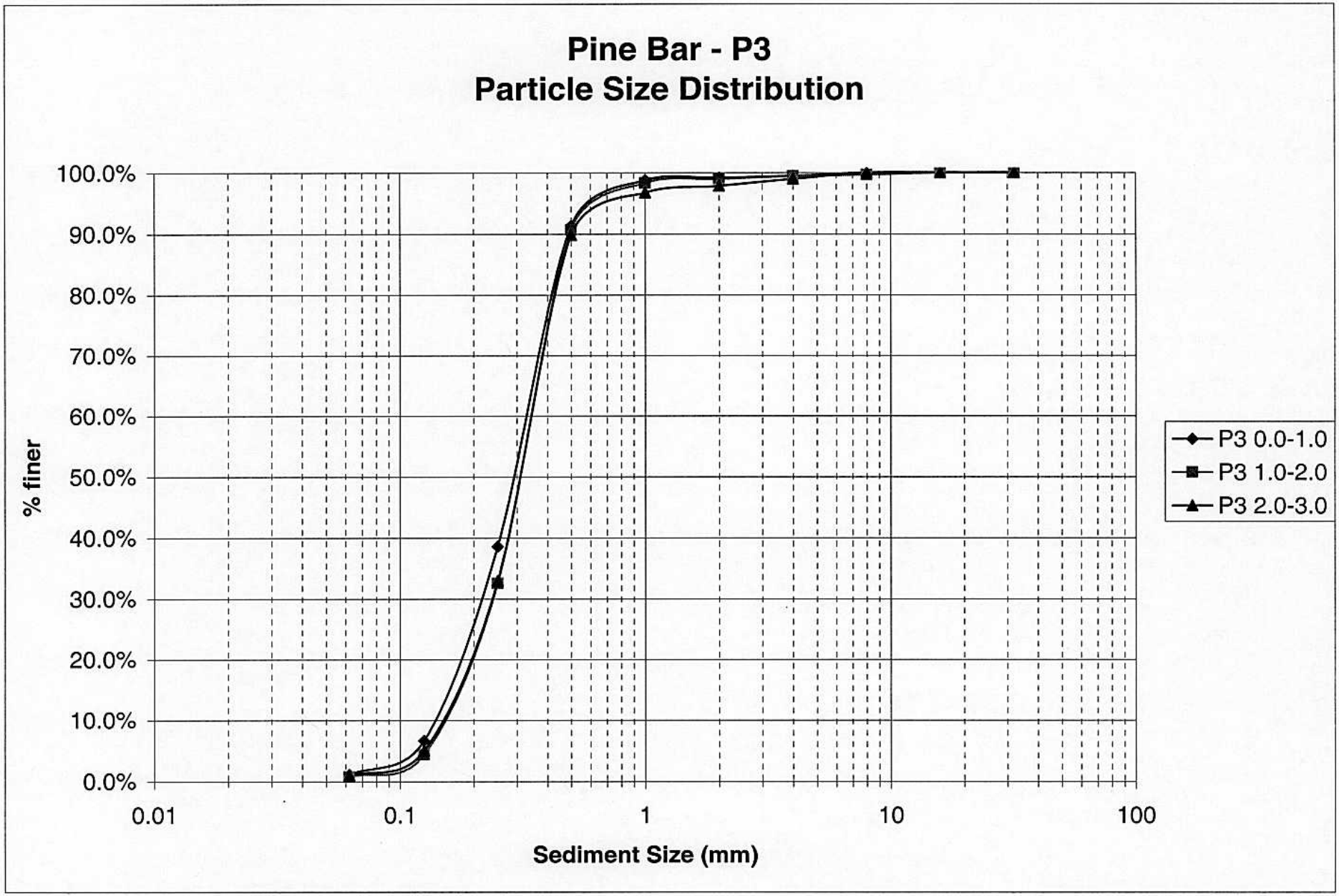
Pine Bar - P3
Particle Size Distribution
100.0%
90.0%
80.0%
70.0%
60.0%
50.0%
40.0%
30.0%
20.0%
10.0%
0.0%
% finer
0.01
0.1
1
10
100
Sediment Size (mm)
P3 0.0-1.0
P3 1.0-2.0
P3 2.0-3.0

Figure 15

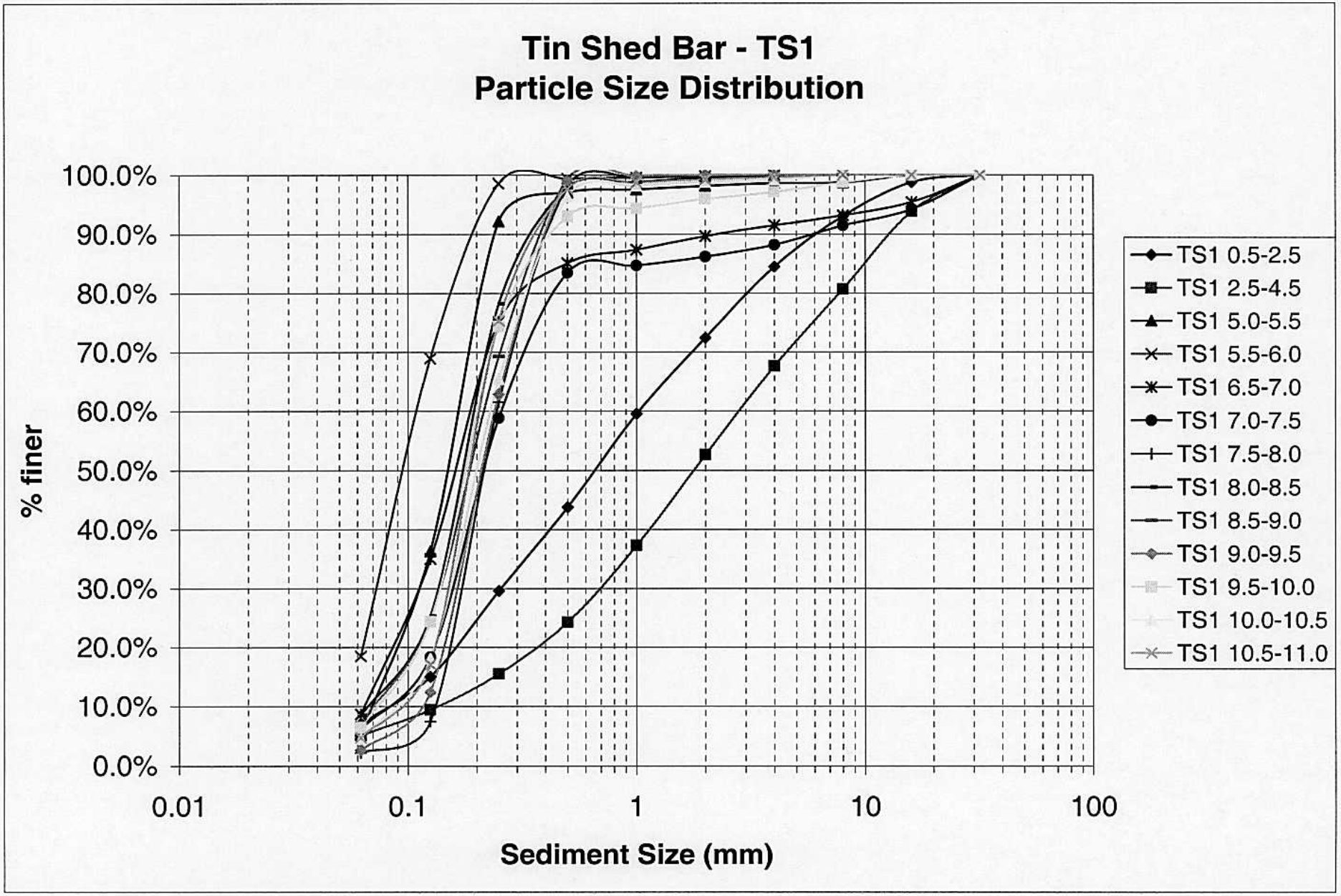
Tin Shed Bar - TS1
Particle Size Distribution
100.0%
90.0%
80.0%
70.0%
60.0%
50.0%
40.0%
30.0%
20.0%
10.0%
0.0%
% finer
0.01
0.1
1
10
100
Sediment Size (mm)
TS1 0.5-2.5
TS1 2.5-4.5
TS1 5.0-5.5
TS1 5.5-6.0
TS1 6.5-7.0
TS1 7.0-7.5
TS1 7.5-8.0
TS1 8.0-8.5
TS1 8.5-9.0
TS1 9.0-9.5
TS1 9.5-10.0
TS1 10.0-10.5
TS1 10.5-11.0

Figure 16

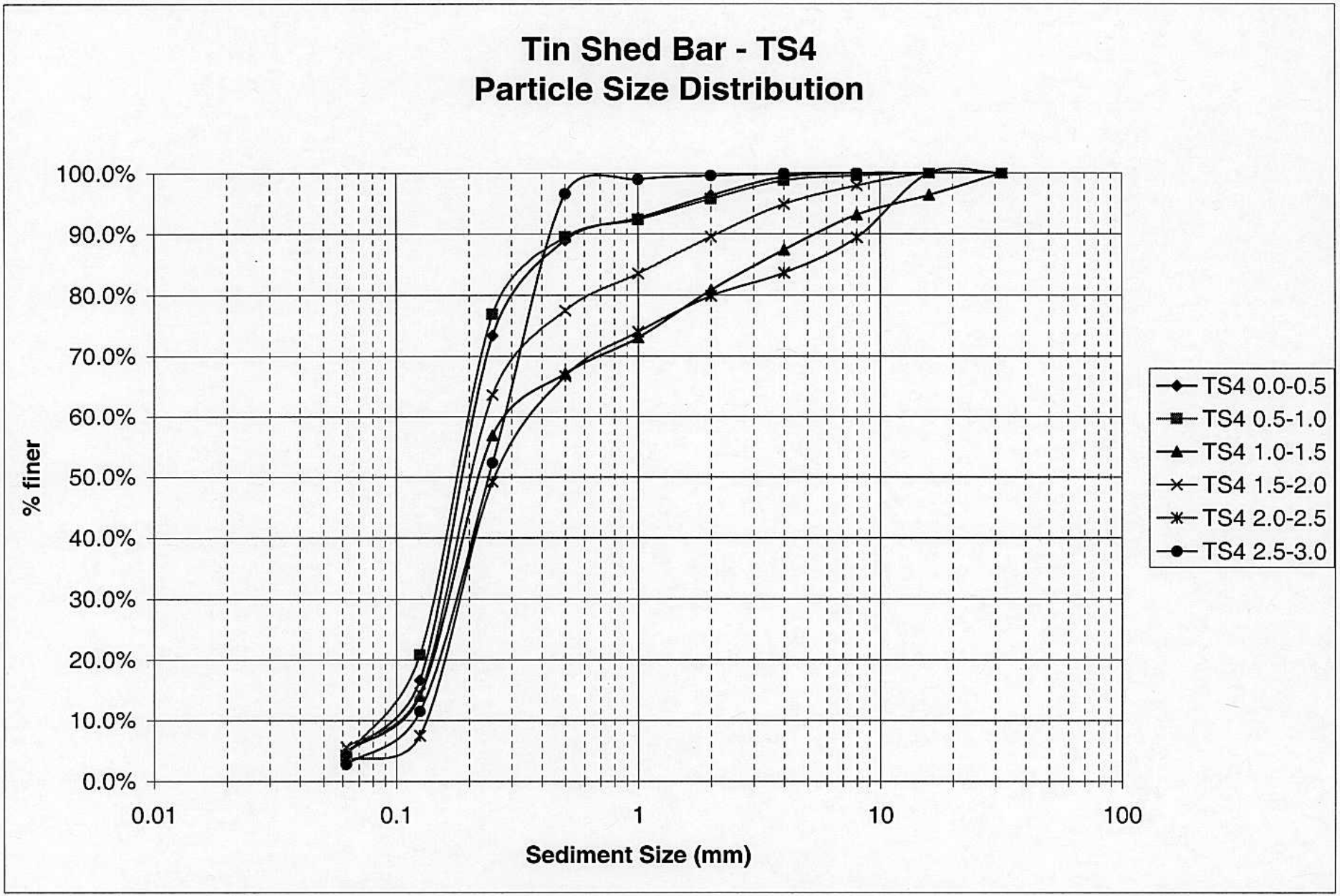
Tin Shed Bar - TS4
Particle Size Distribution
100.0%
90.0%
80.0%
70.0%
60.0%
50.0%
40.0%
30.0%
20.0%
10.0%
0.0%
% finer
0.01
0.1
1
10
100
Sediment Size (mm)
TS4 0.0-0.5
TS4 0.5-1.0
TS4 1.0-1.5
TS4 1.5-2.0
TS4 2.0-2.5
TS4 2.5-3.0

Figure 17


Tin Shed Bar - TS5
Particle Size Distribution
100.0%
90.0%
80.0%
70.0%
60.0%
50.0%
40.0%
30.0%
20.0%
10.0%
0.0%
% finer
0.01
0.1
1
10
100
Sediment Size (mm)
TS5 0.0-1.0
TS5 1.0-1.75

Figure 18

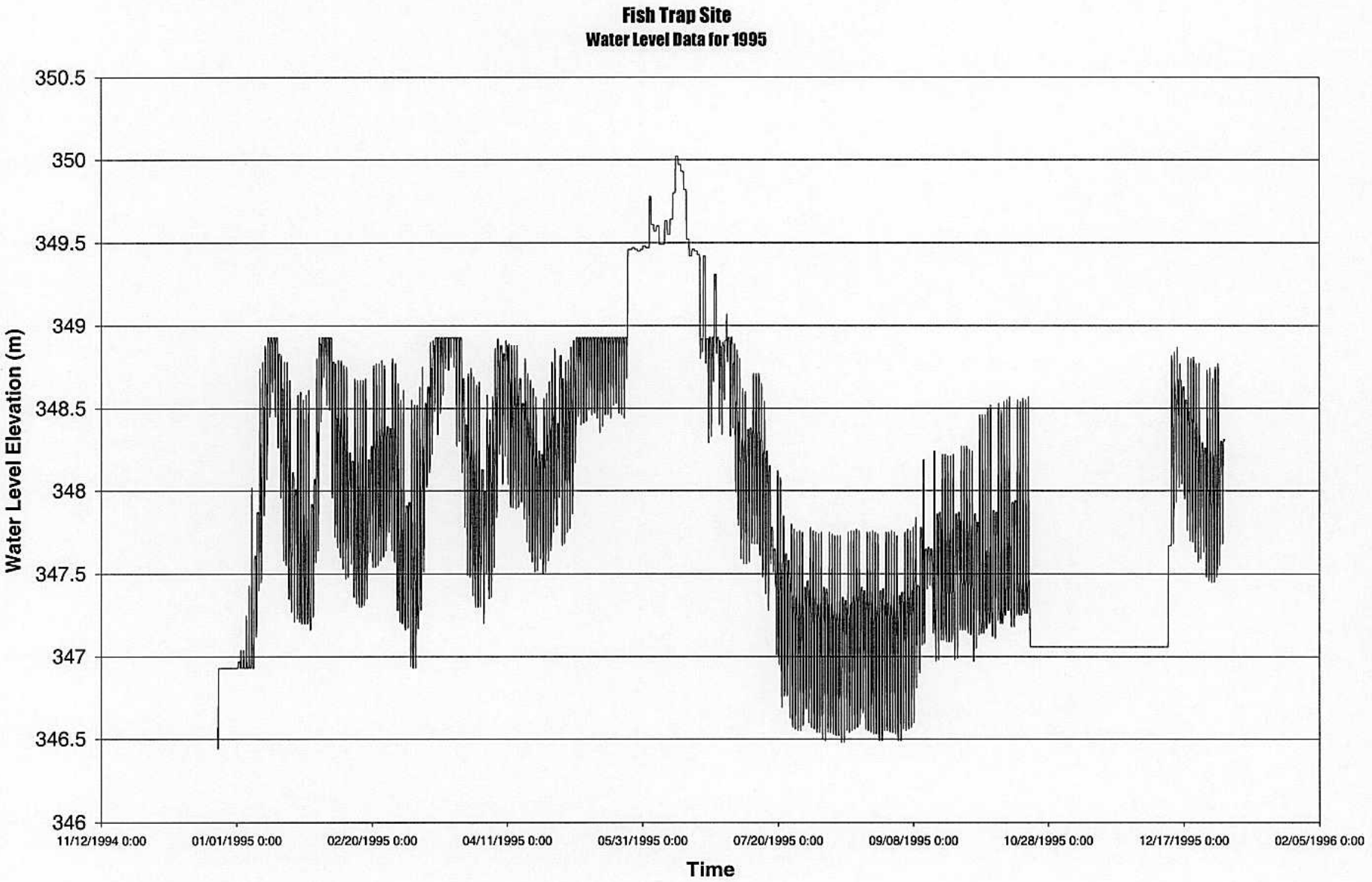
Fish Trap Site
Water Level Data for 1995
Water Level Elevation (m)
350.5
350
349.5
349
348.5
348
347.5
347
346.5
346
11/12/1994 0:00
01/01/1995 0:00
02/20/1995 0:00
04/11/1995 0:00
05/31/1995 0:00
07/20/1995 0:00
09/08/1995 0:00
10/28/1995 0:00
12/17/1995 0:00
02/05/1996 0:00
Time

Figure 19

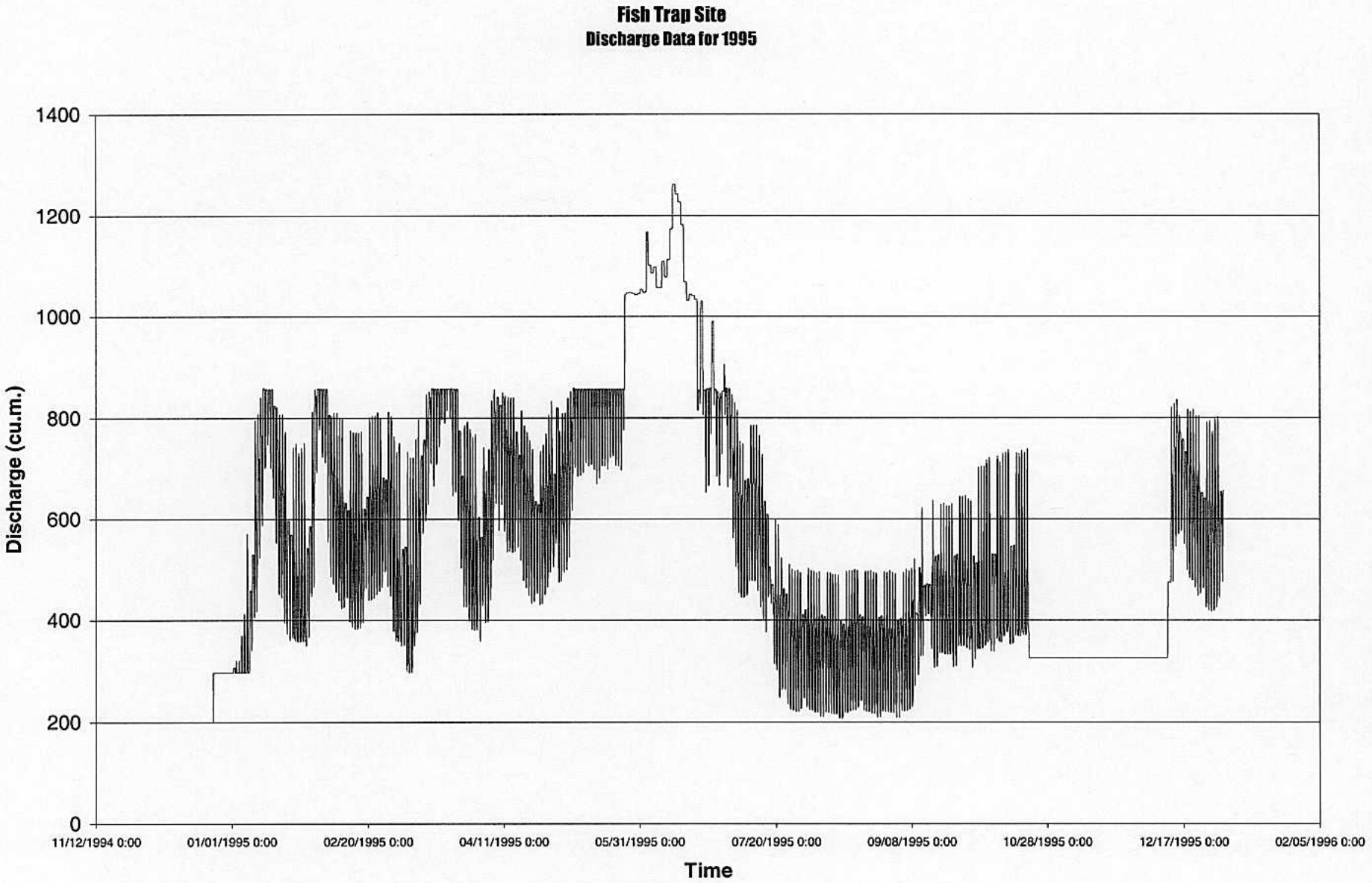
Fish Trap Site
Discharge Data for 1995
Discharge (cu.m.)
1400
1200
1000
800
600
400
200
0
11/12/1994 0:00
01/01/1995 0:00
02/20/1995 0:00
04/11/1995 0:00
05/31/1995 0:00
07/20/1995 0:00
09/08/1995 0:00
10/28/1995 0:00
12/17/1995 0:00
02/05/1996 0:00
Time

Figure 20

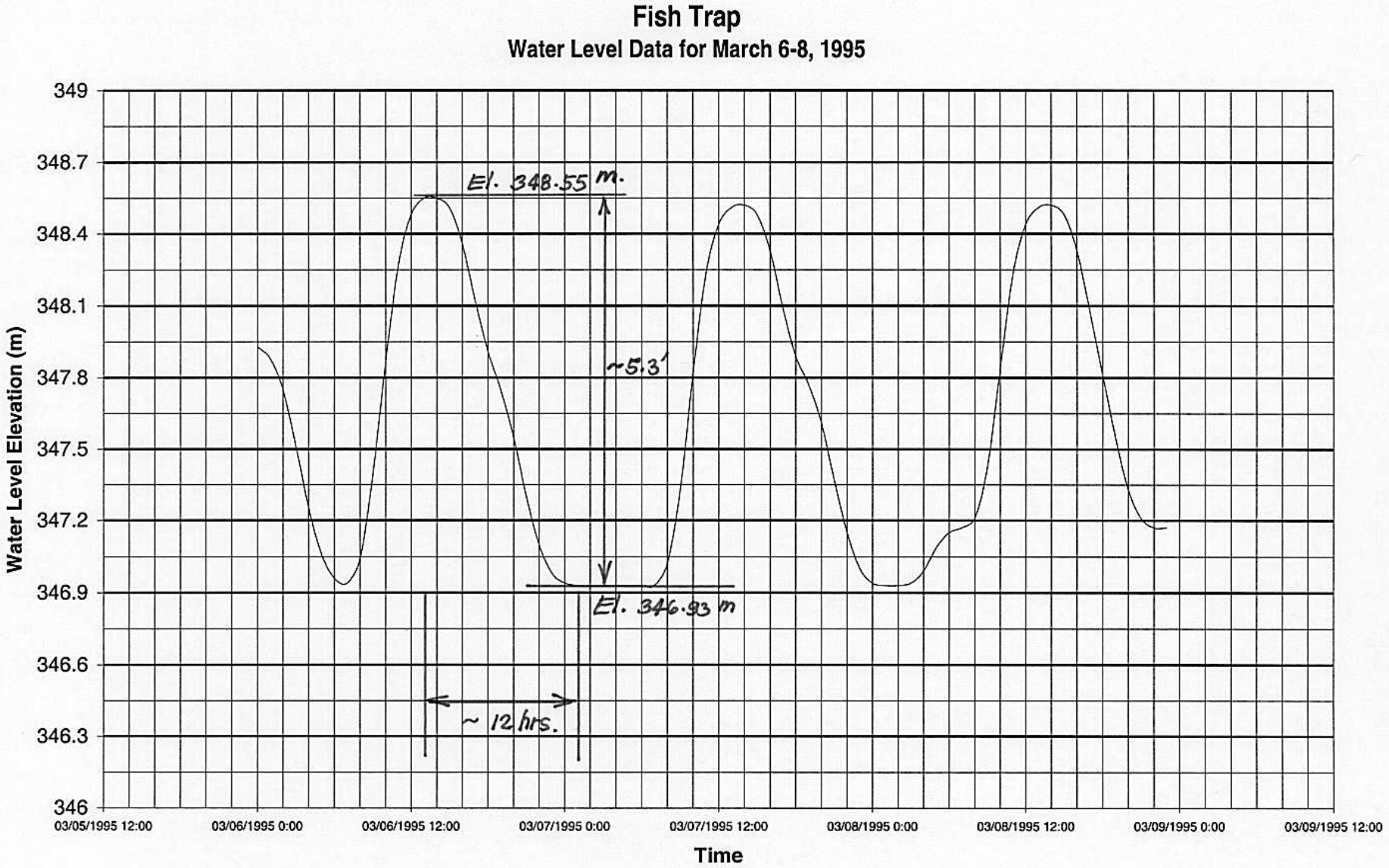
Fish Trap
Water Level Data for March 6-8, 1995
Water Level Elevation (m)
349
348.7
348.4
348.1
347.8
347.5
347.2
346.9
346.6
346.3
346
El. 348.55 m.
~5.3'
El. 346.93 m
~ 12 hrs.
03/05/1995 12:00
03/06/1995 0:00
03/06/1995 12:00
03/07/1995 0:00
03/07/1995 12:00
03/08/1995 0:00
03/08/1995 12:00
03/09/1995 0:00
03/09/1995 12:00
Time

Figure 21

Fish Trap Site
Discharge Data for March 6-8, 1995

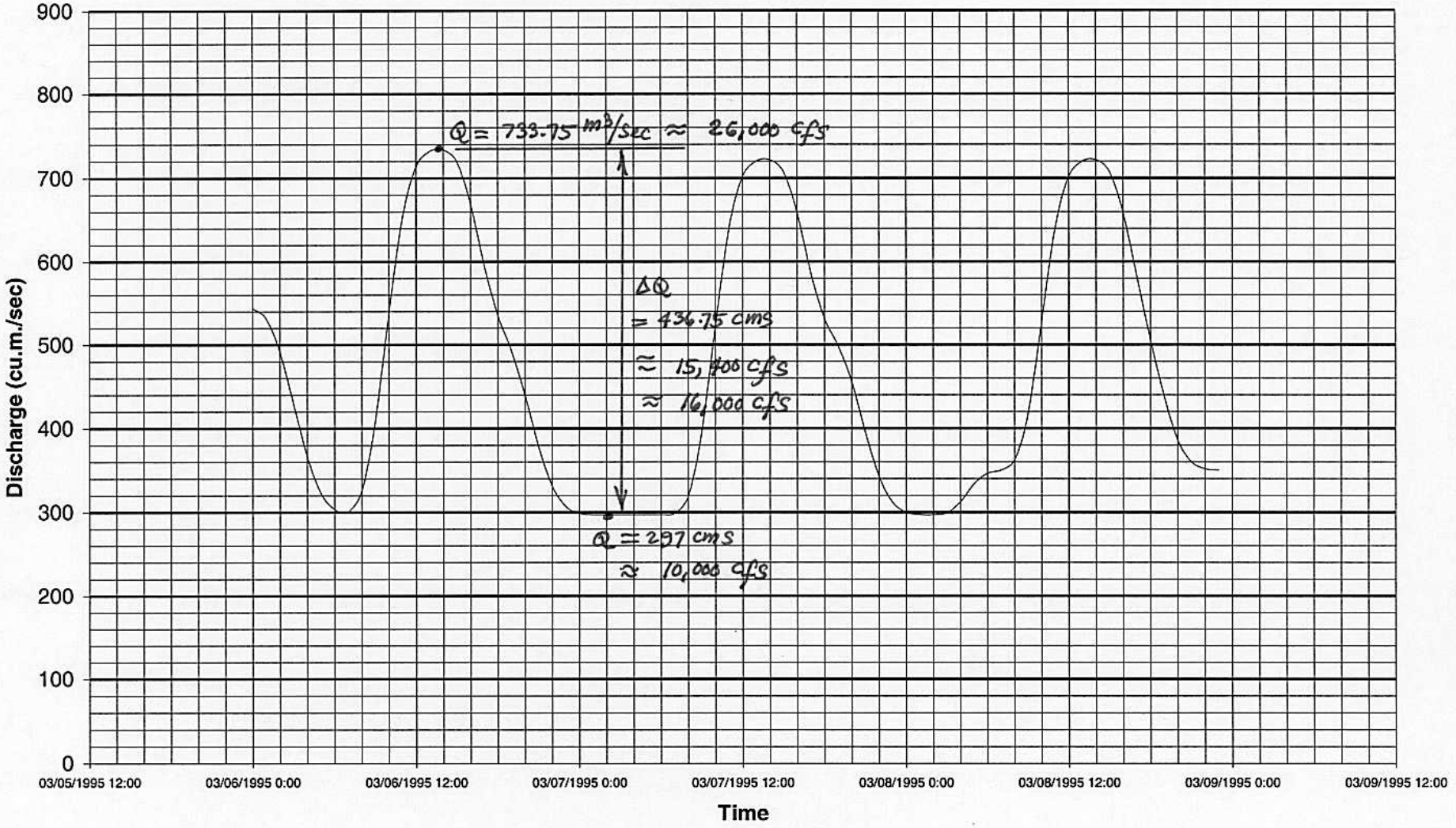

Figure 22

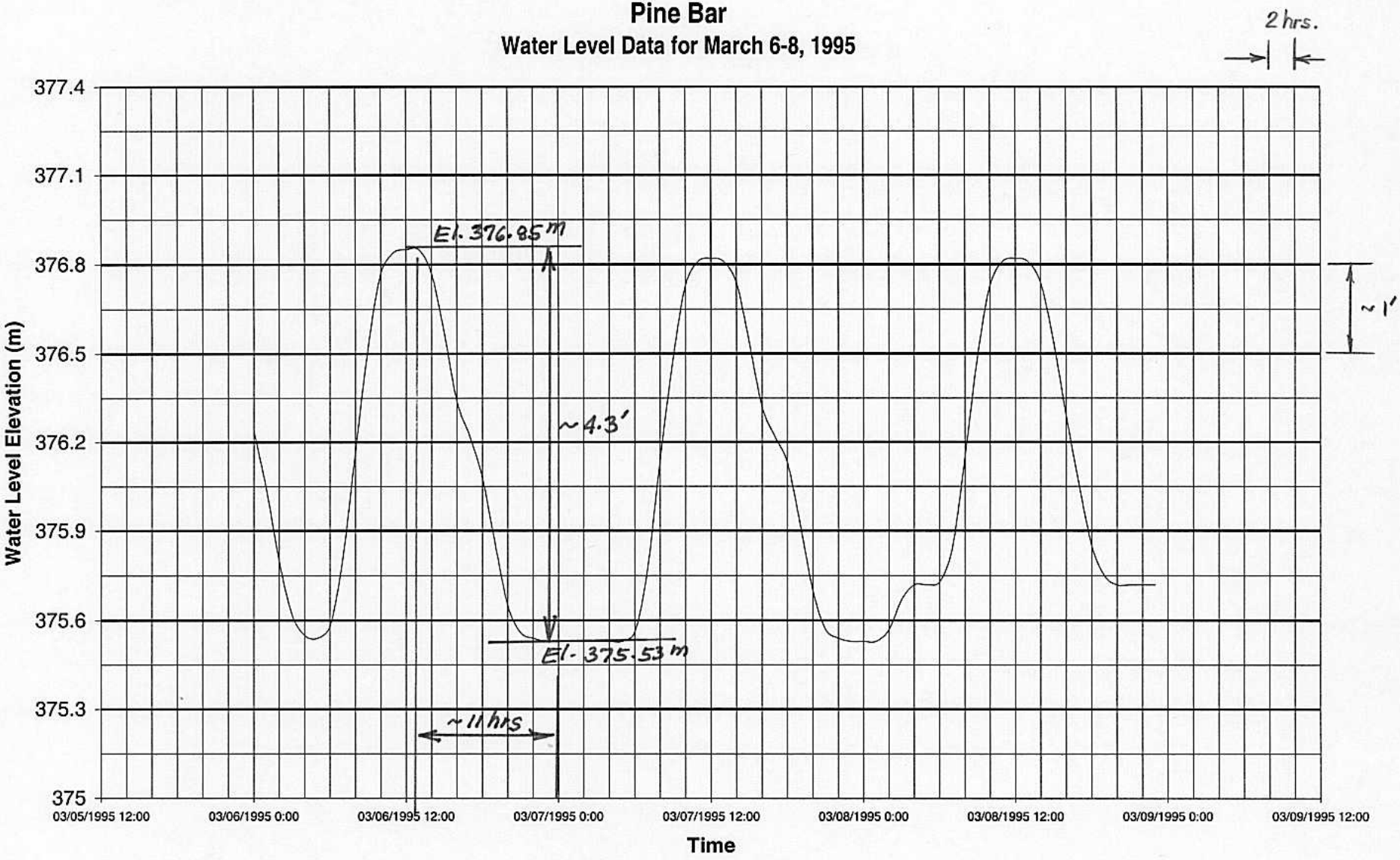
Pine Bar
Water Level Data for March 6-8, 1995
2 hrs.
377.4
377.1
376.8
376.5
376.2
375.9
375.6
375.3
375
Water Level Elevation (m)
El. 376.85 m
~4.3'
El. 375.53 m
~11 hrs
~1'
03/05/1995 12:00
03/06/1995 0:00
03/06/1995 12:00
03/07/1995 0:00
03/07/1995 12:00
03/08/1995 0:00
03/08/1995 12:00
03/09/1995 0:00
03/09/1995 12:00
Time

Figure 23

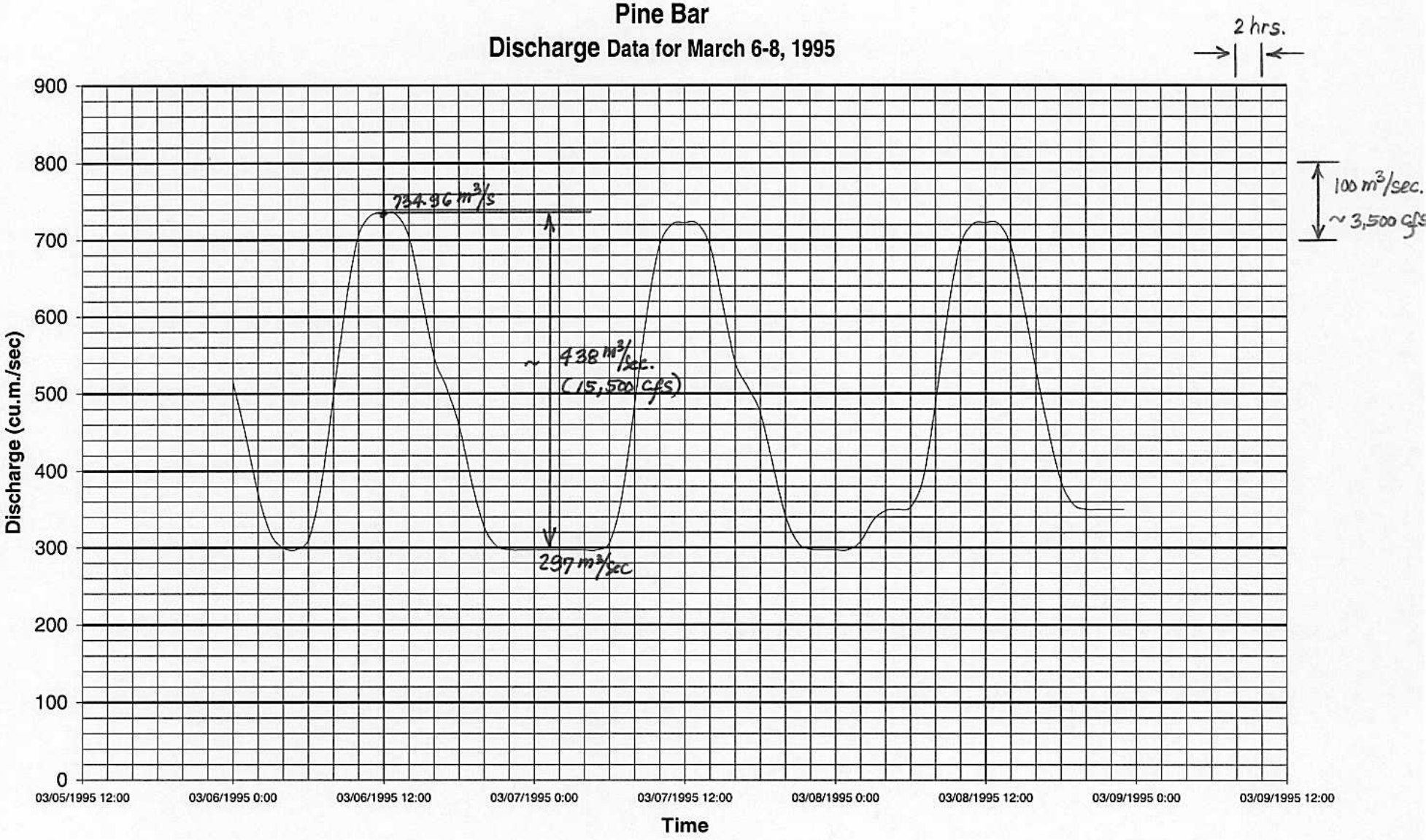
Pine Bar
Discharge Data for March 6-8, 1995
2 hrs.
100 m³/sec.
~ 3,500 cfs
734.96 m³/s
~ 438 m³/sec.
(15,500 cfs)
297 m³/sec
Discharge (cu.m./sec)
900
800
700
600
500
400
300
200
100
0
03/05/1995 12:00
03/06/1995 0:00
03/06/1995 12:00
03/07/1995 0:00
03/07/1995 12:00
03/08/1995 0:00
03/08/1995 12:00
03/09/1995 0:00
03/09/1995 12:00
Time

Figure 24

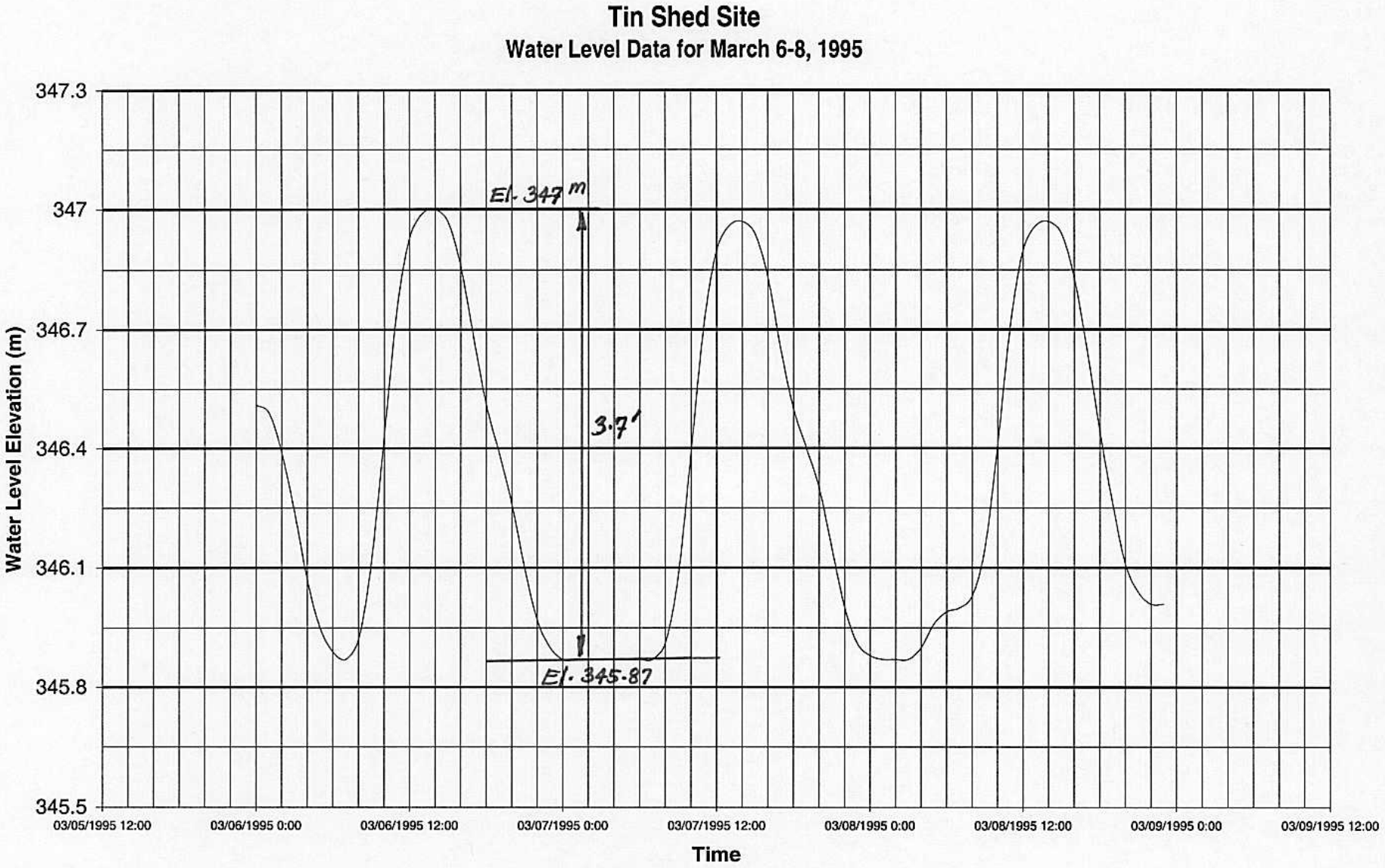
Tin Shed Site
Water Level Data for March 6-8, 1995
Water Level Elevation (m)
347.3
347
346.7
346.4
346.1
345.8
345.5
El. 347 m
3.7'
El. 345.87
03/05/1995 12:00
03/06/1995 0:00
03/06/1995 12:00
03/07/1995 0:00
03/07/1995 12:00
03/08/1995 0:00
03/08/1995 12:00
03/09/1995 0:00
03/09/1995 12:00
Time

Figure 25

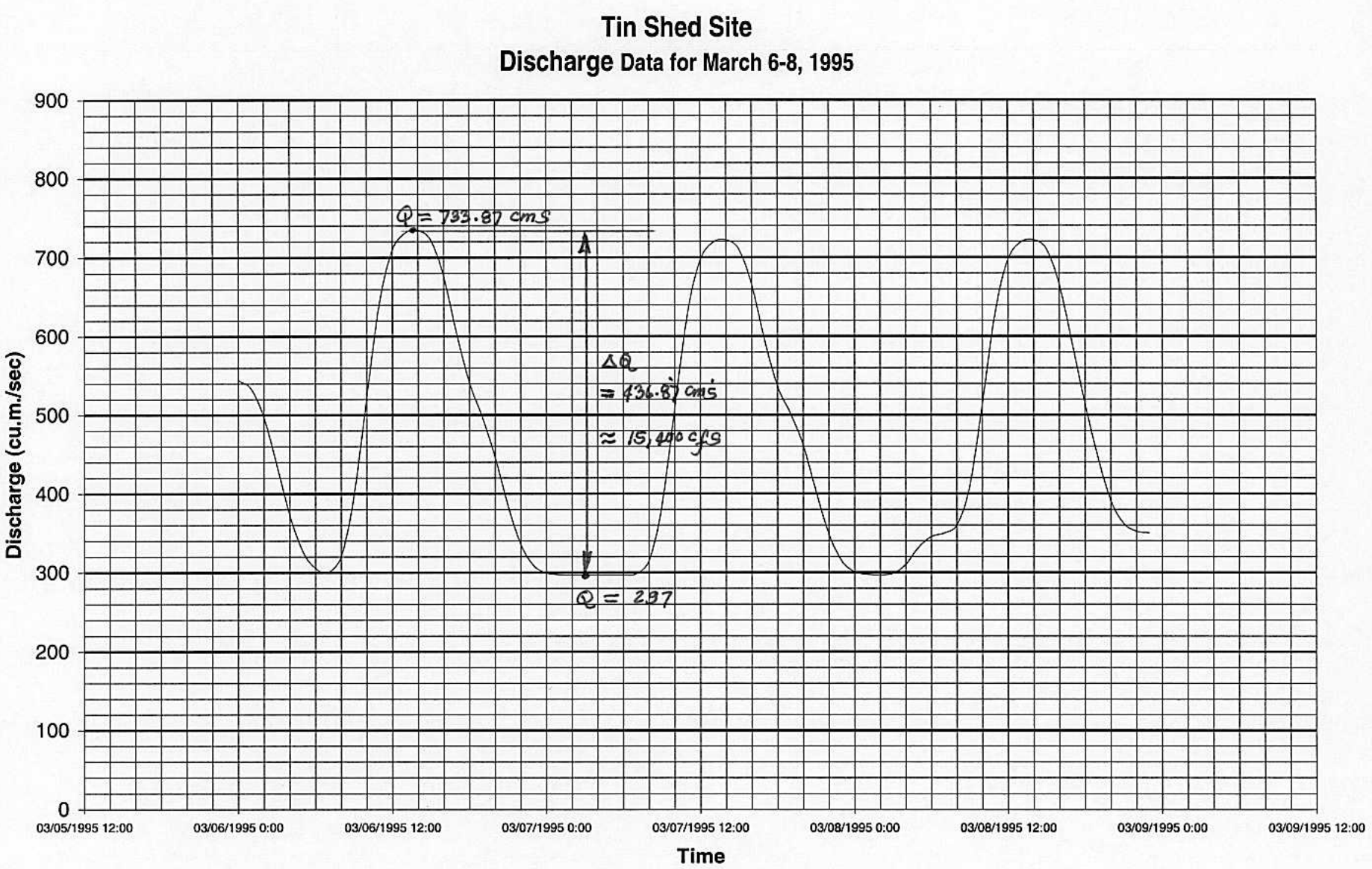
Tin Shed Site
Discharge Data for March 6-8, 1995
Discharge (cu.m./sec)
900
800
700
600
500
400
300
200
100
0
Q = 733.87 cms
A
ΔQ
≈ 436.87 cms
≈ 15,400 cfs
Q = 297
03/05/1995 12:00
03/06/1995 0:00
03/06/1995 12:00
03/07/1995 0:00
03/07/1995 12:00
03/08/1995 0:00
03/08/1995 12:00
03/09/1995 0:00
03/09/1995 12:00
Time

Figure 26

Fish Trap Site
Flood Recession Analysis

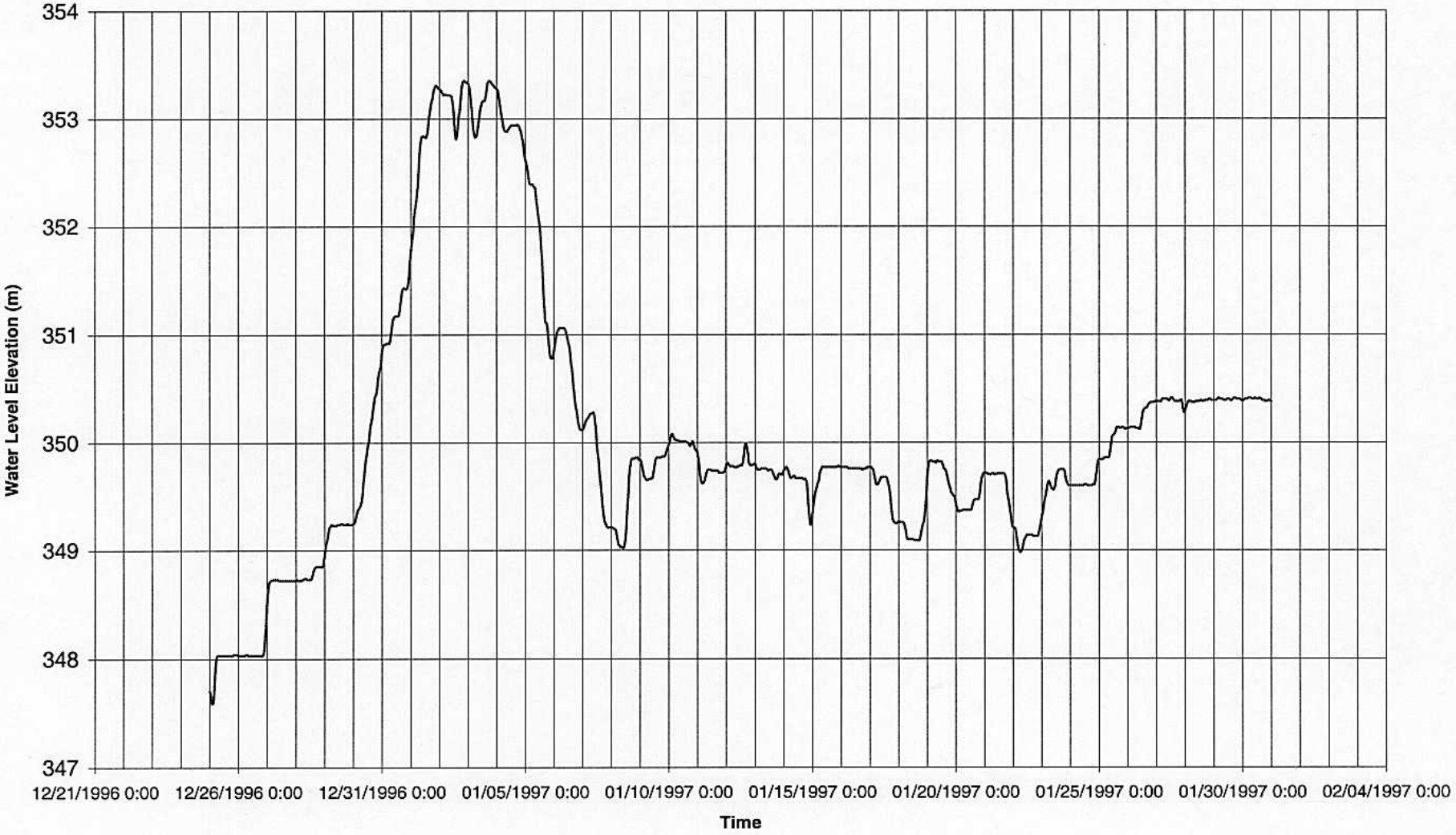

Figure 27

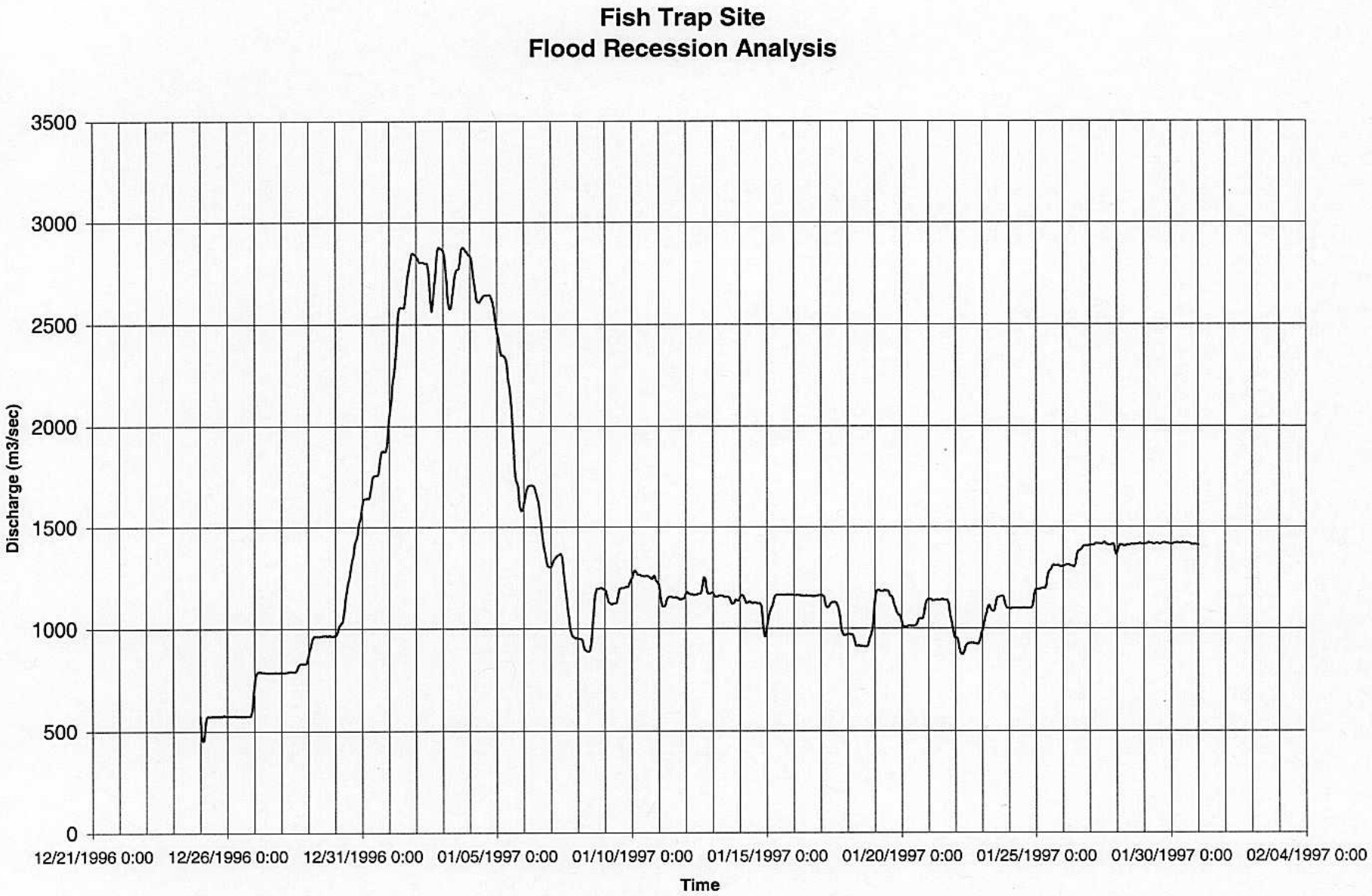
Fish Trap Site
Flood Recession Analysis
Discharge (m3/sec)
3500
3000
2500
2000
1500
1000
500
0
12/21/1996 0:00
12/26/1996 0:00
12/31/1996 0:00
01/05/1997 0:00
01/10/1997 0:00
01/15/1997 0:00
01/20/1997 0:00
01/25/1997 0:00
01/30/1997 0:00
02/04/1997 0:00
Time

Figure 28

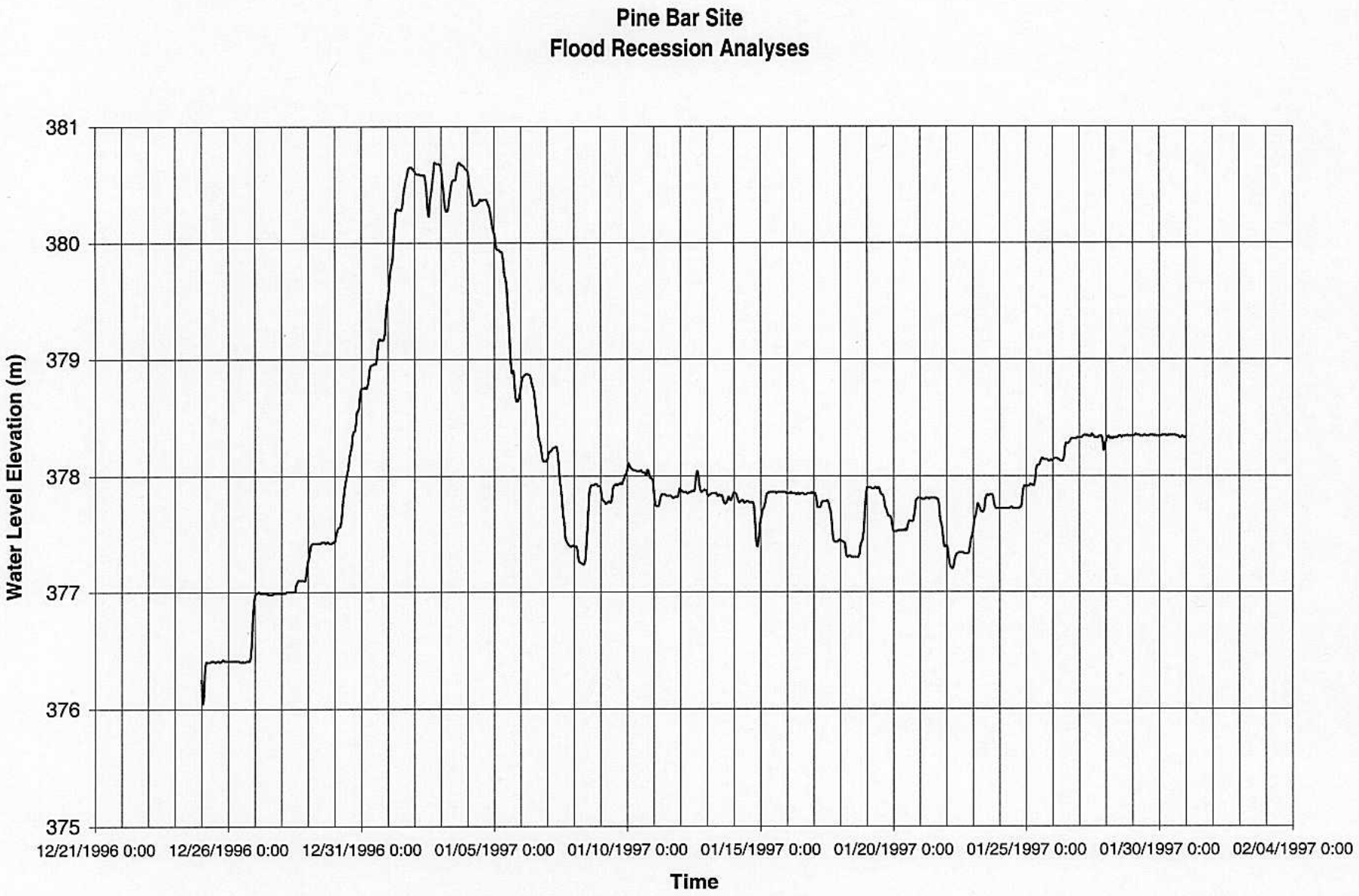
Pine Bar Site
Flood Recession Analyses
Water Level Elevation (m)
381
380
379
378
377
376
375
12/21/1996 0:00
12/26/1996 0:00
12/31/1996 0:00
01/05/1997 0:00
01/10/1997 0:00
01/15/1997 0:00
01/20/1997 0:00
01/25/1997 0:00
01/30/1997 0:00
02/04/1997 0:00
Time

Figure 29

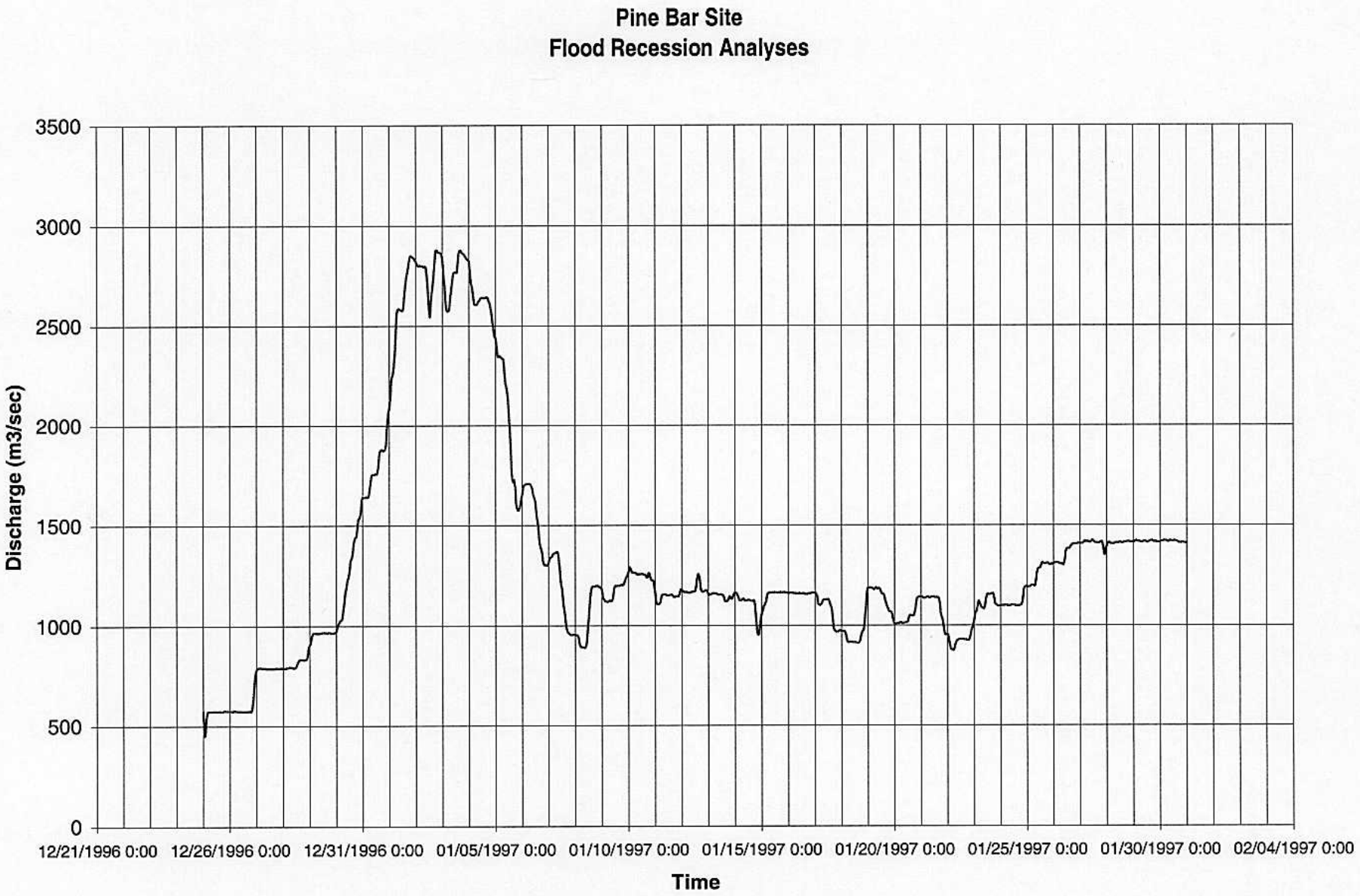
Pine Bar Site
Flood Recession Analyses
Discharge (m3/sec)
3500
3000
2500
2000
1500
1000
500
0
12/21/1996 0:00
12/26/1996 0:00
12/31/1996 0:00
01/05/1997 0:00
01/10/1997 0:00
01/15/1997 0:00
01/20/1997 0:00
01/25/1997 0:00
01/30/1997 0:00
02/04/1997 0:00
Time

Figure 30

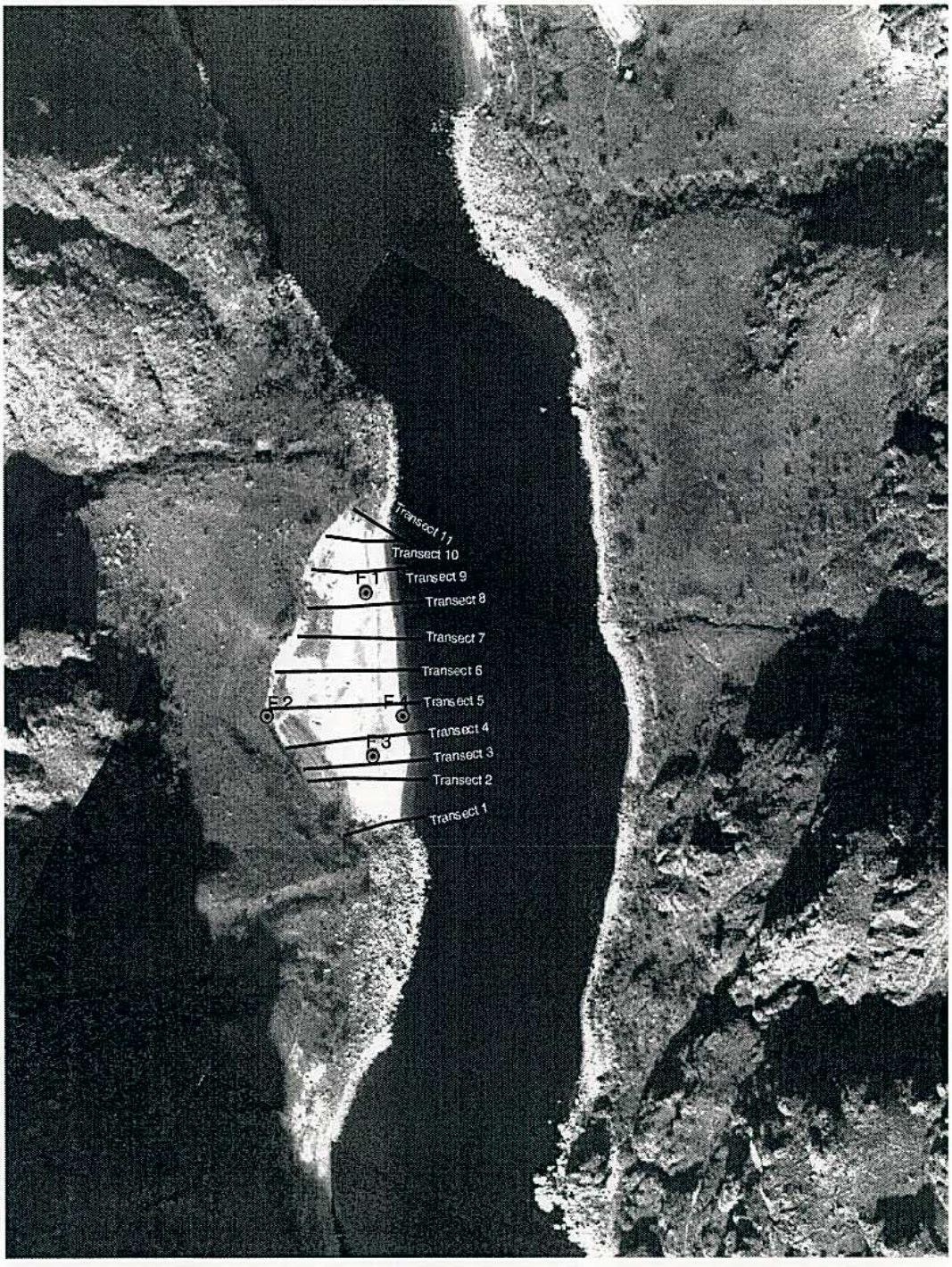

Fish Trap Bar

100 0 100 200 Feet

Figure 31

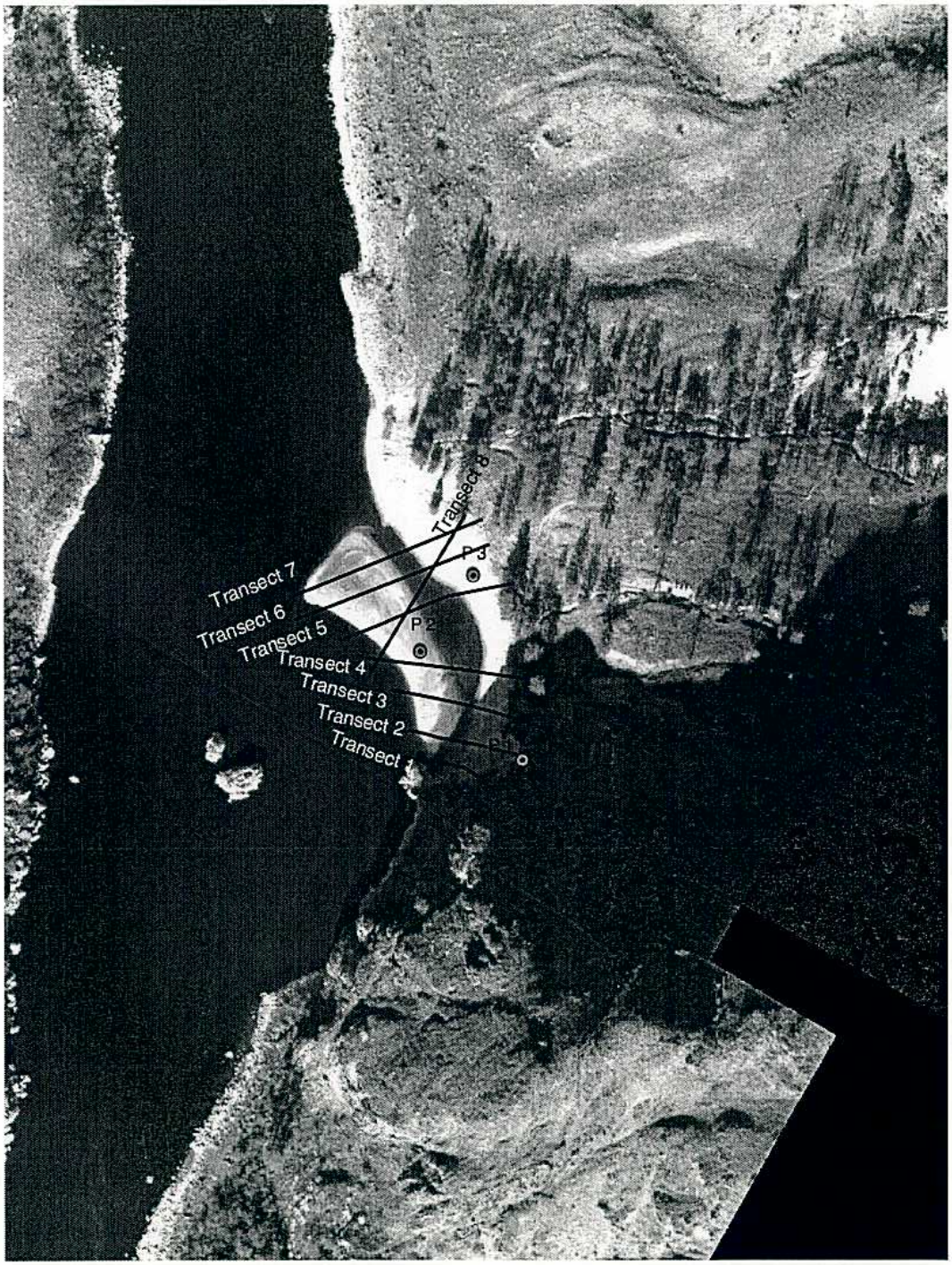
Transect 8
Transect 7
Transect 6
Transect 5
Transect 4
Transect 3
Transect 2
Transect 1
P3
P2
Pine Bar
100 0 100 200 Feet

Figure 32

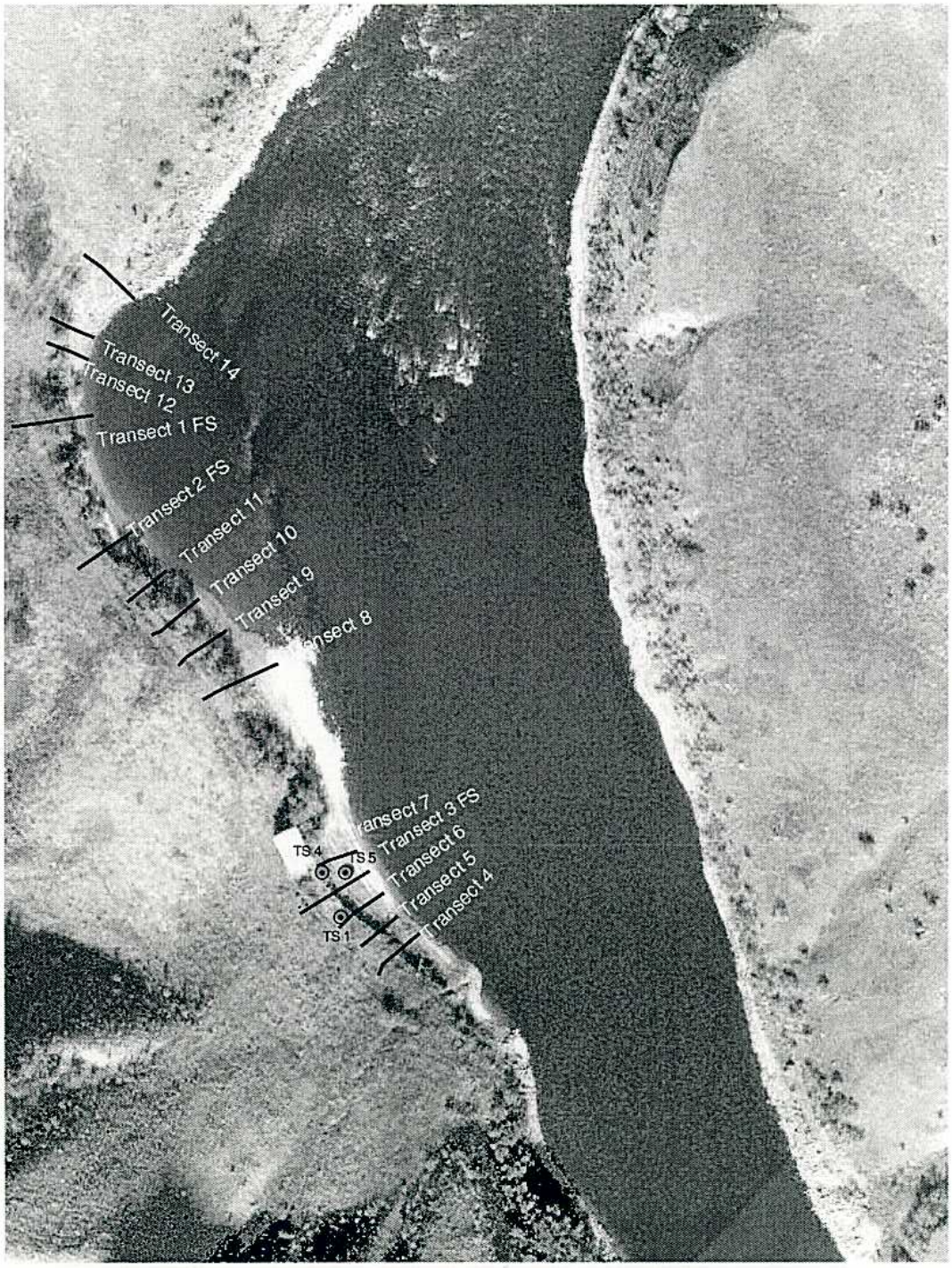

Tin Shed Bar

100 0 100 200 Feet

Figure 33

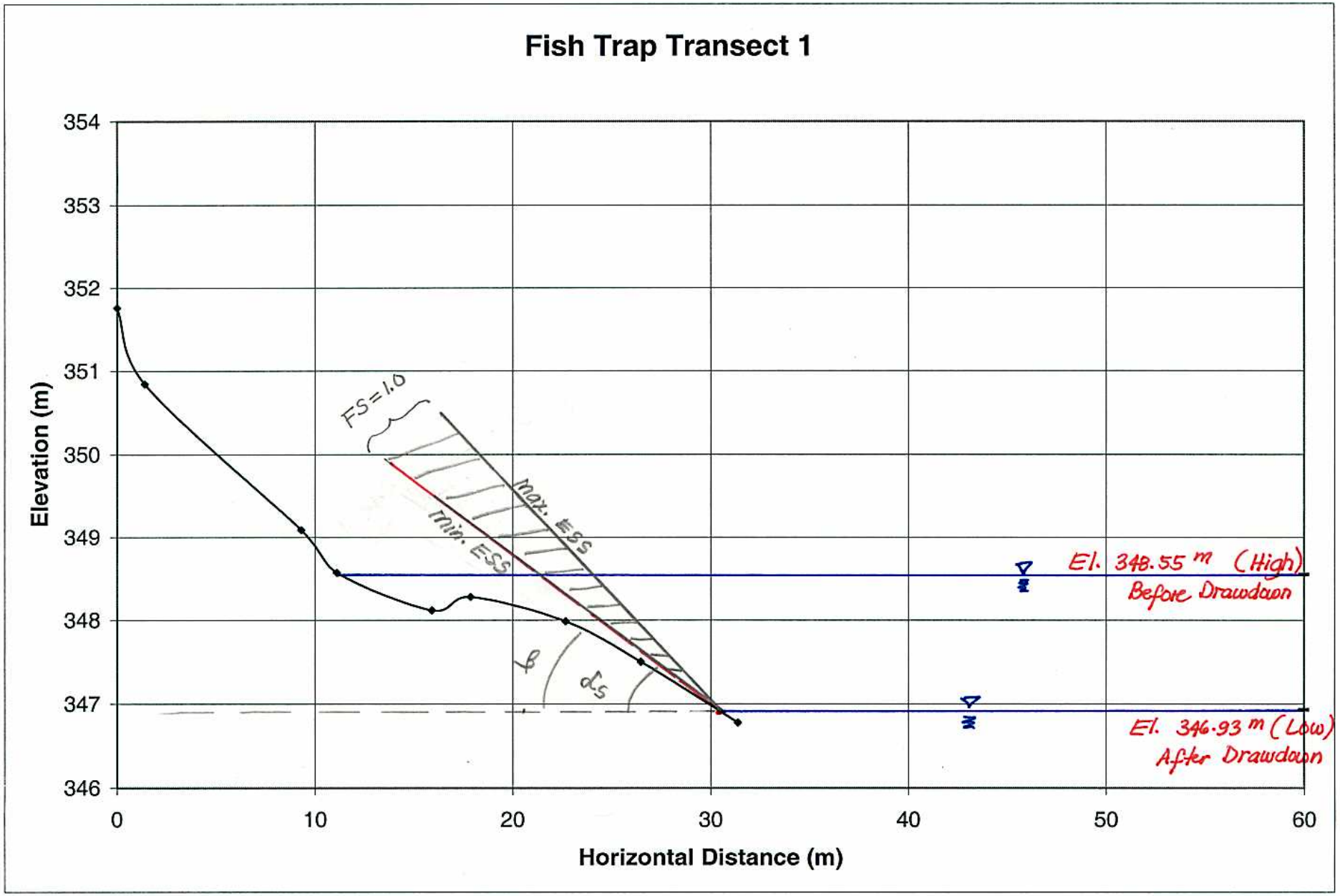
Fish Trap Transect 1
Elevation (m)
354
353
352
351
350
349
348
347
346
0
10
20
30
40
50
60
Horizontal Distance (m)
FS=1.0
max. ESS
min. ESS
El. 348.55 m (High)
Before Drawdown
El. 346.93 m (Low)
After Drawdown

Figure 34

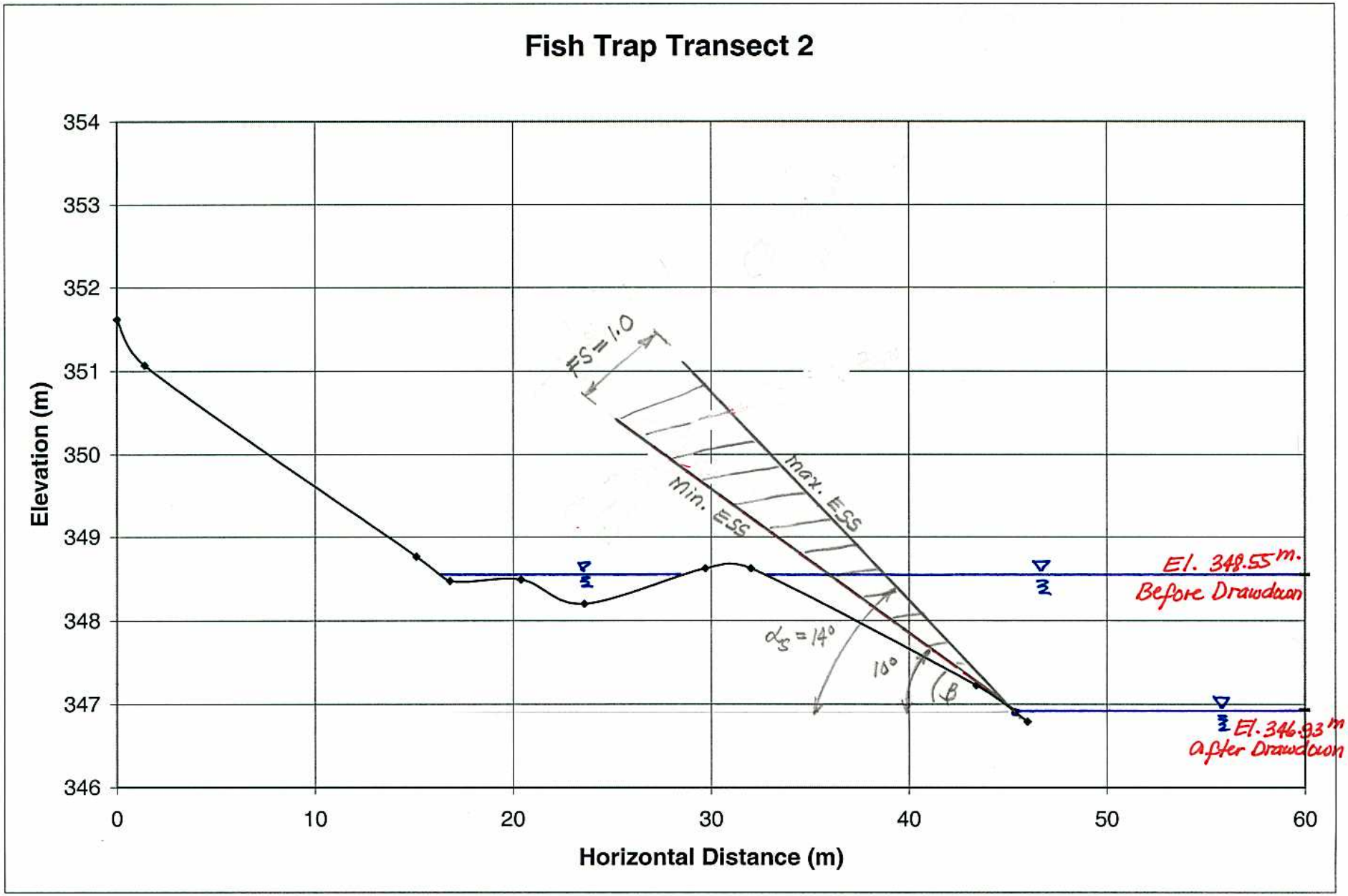
Fish Trap Transect 2
Elevation (m)
354
353
352
351
350
349
348
347
346
0
10
20
30
40
50
60
Horizontal Distance (m)
FS = 1.0
Max. ESS
Min. ESS
El. 348.55 m.
Before Drawdown
$\alpha_s = 14°$
10°
β
El. 346.93 m.
after Drawdown

Figure 35

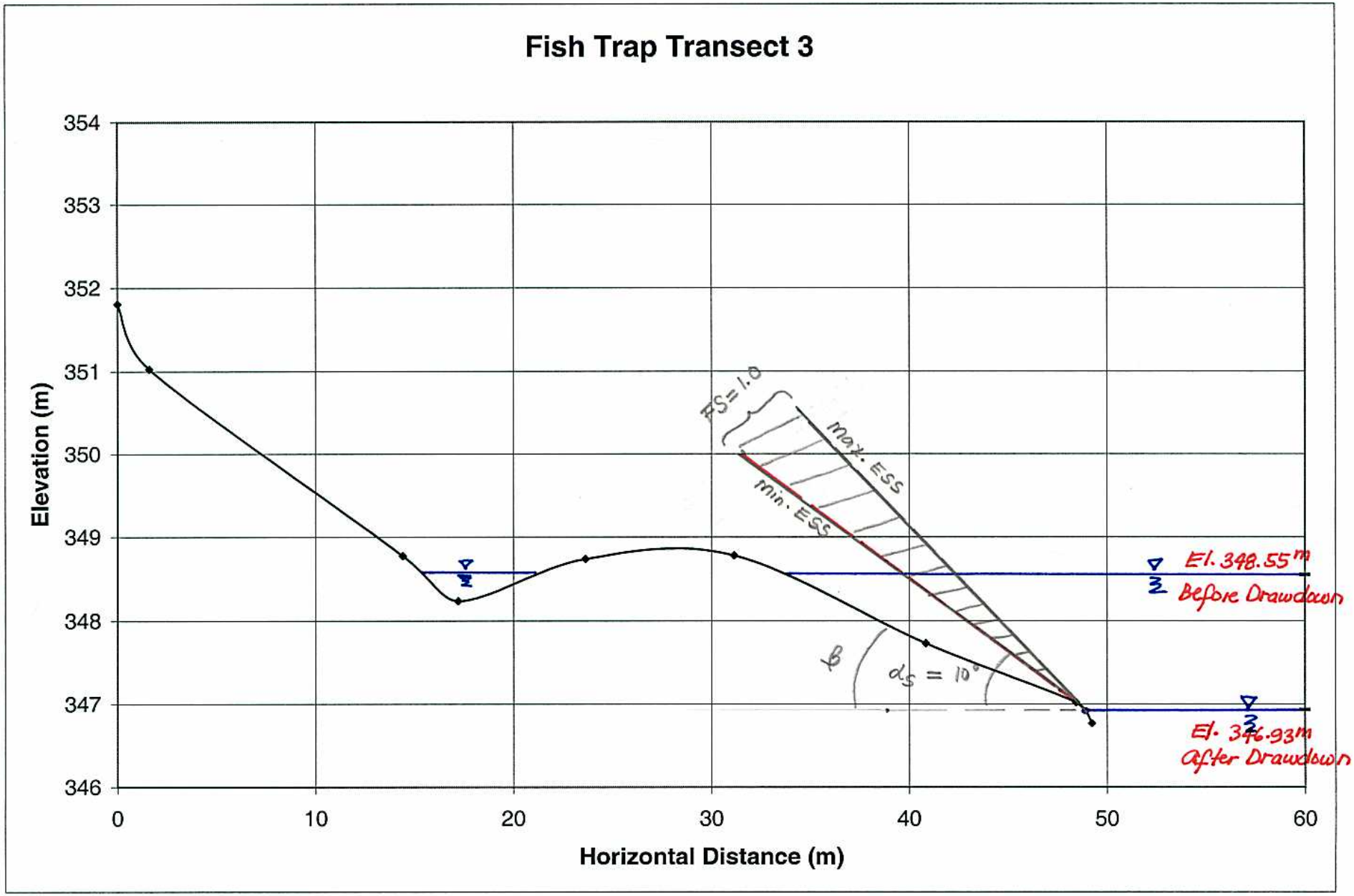
Fish Trap Transect 3
Elevation (m)
354
353
352
351
350
349
348
347
346
0
10
20
30
40
50
60
Horizontal Distance (m)
FS = 1.0
max. ESS
min. ESS
β
d_s = 10°
El. 348.55m
Before Drawdown
El. 346.93m
After Drawdown

Figure 36

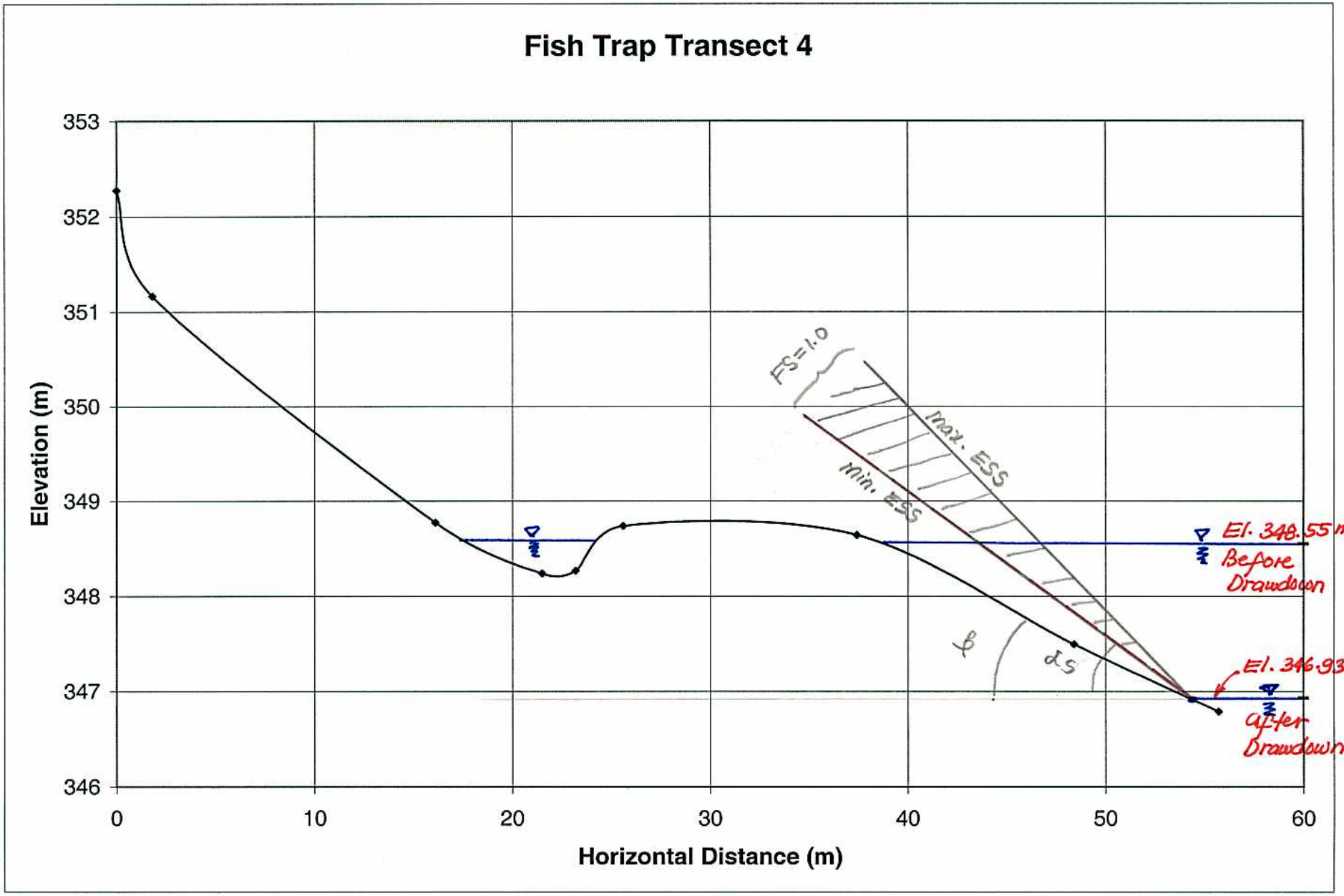
Fish Trap Transect 4
Elevation (m)
353
352
351
350
349
348
347
346
0
10
20
30
40
50
60
Horizontal Distance (m)
FS=1.0
max. ESS
min. ESS
El. 348.55 m
Before Drawdown
El. 346.93 m
After Drawdown
β
αs

Figure 37

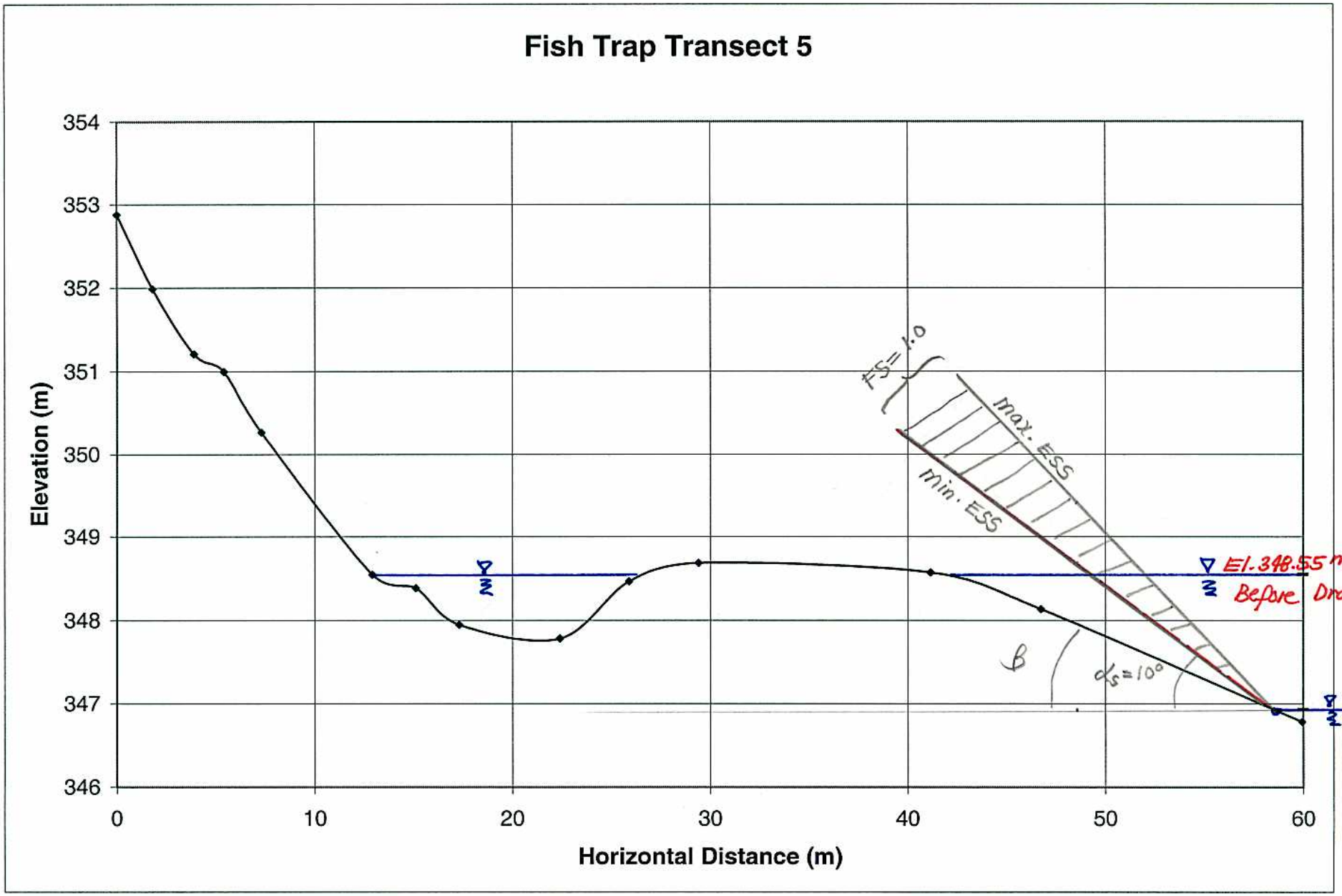
Fish Trap Transect 5
Elevation (m)
354
353
352
351
350
349
348
347
346
0
10
20
30
40
50
60
Horizontal Distance (m)
FS=1.0
max. ESS
min. ESS
El. 348.55 m
Before Drawdown
β
$\phi_s = 10°$
El. 34
after
Drawdo

Figure 38

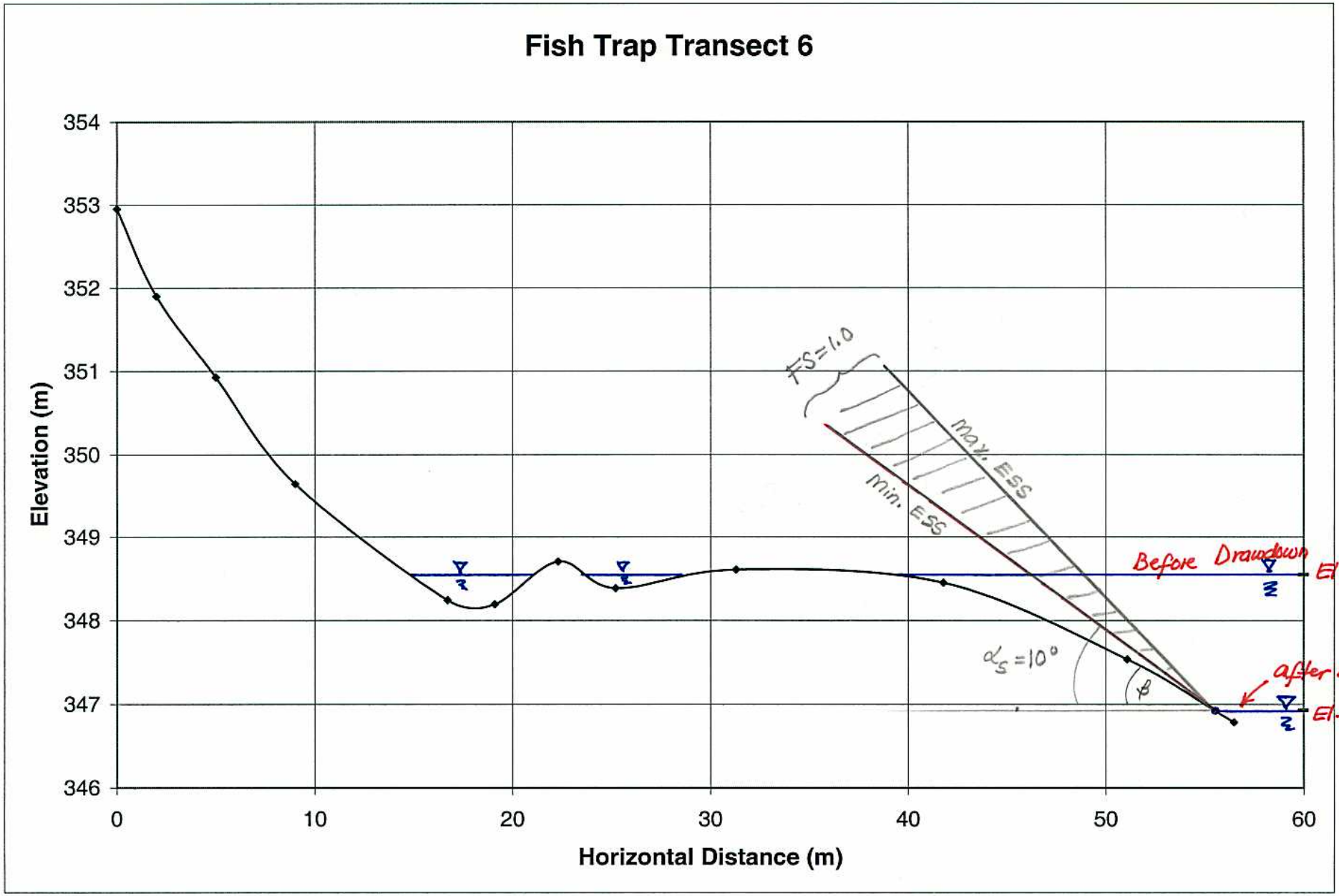
Fish Trap Transect 6
Elevation (m)
354
353
352
351
350
349
348
347
346
0
10
20
30
40
50
60
Horizontal Distance (m)
FS=1.0
max. ESS
min. ESS
Before Drawdown
El.348.55m
after Drawdown
El.346.93m
$\alpha_s = 10°$
β

Figure 39

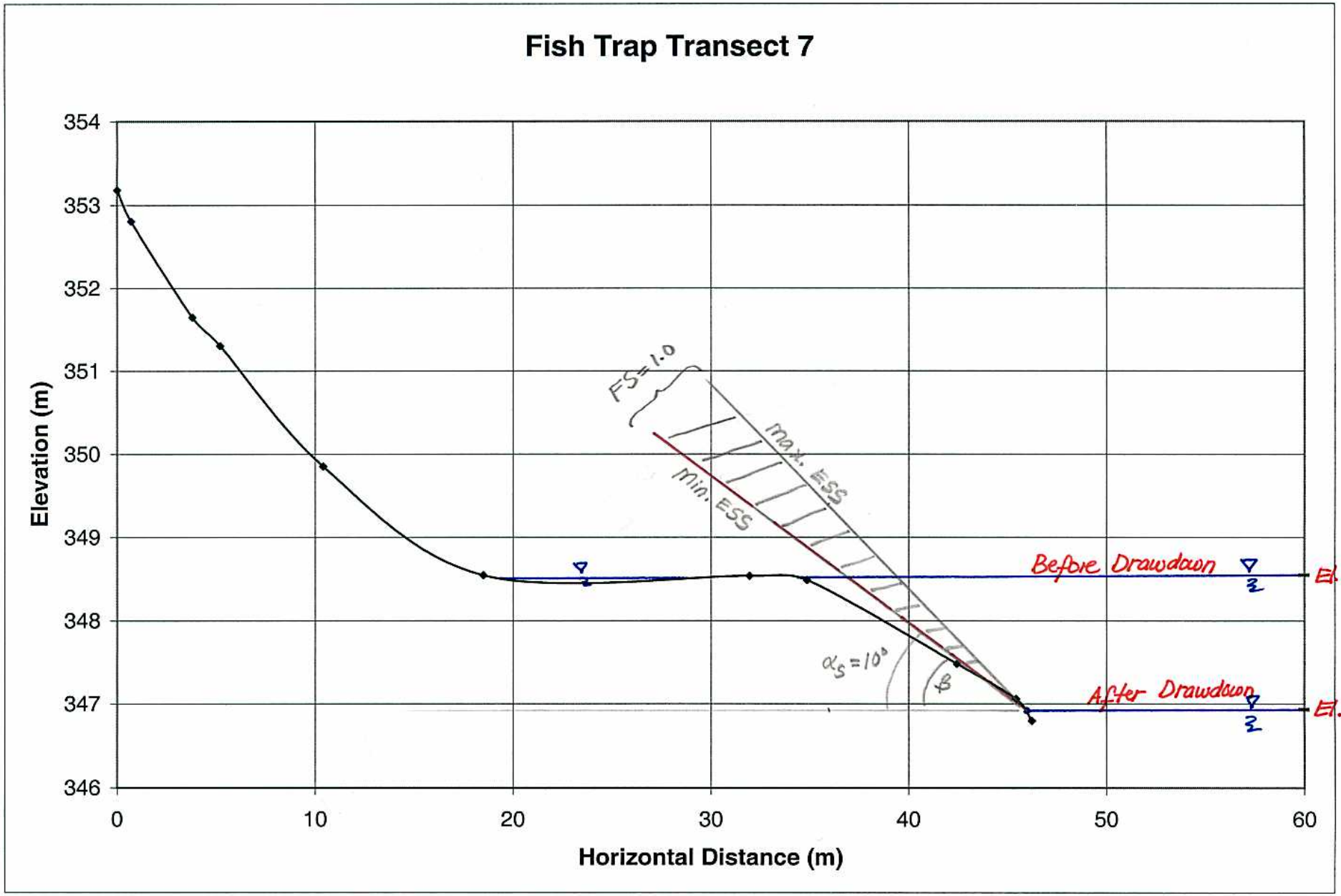
Fish Trap Transect 7
Elevation (m)
354
353
352
351
350
349
348
347
346
0
10
20
30
40
50
60
Horizontal Distance (m)
FS=1.0
max. ESS
min. ESS
Before Drawdown
El. 348.55m
After Drawdown
El. 346.93m
$\alpha_s = 10°$
β

Figure 40

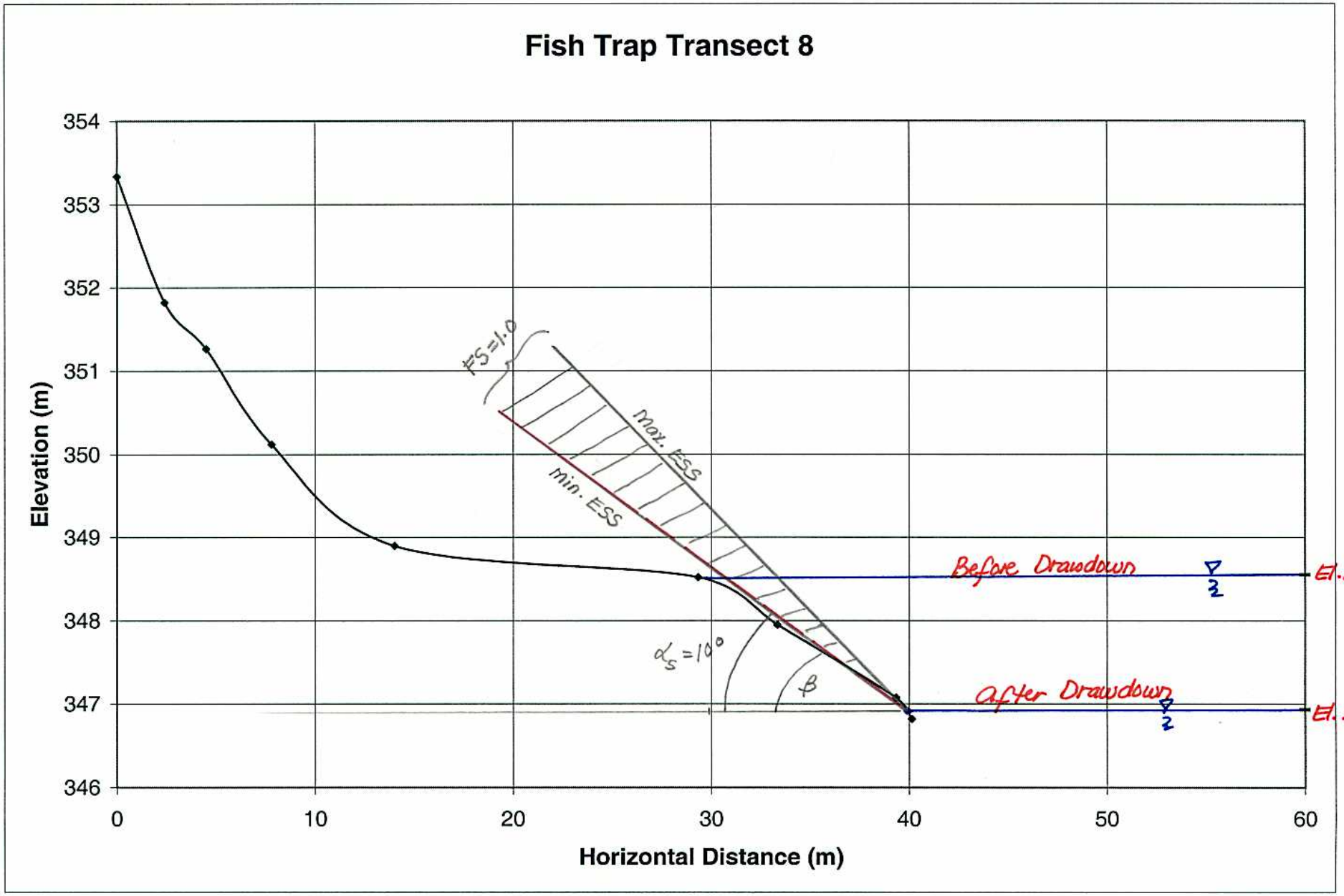
Fish Trap Transect 8
Elevation (m)
354
353
352
351
350
349
348
347
346
0
10
20
30
40
50
60
Horizontal Distance (m)
FS=1.0
Max. ESS
min. ESS
$\alpha_s = 10°$
β
Before Drawdown
El. 348.55 m
after Drawdown
El. 346.93 m.

Figure 41

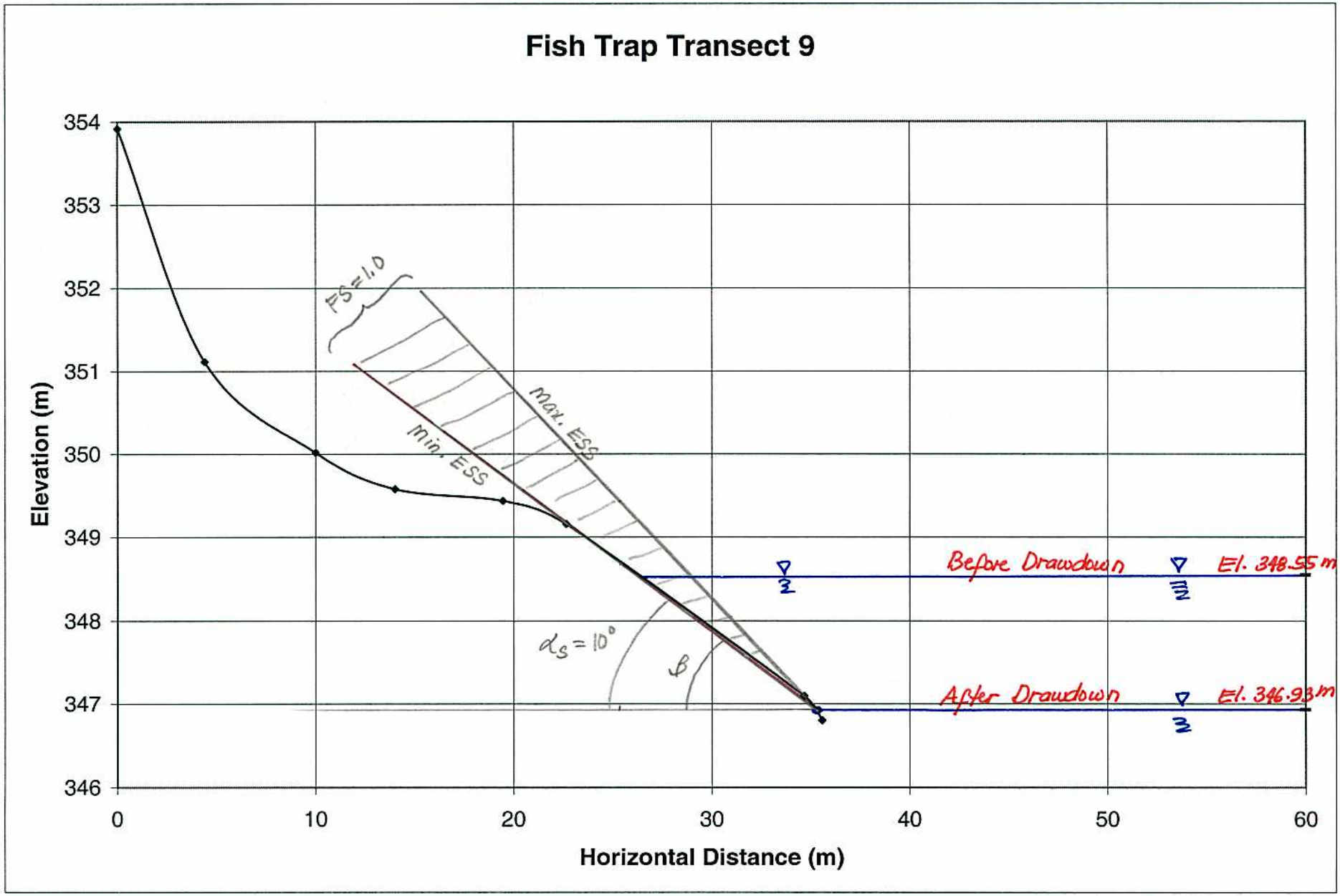
Fish Trap Transect 9
Elevation (m)
354
353
352
351
350
349
348
347
346
0
10
20
30
40
50
60
Horizontal Distance (m)
FS=1.0
max. ESS
min. ESS
$\alpha_s = 10°$
β
Before Drawdown
El. 348.55 m
After Drawdown
El. 346.93 m

Figure 42

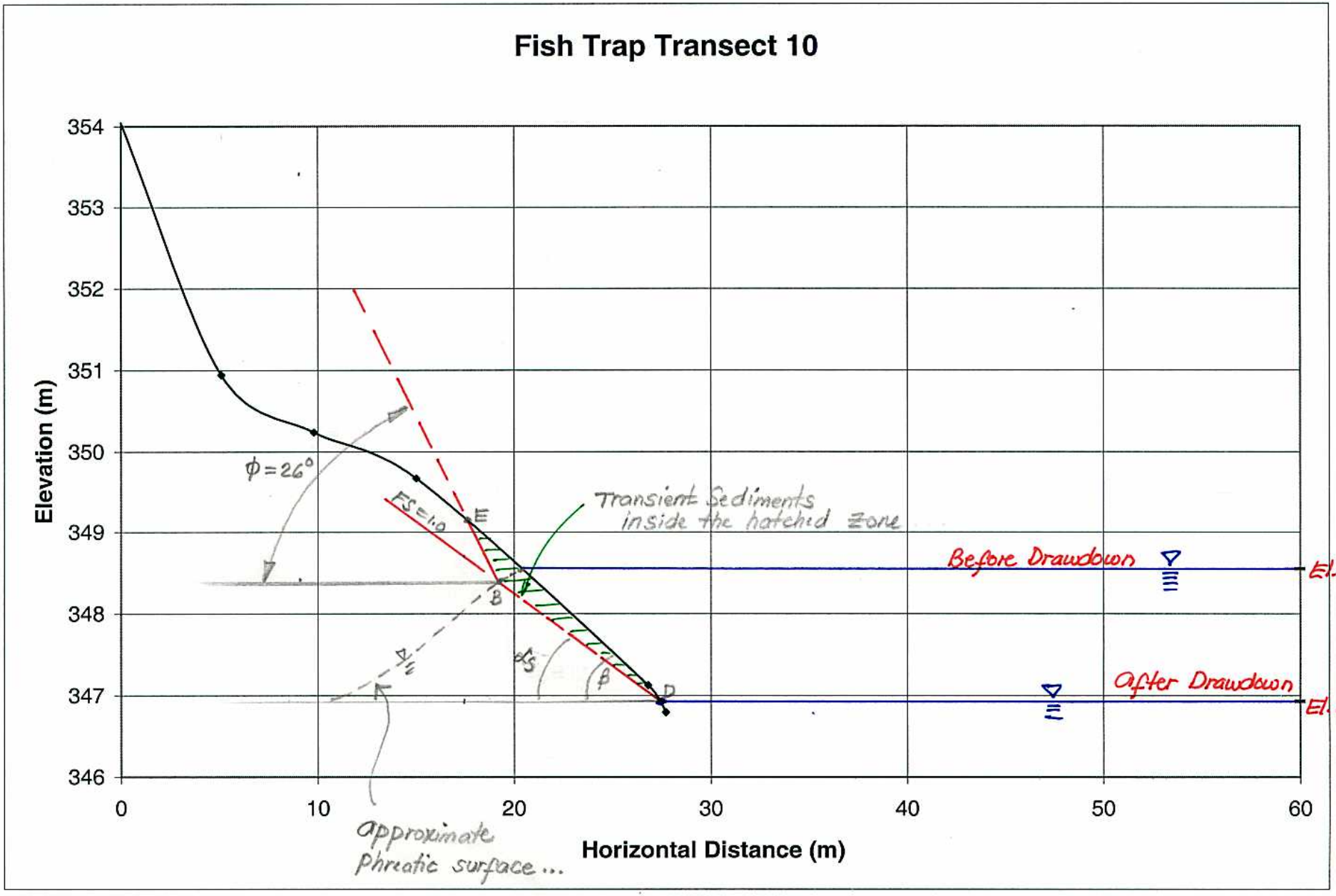
Fish Trap Transect 10
Elevation (m)
354
353
352
351
350
349
348
347
346
0
10
20
30
40
50
60
Horizontal Distance (m)
$\phi = 26°$
FS=1.0
E
B
D
Transient Sediments inside the hatched zone
Before Drawdown
El. 348.55m
after Drawdown
El. 346.93m
approximate Phreatic surface...

Figure 43

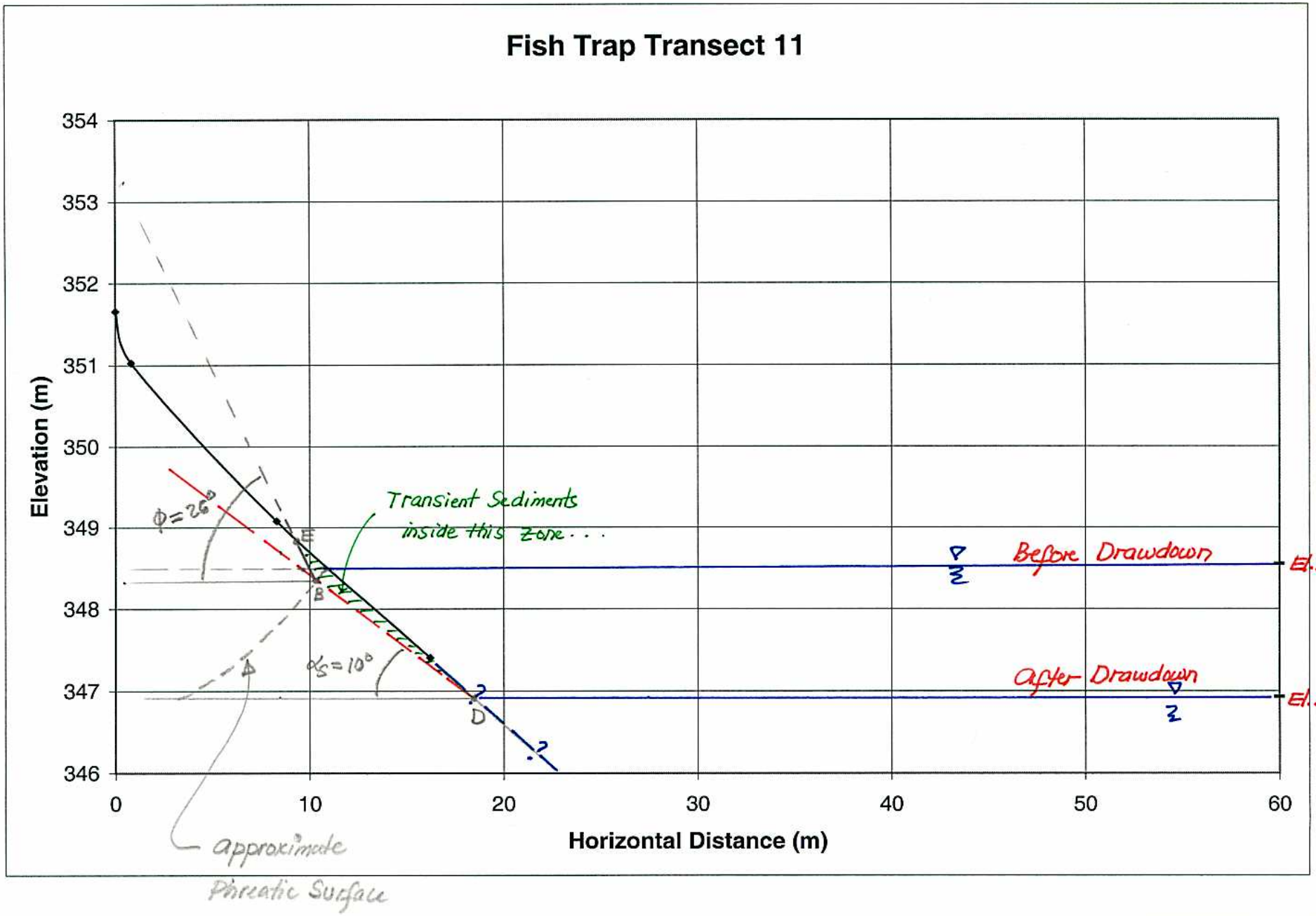
Fish Trap Transect 11
Elevation (m)
354
353
352
351
350
349
348
347
346
0
10
20
30
40
50
60
Horizontal Distance (m)
Transient Sediments
inside this zone . . .
Before Drawdown
El. 348.55m
After Drawdown
El. 346.93m
$\phi = 26°$
$\alpha_s = 10°$
E
B
D
A
approximate
Phreatic Surface

Figure 44

Hells Canyon - Stability Analysis of Sandbars - 16,000 cfs Ld Swing -

C:\KINGSA~1\GEOTEC~1\SOFTWA~1\STEDWIN\HELLLS~1\CASE2.PL2 Run By: King Sampaco - CH2M HILL 02/10/2003 11:31AM

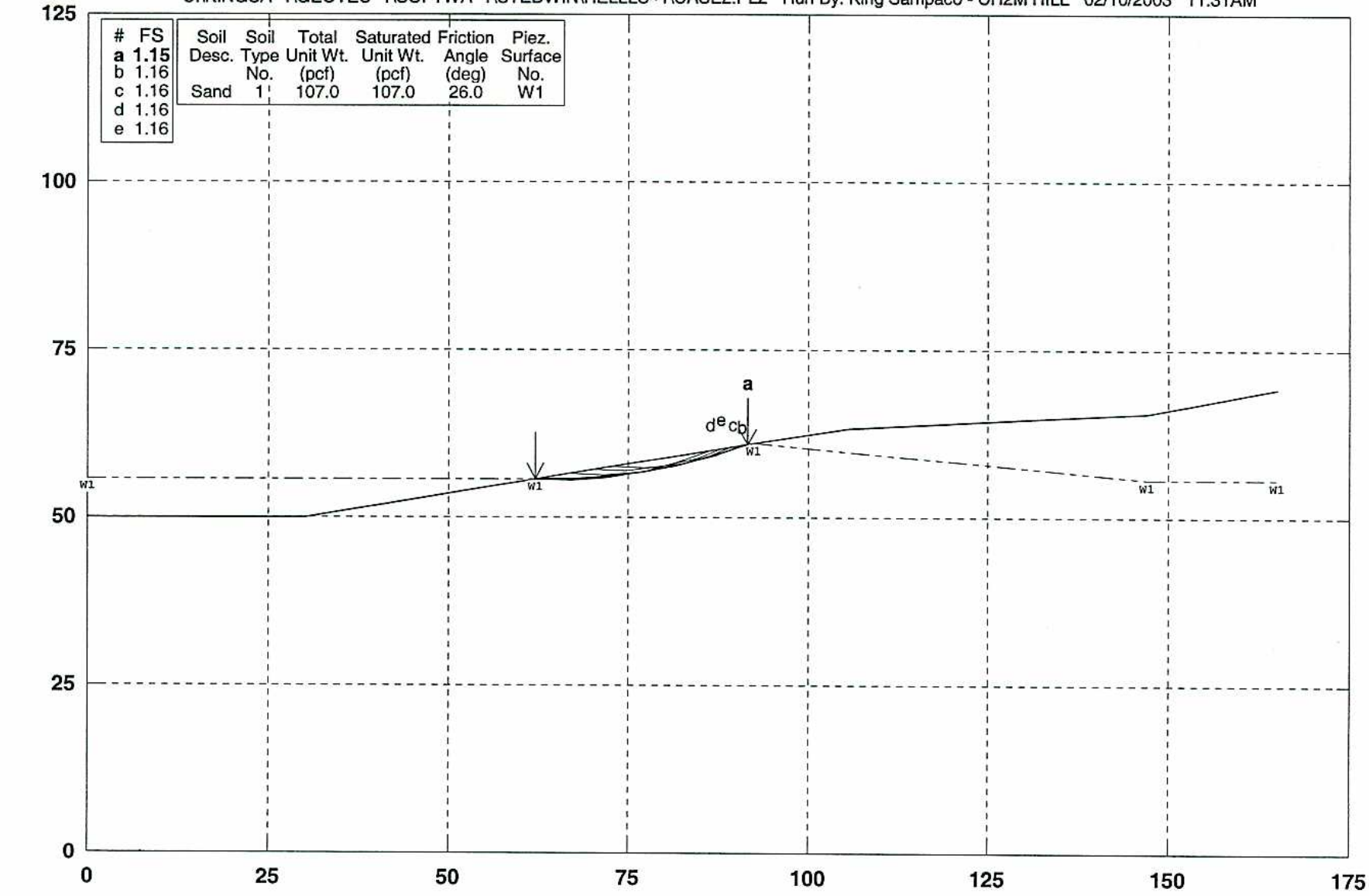

PCSTABL5M/si FSmin=1.15

Safety Factors Are Calculated By The Modified Bishop Method

STED

Figure 45

Hells Canyon - Stability Analysis of Sandbars - 16,000 cfs Ld Swing -

C:\KINGSA~1\GEOTEC~1\SOFTWA~1\STEDWIN\HELLLS~1\CASE4.PL2 Run By: King Sampaco - CH2M HILL 02/10/2003 11:34AM

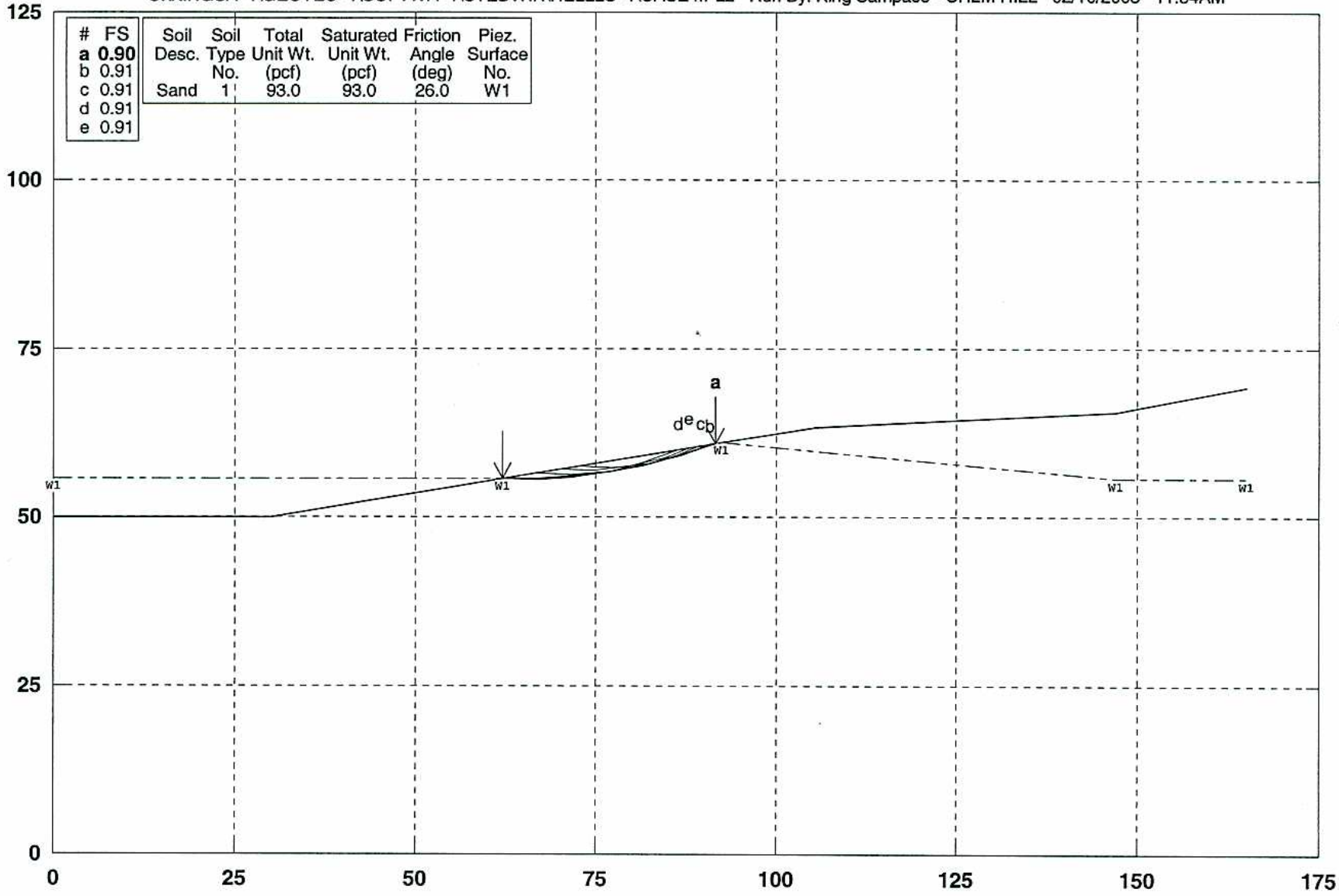

PCSTABL5M/si FSmin=0.90

Safety Factors Are Calculated By The Modified Bishop Method

STED

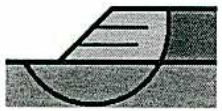

Figure 46

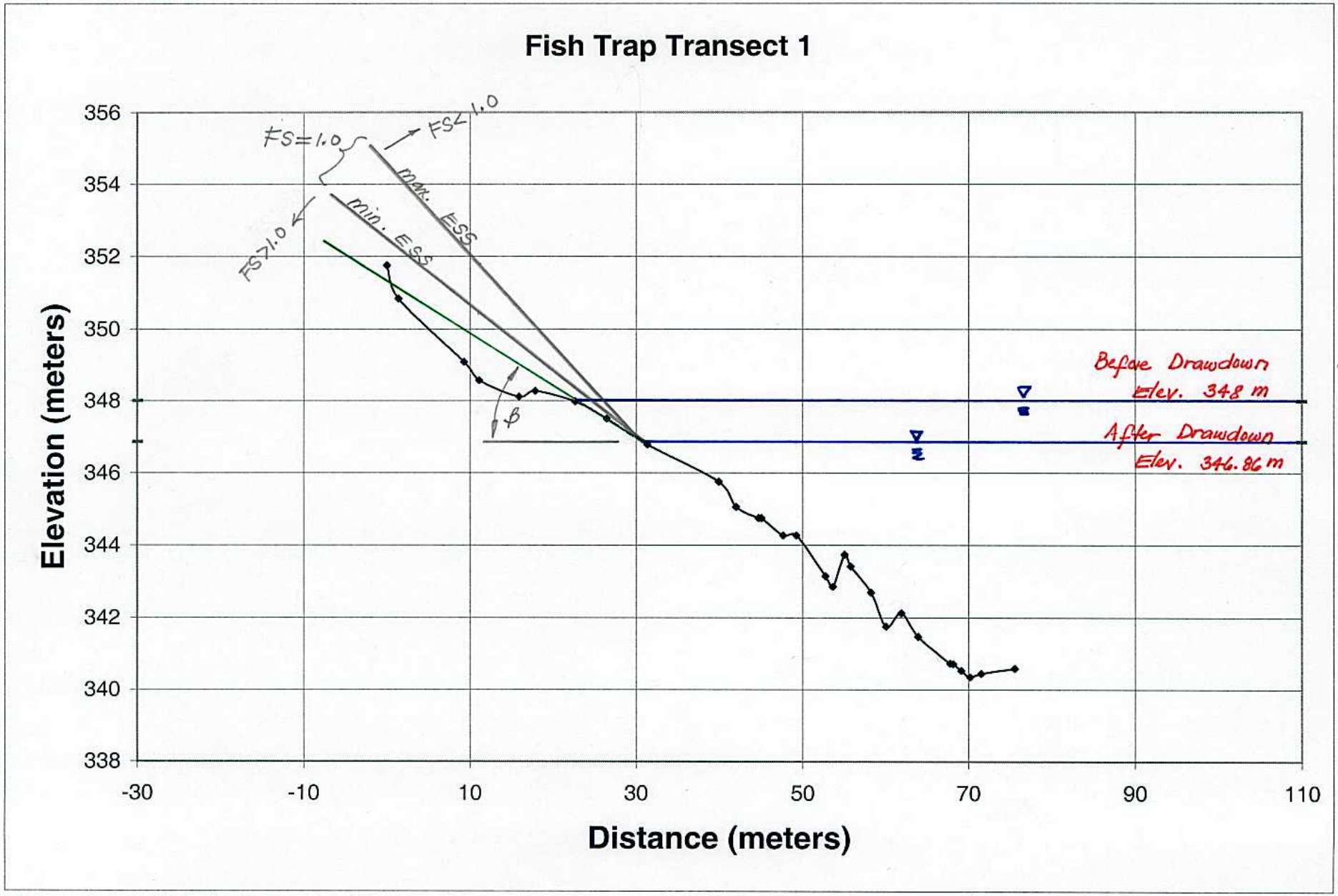
Fish Trap Transect 1
Elevation (meters)
Distance (meters)
356
354
352
350
348
346
344
342
340
338
-30
-10
10
30
50
70
90
110
FS=1.0
FS<1.0
FS>1.0
max. ESS
min. ESS
β
Before Drawdown
Elev. 348 m
After Drawdown
Elev. 346.86 m

Figure 47

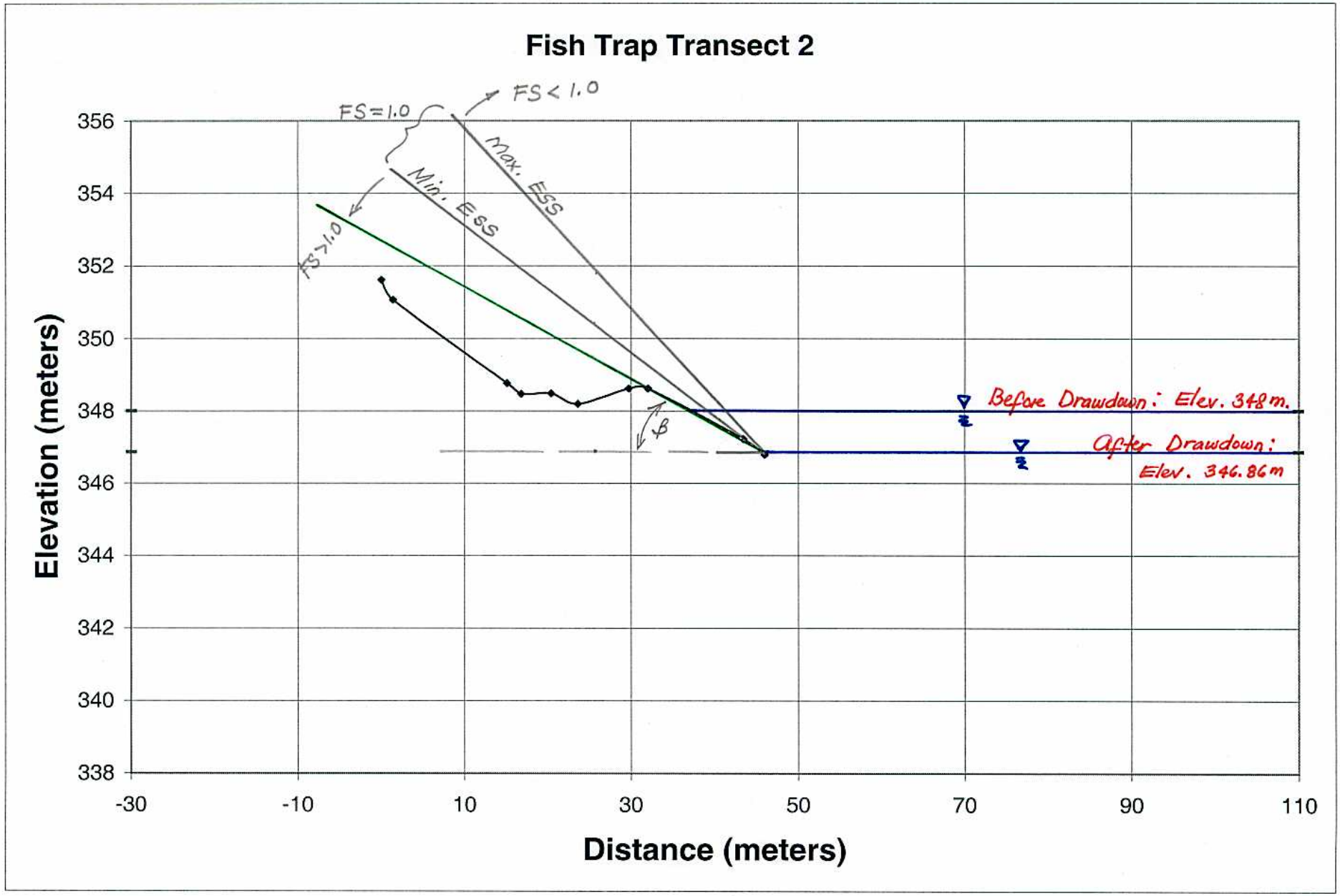
Fish Trap Transect 2
FS = 1.0
FS < 1.0
Max. ESS
Min. ESS
FS > 1.0
β
Before Drawdown: Elev. 348 m.
After Drawdown:
Elev. 346.86 m
Elevation (meters)
356
354
352
350
348
346
344
342
340
338
-30
-10
10
30
50
70
90
110
Distance (meters)

Figure 48

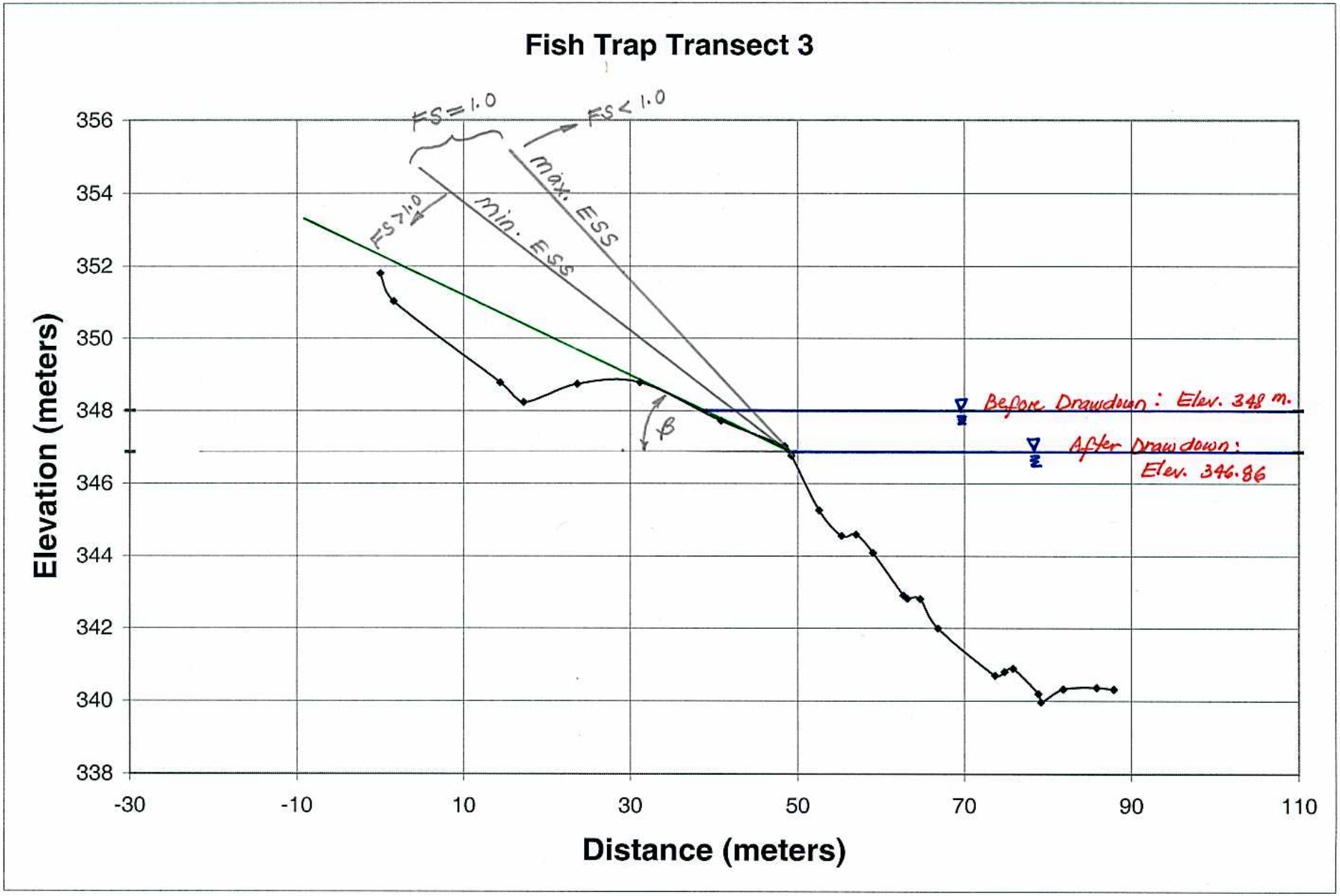
Fish Trap Transect 3
FS = 1.0
FS < 1.0
FS > 1.0
max. ESS
min. ESS
β
Before Drawdown : Elev. 348 m.
After Drawdown : Elev. 346.86
Elevation (meters)
356
354
352
350
348
346
344
342
340
338
-30
-10
10
30
50
70
90
110
Distance (meters)

Figure 49

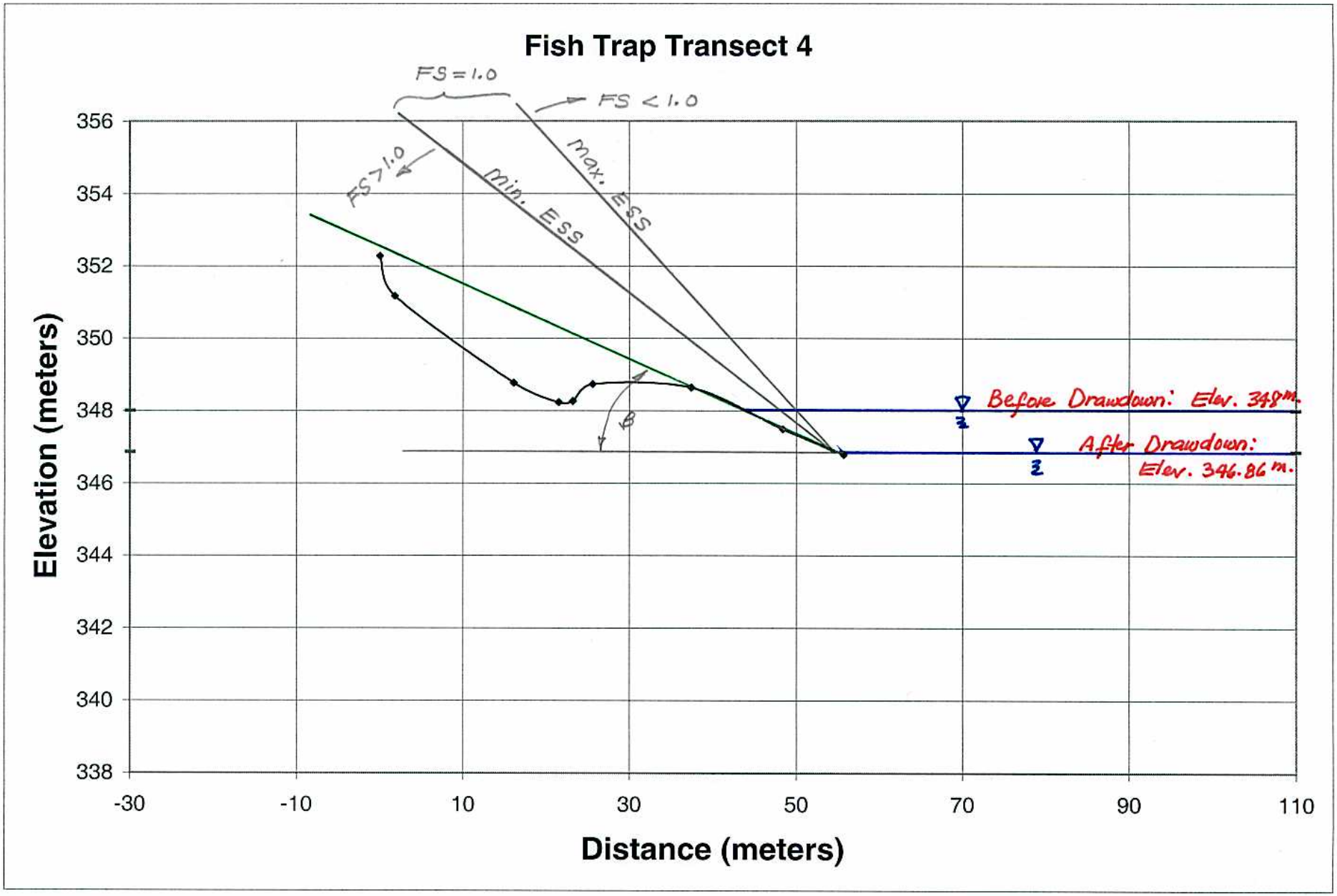
Fish Trap Transect 4
FS = 1.0
FS < 1.0
FS > 1.0
min. ESS
max. ESS
B
Before Drawdown: Elev. 348 m.
After Drawdown:
Elev. 346.86 m.
Elevation (meters)
356
354
352
350
348
346
344
342
340
338
-30
-10
10
30
50
70
90
110
Distance (meters)

Figure 50

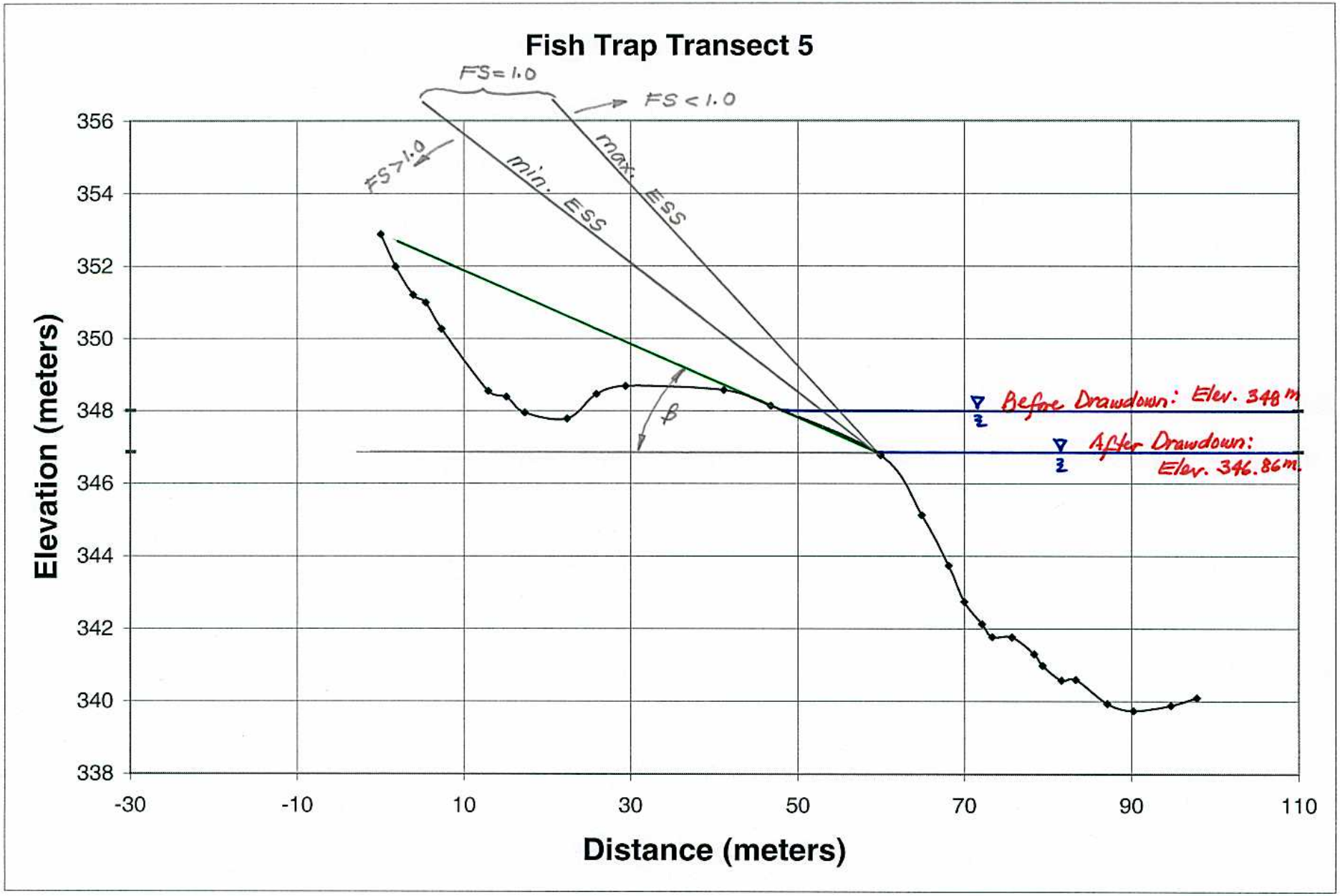
Fish Trap Transect 5
FS=1.0
FS<1.0
FS>1.0
min. ESS
max. ESS
β
Before Drawdown: Elev. 348 m
After Drawdown:
Elev. 346.86m.
Elevation (meters)
356
354
352
350
348
346
344
342
340
338
-30
-10
10
30
50
70
90
110
Distance (meters)

Figure 51

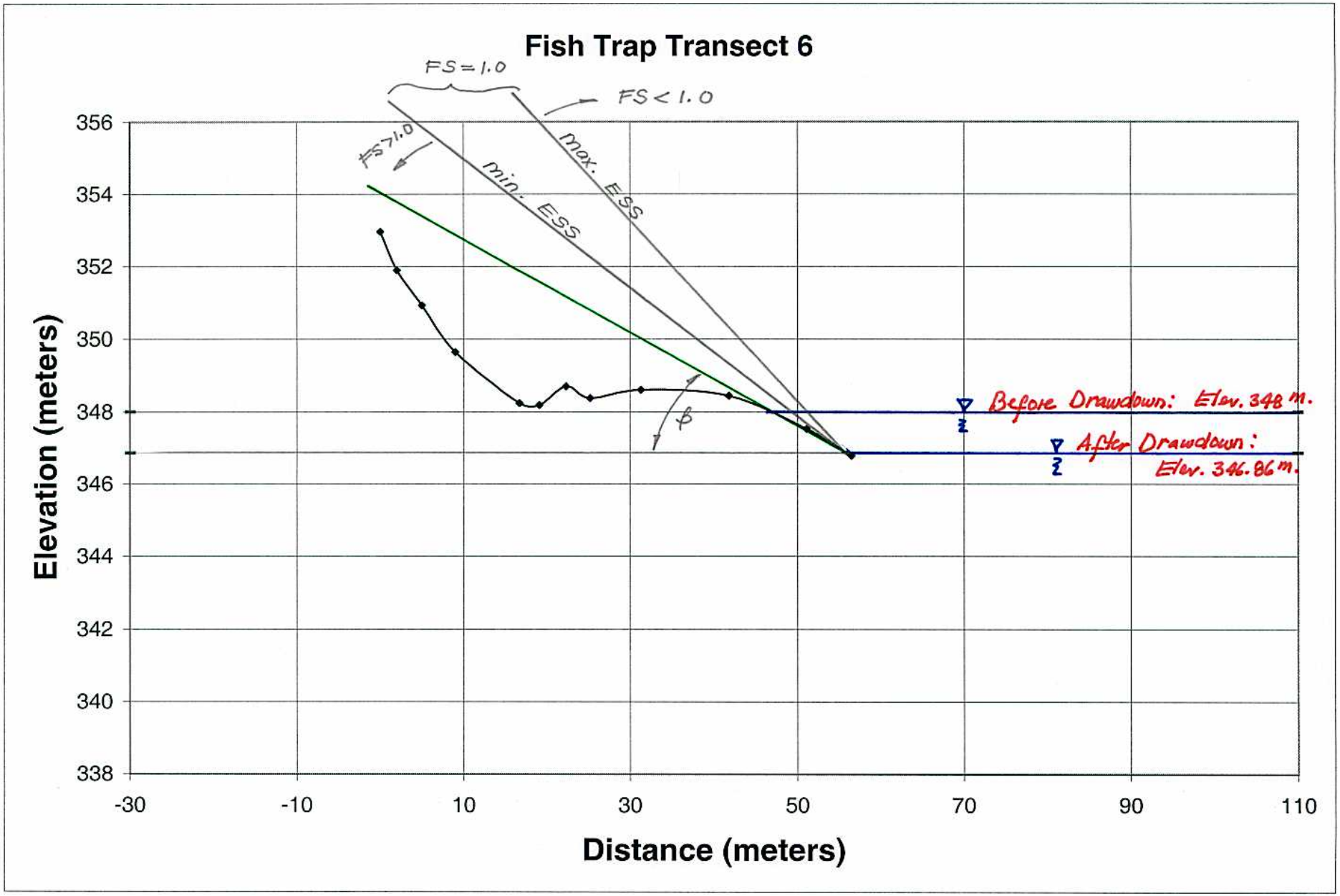
Fish Trap Transect 6
FS = 1.0
FS < 1.0
FS > 1.0
max. ESS
min. ESS
β
Before Drawdown: Elev. 348 m.
After Drawdown: Elev. 346.86 m.
Elevation (meters)
356
354
352
350
348
346
344
342
340
338
-30
-10
10
30
50
70
90
110
Distance (meters)

Figure 52

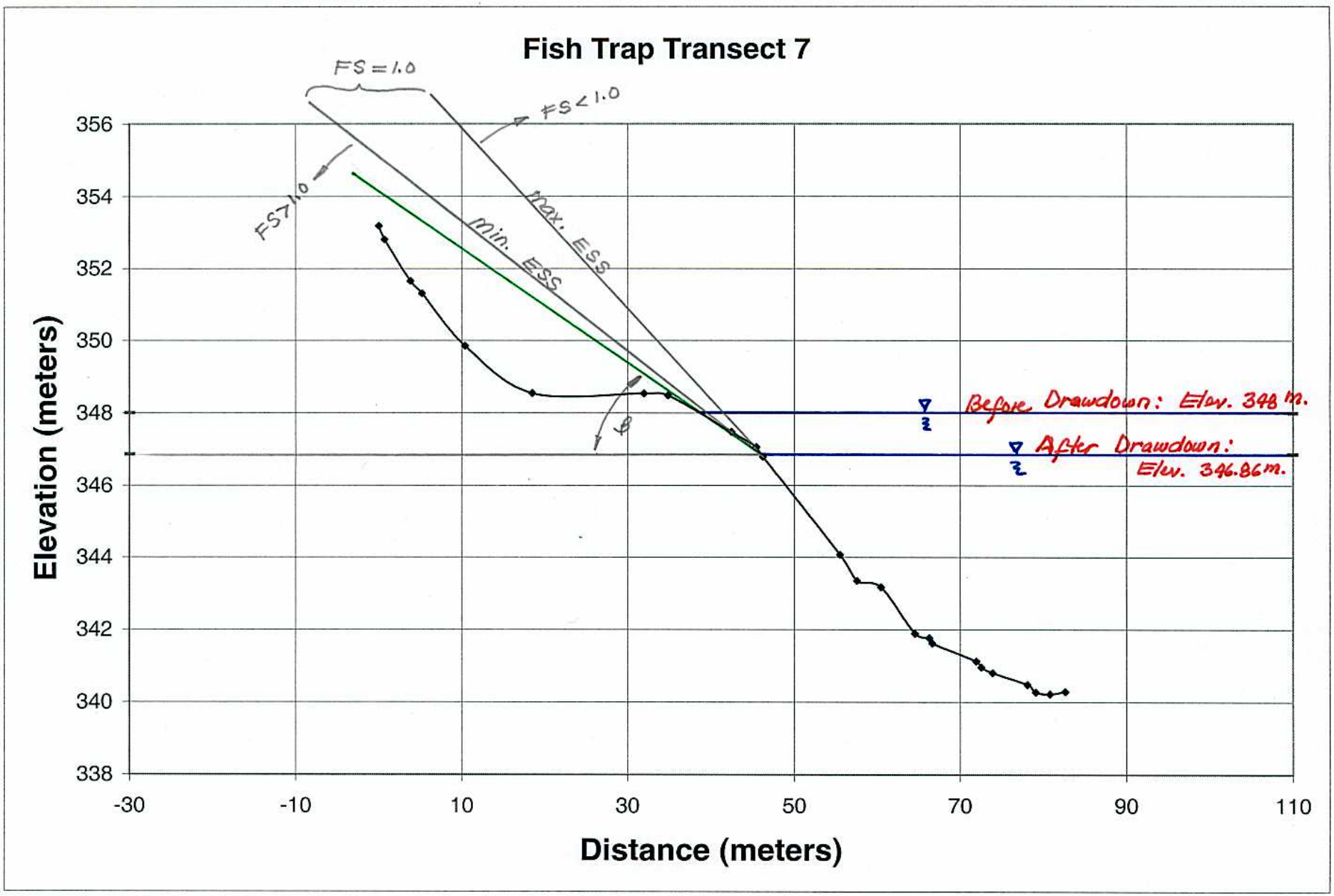
Fish Trap Transect 7
FS = 1.0
FS < 1.0
FS > 1.0
max. ESS
min. ESS
β
Before Drawdown: Elev. 348 m.
After Drawdown:
Elev. 346.86 m.
Elevation (meters)
356
354
352
350
348
346
344
342
340
338
-30
-10
10
30
50
70
90
110
Distance (meters)

Figure 53

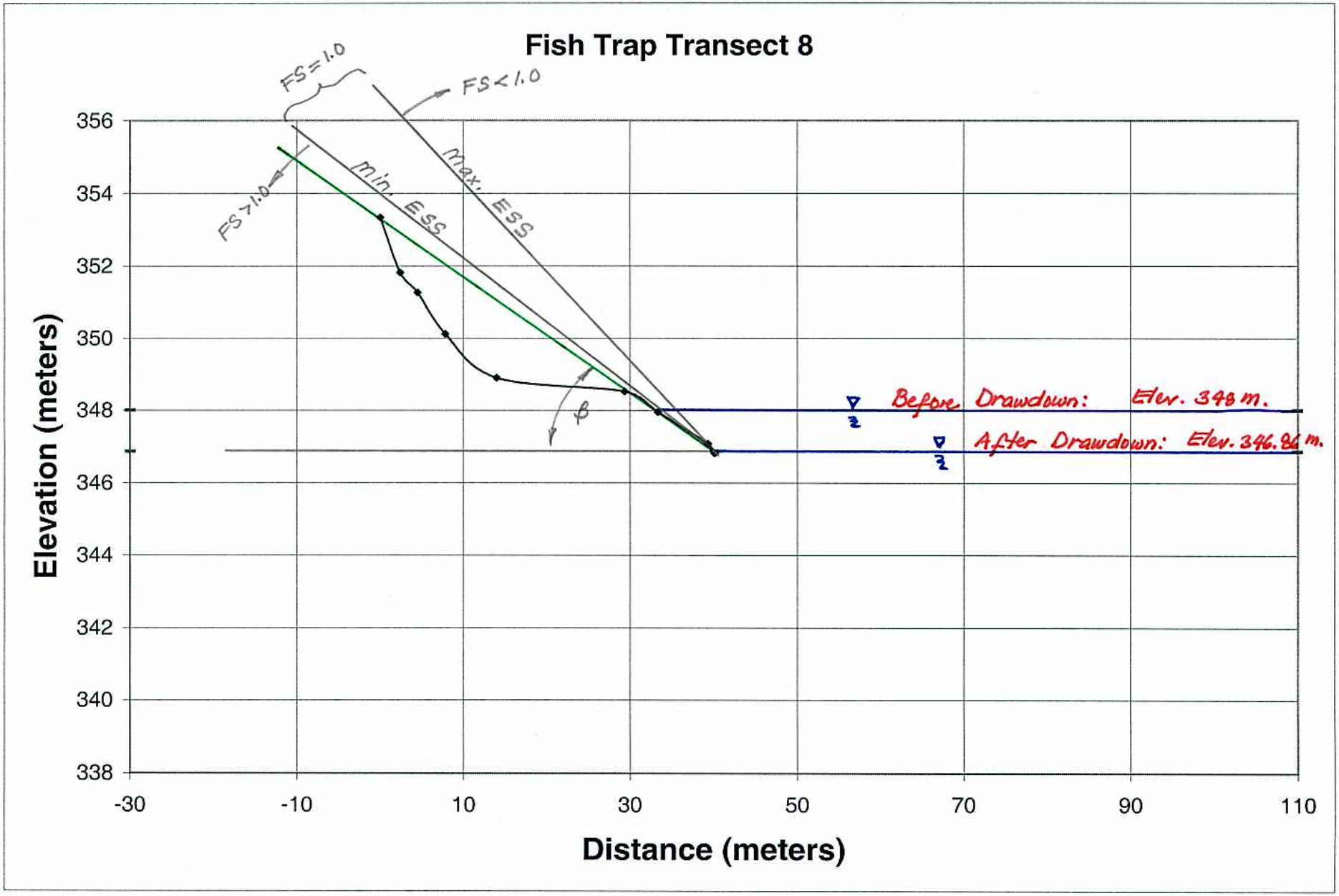
Fish Trap Transect 8
FS=1.0
FS<1.0
FS>1.0
min. ESS
max. ESS
β
Before Drawdown: Elev. 348 m.
After Drawdown: Elev. 346.84 m.
Elevation (meters)
356
354
352
350
348
346
344
342
340
338
-30
-10
10
30
50
70
90
110
Distance (meters)

Figure 54

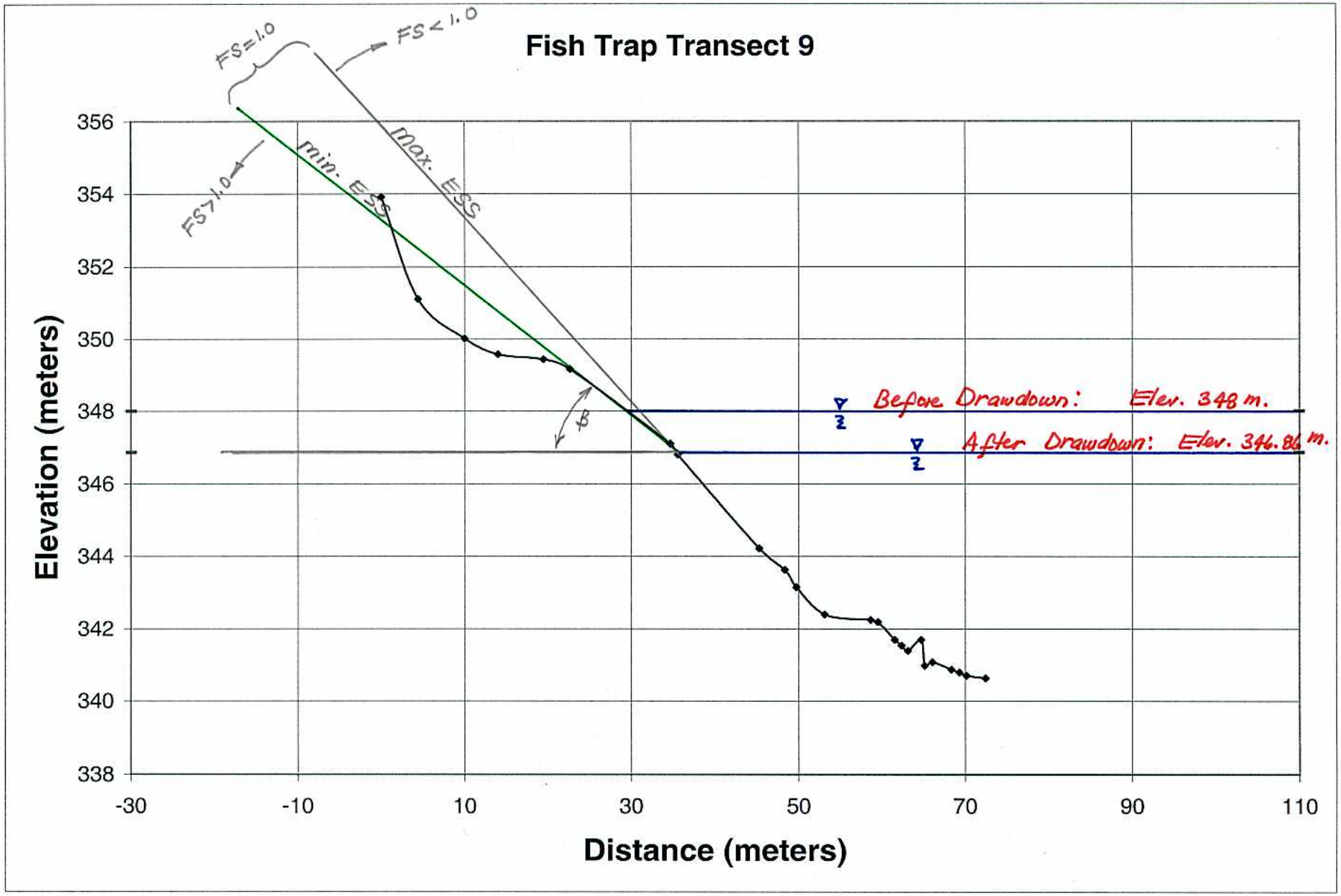
Fish Trap Transect 9
FS=1.0
FS<1.0
FS>1.0
min. ESS
max. ESS
β
Before Drawdown: Elev. 348 m.
After Drawdown: Elev. 346.86 m.
Elevation (meters)
356
354
352
350
348
346
344
342
340
338
-30
-10
10
30
50
70
90
110
Distance (meters)

Figure 55

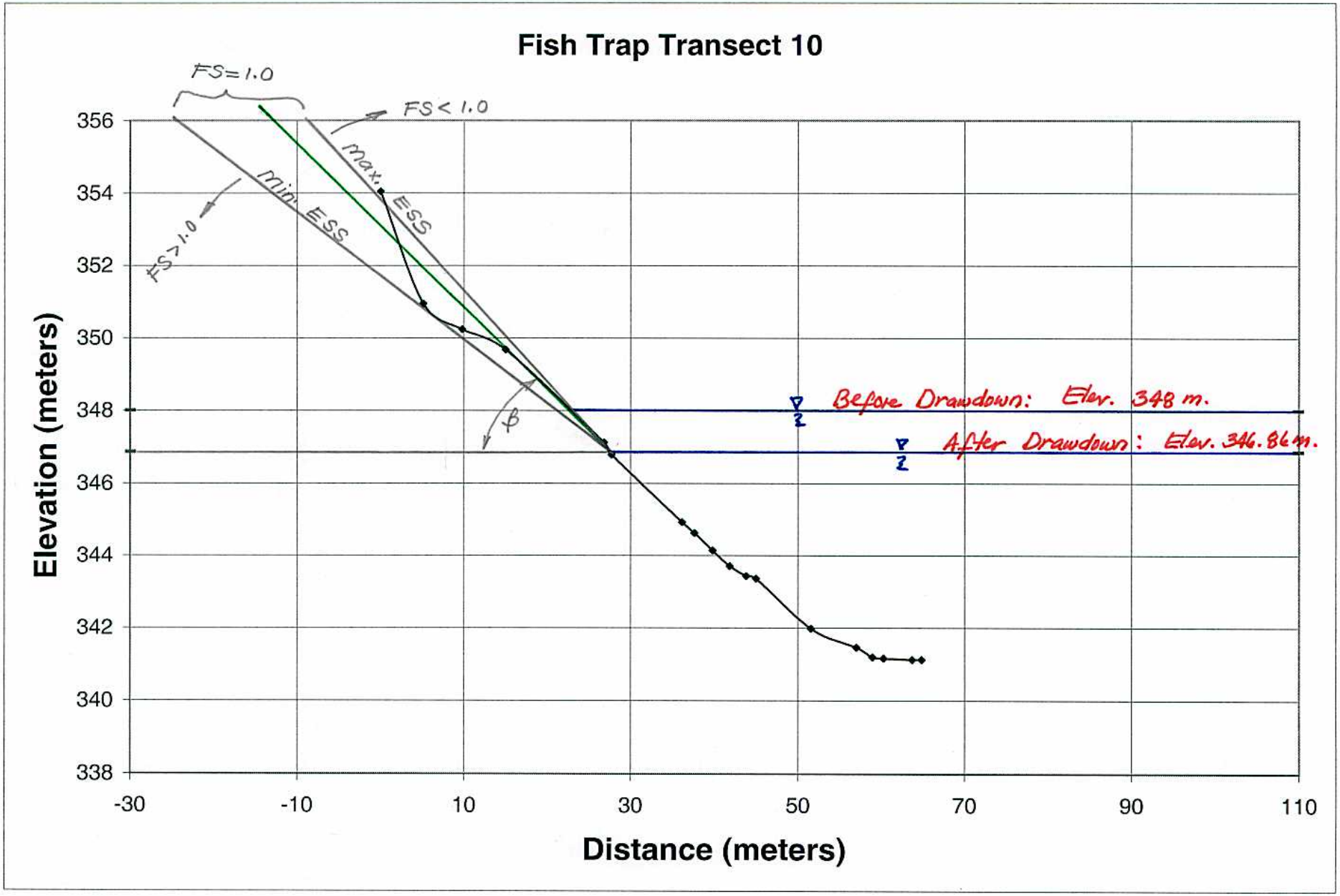
Fish Trap Transect 10
FS = 1.0
FS < 1.0
FS > 1.0
max. ESS
min. ESS
β
Before Drawdown: Elev. 348 m.
After Drawdown: Elev. 346.86 m.
Elevation (meters)
356
354
352
350
348
346
344
342
340
338
-30
-10
10
30
50
70
90
110
Distance (meters)

Figure 56

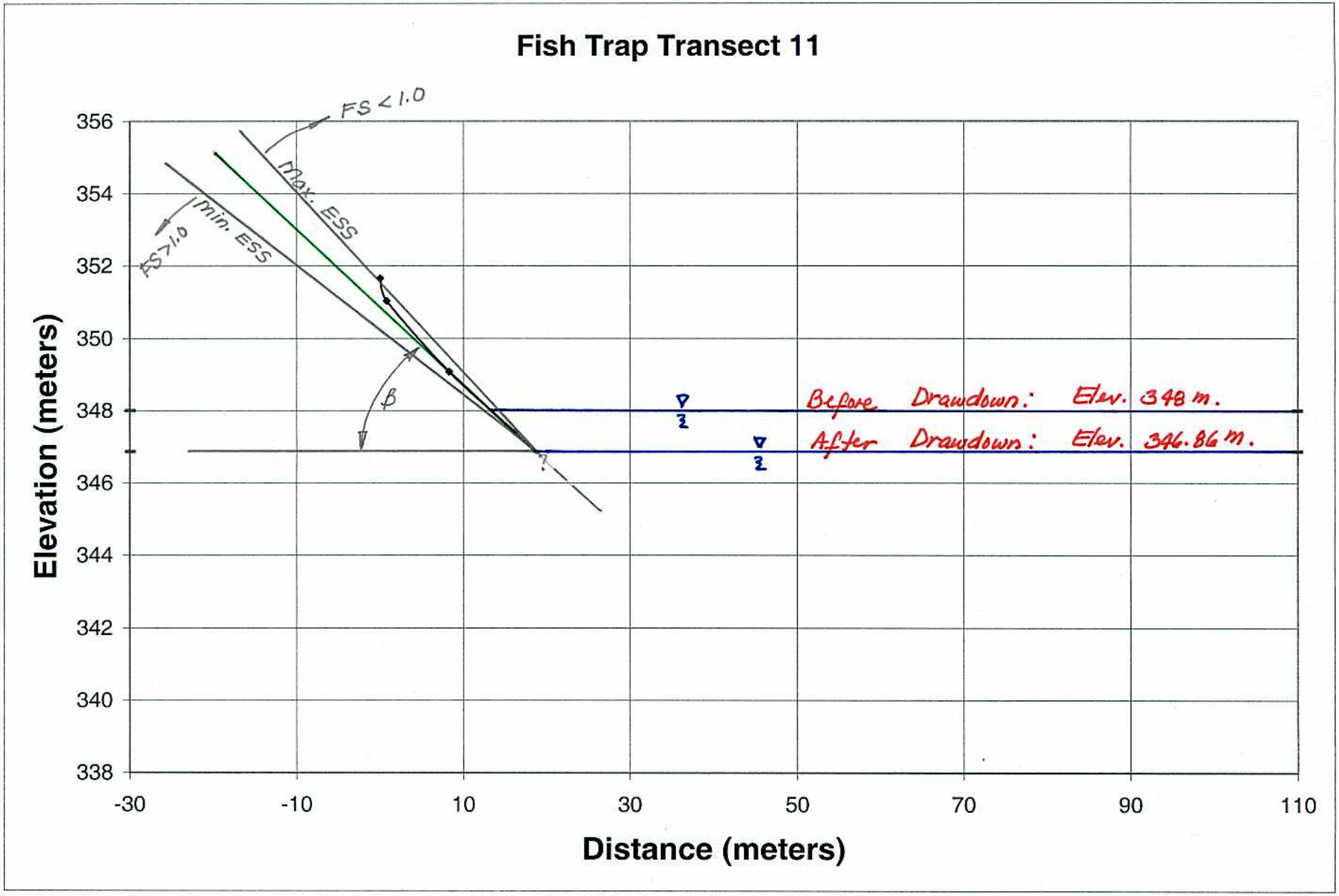
Fish Trap Transect 11
FS < 1.0
Max. ESS
Min. ESS
FS > 1.0
β
Before Drawdown: Elev. 348 m.
After Drawdown: Elev. 346.86 m.
Elevation (meters)
356
354
352
350
348
346
344
342
340
338
-30
-10
10
30
50
70
90
110
Distance (meters)

Figure 57

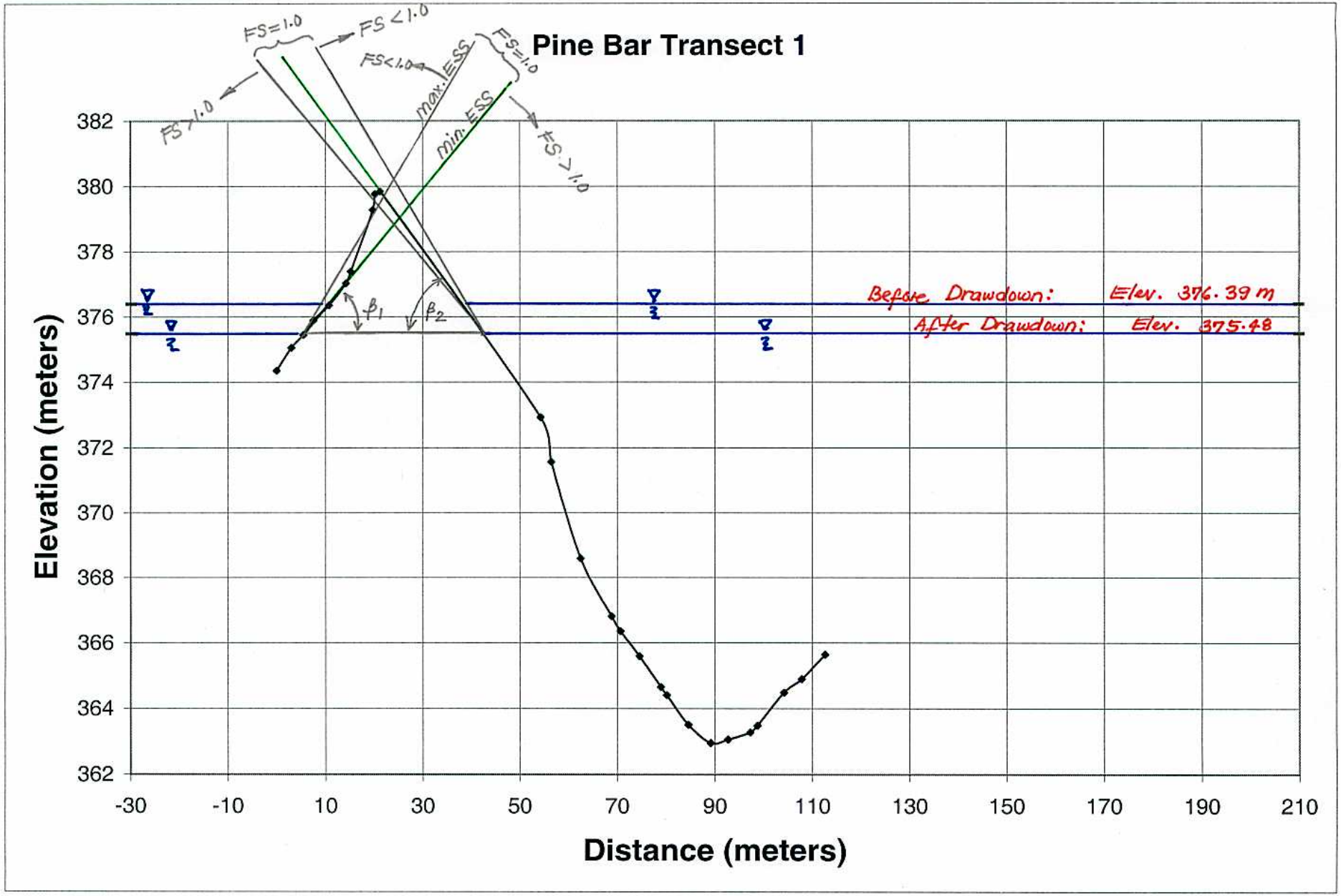
Pine Bar Transect 1
FS=1.0
FS<1.0
FS<1.0
max. ESS
min. ESS
FS=1.0
FS>1.0
FS>1.0
β1
β2
Before Drawdown: Elev. 376.39 m
After Drawdown: Elev. 375.48
Elevation (meters)
382
380
378
376
374
372
370
368
366
364
362
-30
-10
10
30
50
70
90
110
130
150
170
190
210
Distance (meters)

Figure 58

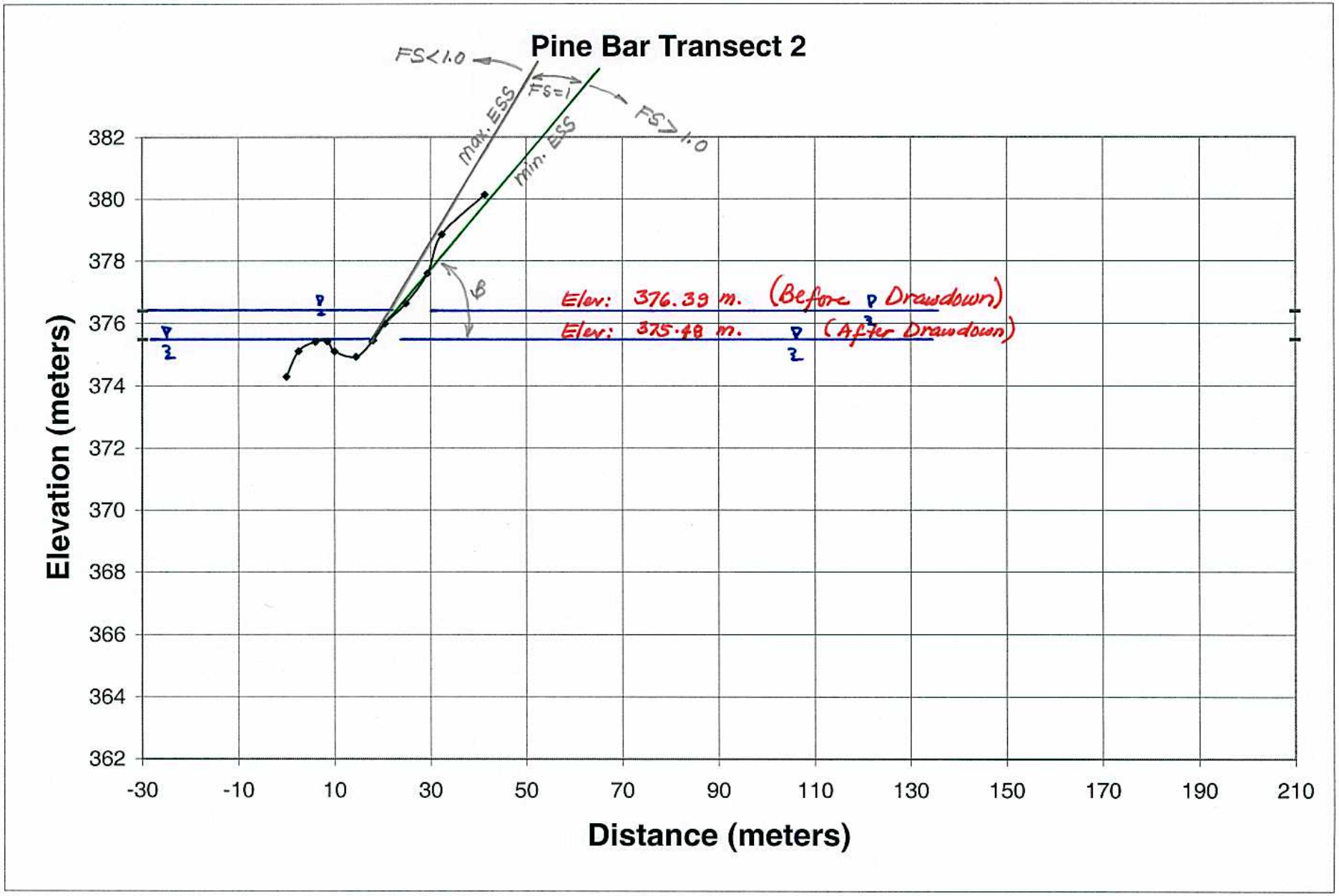
Pine Bar Transect 2
FS<1.0
FS=1
FS>1.0
max. ESS
min. ESS
B
Elev: 376.39 m. (Before Drawdown)
Elev: 375.48 m. (After Drawdown)
Elevation (meters)
382
380
378
376
374
372
370
368
366
364
362
-30
-10
10
30
50
70
90
110
130
150
170
190
210
Distance (meters)

Figure 59

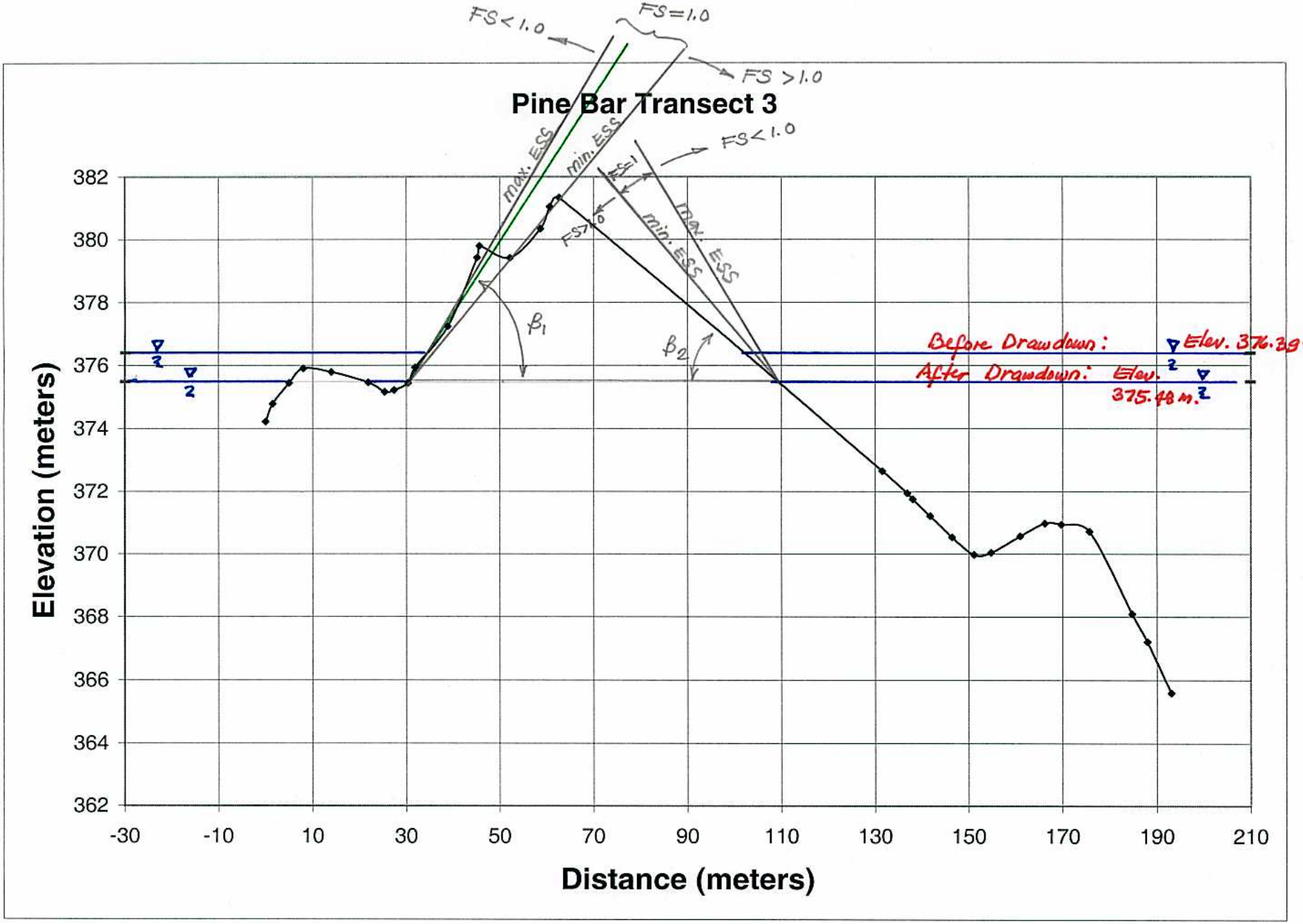
FS<1.0
FS=1.0
FS>1.0
Pine Bar Transect 3
max. ESS
min. ESS
FS<1.0
FS=1.0
min. ESS
max. ESS
β1
β2
Before Drawdown: Elev. 376.39 m.
After Drawdown: Elev. 375.48 m.
Elevation (meters)
382
380
378
376
374
372
370
368
366
364
362
-30
-10
10
30
50
70
90
110
130
150
170
190
210
Distance (meters)

Figure 60

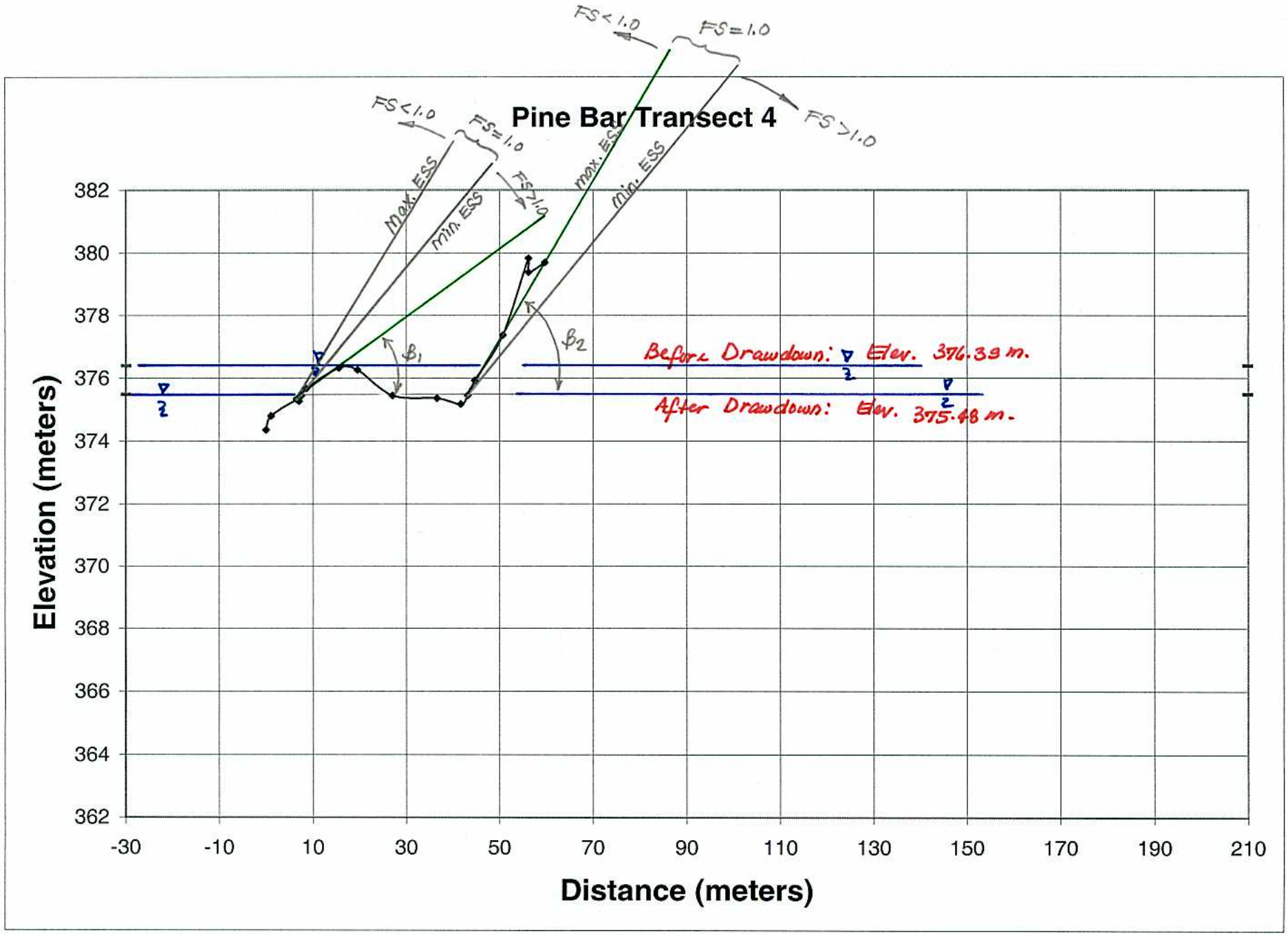
Pine Bar Transect 4
FS<1.0
FS=1.0
FS>1.0
max. ESS
min. ESS
β_1
β_2
Before Drawdown: Elev. 376.39 m.
After Drawdown: Elev. 375.48 m.
Elevation (meters)
382
380
378
376
374
372
370
368
366
364
362
-30
-10
10
30
50
70
90
110
130
150
170
190
210
Distance (meters)

Figure 61

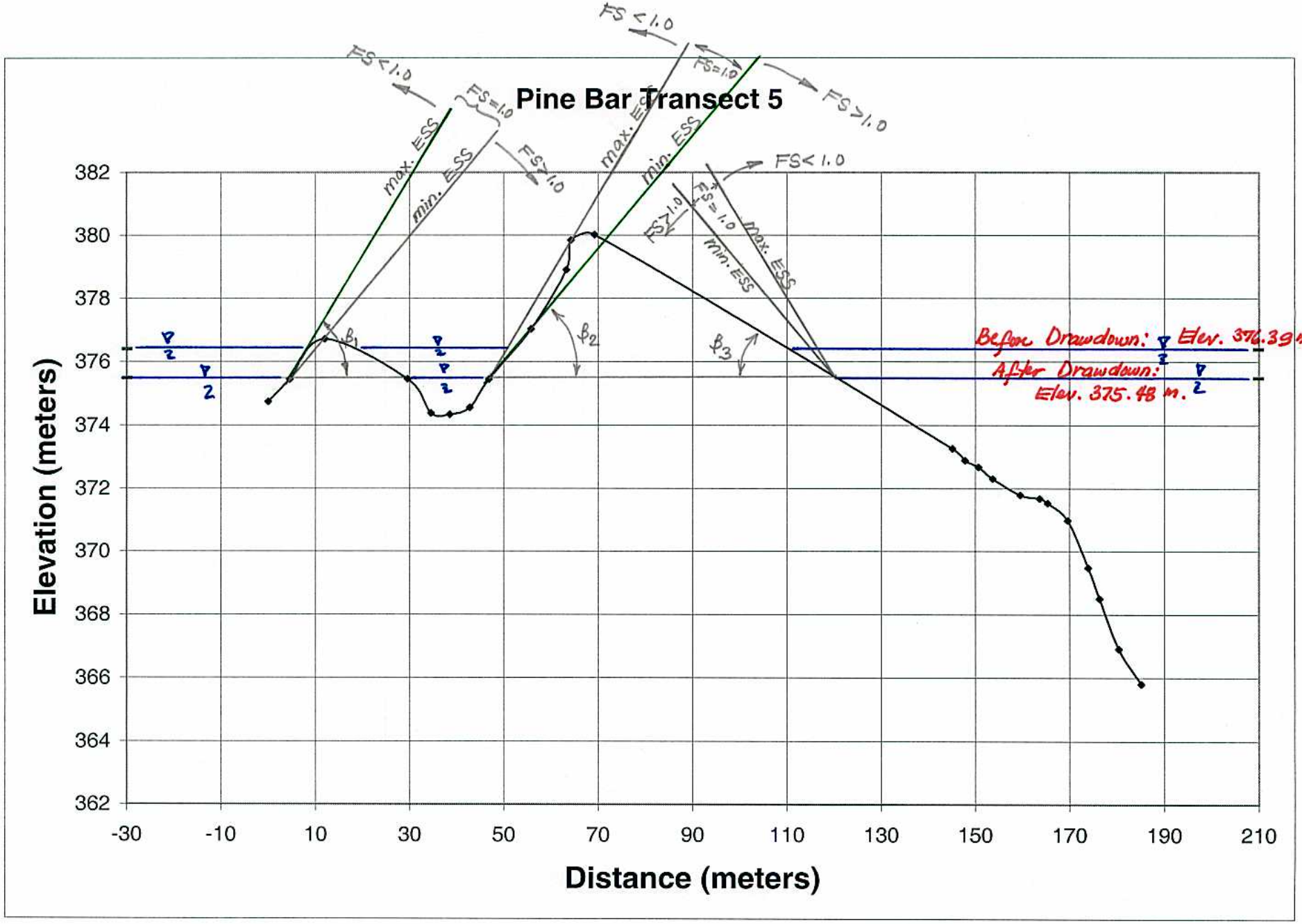
Pine Bar Transect 5
Elevation (meters)
Distance (meters)
382
380
378
376
374
372
370
368
366
364
362
-30
-10
10
30
50
70
90
110
130
150
170
190
210
FS < 1.0
FS = 1.0
FS > 1.0
max. ESS
min. ESS
β1
β2
β3
Before Drawdown: Elev. 376.39 m.
After Drawdown: Elev. 375.48 m.

Figure 62

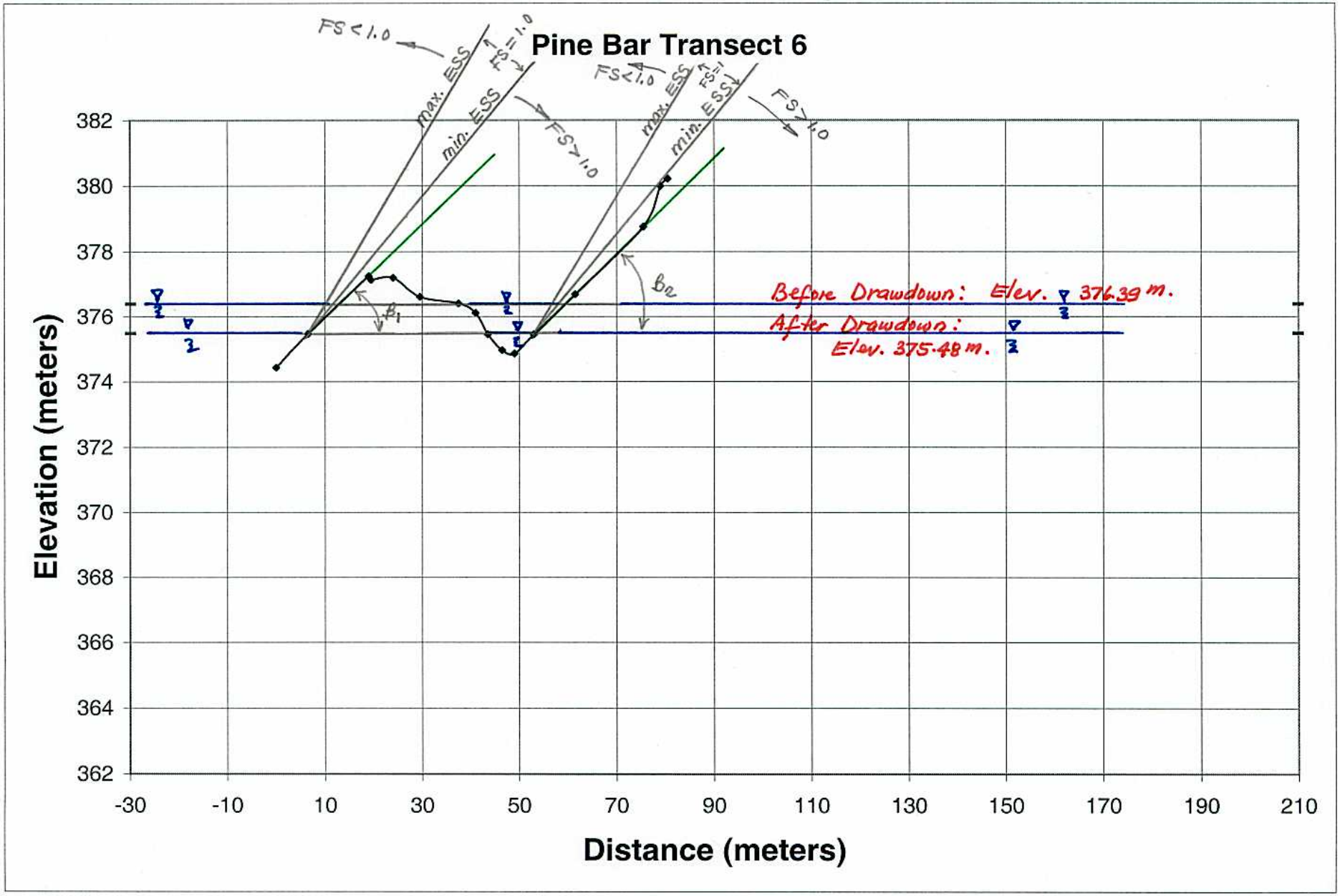
Pine Bar Transect 6
FS<1.0
max. ESS
FS=1.0
min. ESS
FS>1.0
FS<1.0
max. ESS
FS=1
min. ESS
FS>1.0
B_1
B_2
Before Drawdown: Elev. 376.39 m.
After Drawdown:
Elev. 375.48 m.
Elevation (meters)
382
380
378
376
374
372
370
368
366
364
362
-30
-10
10
30
50
70
90
110
130
150
170
190
210
Distance (meters)

Figure 63

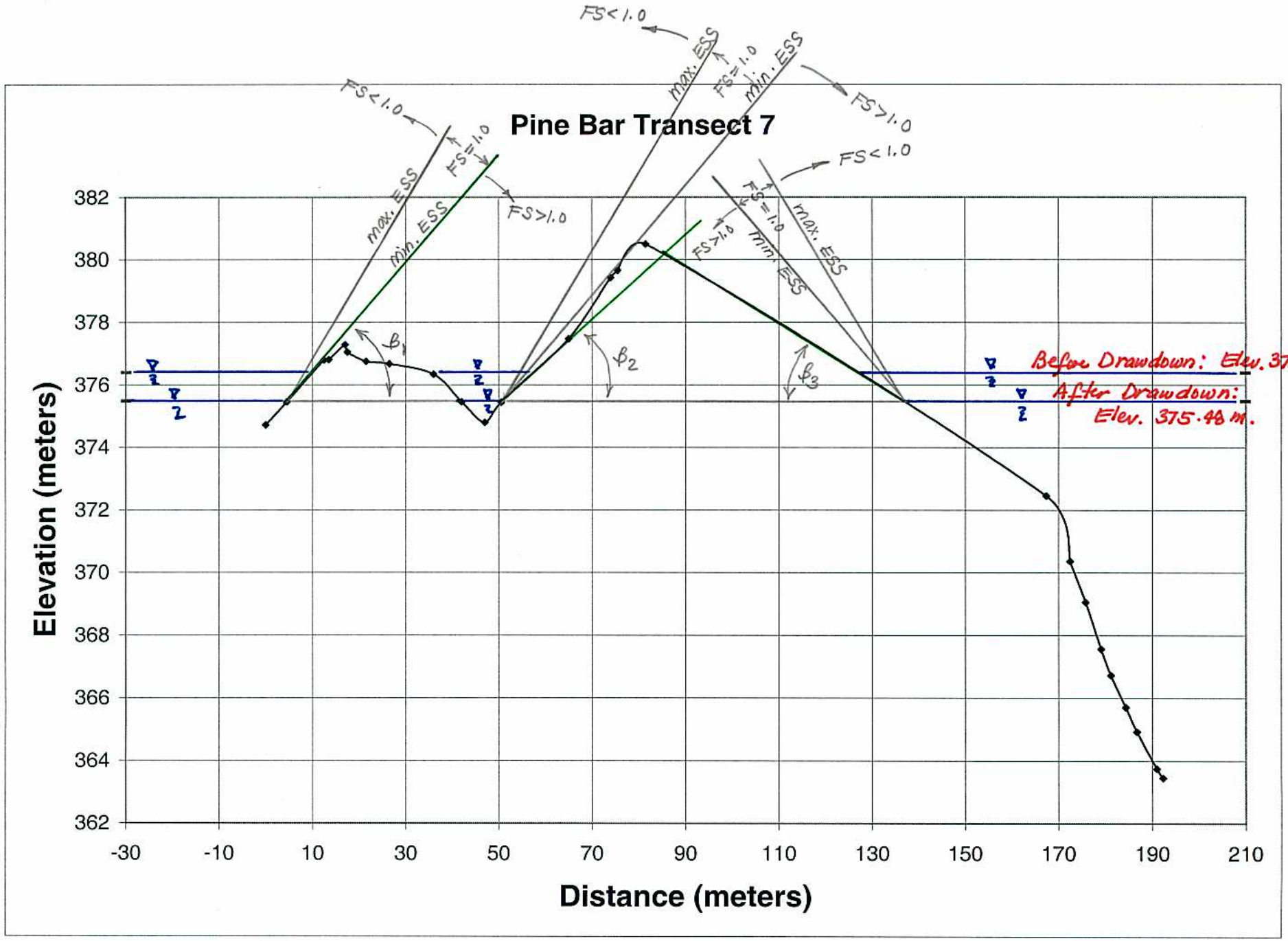
Pine Bar Transect 7
Elevation (meters)
Distance (meters)
382
380
378
376
374
372
370
368
366
364
362
-30
-10
10
30
50
70
90
110
130
150
170
190
210
FS<1.0
max. ESS
FS=1.0
min. ESS
FS>1.0
β1
β2
β3
Before Drawdown: Elev. 376.39 m
After Drawdown:
Elev. 375.48 m.

Figure 64

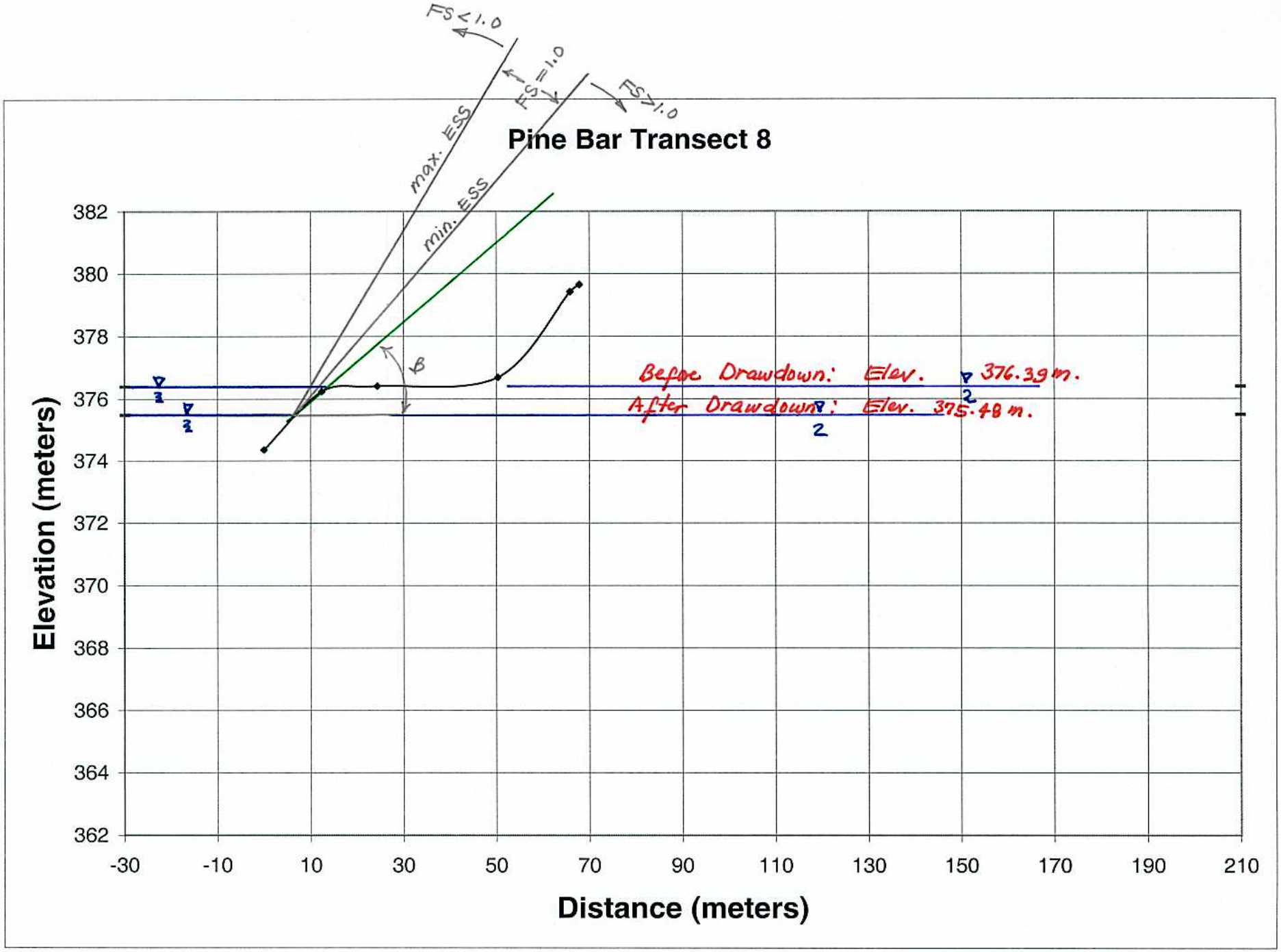
FS < 1.0
FS = 1.0
FS > 1.0
max. ESS
min. ESS
Pine Bar Transect 8
B
Before Drawdown: Elev. 376.39 m.
After Drawdown: Elev. 375.48 m.
Elevation (meters)
382
380
378
376
374
372
370
368
366
364
362
-30
-10
10
30
50
70
90
110
130
150
170
190
210
Distance (meters)

Figure 65

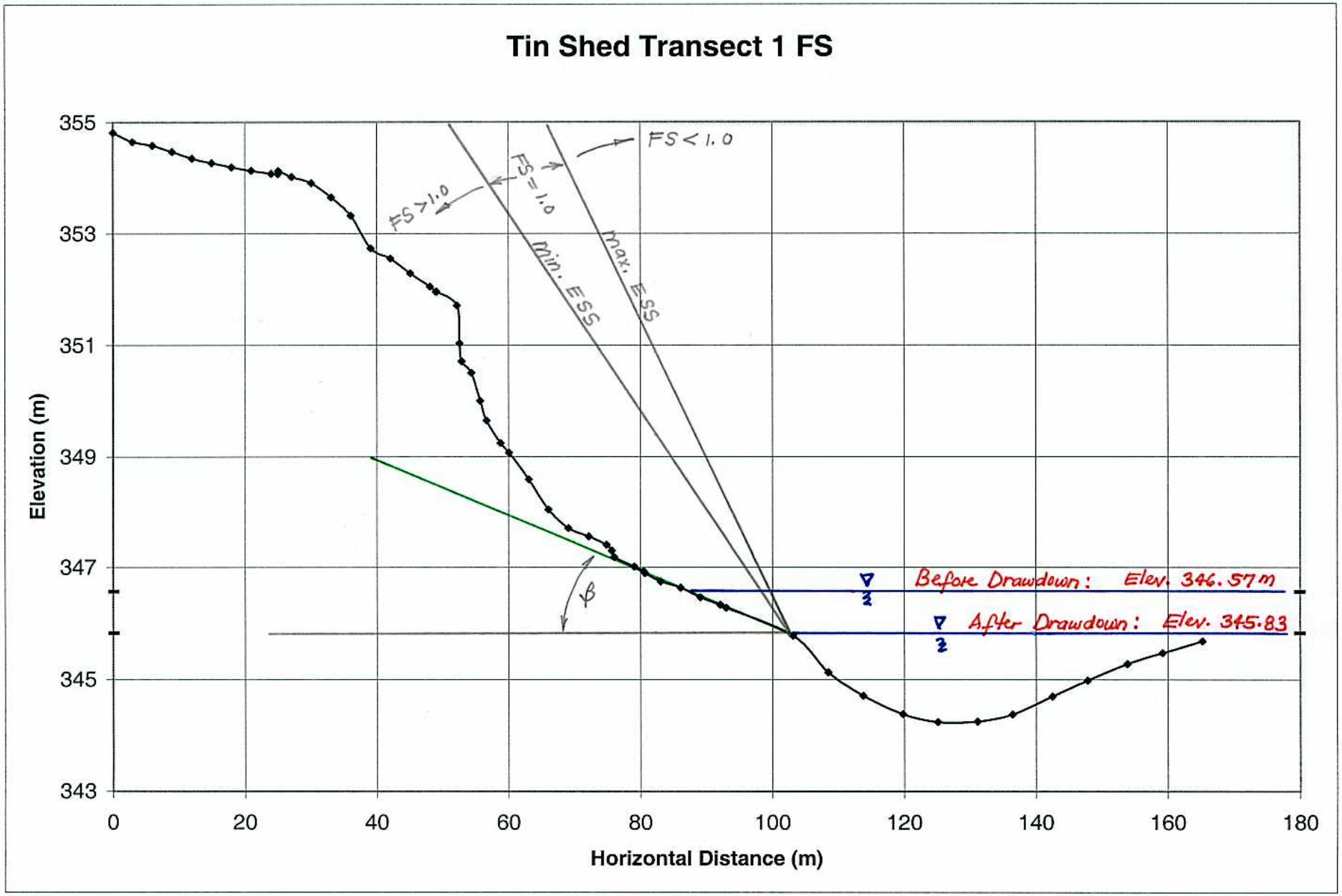
Tin Shed Transect 1 FS
Elevation (m)
355
353
351
349
347
345
343
0
20
40
60
80
100
120
140
160
180
Horizontal Distance (m)
FS > 1.0
FS = 1.0
FS < 1.0
min. ESS
max. ESS
β
Before Drawdown: Elev. 346.57 m
After Drawdown: Elev. 345.83

Figure 66

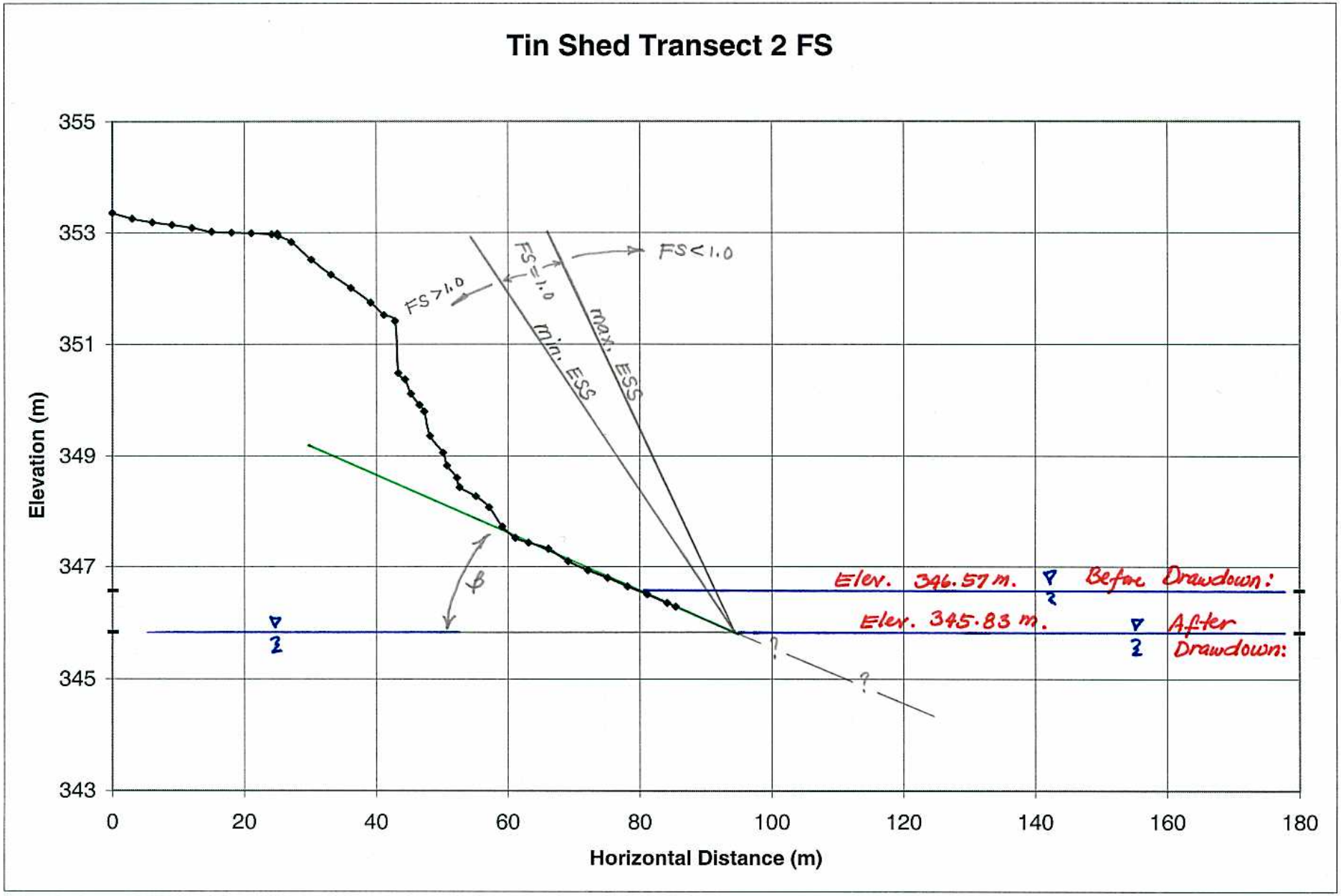
Tin Shed Transect 2 FS
Elevation (m)
355
353
351
349
347
345
343
0
20
40
60
80
100
120
140
160
180
Horizontal Distance (m)
FS>1.0
FS=1.0
min. ESS
max. ESS
FS<1.0
β
Elev. 346.57 m.
Before Drawdown:
Elev. 345.83 m.
After Drawdown:
?
?

Figure 67

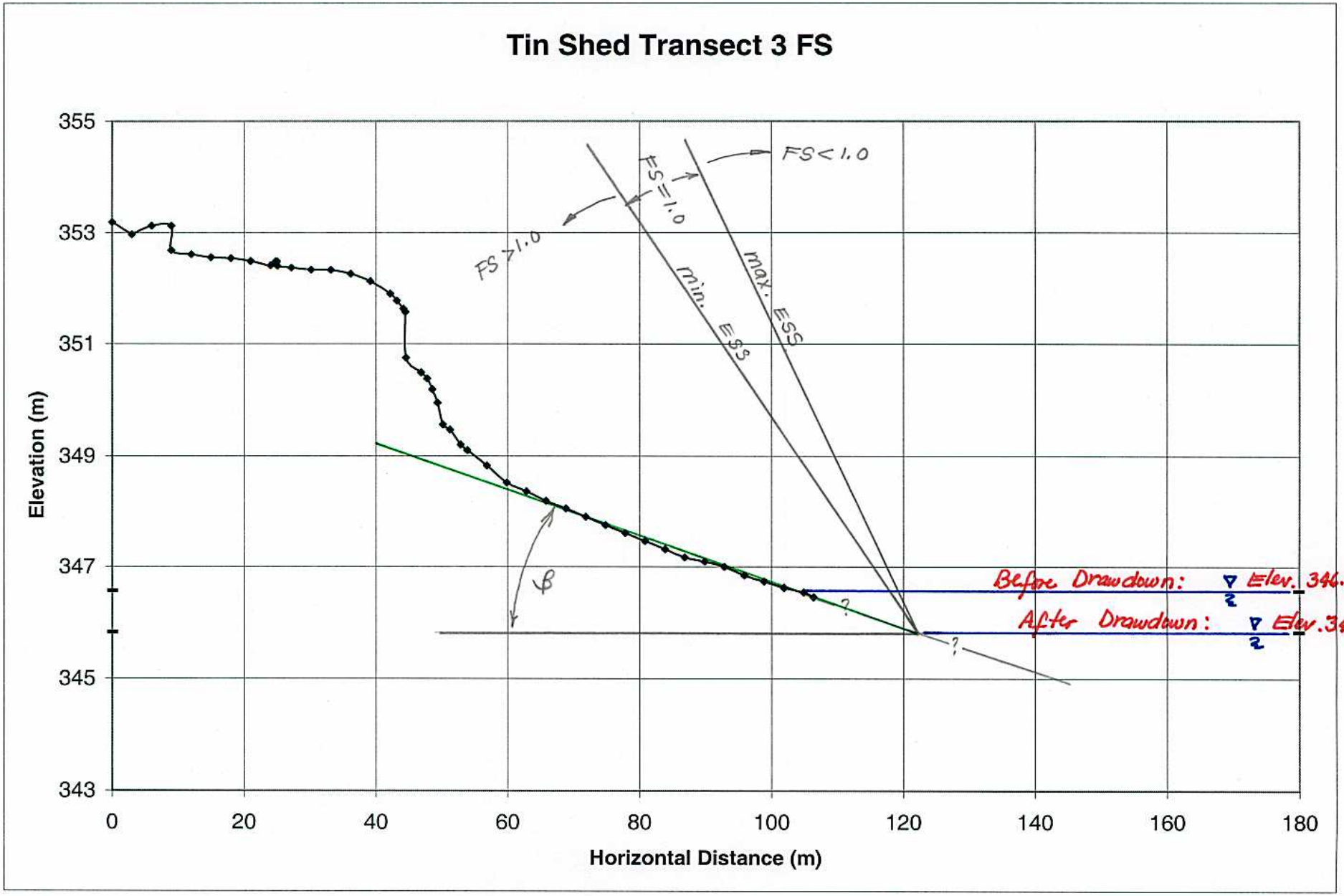
Tin Shed Transect 3 FS
Elevation (m)
355
353
351
349
347
345
343
0
20
40
60
80
100
120
140
160
180
Horizontal Distance (m)
FS < 1.0
FS = 1.0
FS > 1.0
max. ESS
min. ESS
β
?
?
Before Drawdown: ▽ Elev. 346.57 m.
After Drawdown: ▽ Elev. 345.83 m.

Figure 68

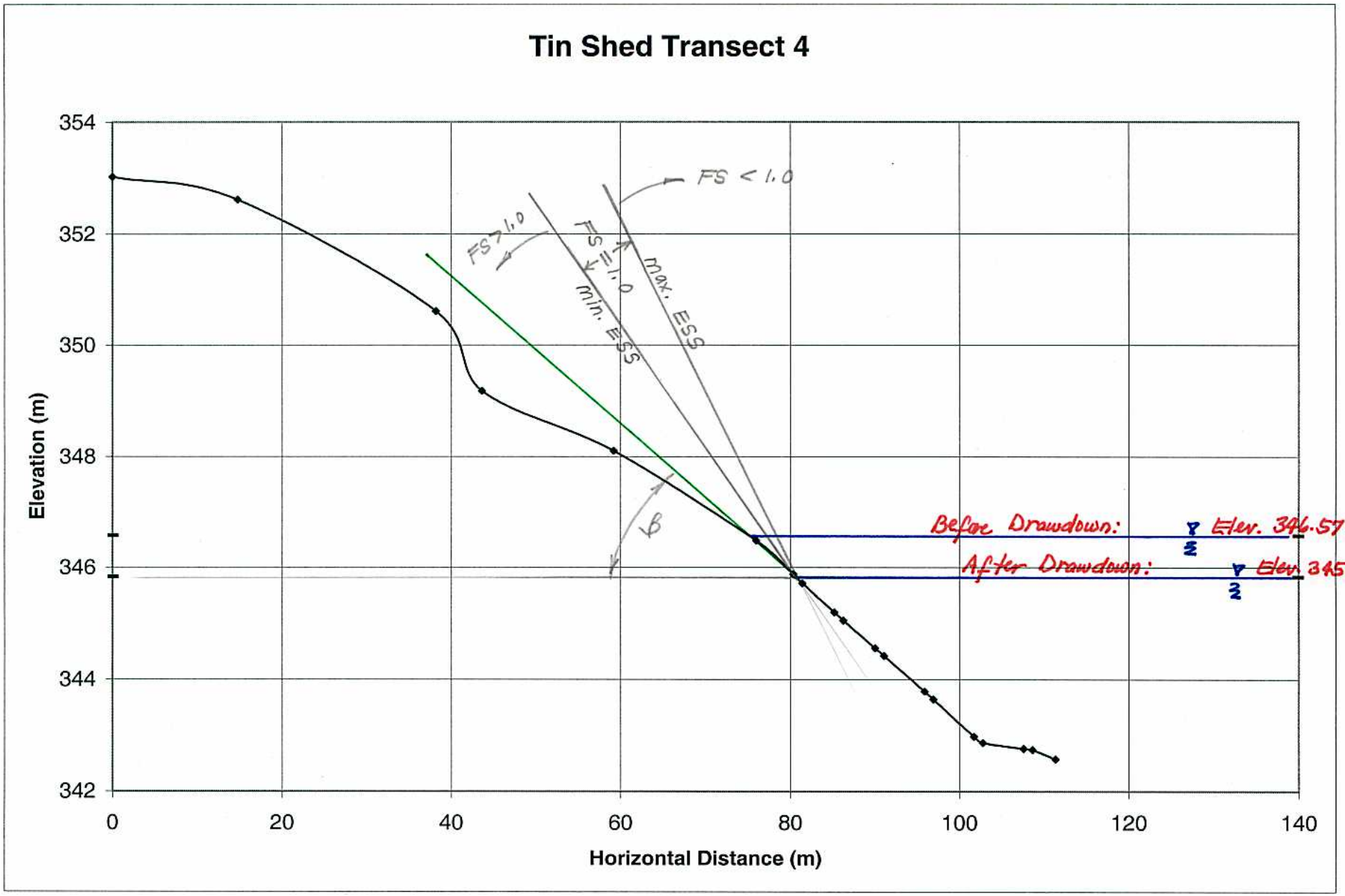
Tin Shed Transect 4
Elevation (m)
354
352
350
348
346
344
342
0
20
40
60
80
100
120
140
Horizontal Distance (m)
FS > 1.0
FS = 1.0
max. ESS
min. ESS
FS > 1.0
β
Before Drawdown:
Elev. 346.57 m.
After Drawdown:
Elev. 345.83 m.

Figure 69

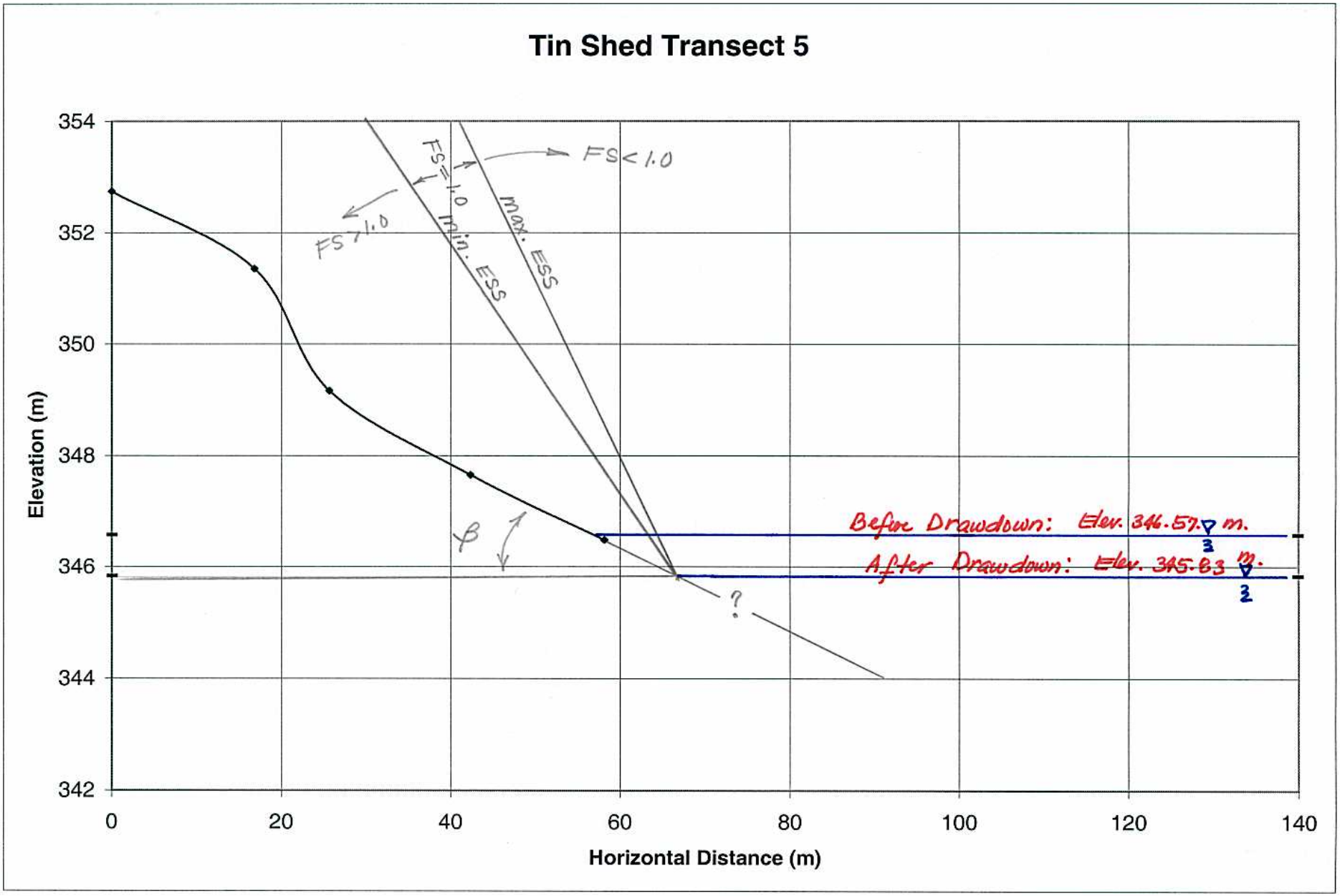
Tin Shed Transect 5
Elevation (m)
354
352
350
348
346
344
342
0
20
40
60
80
100
120
140
Horizontal Distance (m)
FS<1.0
FS=1.0
FS>1.0
min. ESS
max. ESS
β
?
Before Drawdown: Elev. 346.57 m.
After Drawdown: Elev. 345.83 m.

Figure 70

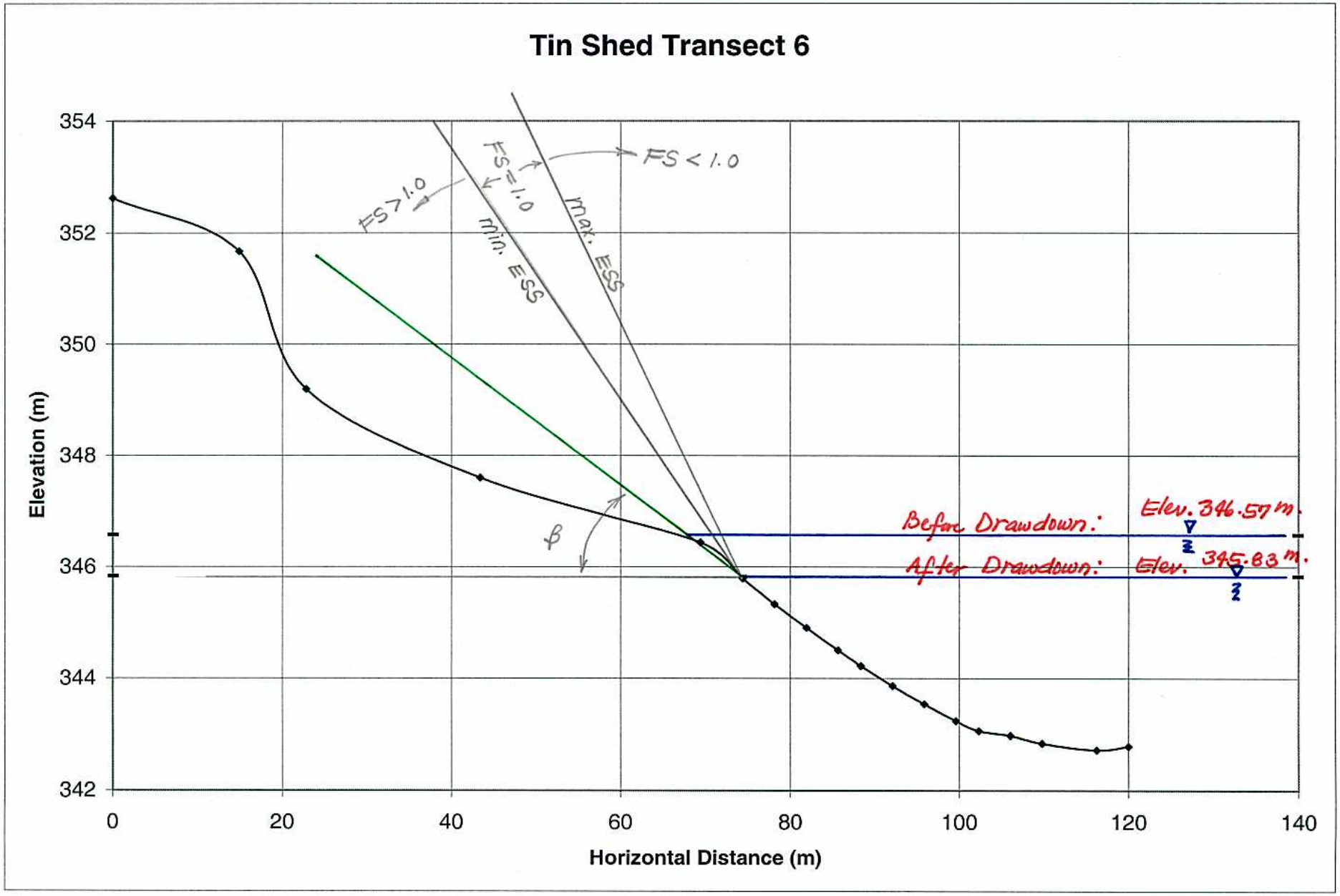
Tin Shed Transect 6
Elevation (m)
354
352
350
348
346
344
342
0
20
40
60
80
100
120
140
Horizontal Distance (m)
FS > 1.0
FS = 1.0
FS < 1.0
min. ESS
max. ESS
β
Before Drawdown:
Elev. 346.57 m.
After Drawdown:
Elev. 345.83 m.

Figure 71

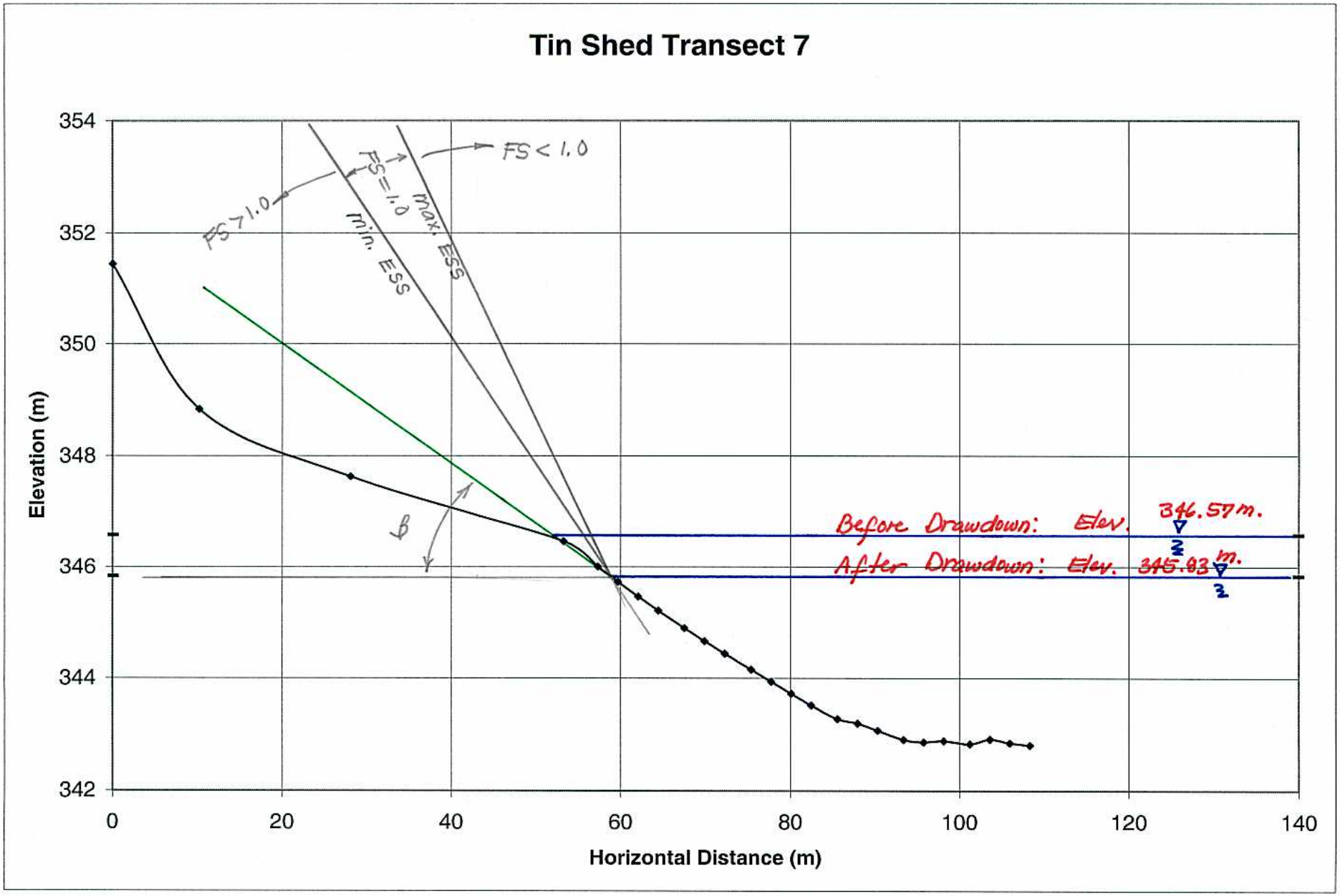
Tin Shed Transect 7
Elevation (m)
354
352
350
348
346
344
342
0
20
40
60
80
100
120
140
Horizontal Distance (m)
FS > 1.0
FS = 1.0
FS < 1.0
max. ESS
min. ESS
β
Before Drawdown: Elev. 346.57 m.
After Drawdown: Elev. 345.83 m.

Figure 72

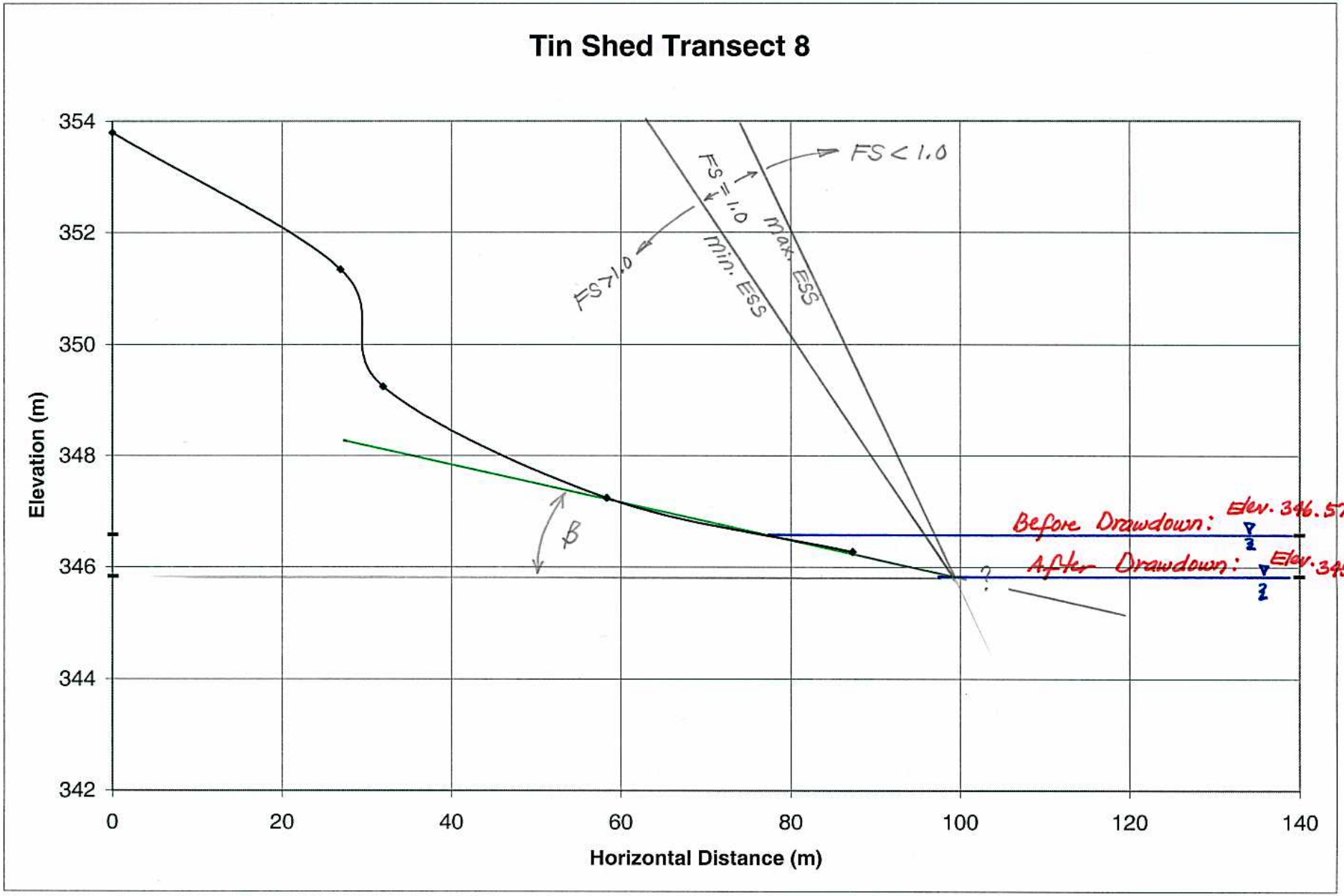
Tin Shed Transect 8
Elevation (m)
354
352
350
348
346
344
342
0
20
40
60
80
100
120
140
Horizontal Distance (m)
FS < 1.0
FS = 1.0
FS > 1.0
max. ESS
min. ESS
β
Before Drawdown: Elev. 346.57m.
After Drawdown: Elev. 345.83 m.
?

Figure 73

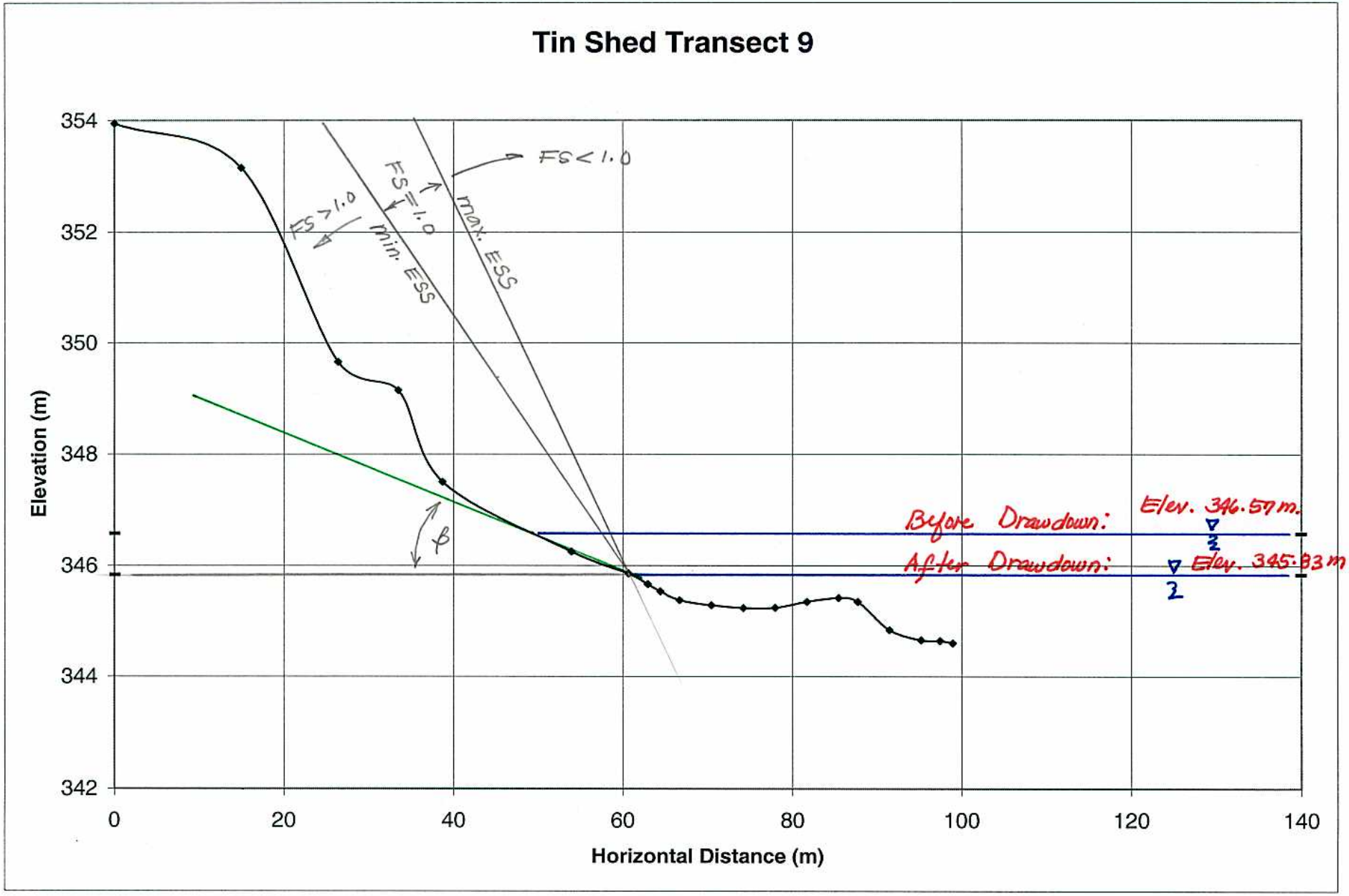
Tin Shed Transect 9
Elevation (m)
354
352
350
348
346
344
342
0
20
40
60
80
100
120
140
Horizontal Distance (m)
FS > 1.0
FS = 1.0
min. ESS
max. ESS
FS < 1.0
β
Before Drawdown:
Elev. 346.57 m.
After Drawdown:
Elev. 345.83 m.

Figure 74

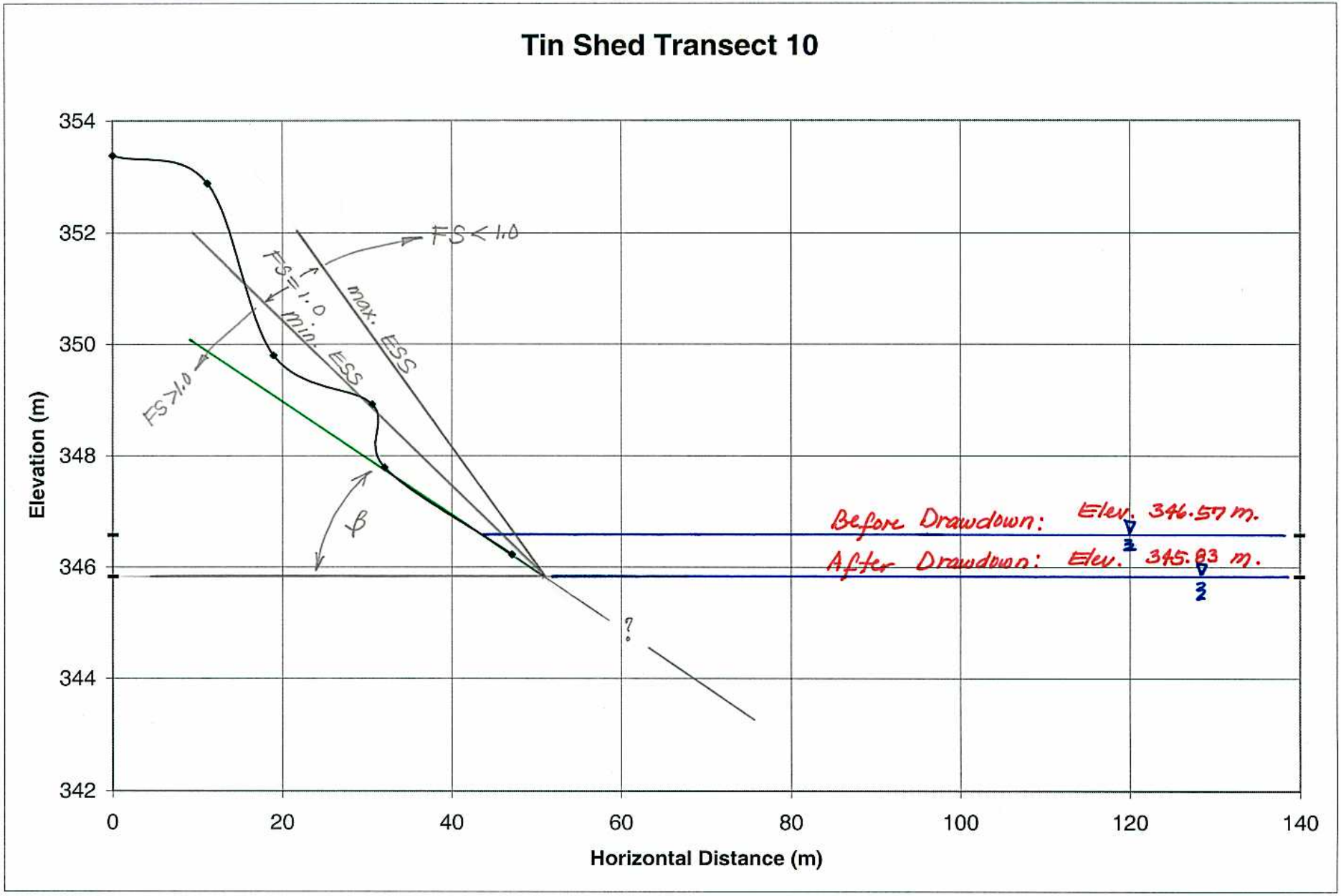
Tin Shed Transect 10
Elevation (m)
354
352
350
348
346
344
342
0
20
40
60
80
100
120
140
Horizontal Distance (m)
FS < 1.0
FS = 1.0
max. ESS
min. ESS
FS > 1.0
β
?
Before Drawdown: Elev. 346.57 m.
After Drawdown: Elev. 345.83 m.

Figure 75

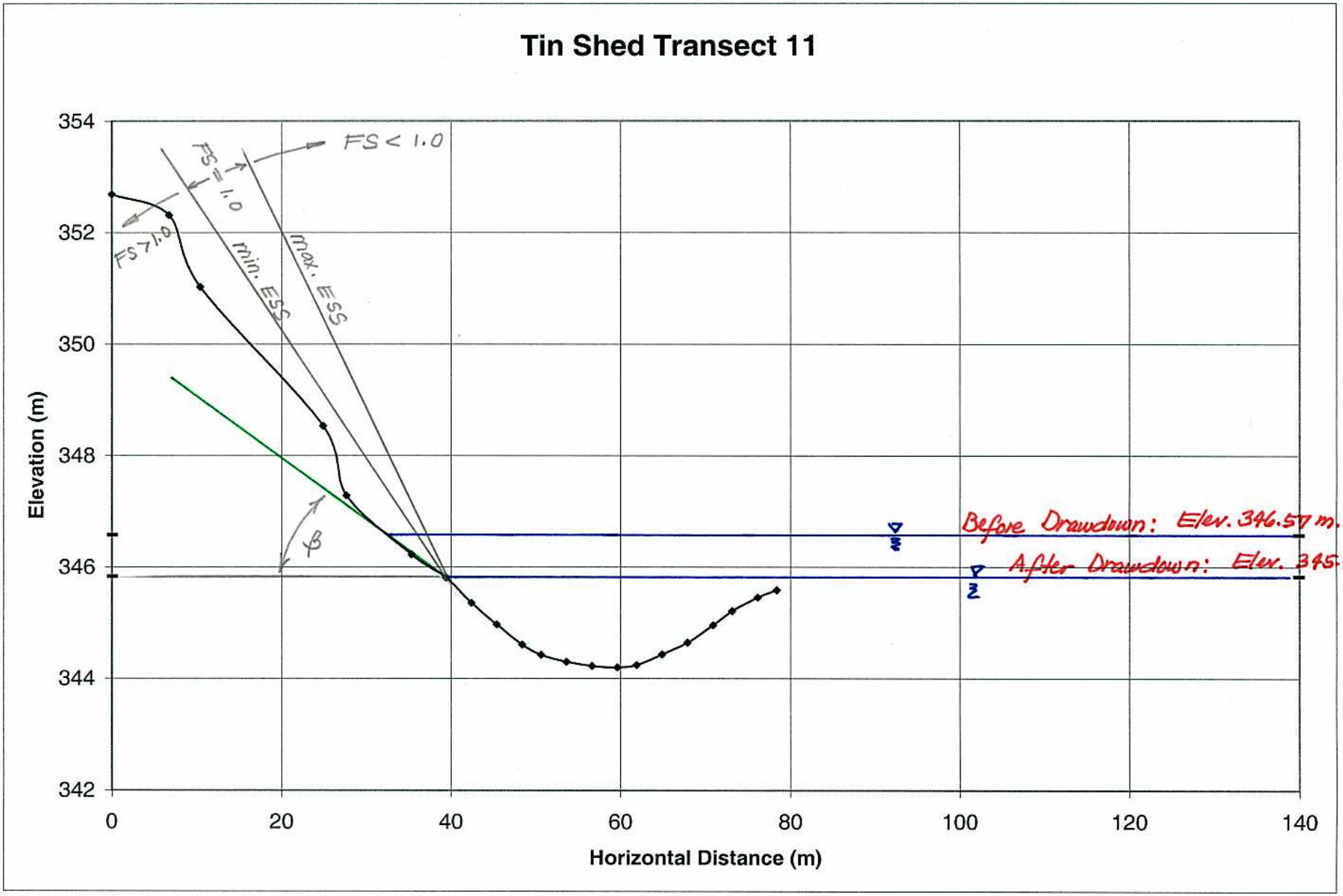
Tin Shed Transect 11
Elevation (m)
354
352
350
348
346
344
342
0
20
40
60
80
100
120
140
Horizontal Distance (m)
FS < 1.0
FS = 1.0
FS > 1.0
min. ESS
max. ESS
β
Before Drawdown: Elev. 346.57 m.
After Drawdown: Elev. 345.83 m.
1
2

Figure 76

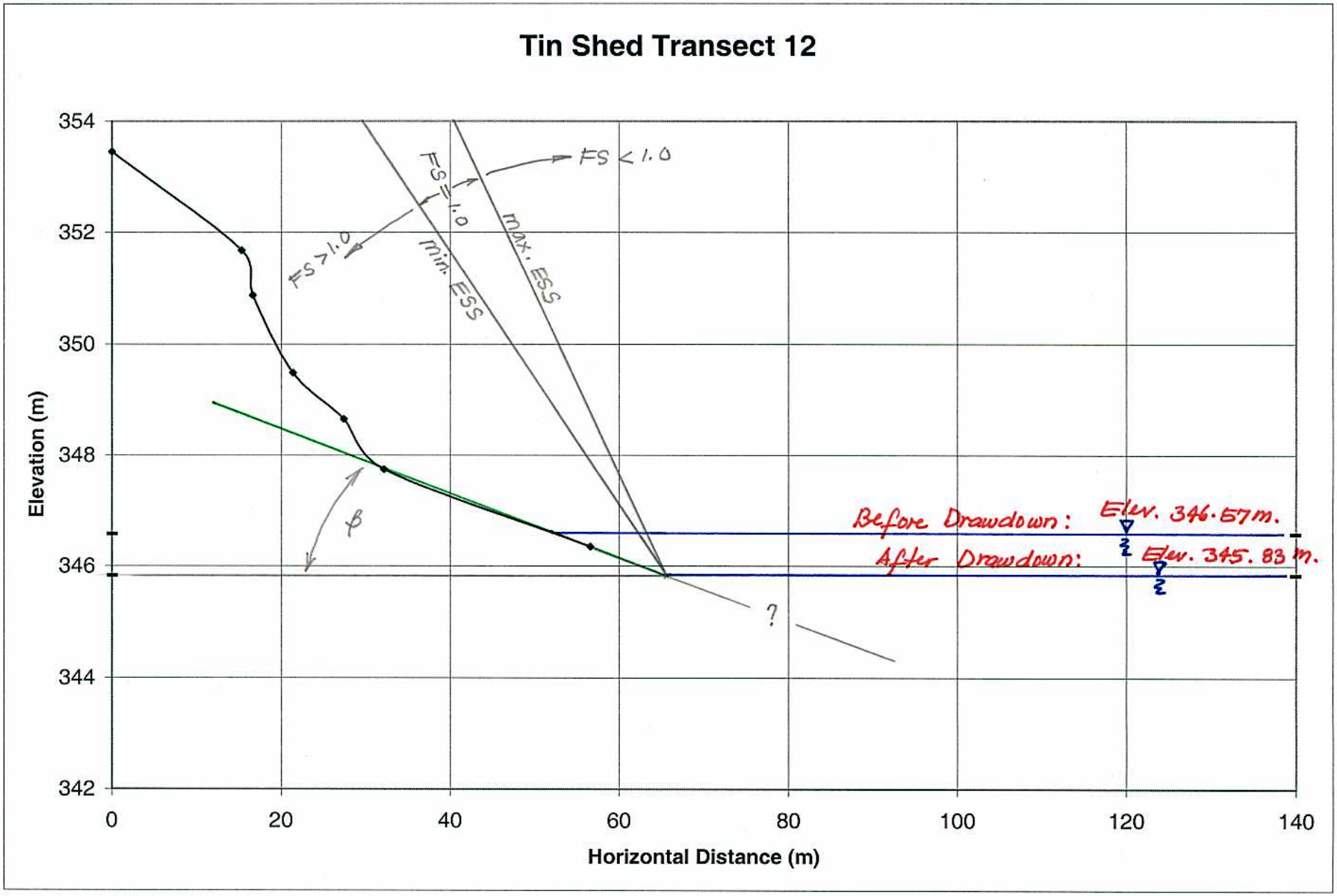
Tin Shed Transect 12
Elevation (m)
354
352
350
348
346
344
342
0
20
40
60
80
100
120
140
Horizontal Distance (m)
FS < 1.0
FS = 1.0
FS > 1.0
min. ESS
max. ESS
β
?
Before Drawdown: Elev. 346.57m.
After Drawdown: Elev. 345.83 m.

Figure 77

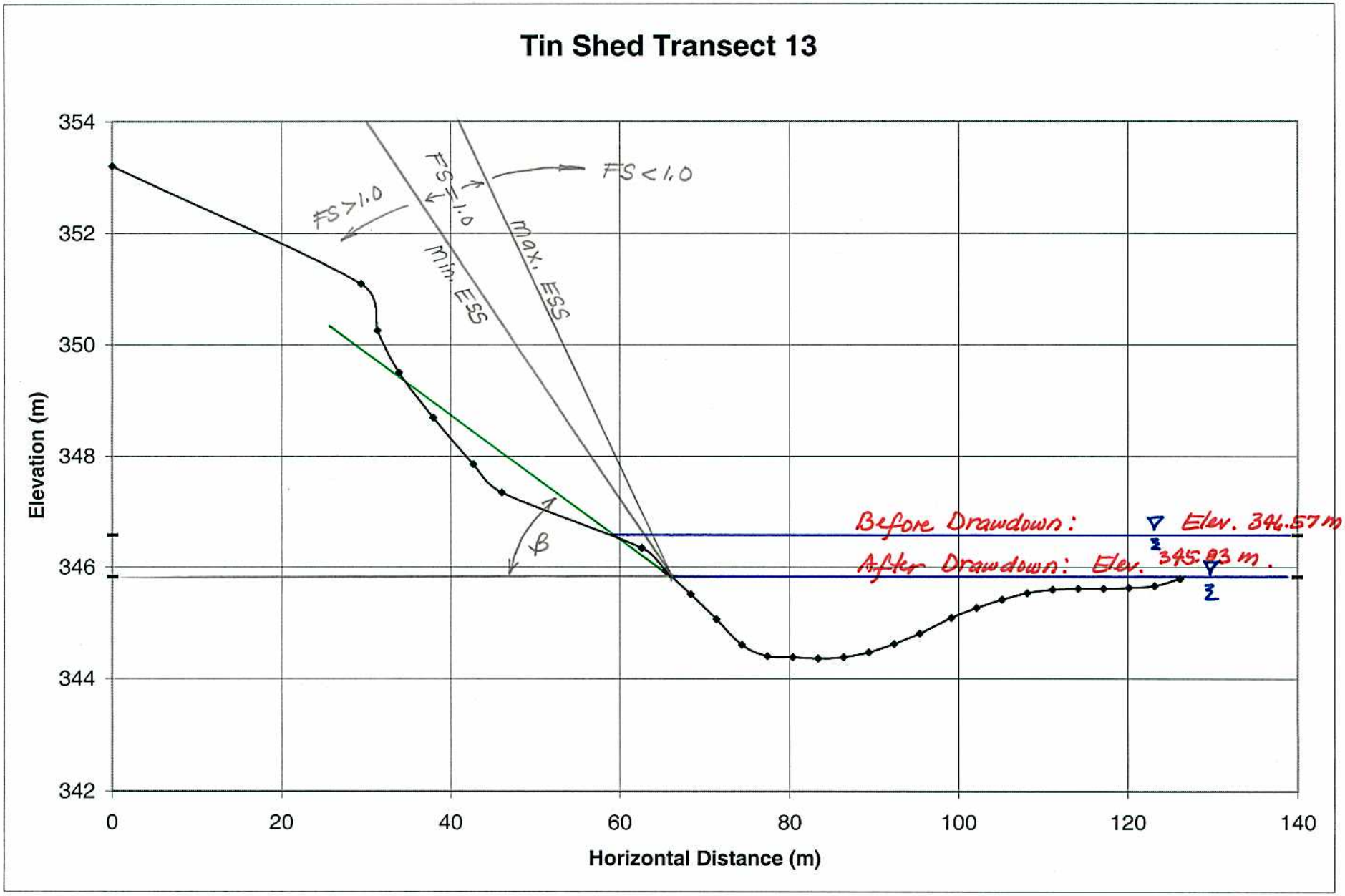
Tin Shed Transect 13
Elevation (m)
354
352
350
348
346
344
342
0
20
40
60
80
100
120
140
Horizontal Distance (m)
FS>1.0
FS≥1.0
FS<1.0
Min. ESS
max. ESS
β
Before Drawdown:
Elev. 346.57 m.
After Drawdown:
Elev. 345.83 m.

Figure 78

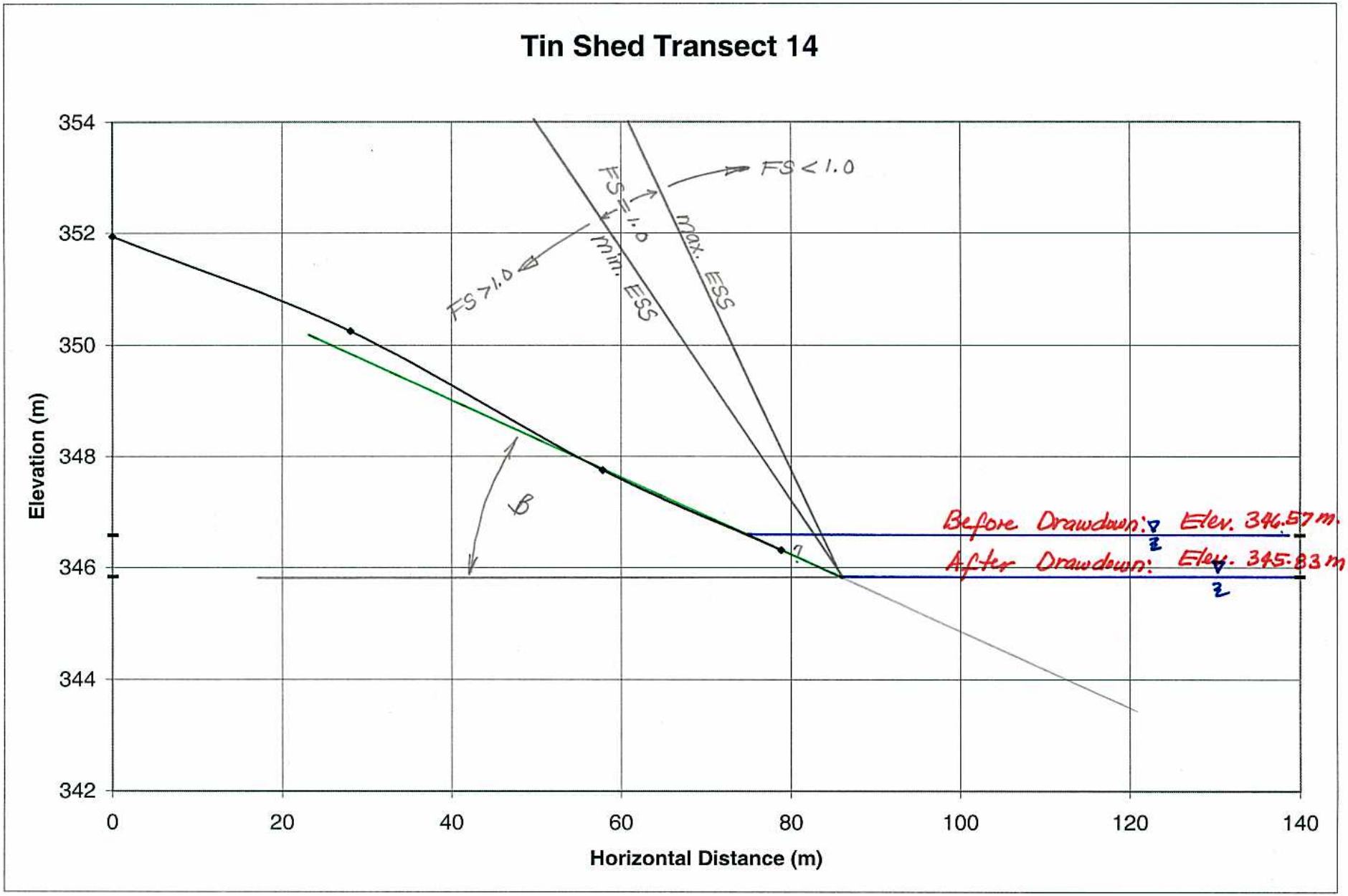
Tin Shed Transect 14
354
352
350
348
346
344
342
Elevation (m)
0
20
40
60
80
100
120
140
Horizontal Distance (m)
FS < 1.0
FS = 1.0
min. ESS
max. ESS
FS > 1.0
b
1
Before Drawdown: Elev. 346.57 m.
After Drawdown: Elev. 345.83 m.

Figure 79

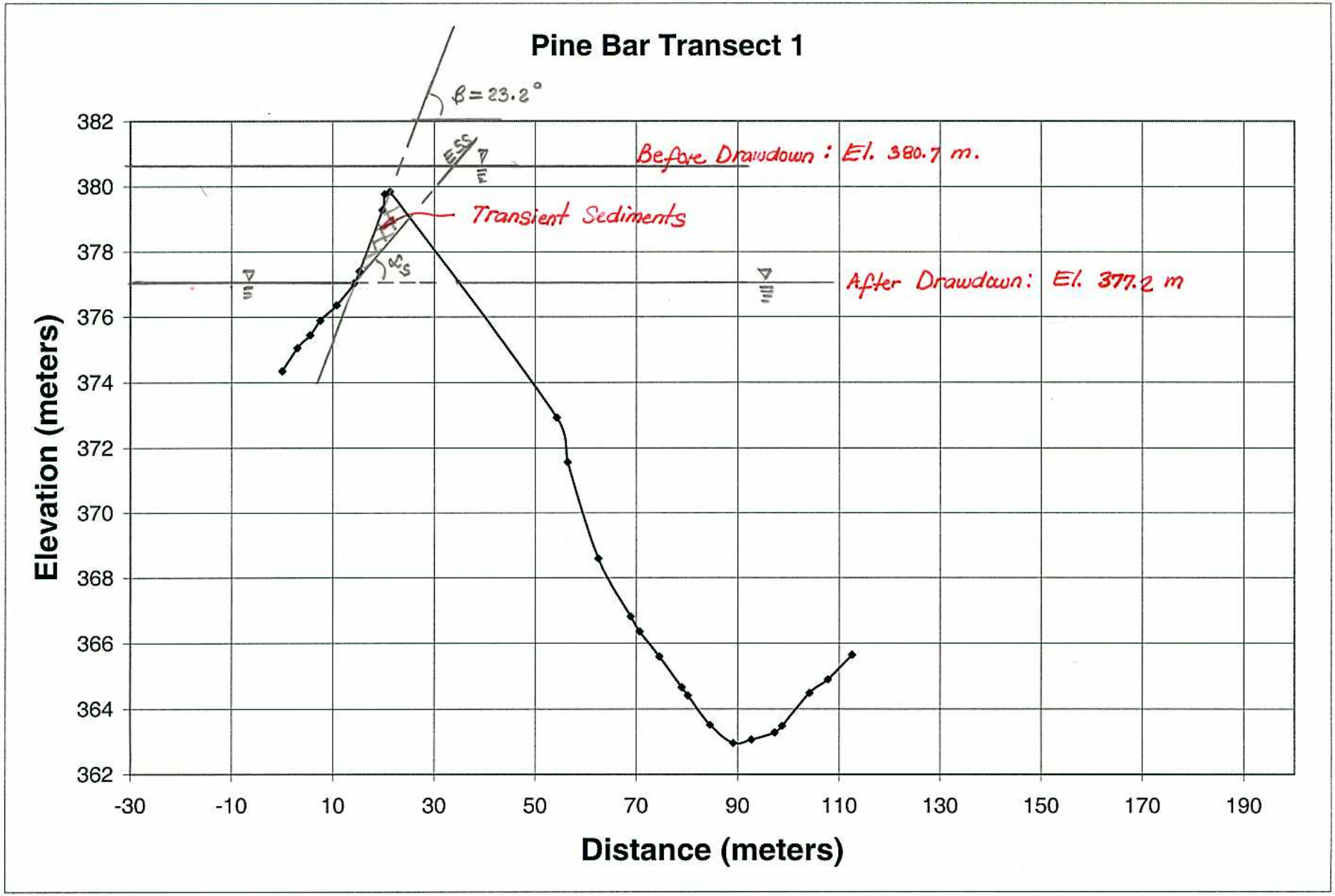
Pine Bar Transect 1
β = 23.2°
Before Drawdown : El. 380.7 m.
Transient Sediments
After Drawdown: El. 377.2 m
Elevation (meters)
382
380
378
376
374
372
370
368
366
364
362
-30
-10
10
30
50
70
90
110
130
150
170
190
Distance (meters)

Figure 80

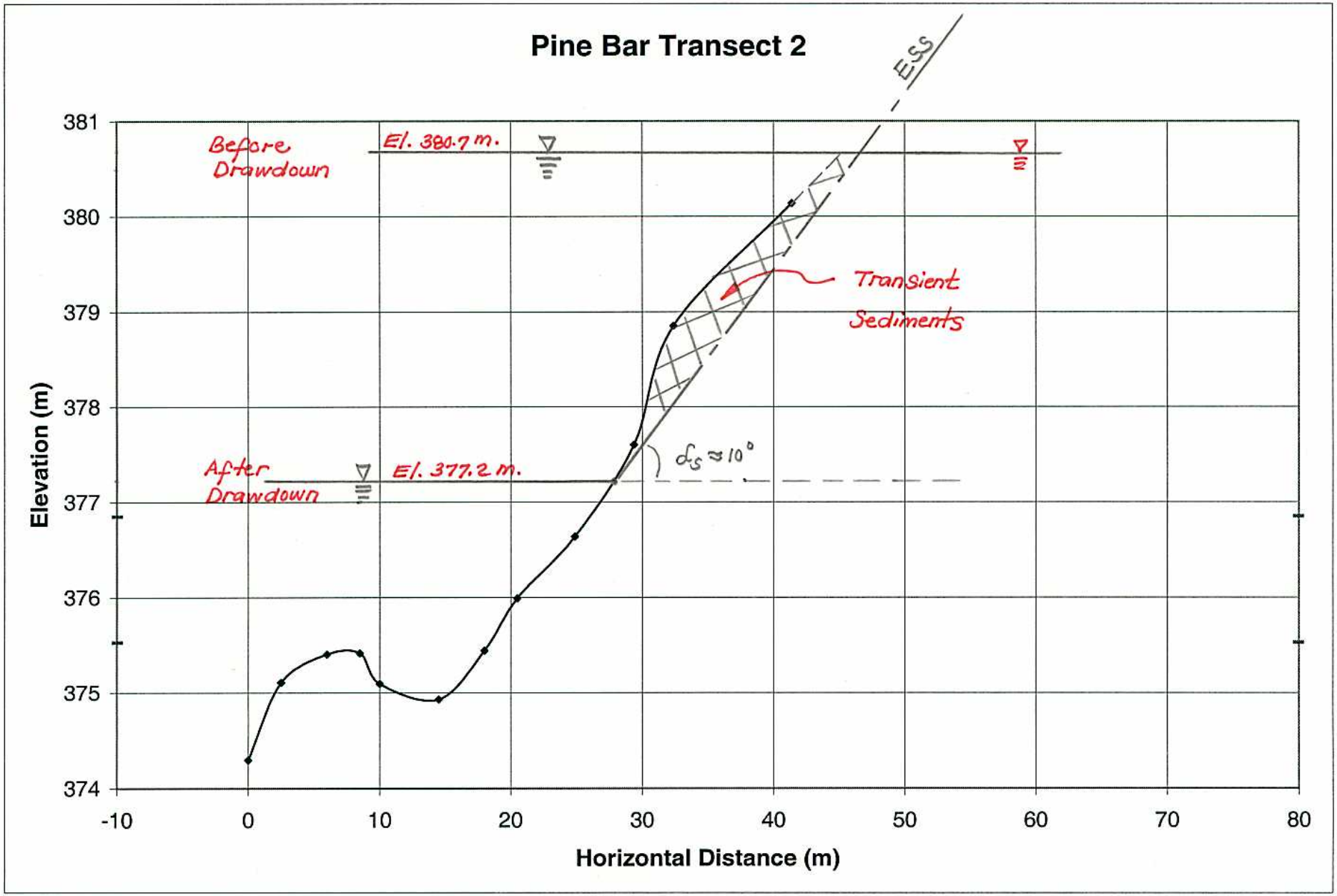
Pine Bar Transect 2
ESS
Before Drawdown
El. 380.7 m.
Transient Sediments
After Drawdown
El. 377.2 m.
$\alpha_s \approx 10°$
Elevation (m)
381
380
379
378
377
376
375
374
-10
0
10
20
30
40
50
60
70
80
Horizontal Distance (m)

Figure 81

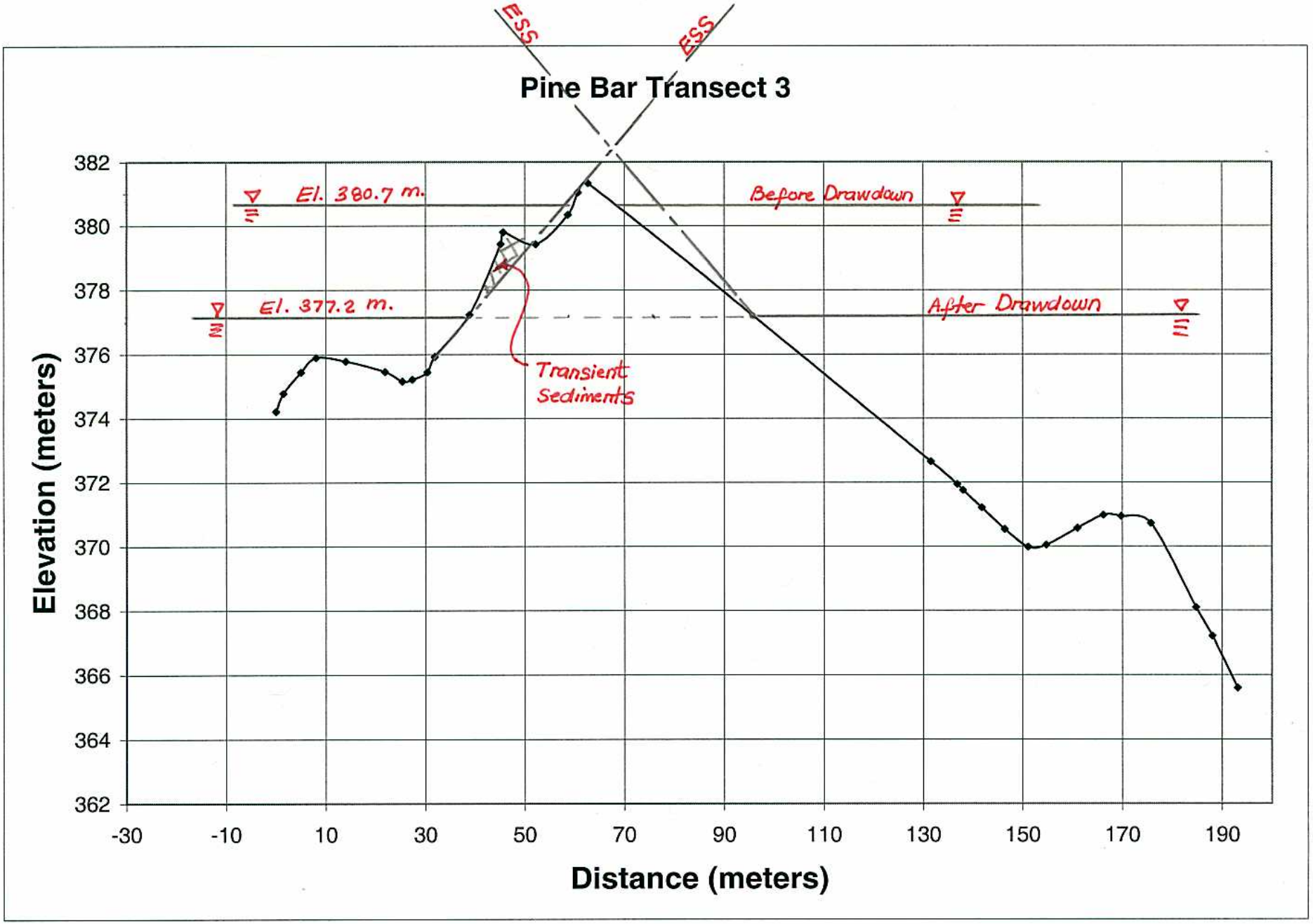
Pine Bar Transect 3
ESS
ESS
El. 380.7 m.
Before Drawdown
El. 377.2 m.
After Drawdown
Transient Sediments
Elevation (meters)
382
380
378
376
374
372
370
368
366
364
362
-30
-10
10
30
50
70
90
110
130
150
170
190
Distance (meters)

Figure 82

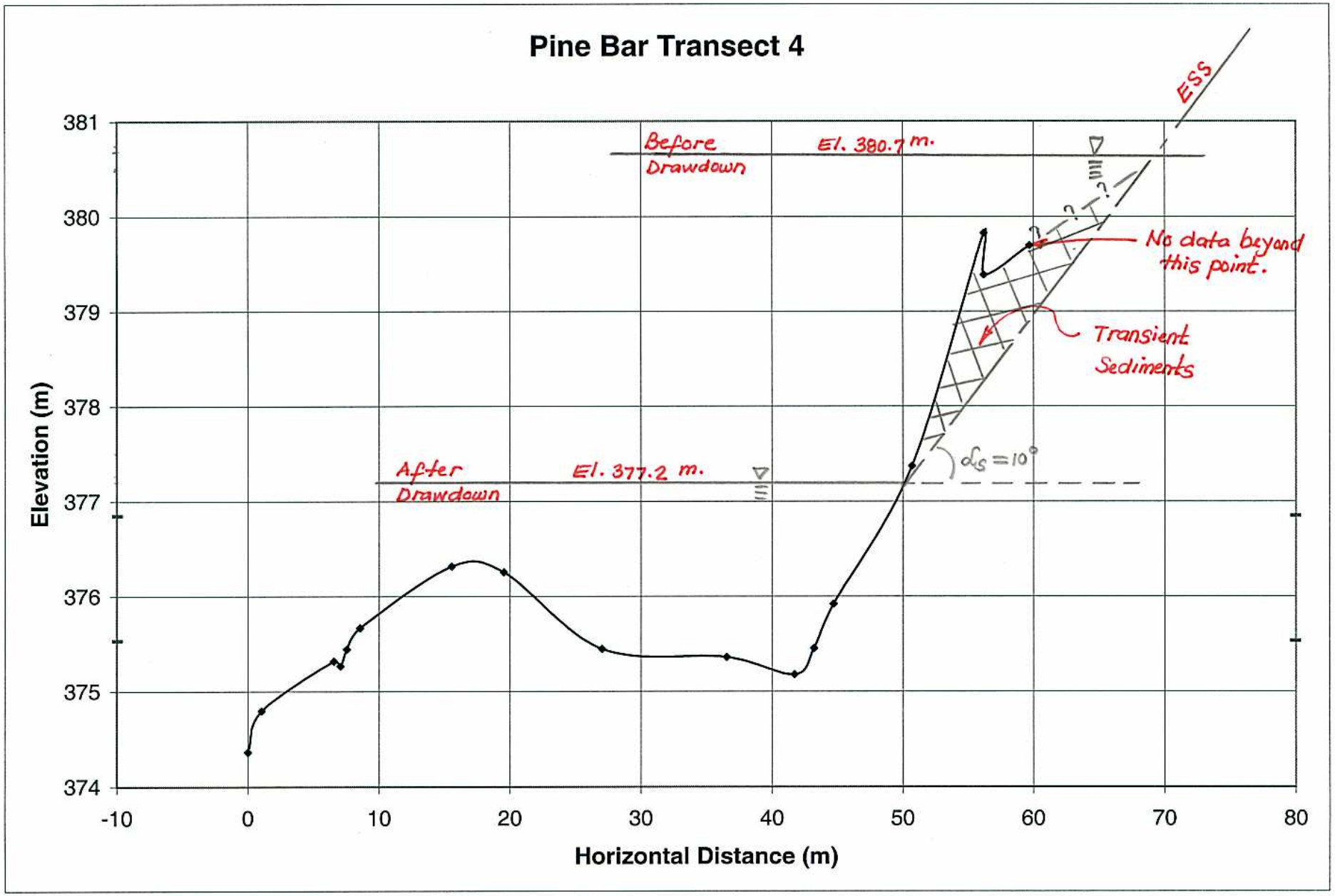
Pine Bar Transect 4
ESS
Before Drawdown
El. 380.7 m.
No data beyond this point.
Transient Sediments
After Drawdown
El. 377.2 m.
$\alpha_s = 10°$
Elevation (m)
381
380
379
378
377
376
375
374
-10
0
10
20
30
40
50
60
70
80
Horizontal Distance (m)

Figure 83

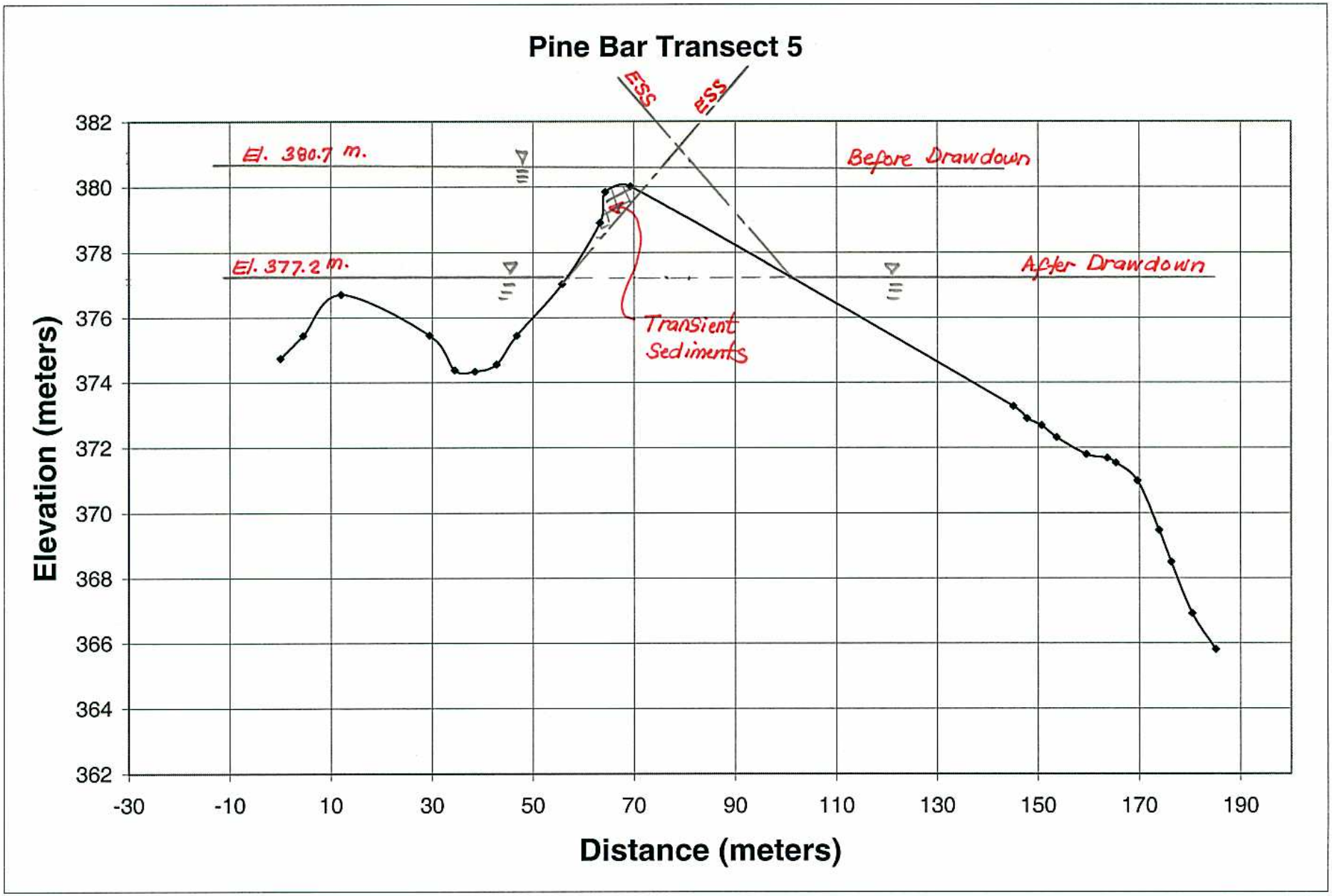
Pine Bar Transect 5
ESS
ESS
El. 380.7 m.
El. 377.2 m.
Before Drawdown
After Drawdown
Transient Sediments
Elevation (meters)
382
380
378
376
374
372
370
368
366
364
362
-30
-10
10
30
50
70
90
110
130
150
170
190
Distance (meters)

Figure 84

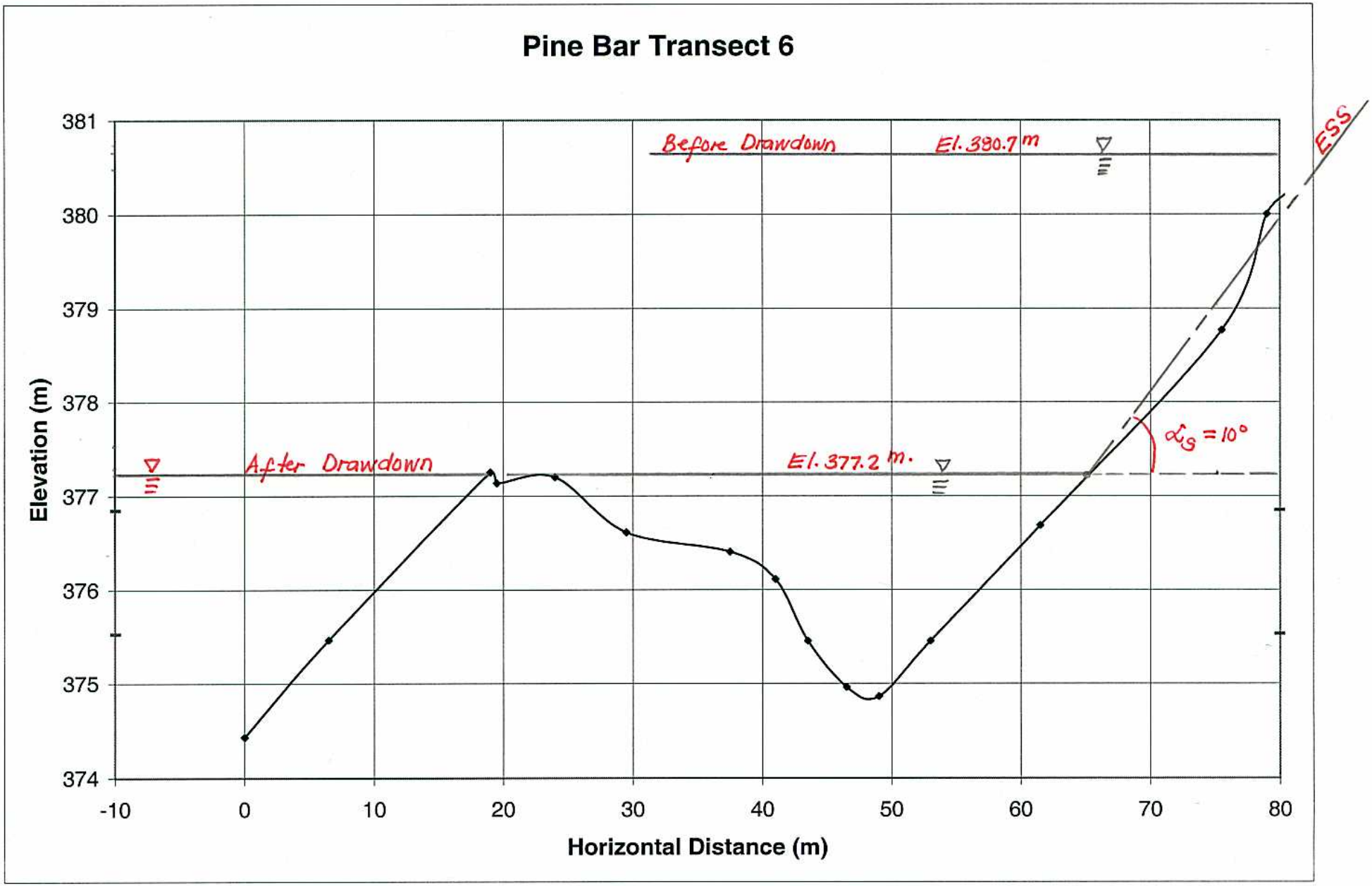
Pine Bar Transect 6
Before Drawdown
El. 380.7 m
After Drawdown
El. 377.2 m.
ESS
$\alpha_s = 10°$
Elevation (m)
Horizontal Distance (m)
381
380
379
378
377
376
375
374
-10
0
10
20
30
40
50
60
70
80

Figure 85

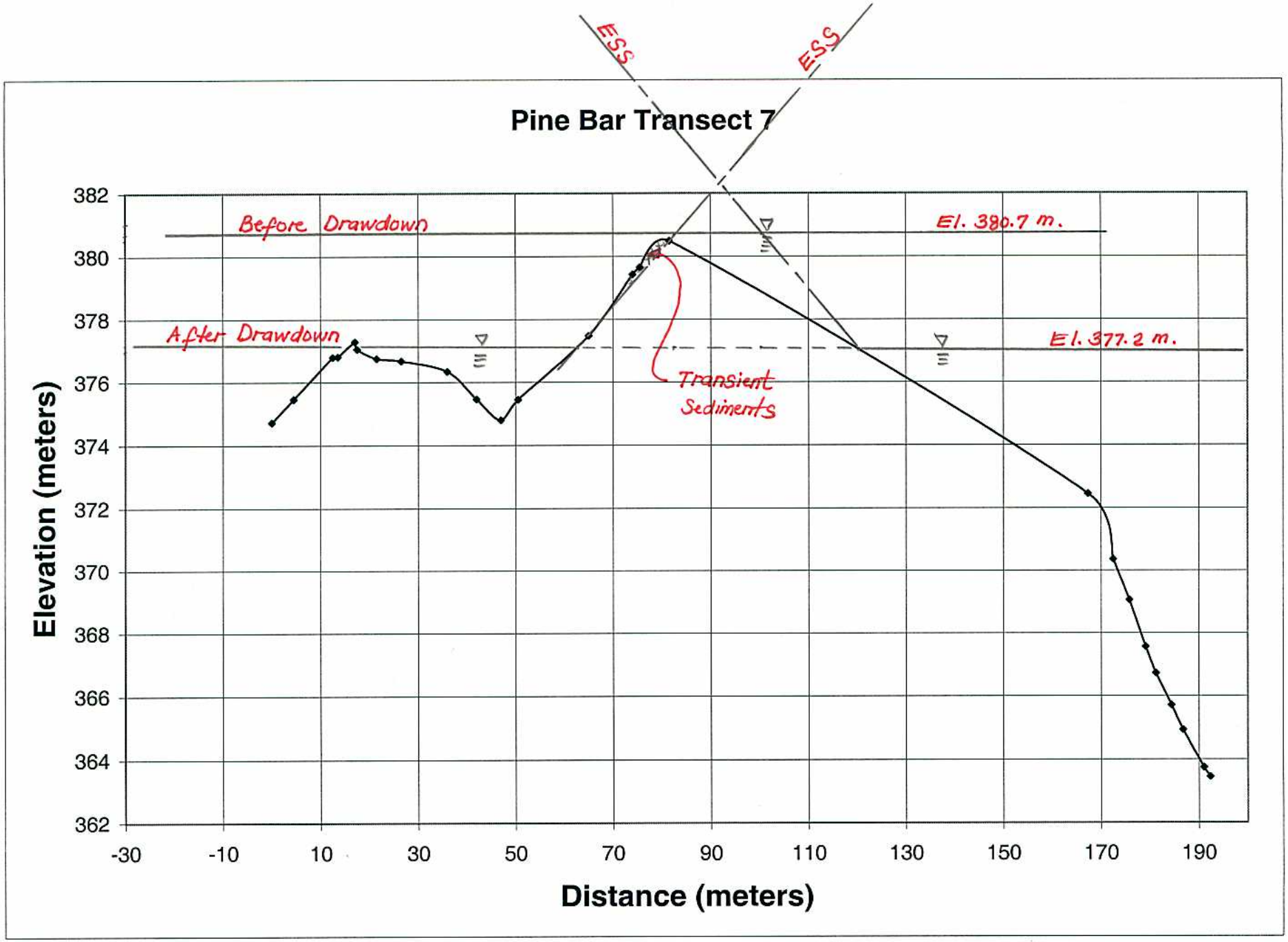
Pine Bar Transect 7
ESS
ESS
Before Drawdown
El. 380.7 m.
After Drawdown
El. 377.2 m.
Transient Sediments
Elevation (meters)
382
380
378
376
374
372
370
368
366
364
362
-30
-10
10
30
50
70
90
110
130
150
170
190
Distance (meters)

Figure 86

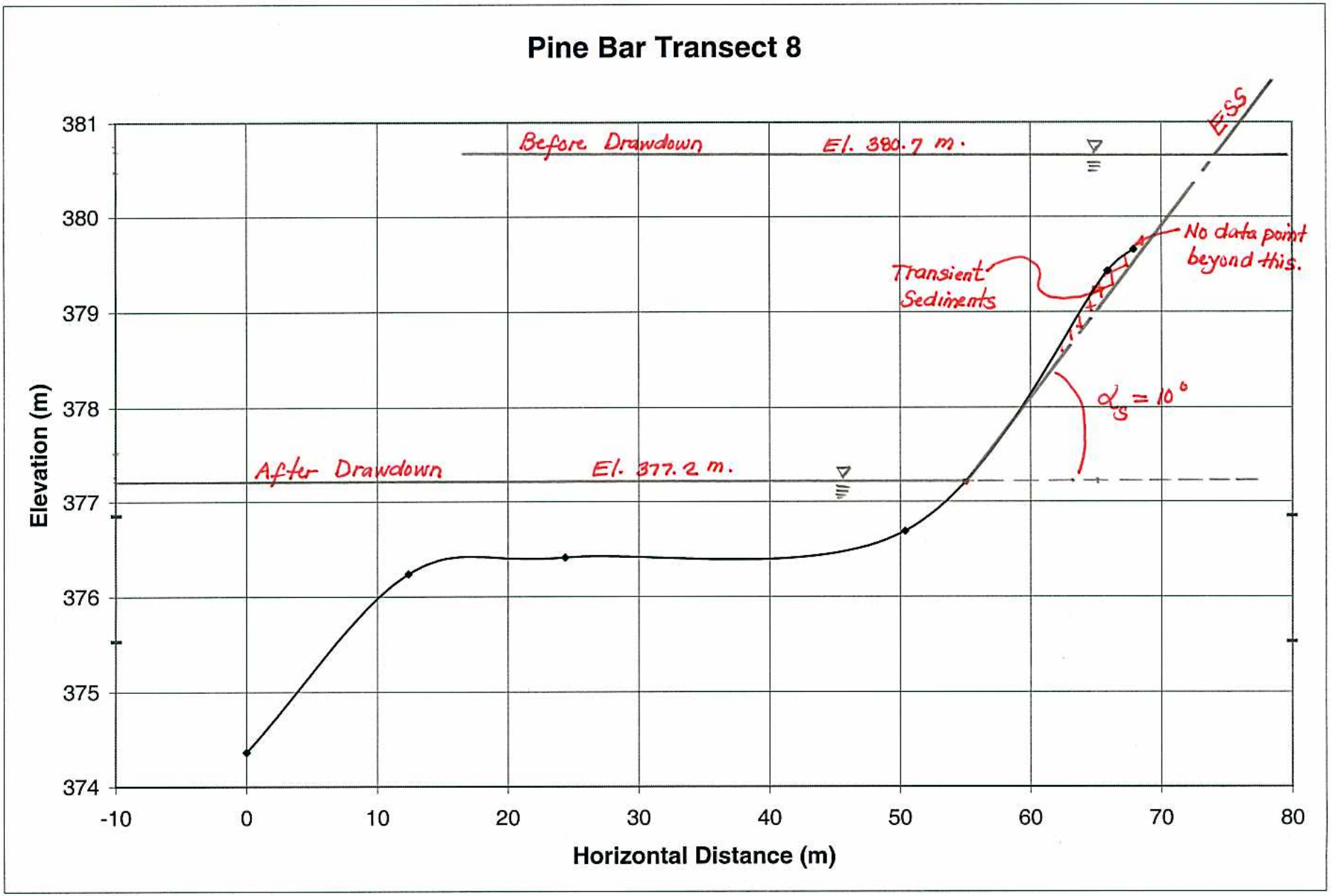
Pine Bar Transect 8
Elevation (m)
381
380
379
378
377
376
375
374
-10
0
10
20
30
40
50
60
70
80
Horizontal Distance (m)
Before Drawdown
El. 380.7 m.
After Drawdown
El. 377.2 m.
ESS
Transient Sediments
No data point beyond this.
$\alpha_s = 10^\circ$

Figure 87

This page left blank intentionally.

Appendix D. Explanation of the content on the 5 DVDs included with Hells Canyon AIR S-1

DVD	Label	Contents	Comments
1	*Hells Canyon AIRs S-1(g)*	1). 1955 Aerial Photos	
	1955 and 2003 Hells Canyon Aerial Photos		
		2). 2003 Aerial Photos	
2	*Hells Canyon AIRs S-1(g)*	1). 1973 Aerial Photos	12,000 cfs flow -- March 23, 1973
	1973_03		
		2). 1973 Aerial Photos	18,000 cfs flow -- March 22, 1973
3	*Hells Canyon AIRs S-1(g)*	1). 1973 Aerial Photos	5,000 cfs flow -- March 25, 1973
	1973_04 & 1977_07		
		2). 1977 Aerial Photos	
4	*Hells Canyon AIRs S-1(g)*	1). 1982 Aerial Photos	
	1982_16		
5	*Hells Canyon AIRs S-1(g)*	1). 1997 Archives (Aerial Photos)	Idaho Power Company
	1997 Archives and IPC & USFS Photos		
		2). IPC & USFS Photos	
		* Idaho Power Photos (1955, 1961, 1968, 1974, 1981)	Photos covering sections of the Snake River
		* Nez Perce National Forest (1948, 1949)	Photos covering sections of the Snake River
		* US Forest Service (1964)	Full set of 1964 Aerial Photos
		* Wallowa-Whitman National Forest (1946)	Photos covering sections of the Snake River
		3). List of Aerial Photos for Hells Canyon.xls	EXCEL worksheet identifying photo number and
			corresonding river miles for photos on this DVD.

This page left blank intentionally.

Appendix E. Tables showing segmentation of unadjusted and flow-adjusted sandbar counts

			Unadjusted Counts													
			(248.8 - 245)	(245 - 240)	(240 - 235)	(235 - 230)	(230 - 225)	(225 - 220)	(220 - 215)	(215 - 210)	(210 - 205)	(205 - 200)	(200 - 195)	(195 - 190)	(190 - 188.28)	
Total	Flow		246	243	238	233	228	223	218	213	208	203	198	193	189	Total
(unadjusted)	(cfs)	Year	HCD													
219	11,000	1955	14	21	20	4	19	21	16	12	18	22	15	26	11	219
242	11,000	1964	11	16	13	9	24	19	24	30	25	27	15	20	9	242
181	5,000	1973	7	7	11	3	15	20	19	14	27	23	12	18	5	181
150	12,000	1973	4	5	3	0	11	9	9	18	33	22	11	19	6	150
132	18,000	1973	3	7	3	0	14	14	13	15	20	19	9	10	5	132
175	5,310	1977	6	9	9	0	11	14	11	20	27	25	13	21	9	175
113	14,000	1982	4	8	1	0	9	12	8	15	20	16	8	10	2	113
118	20,000	1997	3	8	1	0	10	15	13	14	16	16	9	9	4	118
102	8,500	2003	4	5	5	2	15	12	11	7	11	14	7	7	2	102
	9,500															
	10,000															
Adjustment ratio up (bars/1000cfs)			0.43	0.29	1.14	0.43	0.57	1.57	1.43	-0.57	-0.86	0.14	0.14	-0.14	-0.14	4.43
Adjustment ratio down (bars/1000cfs)			-0.17	0.33	0.00	0.00	0.50	0.83	0.67	-0.50	-2.17	-0.50	-0.33	-1.50	-0.17	-3.00
Total	Flow		Flow Adjusted Counts													
(unadjusted)	(cfs)	Year	246	243	238	233	228	223	218	213	208	203	198	193	189	Total
219	11000	1955	13.6	20.7	18.9	3.6	18.4	19.4	14.6	12.6	18.9	21.9	14.9	26.1	11.1	215
242	11000	1964	10.6	15.7	11.9	8.6	23.4	17.4	22.6	30.6	25.9	26.9	14.9	20.1	9.1	238
181	5000	1973	4.0	5.0	3.0	0.0	11.0	9.0	9.0	18.0	33.0	22.0	11.0	19.0	6.0	150
150	12000	1973	4.0	5.0	3.0	0.0	11.0	9.0	9.0	18.0	33.0	22.0	11.0	19.0	6.0	150
132	18000	1973	4.0	5.0	3.0	0.0	11.0	9.0	9.0	18.0	33.0	22.0	11.0	19.0	6.0	150
175	5310	1977	3.1	7.1	1.4	0.0	7.2	3.5	1.4	23.8	32.7	24.0	12.0	22.0	10.0	148
113	14000	1982	4.3	7.3	1.0	0.0	8.0	10.3	6.7	16.0	24.3	17.0	8.7	13.0	2.3	119
118	20000	1997	4.3	5.3	1.0	0.0	6.0	8.3	7.7	18.0	33.3	20.0	11.7	21.0	5.3	142
102	8,500	2003	2.5	4.0	1.0	0.5	13.0	8.1	8.1	8.1	12.7	13.6	6.6	7.4	2.4	88
	9,500															
	10,000															

This page left blank intentionally.